NEW GENOME EDITING TOOLS AND RESOURCES: ENABLING GENE DISCOVERY AND FUNCTIONAL GENOMICS

EDITED BY: Feng Zhang, Bing Yang, Qi-Jun Chen and Wendy Harwood
PUBLISHED IN: Frontiers in Genome Editing

frontiers Research Topics

frontiers

ISSN 1664-8714
ISBN 978-2-88971-786-6
DOI 10.3389/978-2-88971-786-6

About Frontiers

Frontiers is more than just an open-access publisher of scholarly articles: it is a pioneering approach to the world of academia, radically improving the way scholarly research is managed. The grand vision of Frontiers is a world where all people have an equal opportunity to seek, share and generate knowledge. Frontiers provides immediate and permanent online open access to all its publications, but this alone is not enough to realize our grand goals.

Frontiers Journal Series

The Frontiers Journal Series is a multi-tier and interdisciplinary set of open-access, online journals, promising a paradigm shift from the current review, selection and dissemination processes in academic publishing. All Frontiers journals are driven by researchers for researchers; therefore, they constitute a service to the scholarly community. At the same time, the Frontiers Journal Series operates on a revolutionary invention, the tiered publishing system, initially addressing specific communities of scholars, and gradually climbing up to broader public understanding, thus serving the interests of the lay society, too.

Dedication to Quality

Each Frontiers article is a landmark of the highest quality, thanks to genuinely collaborative interactions between authors and review editors, who include some of the world's best academicians. Research must be certified by peers before entering a stream of knowledge that may eventually reach the public - and shape society; therefore, Frontiers only applies the most rigorous and unbiased reviews.
Frontiers revolutionizes research publishing by freely delivering the most outstanding research, evaluated with no bias from both the academic and social point of view. By applying the most advanced information technologies, Frontiers is catapulting scholarly publishing into a new generation.

What are Frontiers Research Topics?

Frontiers Research Topics are very popular trademarks of the Frontiers Journals Series: they are collections of at least ten articles, all centered on a particular subject. With their unique mix of varied contributions from Original Research to Review Articles, Frontiers Research Topics unify the most influential researchers, the latest key findings and historical advances in a hot research area! Find out more on how to host your own Frontiers Research Topic or contribute to one as an author by contacting the Frontiers Editorial Office: frontiersin.org/about/contact

NEW GENOME EDITING TOOLS AND RESOURCES: ENABLING GENE DISCOVERY AND FUNCTIONAL GENOMICS

Topic Editors:
Feng Zhang, University of Minnesota Twin Cities, United States
Bing Yang, University of Missouri, United States
Qi-Jun Chen, China Agricultural University, China
Wendy Harwood, John Innes Centre, United Kingdom

Citation: Zhang, F., Yang, B., Chen, Q.-J., Harwood, W., eds. (2021). New Genome Editing Tools and Resources: Enabling Gene Discovery and Functional Genomics. Lausanne: Frontiers Media SA. doi: 10.3389/978-2-88971-786-6

Table of Contents

frontiers in Genome Editing

EDITORIAL
published: 08 October 2021
doi: 10.3389/fgeed.2021.771622

Editorial: New Genome Editing Tools and Resources: Enabling Gene Discovery and Functional Genomics

Wendy Harwood[1], *Qi-Jun Chen*[2], *Feng Zhang*[3,4,5] *and Bing Yang*[6]*

[1]John Innes Centre, Norwich Research Park, Norwich, United Kingdom, [2]State Key Laboratory of Plant Physiology and Biochemistry, College of Biological Sciences, China Agricultural University, Beijing, China, [3]Department of Plant and Microbial Biology, University of Minnesota, St. Paul, MN, United States, [4]Center for Precision Plant Genomics, University of Minnesota, St. Paul, MN, United States, [5]Center for Genome Engineering, University of Minnesota, St. Paul, MN, United States, [6]Division of Plant Sciences, Bond Life Sciences Center, University of Missouri, Columbia, MO, United States

Keywords: genome editing, gene discovery, functional genomics, CRiSPR/Cas, crop improvement

Editorial on the Research Topic

New Genome Editing Tools and Resources: Enabling Gene Discovery and Functional Genomics

Genome editing technologies are revolutionizing molecular biology research and offer huge potential for development of crops that could help meet the challenge of providing sufficient food, sustainably and under increasingly challenging environmental conditions. The ability to make precise changes in plant genomes, together with the increased genomic resources now available, give unprecedented opportunities to develop crops with desired traits much faster than with traditional techniques. Although there are a range of genome editing technologies available, the one that is currently most widely used, and has generated the most excitement, is CRISPR/Cas. Despite the great progress of CRISPR/Cas-induced genome editing in plants, two main challenges persist: delivery of CRISPR reagents and precise genome editing. The papers in this research topic all feature CRISPR-based systems and highlight some of the latest advances in this fast-moving area including in delivery and precise genome editing technologies.

CRISPR/Cas applications have rapidly moved from allowing simple, single target gene knock-outs to enabling more complex targeted edits. **Figure 1** illustrates the range of tools and resources now available, with those under the headings: Precise editing, Delivery systems and Others highlighted in this research topic. Some of our most important crops have polyploid genomes with multiple gene copies. This can complicate editing strategies (Schaart et al., 2021), however, in the paper entitled "*Multiallelic, Targeted Mutagenesis of Magnesium Chelatase With CRISPR/Cas9 Provides a Rapidly Scorable Phenotype in Highly Polyploid Sugarcane*" Eid et al. show that up to 49 out of 59 copies of the target gene, magnesium chelatase, could be mutated using just two sgRNAs. It was also shown that a heat treatment could increase editing efficiencies 2-fold, while also promoting editing of multiple copies of the target gene.

One attraction of genome editing is that once the required edits have been achieved, the editing components integrated into the genome can be segregated away in subsequent generations, leaving a plant with the required edit only and no foreign DNA. An alternative to this approach is to introduce the editing components as a ribonucleoprotein (RNP) complex (Zhang et al., 2021). Dong et al. in their manuscript "*Efficient Targeted Mutagenesis Mediated by CRISPR-Cas12a Ribonucleoprotein Complexes in Maize*," use this RNP approach, but rather than the common Cas9 RNP, they use a Cas12a RNP and deliver this into maize protoplasts and immature embryos. This RNP approach gave average editing efficiencies of over 60%; comparable to or higher than efficiencies achieved by editing components from transgenes. Several versions of Cas12a have been reported and a comparison by the authors showed improved editing with some Cas12a variants.

Another enhanced Cas12a (FnCas12a) is reported by Negishi et al. in their paper "*Enhanced FnCas12a-Mediated Targeted Mutagenesis Using crRNA with Altered Target*

OPEN ACCESS

Edited and reviewed by:
Yiping Qi,
University of Maryland, United States

***Correspondence:**
Bing Yang
yangbi@missouri.edu

Specialty section:
This article was submitted to Genome Editing in Plants, a section of the journal Frontiers in Genome Editing

Received: *06 September 2021*
Accepted: *20 September 2021*
Published: *08 October 2021*

Citation:
Harwood W, Chen Q-J, Zhang F and Yang B (2021) Editorial: New Genome Editing Tools and Resources: Enabling Gene Discovery and Functional Genomics. Front. Appl. Math. Stat. 3:771622. doi: 10.3389/fgeed.2021.771622

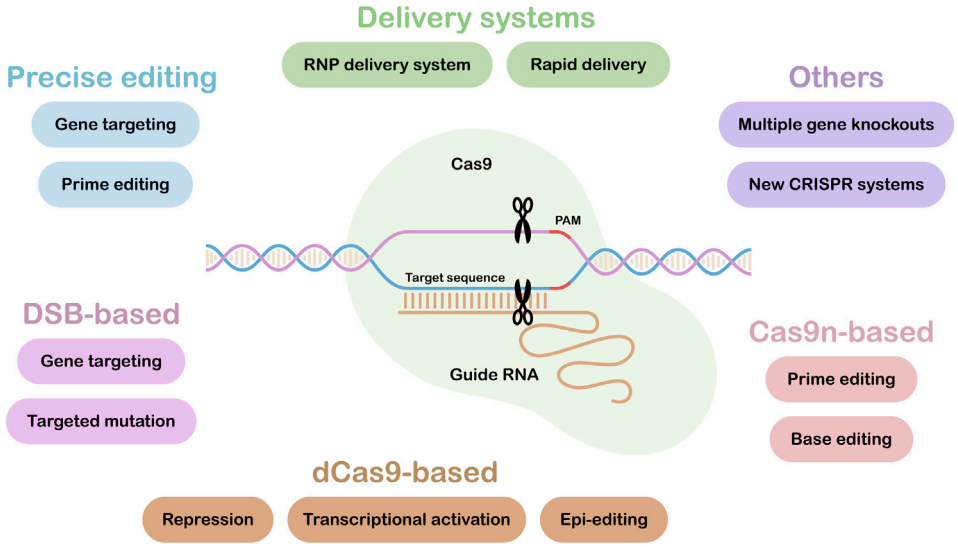

FIGURE 1 | CRISPR/Cas Tools and Resources. Tools and Resources under the headings: Precise editing, Delivery systems and Others are covered in this research topic. The lower part of the figure summarizes current Cas9-based tools and applications. DSB, Double Strand Break; dCas9, dead or inactive Cas9; Cas9n, Cas9 nickase.

Length in Rice." The authors report that the efficiency of FnCas12a-mediated editing depends on the length of the crRNA guide sequence. Altering the length of the crRNA changed the frequency with which large deletions could be obtained, indicating that this approach could fine-tune the editing outcome. The two papers describing the use of Cas12a add to the current literature demonstrating the high potential and versatility of this nuclease family (Bandyopadhyay et al., 2020).

In addition to single and multiple targeted gene knock-outs, there is a need to make other, specific targeted changes in plant genomes. Where a single base change is required, then base editing approaches may be appropriate (**Figure 1**). However, where more than one base change is required, the new technique of prime editing may be used. In the paper "*Spelling Changes and Fluorescent Tagging with Prime Editing Vectors for Plants*," Wang et al. describe a set of easy-to-use vectors for prime editing in both dicot and monocot species. Generally, the size of insertion achieved by prime editing is small (Lin et al., 2020), but Wang et al. showed in their paper that it is possible to insert 66 bp, the largest reported to date. To make even larger genomic insertions at a precise location, gene targeting is required. The targeted insertion of large sequences or entire genes is technically challenging, and efficiencies are generally low (Dong and Ronald 2021). In the paper by Lawrenson et al. "*In-planta Gene Targeting in Barley using Cas9 with and without Geminiviral Replicons*," successful gene targeting in barley is described, with an mCherry marker gene being inserted at the target genomic locus.

As well as tools that expand the range of possible genome editing applications, ways to improve the speed and efficiency of genome editing systems have been examined. The process of plant genome editing can be time consuming, as there is generally a need for regeneration of plants from tissue culture. It is important, therefore, to have confidence that specific genome editing components will work. Nasti et al. in their paper "*Fast-TrACC: A Rapid Method for Delivering and Testing Gene Editing Reagents in Somatic Plant Cells*" address this issue. They describe a system that uses a luciferase reporter to provide a readout of the efficiency of *Agrobacterium*-mediated delivery of genome editing reagents. The ability to test sgRNAs before attempting plant genome editing can save valuable time.

Often it is the generation time of a crop plant that limits fast progress in genome editing. In certain crops, rapid flowering lines have been developed. Fast-flowering mini-maize is one such example (McCaw et al., 2016). As well as the fast-flowering phenotype, mini-maize also needs to be amenable to transformation to make it valuable for rapid genome editing applications. In the paper by McCaw et al. in this research topic, "*Development of a Transformable Fast-Flowering Mini-Maize as a tool for Maize Gene Editing*," the authors describe development of a fast-flowering mini-maize that is also amenable to transformation and editing at efficiencies up to 17 and 79%, respectively, with a seed to T1 seed time of 5.5 months compared to over 9 months for other genotypes.

In summary, this collection of papers highlights some exciting recent developments in provision of CRISPR/Cas tools and resources. These enhanced resources are poised to make a major contribution to more efficient and rapid gene discovery and functional characterization.

AUTHOR CONTRIBUTIONS

WH drafted the editorial and all authors contributed to revision and to the final version.

ACKNOWLEDGMENTS

Joshua Waites from the John Innes Centre is thanked for **Figure 1**.

REFERENCES

Bandyopadhyay, A., Kancharla, N., Javalkote, V. S., Dasgupta, S., and Brutnell, T. P. (2020). CRISPR-Cas12a (Cpf1): A Versatile Tool in the Plant Genome Editing Tool Box for Agricultural Advancement. *Front. Plant Sci.* 11, 1. doi:10.3389/fpls.2020.584151

Dong, O. X., and Ronald, P. C. (2021). Targeted DNA Insertion in Plants. *Proc. Natl. Acad. Sci. USA* 118 (22), e2004834117. doi:10.1073/pnas.2004834117

Lin, Q., Zong, Y., Xue, C., Wang, S., Jin, S., Zhu, Z., et al. (2020). Prime Genome Editing in rice and Wheat. *Nat. Biotechnol.* 38 (5), 582–585. doi:10.1038/s41587-020-0455-x

McCaw, M. E., Wallace, J. G., Albert, P. S., Buckler, E. S., and Birchler, J. A. (2016). Fast-Flowering Mini-Maize: Seed to Seed in 60 Days. *Genetics* 204 (1), 35–42. doi:10.1534/genetics.116.191726

Schaart, J. G., van de Wiel, C. C. M., and Smulders, M. J. M. (2021). Genome Editing of Polyploid Crops: Prospects, Achievements and Bottlenecks. *Transgenic Res.* 30 (4), 337–351. doi:10.1007/s11248-021-00251-0

Zhang, Y., Iaffaldano, B., and Qi, Y. (2021). CRISPR Ribonucleoprotein-Mediated Genetic Engineering in Plants. *Plant Commun.* 2 (2), 100168. doi:10.1016/j.xplc.2021.100168

Conflict of Interest: The authors declare that the research was conducted in the absence of any commercial or financial relationships that could be construed as a potential conflict of interest.

Publisher's Note: All claims expressed in this article are solely those of the authors and do not necessarily represent those of their affiliated organizations, or those of the publisher, the editors and the reviewers. Any product that may be evaluated in this article, or claim that may be made by its manufacturer, is not guaranteed or endorsed by the publisher.

frontiers in Genome Editing

ORIGINAL RESEARCH
published: 14 December 2020
doi: 10.3389/fgeed.2020.608563

Enhanced FnCas12a-Mediated Targeted Mutagenesis Using crRNA With Altered Target Length in Rice

Katsuya Negishi[1†], *Masafumi Mikami*[1,2†], *Seiichi Toki*[1,2,3] *and Masaki Endo*[1,4*]

[1] *Plant Genome Engineering Research Unit, Institute of Agrobiological Sciences, National Agriculture and Food Research Organization, Tsukuba, Japan,* [2] *Graduate School of Nanobioscience, Yokohama City University, Yokohama, Japan,* [3] *Kihara Institute for Biological Research, Yokohama City University, Yokohama, Japan,* [4] *Probabilistic Modeling Team, Research Center for Agricultural Information Technology, National Agriculture and Food Research Organization, Tsukuba, Japan*

The CRISPR/Cas12a (Cpf1) system utilizes a thymidine-rich protospacer adjacent motif (PAM) and generates DNA ends with a 5′ overhang. These properties differ from those of CRISPR/Cas9, making Cas12a an attractive alternative in the CRISPR toolbox. However, genome editing efficiencies of Cas12a orthologs are generally lower than those of SpCas9 and depend on their target sequences. Here, we report that the efficiency of FnCas12a-mediated targeted mutagenesis varies depending on the length of the crRNA guide sequence. Generally, the crRNA of FnCas12a contains a 24-nt guide sequence; however, some target sites showed higher mutation frequency when using crRNA with an 18-nt or 30-nt guide sequence. We also show that a short crRNA containing an 18-nt guide sequence could induce large deletions compared with middle- (24-nt guide sequence) and long- (30-nt guide sequence) crRNAs. We demonstrate that alteration of crRNA guide sequence length does not change the rate of off-target mutation of FnCas12a. Our results indicate that efficiency and deletion size of FnCas12a-mediated targeted mutagenesis in rice can be fine-tuned using crRNAs with appropriate guide sequences.

Keywords: CRISPR/Cas12a, genome editing, targeted mutagenesis, large deletion, *Oryza sativa*

OPEN ACCESS

Edited by:
Bing Yang,
University of Missouri, United States

Reviewed by:
Keunsub Lee,
Iowa State University, United States
Qinlong Zhu,
South China Agricultural University, China

***Correspondence:**
Masaki Endo
mendo@affrc.go.jp

[†]These authors have contributed equally to this work

Specialty section:
This article was submitted to Genome Editing in Plants, a section of the journal Frontiers in Genome Editing

Received: *21 September 2020*
Accepted: *18 November 2020*
Published: *14 December 2020*

Citation:
Negishi K, Mikami M, Toki S and Endo M (2020) Enhanced FnCas12a-Mediated Targeted Mutagenesis Using crRNA With Altered Target Length in Rice. Front. Genome Ed. 2:608563. doi: 10.3389/fgeed.2020.608563

INTRODUCTION

The CRISPR/Cas9 (clustered regularly interspaced short palindromic repeats/CRISPR-associated protein 9) system was first reported as an adaptive immune system in archaea and bacteria and is now used for genome editing in various organisms, including plants (Li et al., 2013; Nekrasov et al., 2013; Shan et al., 2013). Cas9 endonuclease protein makes a complex with two small RNAs named CRISPR RNA (crRNA) and trans-activating crRNA (tracrRNA) (Jinek et al., 2012). The Cas9-RNA complex first recognizes a protospacer adjacent motif (PAM) sequence in the double-stranded DNA and then interrogates a target sequence next to the PAM (Shibata et al., 2017). Cas9 binds and cleaves target DNA with a sequence complementary to that of the crRNA to produce a DNA double-stranded break (DSB) that causes genome mutations as a failure of DNA repair pathways. In CRISPR/Cas9-mediated genome editing, the PAM restricts the selectivity of target sites because each Cas9 requires a specific

PAM sequence for target recognition. The widely used Cas9 from *Streptococcus pyogenes* (SpCas9) recognizes an NGG sequence as a PAM. Cas9 orthologs from *Streptococcus thermophilus* (StCas9) and *Staphylococcus aureus* (SaCas9) recognize NNAGAA and NNGRRT as PAM sequences, respectively, and have been utilized for genome editing in plants (Steinert et al., 2015; Kaya et al., 2016). Furthermore, engineered SpCas9 variants that recognize different PAM sequences have been developed, expanding the application of genome editing in plants (Hu et al., 2018; Meng et al., 2018; Endo et al., 2019). These Cas9 orthologs and variants can expand target selectivity. However, Cas9 orthologs mainly require a guanine-rich sequence as a PAM. Cas12a—also known as CRISPR from *Prevotella* and *Francisella* 1 (Cpf1)—has been reported as another type of RNA-guided endonuclease derived from a Class 2/type V CRISPR/Cas system (Zetsche et al., 2015). While Cas9 requires a mainly G-rich sequence as a PAM, Cas12a can recognize a T-rich sequence as a PAM. Therefore, CRISPR/Cas12a-based genome editing technology can be a useful tool to complement CRISPR/Cas9 and further expand the targeting range. In addition, Cas12a has several features that differ from those of Cas9. Cas12a cleaves target DNA downstream of the PAM and produces cohesive ends with 5′ sticky overhangs, whereas Cas9 generates blunt ends upstream of the PAM (Zetsche et al., 2015). While Cas9 needs crRNA and tracrRNA, Cas12a requires only crRNA. The length of Cas12a crRNA is 40–45 nucleotides (nt), i.e., less than half the length of the SpCas9 single-guide RNA (sgRNA), which is a fusion RNA of crRNA and tracrRNA with an artificial linker (Jinek et al., 2012). Cas12a has both DNA and RNA cleavage activities to process the CRISPR precursor transcript (pre-crRNA) to mature crRNA, whereas Cas9 has DNA cleavage activity only (Fonfara et al., 2016). Three Cas12a orthologs, from *Acidaminococcus* sp. BV3L6 (AsCas12a), *Lachnospiraceae bacterium* ND2006 (LbCas12a), and *Francisella novicida* U112 (FnCas12a), have been used for genome editing in plants (Endo et al., 2016; Tang et al., 2017; Wang et al., 2017; Xu et al., 2019). AsCas12a and LbCas12a recognize TTTV and FnCas12a recognizes TTV as PAMs (Zetsche et al., 2015). However, mutagenesis efficiency using AsCas12a or LbCas12a was found to be generally lower than that using SpCas9 in maize (Lee et al., 2019). In our previous study of FnCas12a, the mutation efficiencies in several target sites designed in the *Nicotiana tabacum* genome were also very low—even below detection level (Endo et al., 2016). Because of the low mutation efficiency, Cas12a orthologs are thus harder to use for genome editing in plants than SpCas9 despite the many inherent advantages of Cas12a. Thus, the CRISPR/Cas12a system needs further optimization to improve genome editing efficiency. In SpCas9-mediated genome editing, there are several reports of enhancement of genome editing activity through gRNA engineering, such as changing the length of the sgRNA or scaffold sequence (Fu et al., 2014; Dang et al., 2015) or chemical modification of the sgRNA (Hendel et al., 2015; Ryan et al., 2018). In CRISPR/Cas12a, it has also been reported that engineering of the crRNA can affect genome editing activity. Modifications of the 3′-end sequence of crRNA can improve AsCas12a activity in human cells (Li et al., 2017). The FnCas12a-crRNA complex has DSB activity in *in vitro* assays when using crRNAs with 16- to 24-nt and 30-nt guide sequences (Lei et al., 2017). Although the most commonly used crRNAs of LbCas12a have a 25-nt guide and 21-nt scaffold sequence, LbCas12a can induce targeted mutations when using a crRNA containing a 31-nt guide, 21-nt scaffold, and 15-nt repeat spacer sequence in rice (Xu et al., 2017). Furthermore, the cleavage site recognized by FnCas12a could be altered by changing the crRNA length *in vitro*. The lengths of 5′ protruding ends were extended when the length of the guide sequence was 18-nt or less (Lei et al., 2017). In this work, we compared the mutation frequencies in rice using crRNAs with four different guide sequence lengths (18-nt, 24-nt, 30-nt, and 45-nt) and showed that the length of the guide sequence affects genome editing efficiency and mutation pattern. We also investigated the effect of guide sequence length on the rate of off-target mutation. Our results suggest that optimizing target length can lead to more efficient CRISPR/FnCas12a-mediated genome editing in plants.

MATERIALS AND METHODS

Vector Construction

The FnCas12a vector used in this study is based on our previously described FnCas12a expression vectors, which include the FnCas12a expression cassette and the hygromycin B phosphotransferase (HPT) expression cassette (Endo et al., 2016). The crRNA of FnCas12a was placed under the control of the rice *U6-2* promoter (Mikami et al., 2015). crRNAs with 24-nt, 18-nt, 30-nt, or 45-nt guide sequences were inserted into the *Bbs*I site next to the crRNA scaffold. The expression cassette of crRNA was cloned into the binary vector using the restriction enzymes *Asc*I and *Pac*I (Endo et al., 2016).

Transformation of Rice With FnCas12a/crRNA Expression Constructs

Agrobacterium tumefaciens-mediated transformation of rice (*Oryza sativa* L. cv. Nipponbare) using scutellum-derived calli was performed as described previously (Toki, 1997; Toki et al., 2006). Rice calli were infected by *A. tumefaciens* strain EHA105 transformed with the FnCas12a/crRNA vectors. Transgenic calli were selected for hygromycin resistance and cultured for 1 month at 30°C on callus induction medium containing 50 mg/L hygromycin B. Details of the rice transformation procedure have been described in a previous report (Mikami et al., 2017).

Cleaved Amplified Polymorphic Sequences Analysis

To detect targeted mutations in the rice genome, genomic DNA was extracted from 18 to 25 independent transgenic calli or regenerated plants per construct using an Agencourt Chloropure Kit (Beckman Coulter). Target loci were amplified using the primers listed in **Supplementary Table 1**. PCR products were subjected to restriction enzyme digestion and analyzed by agarose gel electrophoresis. The number of samples for cleaved amplified polymorphic sequences (CAPS) analysis and the number of mutations detected in calli are shown in **Supplementary Table 2**.

TABLE 1 | Target sequences and lengths of DL-1 and DL-2.

Target gene	crRNA	PAM	Sequence	Length (nt)
DL	DL-1_Short	TTC	GTCTTTTGGGTAG CTGCA	18
	DL-1_Middle		GTCTTTTGGGTAG CTGCAGGTTGG	24
	DL-1_Long		GTCTTTTGGGTAG CTGCAGGTTGGAGTCCC	30
	DL-2_Short	TTG	GGGAGAGCGG CTGCACCA	18
	DL-2_Middle		GGGAGAGCGGCTGCACC ATCGGCG	24
	DL-2_Long		GGGAGAGCGGCTGCA CCATCGGCGGCCGCG	30

Underlined sequences indicate the restriction enzyme sites for CAPS assay.

Sequencing Analysis

To determine mutation frequency in rice calli, we selected two representative lines for each construct whose CAPS analysis revealed a clear undigested PCR fragment, and their PCR products were cloned into pCR-BluntII-TOPO (Invitrogen) and subjected to sequence analysis using an Applied Biosystems 3500xl sequencer (Applied Biosystems).

Amplicon Deep Sequencing Analysis

For amplicon deep sequencing analysis, the PCR products were adjusted in four steps: (1) in five target sites (DL-1, DL-2, ALS-1, ALS-2, and AAO2-1), crRNAs with short, middle, and long guide sequences were prepared and expressed with FnCas12a. Four independent transgenic calli with high mutation frequencies were selected by CAPS analysis. (2) Undigested PCR products indicating the occurrence of mutation were extracted using a DNA Gel Extraction Kit (QIAGEN) after agarose gel electrophoresis, and re-amplified to concentrate PCR products containing FnCas12a-mediated mutations. (3) PCR products derived from four independent calli were mixed in equal amounts. (4) Multiplex identifiers-labeled PCR products were sequenced on an Illumina MiSeq platform at FASMAC Co. (Japan). Mutations detected on fewer than 50 reads and at locations that were not around the target region were considered false positives due to PCR errors and were excluded from analysis. All primers for PCR are listed in **Supplementary Table 1**. The sequence data have been deposited with the DDBJ Sequence Read Archive (DRA) under accession number DRA010861.

RESULTS

Effect of Guide Sequence Length on Mutation Frequency

The length of the crRNA of FnCas12a is generally 43-nt, comprising a 24-nt guide sequence that is complementary to the target DNA sequence and a 19-nt scaffold sequence (Zetsche et al., 2015). To investigate whether the length of guide sequence of crRNA affects targeted mutation efficiency in rice, we designed FnCas12a/crRNA vectors expressing crRNAs with 24-nt (middle), 18-nt (short), and 30-nt (long) guide sequences (**Supplementary Figure 1**). We selected two target sites in the rice *DROOPING LEAF* (*DL*) gene (**Table 1**). FnCas12a/crRNA vectors were transformed into rice calli via *A. tumefaciens* strain EHA105, and mutations were detected by CAPS analysis (**Figure 1**). In DL-1_Middle transformed calli, undigested DNA fragments, indicating the presence of mutation, were rarely detected (**Figure 1A**, middle panel). To estimate the mutation frequencies in independent transgenic calli, PCR products derived from calli lines #5 and #8 were cloned into plasmids and sequenced, showing that mutation frequencies in these lines were 4.1 and 8.3%, respectively (**Figure 1A**, middle panel). In contrast, when DL-1_Short was used, undigested DNA fragments were clearly detected in all transgenic calli, and mutation frequencies at the DL-1 target site were higher (up to 96.8% in callus line #2) than that of DL-1_Middle (**Figure 1A**, upper panel). The mutation frequency of DL-1_Long was comparable to that of DL-1_Middle (**Figure 1A**, lower panel). In the case of another target site, DL-2, the mutation frequencies of DL-2_Short were also higher than those of DL-2_Middle and DL-2_Long (**Figure 1B**). These results show that the use of crRNA with a shortened guide sequence at the DL-1 and DL-2 target sites could improve FnCas12a-mediated genome editing efficiency. To further investigate the effect of guide sequence length on mutation frequency, we selected additional eight target sites in five genes, *DL*, *ACETOLACTATE SYNTHASE* (*ALS*), *LOW CADMIUM* (*LCD*), *INDOLE-3-ACETALDEHYDE OXIDASE2* (*AAO2*), and *9-CIS-EPOXYCAROTENOID DIOXYGENASE1* (*NCED1*), and assessed their mutation frequencies (**Figure 4A**, **Supplementary Figures 2**–**4**, **9A**). A summary of mutation frequency at each target site is shown in **Table 2**. In 4 out of 10 target sites (DL-1, DL-2, AAO2-1, and NCED1-1), using shortened guide sequences led to the highest mutation frequencies. On the other hand, in two target sites (ALS-1 and ALS-2), longer guide sequences improved mutation frequency compared with the middle guide sequence. For the other four target sites, the middle guide sequences showed the highest mutation frequencies, or we detected no mutations in all transgenic calli. These results suggest that FnCas12a-mediated mutation frequency could be improved by changing the length of the guide sequence. Previous *in vitro* experiments showed that FnCas12a could cleave the target DNA with crRNAs with a 16–30 nt guide (Zetsche et al., 2015; Lei et al., 2017), consistent with our *in vivo* results. We next investigated whether a guide sequence longer than 30 nt could further improve mutation frequencies *in vivo*. We designed four very-long-crRNAs with a 45-nt guide sequence at the *DL* gene (**Supplementary Table 3**). In CAPS assay, undigested DNA fragments were clearly detected in DL-2 and DL-3 target sites, meaning that very-long-crRNAs were functional in these target sites (**Supplementary Figure 5**). The mutation frequencies in DL-2 and DL-3 sites using very long guide sequences were 19.3 and 53.1%, respectively, i.e., slightly lower than frequencies achieved using middle guide sequences (**Table 2**). These results suggest that FnCas12a can work using crRNA with various lengths of guide sequence in plants.

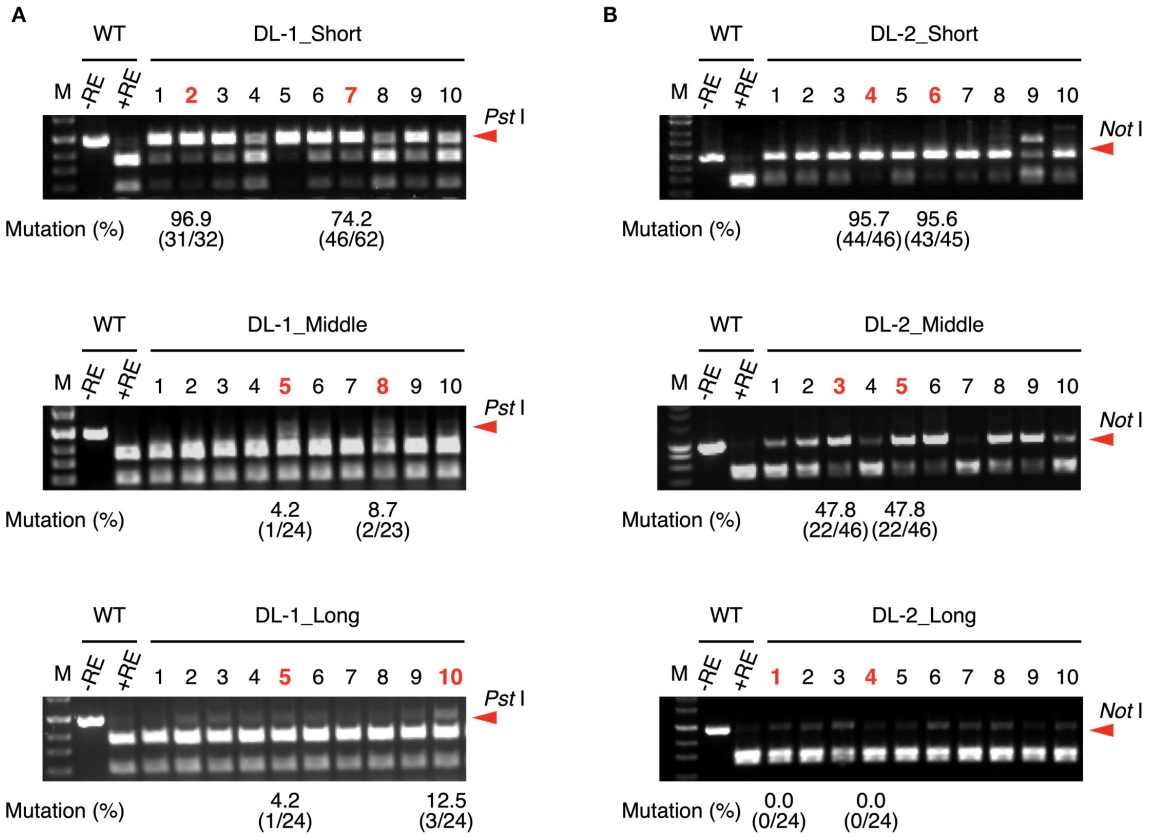

FIGURE 1 | CAPS analysis and mutation frequency using crRNA with guide sequences of different lengths at DL-1 **(A)** and DL-2 **(B)** target sites. Mutation frequencies of selected calli (shown in red) were calculated from the ratio of sequenced clones with mutation. M, DNA molecular weight; –RE, without restriction enzyme; +RE, with restriction enzyme. Red arrowheads indicate the position of undigested PCR fragments.

Analysis of Mutation Patterns Induced by Different Lengths of Guide Sequence

Next, we examined the effect of guide sequence length on mutation pattern. We investigated deletion size at DL-1 and DL-2 target sites by amplicon deep sequencing analysis (**Figure 2**). In DL-1_Middle and DL-1_Long, deletions of <31 bp accounted for more than 90%, and large deletions (≥31 bp) were rarely detected (**Figure 2A**, **Supplementary Figure 7A**). On the other hand, in DL-1_Short, large deletions were generated at a high frequency (38.9%) (**Figure 2A**). At the DL-2 target site, large deletions were also detected at high frequency in DL-2_Short (38.0%) compared with DL-2_Middle (6.6%) and DL-2_Long (4.1%) (**Figure 2B**, **Supplementary Figure 7B**). We also analyzed the deletion size in other target sites: ALS-1, ALS-2, and AAO2-1. Although the differences were less clear than in DL-1 and DL-2, the proportion of large deletions at these target sites also increased when using shorter guide sequences compared with middle and long guides (**Supplementary Figures 6**, **7**). These results indicate that the use of short guide sequences tended to induce large deletions compared with those induced by middle and long guides. We next focused on the position of the deleted nucleotides. To investigate the frequency of deletion at each position of the target region, we collected deletion mutations from the NGS data and examined the frequency of deletion, which is the percentage of deletions at each position among all deletion mutations (**Figure 3**, **Supplementary Figure 8**). In DL-2 target sites, frequencies of deletion at 18–23 bp downstream of the PAM were >50% among the deletion mutations detected using all short, middle, and long guides (**Figure 3A–C**). In the case of the short guide, the frequency of deletion of nucleotides located at 24–51 bp downstream of PAM was ≥31% (**Figure 3A**). On the other hand, when using middle and long guides, the frequency of deletion in this region reduced gradually as the distance increased (**Figures 3B**,**C**). A similar result was obtained with DL-1 (**Supplementary Figure 8**). These results show that the large deletions detected using the short guide were due mainly to deletions in the region downstream of PAM.

Off-Target Analysis Using Short and Long Guides

To investigate the effect of guide sequence length on off-target mutations, we focused on the *AAO* and *NCED* gene families (Tan et al., 2003; Hirano et al., 2008; Endo et al., 2016). We

TABLE 2 | Mutation frequencies using crRNA with different lengths of guide sequences.

Target site	Mutation frequency (%)				Sequence
	Short (18 nt)	Middle (24 nt)	Long (30 nt)	Very long (45 nt)	
DL-1	**81.9**	6.4	8.3	*	**Table 1**, **Supplementary Table 3**
DL-2	**95.6**	47.8	0.0	19.3	**Table 1**, **Supplementary Table 3**
DL-3	4.3	**85.4**	*	53.1	**Supplementary Table 3**
DL-4	8.2	**21.3**	*	*	**Supplementary Table 3**
ALS-1	20.0	46.8	**88.4**		**Supplementary Table 3**
ALS-2	63.4	78.3	**93.5**		**Supplementary Table 3**
LCD-1	0.0	*	*		**Supplementary Table 3**
LCD-2	*	*	*		**Table 3**
AAO2-1	**75.8**	41.0	32.8		**Supplementary Table 3**
NCED1-1	**25.0**	20.0	18.8		**Supplementary Table 3**

**Undigested DNA fragments were not detected in all transgenic line in CAPS assay.*
The highest mutation frequencies among the different guide lengths are shown in bold.

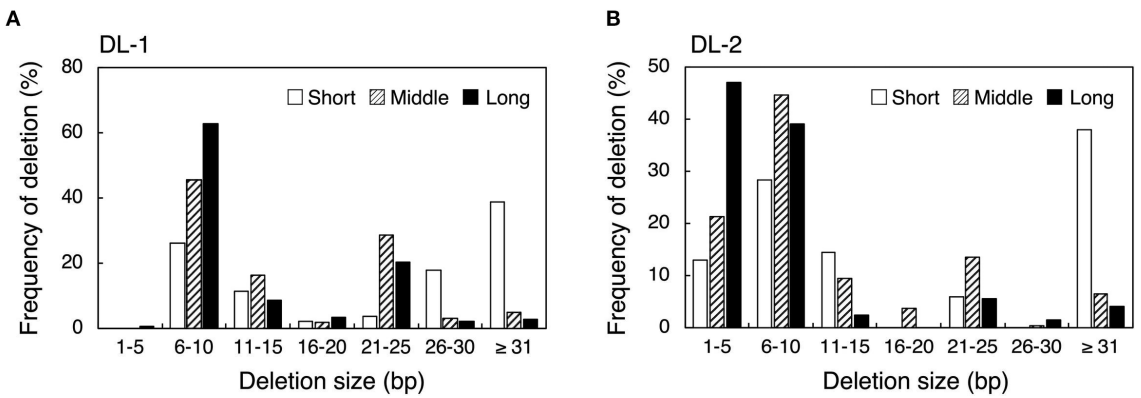

FIGURE 2 | Comparison of deletion sizes using crRNA with guide sequences of different lengths at DL-1 **(A)** and DL-2 **(B)** target sites. Deletion size and mutation number were detected by targeted amplicon sequencing. Frequency of deletion means the percentage of deletions within the range of each deletion size per total number of deletion mutations.

designed target sites in *AAO2* and *NECD1* genes as on-target (**Table 3**, **Supplementary Table 4**). The *AAO* gene family has three off-target candidate sites that have 1- or 2-nt mismatched sequence compared with the AAO2-1 guide sequence (AAO_off-1 to -3) (**Table 3**). We analyzed the mutation frequencies in these target sites by CAPS and sequence analysis (**Figure 4**). The mutation frequencies of the top two independent calli at on-target sites in *AAO2* were 67.7 and 83.8% in AAO2-1_Short, 23.3 and 58.1% in AAO2-1_Middle, and 22.5 and 43.3% in AAO2-1_Long, respectively (**Figure 4A**). On the other hand, at the off-target candidate sites (AAO_off-1 to -3), no undigested PCR fragments were detected for any guide length, meaning no mutation at these sites (**Figure 4B**, **Supplementary Figure 9**). *NCED2* and *NCED3* genes have 2-nt or 3-nt mismatched off-target candidate sites (NCED_off-1 and NCED_off-2) of NCED1-1 guide (**Supplementary Table 4**). Similar to the result of on- and off-target mutation analyses in the *AAO* gene family, mutations were clearly detected at the *NCED1* on-target site using NCED1-1_Short, _Middle, and _Long, and we could not detect any undigested fragment at the off-target candidate sites, even in NCED1-1_Short, by CAPS analysis (**Supplementary Figure 10**). Finally, we checked the genotypes of regenerated plants expressing AAO2-1_Short, AAO2-1_Long, NCED1-1_Short, and NCED1-1_Long, respectively, and no regenerated plants with off-target mutations were obtained (**Supplementary Table 5**). These results indicate that, while changing the length of the guide sequence could improve the mutation frequencies of on-target sites, it appears to have little effect on the accuracy of target sequence recognition of FnCas12a

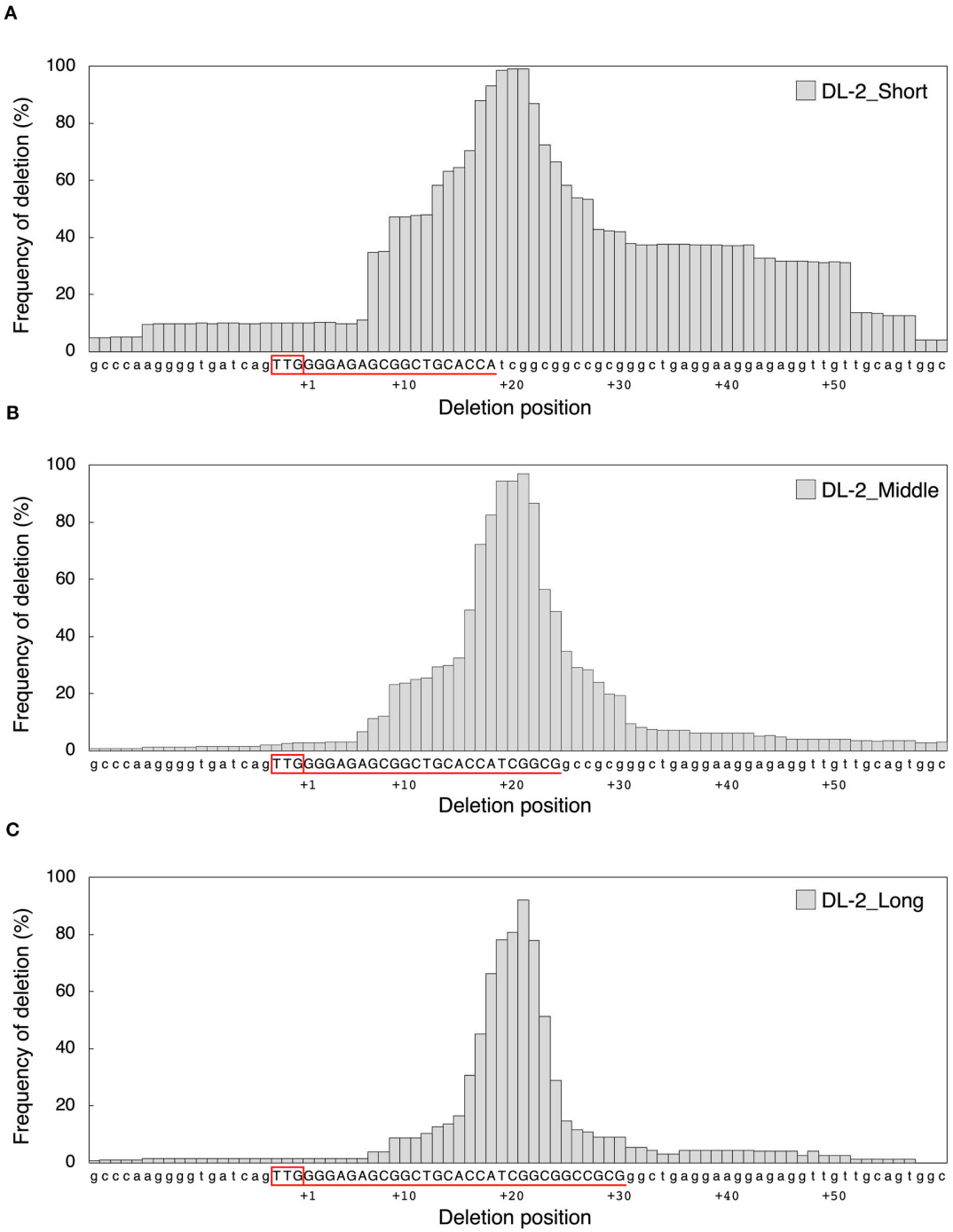

FIGURE 3 | Comparison of deletion position according to the **(A)** DL2-Short, **(B)** DL-2_Middle, and **(C)** DL-2_Long guides at DL-2 target sites. Deletion size and mutation number were detected by targeted amplicon sequencing. Frequency of deletion means the percentage of deletions in each position among all deletion mutations. The target sequence of each guide is shown in red, underlined, and in capital letters. The PAM sequence is boxed in red upstream of the target sequence.

DISCUSSION

In this study, we selected 10 target sites in five rice genes and showed that FnCas12a-mediated mutation efficiency could be improved by using different lengths of guide sequences. We detected mutations at eight target sites when using crRNA containing middle guide (24-nt). In four of the eight target sites (DL-1, DL-2, AAO2-1, and NCED1-1), short guide showed high mutation frequencies compared with middle guide (**Figures 1**, **4**). On the other hand, using long guide

improved mutation frequencies at the ALS-1 and ALS-2 sites (**Supplementary Figure 3**). These results suggest that, for efficient genome editing, an optimal length exists for each gene or target sequence. It would be useful if we could predict the best guide length *in silico*. Therefore, the secondary structure and GC contents of the crRNA were investigated for target sites whose mutation frequencies were improved by changing the length of the guide sequence (**Supplementary Tables 6**, **7**). However, we were unable to find any relationship between these factors and mutation frequencies in our study. Previous studies have revealed that extension and modification of the 5′ and 3′ ends of the crRNA enhance the efficiency of AsCas12a-mediated genome editing in human cells (Moon et al., 2018; Park et al., 2018). These studies, together with our findings, emphasize the importance of designing crRNAs of appropriate length for each target sequence to further improve genome editing efficiency by FnCas12a. It has also been reported that the ability of Cas12a to self-process crRNA can be used to modify the crRNA expression vectors and improve the efficiency of multiple gene editing in plants (Tang et al., 2019; Xu et al., 2019). Combining these methods with our results may enable efficient multi-gene modification by FnCas12a.

TABLE 3 | Target sequences of AAO2-1 on-target site and off-target candidate site.

Target site	crRNA	PAM	On- or off-target sequence
AAO2-1	AAO2-1_Short	TTG	GCAATGCTGTGTCATATG
	AAO2-1_Middle		GCAATGCTGTGTCATATG TTAATT
	AAO2-1_Long		GCAATGCTGTGTCATATG TTAATTCTGCAT
AAO_off-1	–	TTG	GCAATGCTGTTTCATATG TTAATTCTGCTT
AAO_off-2	–	TTG	GCAATGCTGTTTCATATG TTAATTCTGCTT
AAO_off-3	–	TTG	GCAATGCTGTCTCATATG TGAATTCTGCAT

Red characters indicate mismatched nucleotide of off-target candidate sites.
Underlines at on- or off-target sequence indicate restriction enzyme sites for CAPS assay.

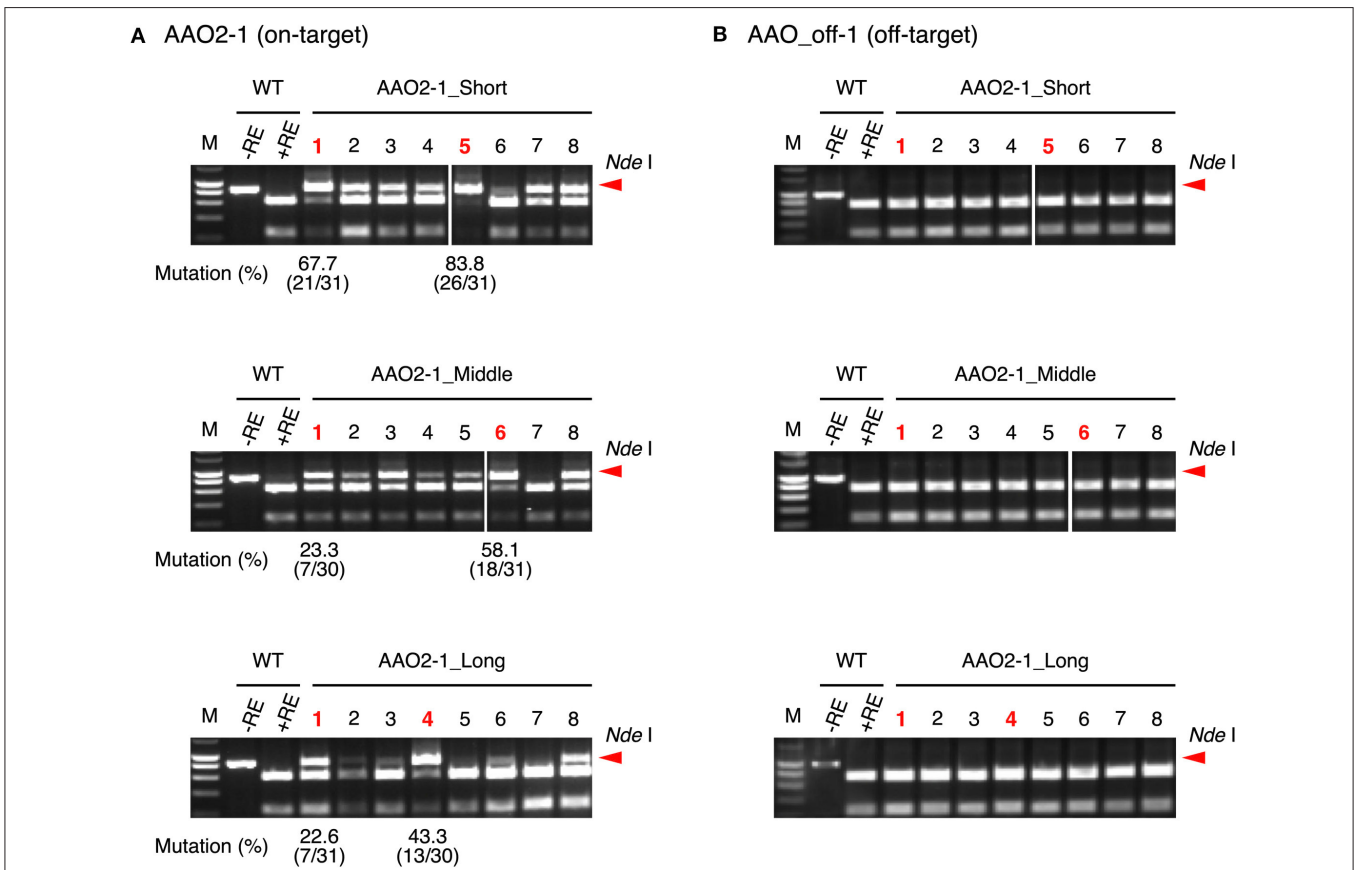

FIGURE 4 | Off-target mutation analysis using CAPS assay at **(A)** AAO2-1 on-target site and **(B)** AAO_off-1 off-target candidate site using crRNA with guide sequences of different lengths. Mutation frequencies of selected calli (shown in red) were calculated from the ratio of sequenced clones with mutation. M, DNA molecular weight; –RE, without restriction enzyme; +RE, with restriction enzyme. Red arrowheads indicate the position of undigested PCR fragments. CAPS images of AAO2-1_Short and AAO2-1_Middle guides in AAO2-1 target site (A: upper and middle sides) and AAO2-1_Short and AAO2-1_Middle guides in AAO_off-1 target site (B: upper and middle sides) were grouping images from different parts of the same agarose gel electrophoresis image, respectively.

Nucleotides 1–20 of the crRNA guide make an RNA–DNA heteroduplex with target DNA strands in AsCas12a and LbCas12a, and it has been suggested that Cas12a orthologs, including FnCas12a, recognize their target DNA region in a similar manner (Yamano et al., 2016, 2017). After forming the complex, FnCas12a introduces a DSB with a 5-nt 5′ overhang generated by cleaving after the 18th base on the non-targeted strand and after the 23rd base on the targeted strand from the PAM (Zetsche et al., 2015). However, Lei and colleagues reported that, when the guide sequence of crRNA was shorter than 20-nt, FnCas12a could cleave after the 14th base on the non-target strand from the PAM, generating longer 5′ overhangs (Lei et al., 2017). We showed that the frequency of large deletions was increased using the 18-nt short guide compared with the middle or long guide (**Figure 2**, **Supplementary Figure 6**), implying the importance of overhang length for deletion size. We also observed an increase in the frequency of deletions away from the PAM when using short guide (**Figure 3**, **Supplementary Figure 8**). It has been reported that SpCas9-RNA molecules remain tightly bound to the PAM-distal region after cleavage (Sternberg et al., 2014; Shibata et al., 2017). Since the DSB produced by FnCas12a was at the end of the target sequence, FnCas12a may continue to bind to the PAM side of the cleaved DNA, preventing DNA degradation at the PAM side.

It has been reported that shortened guide can reduce undesired mutagenesis at off-target sites in SpCas9-mediated genome editing (Fu et al., 2014). Furthermore, the off-target activity of Cas12a orthologs is relatively low compared with that of SpCas9 in human cells and plants (Endo et al., 2016; Kim et al., 2016, 2017; Kleinstiver et al., 2016). Consistent with these results, no mutations were introduced at off-target candidate sites with shortened guide in either rice calli or regenerated plants in our experiments (**Figure 4**, **Supplementary Figure 10**, **Supplementary Table 5**). The knowledge obtained in our study may help provide accurate genome editing with minimal off-target mutations. Further study is needed to clarify the relationship between off-target mutation and the length of guide sequence in FnCas12a-mediated genome editing.

It has been reported that 5′ sticky ends could increase the frequencies of targeted gene insertions and replacements via homologous recombination in the CRISPR/Cas9 paired nickase system (Bothmer et al., 2017). FnCas12a-mediated targeted gene insertions and replacements via homologous recombination have also been reported in rice (Begemann et al., 2017; Li et al., 2018). The FnCas12a-mediated genome editing platform has the potential to provide precise gene targeting with high frequencies. For this purpose, it is important to design effective crRNAs that can generate precise DSB at target sites. Our study results provide a basis for improved FnCas12a-mediated gene targeting efficiency through high efficiently and precise DSB induction.

DATA AVAILABILITY STATEMENT

The datasets presented in this study can be found in online repositories. The names of the repository/repositories and accession number(s) can be found below: DDBJ BioProject, PRJDB10598.

AUTHOR CONTRIBUTIONS

MM, ST, and ME designed the experiments. MM performed the experiments. KN and MM analyzed the results. KN and ME wrote the manuscript. All authors contributed to the article and approved the submitted version.

FUNDING

This work was supported by the Cabinet Office, Government of Japan, Cross-ministerial Strategic Innovation Promotion Program (SIP) Technologies for Smart Bio-industry and Agriculture (funding agency: Bio-oriented Technology Research Advancement Institution, NARO) to ST and Research Fellowship of the Japan Society for the Promotion of Science for Young Scientists (Grant Number: 16J06425) to MM.

ACKNOWLEDGMENTS

We thank Dr. H.M. Rothnie for English proofreading, Dr. J. Sun (National Agriculture and Food Research Organization, Japan) for helpful advice about data analysis, and members of the Toki Laboratory for technical assistance and discussion.

SUPPLEMENTARY MATERIAL

The Supplementary Material for this article can be found online at: https://www.frontiersin.org/articles/10.3389/fgeed.2020.608563/full#supplementary-material

REFERENCES

Begemann, M., Gray, B., January, E., Gordon, G., He, Y., Liu, H., et al. (2017). Precise insertion and guided editing of higher plant genomes using Cpf1 CRISPR nucleases. *Sci. Rep.* 7:11606. doi: 10.1038/s41598-017-11760-6

Bothmer, A., Phadke, T., Barrera, L., Margulies, C., Lee, C., Buquicchio, F., et al. (2017). Characterization of the interplay between DNA repair and CRISPR/Cas9-induced DNA lesions at an endogenous locus. *Nat. Commun.* 8:13905. doi: 10.1038/ncomms13905

Dang, Y., Jia, G., Choi, J., Ma, H., Anaya, E., Ye, C., et al. (2015). Optimizing sgRNA structure to improve CRISPR-Cas9 knockout efficiency. *Genome Biol.* 16:280. doi: 10.1186/s13059-015-0846-3

Endo, A., Masafumi, M., Kaya, H., and Toki, S. (2016). Efficient targeted mutagenesis of rice and tobacco genomes using Cpf1 from *Francisella novicida*. *Sci. Rep.* 6:38169. doi: 10.1038/srep38169

Endo, M., Mikami, M., Endo, A., Kaya, H., Itoh, T., Nishimasu, H., et al. (2019). Genome editing in plants by engineered CRISPR–Cas9 recognizing NG PAM. *Nat. Plants* 5, 14–17. doi: 10.1038/s41477-018-0321-8

Fonfara, I., Richter, H., Bratovič, M., Rhun, A., and Charpentier, E. (2016). The CRISPR-associated DNA-cleaving enzyme Cpf1 also processes precursor CRISPR RNA. *Nature* 532, 517–521. doi: 10.1038/nature17945

Fu, Y., Sander, J., Reyon, D., Cascio, V., and Joung, J. (2014). Improving CRISPR-Cas nuclease specificity using truncated guide RNAs. *Nat. Biotechnol.* 32, 279–284. doi: 10.1038/nbt.2808

Hendel, A., Bak, R., Clark, J., Kennedy, A., Ryan, D., Roy, S., et al. (2015). Chemically modified guide RNAs enhance CRISPR-Cas genome editing in human primary cells. *Nat. Biotechnol.* 33, 985–989. doi: 10.1038/nbt.3290

Hirano, K., Aya, K., Hobo, T., Sakakibara, H., Kojima, M., Shim, R., et al. (2008). Comprehensive transcriptome analysis of phytohormone biosynthesis and signaling genes in microspore/pollen and tapetum of rice. *Plant Cell Physiol.* 49, 1429–1450. doi: 10.1093/pcp/pcn123

Hu, X., Meng, X., Liu, Q., Li, J., and Wang, K. (2018). Increasing the efficiency of CRISPR-Cas9-VQR precise genome editing in rice. *Plant Biotechnol. J.* 16, 292–297. doi: 10.1111/pbi.12771

Jinek, M., Chylinski, K., Fonfara, I., Hauer, M., Doudna, A., and Charpentier, E. (2012). A programmable dual-RNA-guided DNA endonuclease in adaptive bacterial immunity. *Science* 337, 816–821. doi: 10.1126/science.1225829

Kaya, H., Mikami, M., Endo, A., Endo, M., and Toki, S. (2016). Highly specific targeted mutagenesis in plants using *Staphylococcus aureus* Cas9. *Sci. Rep.* 6:26871. doi: 10.1038/srep26871

Kim, H., Kim, S., Ryu, J., Kang, B., Kim, J., and Kim, S. (2017). CRISPR/Cpf1-mediated DNA-free plant genome editing. *Nat. Commun.* 8:14406. doi: 10.1038/ncomms14406

Kim, Y., Cheong, S., Lee, J., Lee, S., Lee, M., Baek, I., et al. (2016). Generation of knockout mice by Cpf1-mediated gene targeting. *Nat. Biotechnol.* 34, 808–810. doi: 10.1038/nbt.3614

Kleinstiver, B., Tsai, S., Prew, M., Nguyen, N., Welch, M., Lopez, J., et al. (2016). Genome-wide specificities of CRISPR-Cas Cpf1 nucleases in human cells. *Nat. Biotechnol.* 34, 869–874. doi: 10.1038/nbt.3620

Lee, K., Zhang, Y., Kleinstiver, B., Guo, J., Aryee, M., Miller, J., et al. (2019). Activities and specificities of CRISPR/Cas9 and Cas12a nucleases for targeted mutagenesis in maize. *Plant Biotechnol. J.* 17, 362–372. doi: 10.1111/pbi.12982

Lei, C., Li, S., Liu, J., Zheng, X., Zhao, G., and Wang, J. (2017). The CCTL (Cpf1-assisted cutting and Taq DNA ligase-assisted Ligation) method for efficient editing of large DNA constructs *in vitro*. *Nucleic Acids Res.* 45:9. doi: 10.1093/nar/gkx018

Li, B., Zhao, W., Luo, X., Zhang, X., Li, C., Zeng, C., et al. (2017). Engineering CRISPR-Cpf1 crRNAs and mRNAs to maximize genome editing efficiency. *Nat. Biomed. Eng.* 1:0066. doi: 10.1038/s41551-017-0066

Li, J., Norville, J., Aach, J., McCormack, M., Zhang, D., Bush, Z., et al. (2013). Multiplex and homologous recombination–mediated genome editing in *Arabidopsis* and *Nicotiana benthamiana* using guide RNA and Cas9. *Nat. Biotechnol.* 31, 688–691. doi: 10.1038/nbt.2654

Li, S., Li, J., Zhang, J., Du, W., Fu, J., Sutar, S., et al. (2018). Synthesis-dependent repair of Cpf1-induced double strand DNA breaks enables targeted gene replacement in rice. *J. Exp. Bot.* 69, 4715–4721. doi: 10.1093/jxb/ery245

Meng, X., Hu, X., Liu, Q., Song, X., Gao, C., Li, J., et al. (2018). Robust genome editing of CRISPR-Cas9 at NAG PAMs in rice. *Sci. China Life Sci.* 61, 122–125. doi: 10.1007/s11427-017-9247-9

Mikami, M., Toki, S., and Endo, M. (2015). Comparison of CRISPR/Cas9 expression constructs for efficient targeted mutagenesis in rice. *Plant Mol. Biol.* 88, 561–572. doi: 10.1007/s11103-015-0342-x

Mikami, M., Toki, S., and Endo, M. (2017). In planta processing of the SpCas9-gRNA complex. *Plant Cell Physiol.* 58, 1857–1867. doi: 10.1093/pcp/pcx154

Moon, S., Lee, J., Kang, J., Lee, N., Ha, D., Kim, D., et al. (2018). Highly efficient genome editing by CRISPR-Cpf1 using CRISPR RNA with a uridinylate-rich 3′-overhang. *Nat. Commun.* 9, 3651. doi: 10.1038/s41467-018-06129-w

Nekrasov, V., Staskawicz, B., Weigel, D., Jones, J., and Kamoun, S. (2013). Targeted mutagenesis in the model plant *Nicotiana benthamiana* using Cas9 RNA-guided endonuclease. *Nat. Biotechnol.* 31, 691–693. doi: 10.1038/nbt.2655

Park, H., Liu, H., Wu, J., Chong, A., Mackley, V., Fellmann, C., et al. (2018). Extension of the crRNA enhances Cpf1 gene editing in vitro and in vivo. *Nat. Commun.* 9:3313. doi: 10.1038/s41467-018-05641-3

Ryan, D., Taussig, D., Steinfeld, I., Phadnis, S., Lunstad, B., Singh, M., et al. (2018). Improving CRISPR-Cas specificity with chemical modifications in single-guide RNAs. *Nucleic Acids Res.* 46, 792–803. doi: 10.1093/nar/gkx1199

Shan, Q., Wang, Y., Li, J., Zhang, Y., Chen, K., Liang, Z., et al. (2013). Targeted genome modification of crop plants using a CRISPR-Cas system. *Nat. Biotechnol.* 31, 686–688. doi: 10.1038/nbt.2650

Shibata, M., Nishimasu, H., Kodera, N., Hirano, S., Ando, T., Uchihashi, T., et al. (2017). Real-space and real-time dynamics of CRISPR-Cas9 visualized by high-speed atomic force microscopy. *Nat. Commun.* 8:1430. doi: 10.1038/s41467-017-01466-8

Steinert, J., Schiml, S., Fauser, F., and Puchta, H. (2015). Highly efficient heritable plant genome engineering using Cas9 orthologues from *Streptococcus thermophilus* and *Staphylococcus aureus*. *Plant J.* 84, 1295–1305. doi: 10.1111/tpj.13078

Sternberg, S., Redding, S., Jinek, M., Greene, E., and Doudna, J. (2014). DNA interrogation by the CRISPR RNA-guided endonuclease Cas9. *Nature* 507, 62–67. doi: 10.1038/nature13011

Tan, B., Joseph, L., Deng, W., Liu, L., Li, Q., Cline, K., et al. (2003). Molecular characterization of the *Arabidopsis* 9-*cis* epoxycarotenoid dioxygenase gene family. *Plant J.* 35, 44–56. doi: 10.1046/j.1365-313X.2003.01786.x

Tang, X., Lowder, L., Zhang, T., Malzahn, A., Zheng, X., Voytas, D., et al. (2017). A CRISPR-Cpf1 system for efficient genome editing and transcriptional repression in plants. *Nat. Plants* 3:17018. doi: 10.1038/nplants.2017.18

Tang, X., Ren, Q., Yang, L., Bao, Y., Zhong, Z., He, Y., et al. (2019). Single transcript unit CRISPR 2.0 systems for robust Cas9 and Cas12a mediated plant genome editing. *Plant Biotechnol. J.* 17, 1431–1445. doi: 10.1111/pbi.13068

Toki, S. (1997). Rapid and efficient *Agrobacterium*-mediated transformation in rice. *Plant Mol. Biol. Rep.* 15, 16–21. doi: 10.1007/BF02772109

Toki, S., Hara, N., Ono, K., Onodera, H., Tagiri, A., Oka, S., et al. (2006). Early infection of scutellum tissue with *Agrobacterium* allows high-speed transformation of rice. *Plant J.* 47, 969–976. doi: 10.1111/j.1365-313X.2006.02836.x

Wang, M., Mao, Y., Lu, Y., Tao, X., and Zhu, J. (2017). Multiplex gene editing in rice using the CRISPR-Cpf1 system. *Mol. Plant* 10, 1011–1013. doi: 10.1016/j.molp.2017.03.001

Xu, R., Qin, R., Li, H., Li, D., Li, L., Wei, P., et al. (2017). Generation of targeted mutant rice using a CRISPR-Cpf1 system. *Plant Biotechnol. J.* 15, 713–717. doi: 10.1111/pbi.12669

Xu, R., Qin, R., Li, H., Li, J., Yang, J., and Wei, P. (2019). Enhanced genome editing in rice using single transcript unit CRISPR-*Lb*Cpf1 systems. *Plant Biotechnol. J.* 17, 553–555. doi: 10.1111/pbi.13028

Yamano, T., Nishimasu, H., Zetsche, B., Hirano, H., Slaymaker, I., Li, Y., et al. (2016). Crystal structure of Cpf1 in complex with guide RNA and target DNA. *Cell* 165, 949–962. doi: 10.1016/j.cell.2016.04.003

Yamano, T., Zetsche, B., Ishitani, R., Zhang, F., Nishimasu, H., and Nureki, O. (2017). Structural basis for the Canonical and non-Canonical PAM Recognition by CRISPR-Cpf1. *Mol. Cell* 67, 633–645. doi: 10.1016/j.molcel.2017.06.035

Zetsche, B., Gootenberg, J., Abudayyeh, O., Slaymaker, I., Makarova, K., Essletzbichler, P., et al. (2015). Cpf1 is a single RNA-guided endonuclease of a class 2 CRISPR-Cas system. *Cell* 163, 759–771. doi: 10.1016/j.cell.2015.09.038

Conflict of Interest: The authors declare that the research was conducted in the absence of any commercial or financial relationships that could be construed as a potential conflict of interest.

frontiers in Genome Editing

ORIGINAL RESEARCH
published: 11 January 2021
doi: 10.3389/fgeed.2020.622227

Development of a Transformable Fast-Flowering Mini-Maize as a Tool for Maize Gene Editing

Morgan E. McCaw[1,2], *Keunsub Lee*[1,2], *Minjeong Kang*[1,2,3], *Jacob D. Zobrist*[1,2,4], *Mercy K. Azanu*[1,2,3], *James A. Birchler*[2,5] *and Kan Wang*[1,2]*

[1] *Department of Agronomy, Iowa State University, Ames, IA, United States,* [2] *Crop Bioengineering Center, Iowa State University, Ames, IA, United States,* [3] *Interdepartmental Plant Biology Major, Iowa State University, Ames, IA, United States,* [4] *Interdepartmental Genetics and Genomics Major, Iowa State University, Ames, IA, United States,* [5] *Division of Biological Sciences, University of Missouri, Columbia, MO, United States*

Maize (*Zea mays* ssp. *mays*) is a popular genetic model due to its ease of crossing, well-established toolkits, and its status as a major global food crop. Recent technology developments for precise manipulation of the genome are further impacting both basic biological research and biotechnological application in agriculture. Crop gene editing often requires a process of genetic transformation in which the editing reagents are introduced into plant cells. In maize, this procedure is well-established for a limited number of public lines that are amenable for genetic transformation. Fast-Flowering Mini-Maize (FFMM) lines A and B were recently developed as an open-source tool for maize research by reducing the space requirements and the generation time. Neither line of FFMM were competent for genetic transformation using traditional protocols, a necessity to its status as a complete toolkit for public maize genetic research. Here we report the development of new lines of FFMM that have been bred for amenability to genetic transformation. By hybridizing a transformable maize genotype high Type-II callus parent A (Hi-II A) with line A of FFMM, we introgressed the ability to form embryogenic callus from Hi-II A into the FFMM-A genetic background. Through multiple generations of iterative self-hybridization or doubled-haploid method, we established maize lines that have a strong ability to produce embryogenic callus from immature embryos and maintain resemblance to FFMM-A in flowering time and stature. Using an *Agrobacterium*-mediated standard transformation method, we successfully introduced the CRISPR-Cas9 reagents into immature embryos and generated transgenic and mutant lines displaying the expected mutant phenotypes and genotypes. The transformation frequencies of the tested genotypes, defined as the numbers of transgenic event producing T1 seeds per 100 infected embryos, ranged from 0 to 17.1%. Approximately 80% of transgenic plants analyzed in this study showed various mutation patterns at the target site. The transformable FFMM line, FFMM-AT, can serve as a useful genetic and genomic resource for the maize community.

Keywords: ***Agrobacterium*-mediated transformation, CRISPR, embryogenic callus, gene editing, transgenesis, *Zea mays***

OPEN ACCESS

Edited by:
Feng Zhang,
University of Minnesota Twin Cities, United States

Reviewed by:
Gunvant B. Patil,
Texas Tech University, United States
Qiudeng Que,
Syngenta, United States

***Correspondence:**
Kan Wang
kanwang@iastate.edu

Specialty section:
This article was submitted to Genome Editing in Plants, a section of the journal Frontiers in Genome Editing

Received: *28 October 2020*
Accepted: *26 November 2020*
Published: *11 January 2021*

Citation:
McCaw ME, Lee K, Kang M, Zobrist JD, Azanu MK, Birchler JA and Wang K (2021) Development of a Transformable Fast-Flowering Mini-Maize as a Tool for Maize Gene Editing. Front. Genome Ed. 2:622227. doi: 10.3389/fgeed.2020.622227

INTRODUCTION

Recent years have ushered in rapid advances in precise gene editing technologies such as clustered regularly interspaced short palindromic repeats (CRISPR)-Cas systems (Jinek et al., 2012; Zetsche et al., 2015). The advent of gene editing has placed increased importance on the ability to genetically transform plants. Methods of plant transformation and their difficulty differ greatly between species; what works well for one species may not work at all in other species. In maize, the most successful methods have traditionally relied on transformation of embryogenic callus derived from the scutellum of immature zygotic embryos (IZEs). Although this method has been widely used in maize transformation, few inbred maize lines are capable of readily producing embryogenic callus that can be transformed and regenerated into plants.

Maize embryogenic callus has been traditionally classified as either Type-I: hard, compact, and relatively slow growing; or Type-II: highly friable, relatively fast growing, and with abundant somatic embryos (Tomes and Smith, 1985). Type-I callus response is typically induced by a Murashige and Skoog (MS) based medium and is more common than Type-II. B104 is a popular line for Type-I transformation (Frame et al., 2006; Raji et al., 2018), due to its high percentage (∼60%) of genetic similarity to B73 (Liu et al., 2003), which was used to produce the first maize reference genome (Schnable et al., 2009). Success has also been reported in A188 and H99 (Ishida et al., 2003), B114 and Ky21 (Frame et al., 2006) as well as a number of tropical lines (Carvalho et al., 1997; Bohorova et al., 1999; Valdez-Ortiz et al., 2007; Anami et al., 2010; Ombori et al., 2013). Type-II callus in maize is typically induced by an N6-based medium and was originally derived from embryos of A188 or B73 × A188 hybrids (Armstrong and Green, 1985; Tomes and Smith, 1985). A maize genotype with a high Type-II callus induction rate (Hi-II) is one of the most popular and user-friendly lines for transformation (Armstrong et al., 1991). The Hi-II system is a hybrid formed by a cross of lines "Parent A" and "Parent B". These lines were selected from two independent F2 embryos of an A188 × B73 hybrid with the ability to generate Type-II callus. The regenerant seed (R1) plants were then grown and tested for ∼100% Type-II callus formation in half ears and the remaining R2 seed from two plants of each embryo lineage were used to produce sib populations that comprise "Parent A" and "Parent B" (Armstrong et al., 1991).

Fast-Flowering Mini-Maize (FFMM) was developed to accelerate maize genetic research by reducing the long generation time and substantial space requirements of maize (McCaw et al., 2016). Two independent inbred lines, FFMM-A and FFMM-B, were generated using single-seed descent from a modified double-cross hybrid of four early flowering lines. Both lines can go from seed-to-seed in 60 days, producing 5–6 generations per year as compared to the 2–3 generations in traditional lines. Both FFMM lines also require less growth substrate per plant and about four plants can be grown in the same footprint of a traditional maize plant. FFMM also performs well in inexpensive, modular growth chamber setups, which makes it more accessible to researchers without access to greenhouses (Tran and Braun, 2017). FFMM plants are short enough to grow on stackable shelves with a proper lighting system. The original FFMM lines are not capable of genetic transformation by traditional protocols, though they work very well with the QuickCorn Babyboom/Wuschel morphogenic genes technology (Lowe et al., 2016, 2018; Jones et al., 2019; Masters et al., 2020). This morphogenic gene technology, while effective, does have some limitations such as large construct size and restrictive licensing options. The ability to transform FFMM through traditional methods completes this germplasm as an open-source tool for maize genetics research. In this work, we report the breeding and tissue culture efforts toward generation of FFMM lines with a robust ability to produce embryogenic callus from IZEs. We then demonstrate that these lines can be transformed using an *Agrobacterium*-mediated standard transformation method for efficient targeted mutagenesis by a CRISPR-Cas9 system.

MATERIALS AND METHODS

Germplasm Availability, Development, and Greenhouse Care

Fast-Flowering Mini-Maize A (FFMM-A, McCaw and Birchler, 2017) and maize haploid inducer line RWS-GFP (Yu and Birchler, 2016) can be obtained from James A. Birchler at the University of Missouri. Maize high Type-II Parent A (Hi-II A, Armstrong et al., 1991) can be obtained from the Maize Genetics Cooperation Stock Center (http://maizecoop.cropsci.uiuc.edu/).

FFMM-AT lines were generated through introgression of competency to form embryogenic callus in tissue culture from Hi-II A into the FFMM-A genetic background. All plants were grown in a greenhouse set to 28°C, 16 h day/25°C, 8 h night in a soilless substrate (Promix BR or Sun Gro LC1) as described previously (McCaw and Birchler, 2017). Seeds were started in seedling flats to germinate for 9–10 days with only deionized (DI) water supplemented. Once established, the plantlets were moved to 1 gallon pots supplemented with 0.66 g 10% iron chelate (Grow More Inc., CA, USA) and watered to ∼50% soil saturation with a 15-5-15 (N-P-K) fertilizer at 200 ppm nitrogen whenever the soil was dry ∼2 cm below the surface. Once a tassel was visible in the whorl (∼26 days) they were switched back to DI water and kept between ∼50–75% soil saturation.

To achieve a well-pollinated ear, ear shoots were bagged when flag leaves emerge and tended every day to trim flag leaves and watch for silks. Shoot bags were marked on the 1st day of silking and silks were trimmed on the second day and re-covered with the top of the bag folded to indicate the cut. Pollination was performed on the following morning as previously described (McCaw, 2017).

After pollination, watering with fertilizer resumes and plants were kept well-watered. Watering was ceased 23 days after pollination (DAP) and the ears were de-husked while still attached to plants to facilitate drying and to reduce mold. Once the seed was dry enough that the endosperm could not be marred by a thumbnail (∼30 DAP) the ear was harvested and dried in a seed dryer or sunny part of the greenhouse.

Doubled Haploid

Doubled haploid (DH) lines were produced from F1 seeds of reciprocal crosses between two FFMM-AT lines, AT1 self-generation 4 (self-4, 91% Type-II callus) × AT4R self-3 (regenerated from callus of a self-2 ear that produced 66% Type-II callus). Seed from these F1 crosses were grown and crossed as a female by RWS-GFP, a haploid inducer line carrying an EGFP driven by 2x Cauliflower Mosaic Virus (CaMV) 35S promoter to facilitate identification of haploids (Röber et al., 2005, Yu and Birchler, 2016). Immature embryos were harvested 9–10 DAP for haploid doubling using two different methods described below.

Embryo Rescue Doubling (ERD)

For lines ATDH1 and ATDH4, embryos were plated embryo axis-side down, scutellum-side up onto a MS Rooting Medium supplemented with colchicine (Barton et al., 2014) that blocks spindle fiber formation during mitosis to cause genome doubling (**Supplemental Material**). Embryos were incubated in the dark at 28°C for ∼24 h. All embryos were then moved to the MS Rooting Medium without colchicine and with the embryo axis-side up, scutellum-side down, to encourage the embryo to germinate. After 3–5 days incubation in the dark at 28°C, embryos were checked for GFP expression in a dark room using a NIGHTSEA BlueStar flashlight and filter glasses (NIGHTSEA, MA, USA). GFP positive (diploid) embryos were discarded and GFP negative (haploid) embryos were allowed to continue germinating. Once the coleoptile was about 2 cm long, the germinating embryos were buried upright in a sundae cup (Solo SD-12) containing the MS Rooting Medium, with just the tip of the coleoptile protruding from the MS Rooting Medium. The corresponding lids were sealed to the sundae cups and the germinating embryos were moved to a lighted biological incubator (28°C, 16 h day, 8 h night, 20-150 μmol/m^2/s) to root. Once roots and leaves were established, the plants were transplanted to soil in a similar manner as a regenerated plantlet from transformation as described later. Doubled haploid plants showed restored fertility throughout the whole tassel and were self-pollinated to produce ears.

Haploid Callus Spontaneous Doubling (HCSD)

Line ATU1 was generated by plating embryos directly on Callus Development Medium (605J, **Supplemental Material**, Lowe et al., 2016) with the scutellum-side up and incubating in the dark at 28°C. After 3–5 days the embryos were screened for GFP expression using a NIGHTSEA Bluestar flashlight and filter glasses and GFP expressing diploid embryos were discarded. Haploid embryo callus was transferred to fresh 605J medium after 2 weeks, and incubated for additional 2 weeks. Plantlets were regenerated using Shoot Formation Medium (289O) as described (**Supplemental Material**, Lowe et al., 2016). Shoots were transferred to the MS Rooting Medium described above in a lighted biological incubator (28°C, 16 h day, 8 h night, 20–150 μmol/m^2/s) until leaves and roots developed. Rooted plants were then transferred to soil as described in the transformation section below. Regenerated plantlet clones showed good fertility restoration in the tassels and were sib-crossed to produce seeds.

Construct and *Agrobacterium* Strain

The CRISPR-Cas9 construct, pKL2013 (**Supplementary Figure 1**), was made by inserting a red fluorescent protein marker (mCherry) from pPT5 (Lee et al., 2019a) into A844B, which contains a gRNA targeting the maize *Glossy2* gene (Lee et al., 2019b). The mCherry cassette (CaMV 35S promoter-mCherry-Tvsp terminator) was PCR amplified from pPT5 using the primers P35S-F1 (5′-CCTTAATTAAGGGAAGACCAAAGGGCTATTGAGA-3′) and Tvsp-R1 (5′-TCCGCGATCGCCGCTTATTGCACTCCCTTTT-3′), and digested with *Pac*I and *Pvu*I (NEB, MA, USA). A844B was digested with *Pac*I and treated with thermosensitive alkaline phosphatase according to the manufacturer's instruction (Promega, WI, USA), and purified using the QIAquick PCR purification kit (Qiagen, Hilden, Germany). Ligation was performed using the T4 DNA ligase (NEB) with 50 ng of the digested A844B DNA and 15 ng the mCherry cassette in 10 μl of total reaction volume. After incubating for 15 min at 25°C, 3 μl of the ligation mixture was used for *E. coli* transformation (DH5α) using a heat shock method (Froger and Hall, 2007). Plasmid DNA was isolated using the QIAprep Spin Miniprep kit (Qiagen) and sequenced using primers pKL2013-F1 (5′-Tgaattcgacccagctttct-3′) and pKL2013-R1 (5′-tgtggaattgtgagcggata-3′) to verify the insertion of the mCherry cassette.

Agrobacterium strain LBA4404Thy- (Ranch et al., 2010) harboring a plasmid PHP71539 (Anand et al., 2018) was obtained from Corteva Agriscience Inc. This strain is a thymidine auxotrophic *Agrobacterium* strain that can only survive in media supplemented with thymidine (Ranch et al., 2010). The plasmid PHP71539 (Anand et al., 2018) carries extra sets of *Agrobacterium* virulence (*vir*) genes that can further enhance the *Agrobacterium*'s T-DNA transfer ability. We introduced pKL2013 into the *Agrobacterium* strain via electroporation as previously described (Mattanovich et al., 1989). After 2-day incubation at 28°C, *Agrobacterium* colonies appeared on the solid Yeast Extract Peptone medium (YP) amended with 30 mg/L gentamicin, 50 mg/L kanamycin, and 50 mg/L thymidine. Two single colonies were grown in 10 mL of liquid YP medium containing 30 mg/L gentamicin, 50 mg/L kanamycin, and 50 mg/L thymidine for 20 h at 28°C with a shaking at 200 rpm and the plasmid DNA was extracted using the QIAprep Spin Miniprep kit (Qiagen). Extracted plasmid DNA from the *Agrobacterium* cells and the original pKL2013 DNA from *E. coli* were digested with *Hin*dIII and *Pvu*I (NEB) and resolved by 1% Agarose gel electrophoresis to confirm the presence and stability of pKL2013 within LBA4404Thy- cells.

Maize Transformation

FFMM-AT transformation experiments for delivery of the construct carrying CRISPR reagents were carried out using standard transformation protocol similar to Hi-II genotype described previously (Wang and Frame, 2004) with modifications. Briefly, the media of Wang and Frame (2004) were replaced with the following media (**Supplementary Material**): Liquid Infection Medium (700A), Cocultivation Medium (562V), Callus Development Medium (605J or 605T), Selection Media I and II, and Shoot Formation

Medium (289O plus 3 mg/L bialaphos) per Lowe et al. (2016), Jones et al. (2019) and Masters et al. (2020).

Immature embryos of 1.5 mm average length were dissected and transferred into 700A Liquid Infection Medium in a 1.5 mL Eppendorf tube (up to 100 embryos/mL). For infection, the 700A liquid was replaced with 1 mL of *Agrobacterium* culture ($OD_{600} = 0.4$) that was suspended in the 700A liquid medium supplemented with 100 μM acetosyringone (AS). The embryos were infected for ∼5 min at room temperature before the embryos and the liquid culture were transferred onto 562V Cocultivation Medium. Afterwards any excess *Agrobacterium* culture was removed, and the embryos were oriented scutellum-side up. The plates were wrapped with parafilm and incubated at 20°C in the dark for 3 days. After cocultivation, embryos were transferred to 605T Resting Medium and incubated for 7–10 days to begin callus initiation. Next, embryos were transferred to Selection I Medium (605J plus 3 mg/L bialaphos) and incubated at 28°C in the dark. After 2 weeks, callus pieces were transferred to Selection II Medium (605J plus 6 mg/L bialaphos) for continued selection and callus growth. Rapidly growing calli were transferred with about 6–8 calli per plate to give room for growth. Friable callus pieces were separated and put in contact with the medium. These calli were then incubated for additional 2–3 weeks in the dark at 28°C.

After selection, healthy-looking callus was evaluated with a NIGHTSEA dual fluorescent protein flashlight and RFP filter glasses. Both RFP-positive and RFP-negative healthy calli were identified and placed on Shoot Formation Medium (289O plus 3 mg/L bialaphos). These calli were incubated in the dark at 28°C for 7 days then moved to the lighted chamber described above. Within 1–2 weeks, developing shoots were transferred to MS Rooting Medium (plus 2 mg/L bialaphos). To ensure good root formation, remnant callus materials surrounding the base of the shoot were removed before the shoots were buried in MS Rooting Medium. For successful outcrossing, pollen donor seeds were planted about 9 days after the plantlets were moved to MS Rooting Medium.

Once the plants grew a total of about 7 cm of root length (either in one root or several lengths added up but not counting hair-fine roots) they were removed from medium, the roots were washed off with water, and transferred to soil (**Supplementary Material**). Multiple connected plantlets growing from a single piece of callus were gently teased apart for separate planting. Plantlets with one or two leaves and a good start to roots were transferred to a minimal amount of soilless substrate that was kept moist but not soaked to encourage root growth. Plantlets were covered with a humidity dome and moved to a growth chamber set to 26°C 16 h/8 h day night cycle or to the greenhouse. During the first 5–8 days in soil the plants remained covered with a humidity dome to avoid desiccation due to changing conditions.

Once established, plantlets were moved to 3 inch (7.6 cm) square nursery pots and watered with fertilizer as described above until a tassel became visible. Some plants flowered in these square nursery pots but some outgrew those pots and were moved to larger half-gallon or gallon (3.7-liter) size nursery pots before maturing. Before flowering, ear shoots were bagged similarly to seed grown plants using half shoot bags, but tassels were not covered and silks were not cut because they tended not to regrow. To pollinate, the tips of shoot bags were cut and pollen was poured onto the silks. The shoot bag was then folded over and covered by a second half shoot bag because the plants were generally not sturdy enough to hold a half tassel bag. T0 plants were also reciprocally crossed with individuals started from seed.

To prevent mold caused by unusually moist conditions within ears of regenerated plants, ears were dehusked at 11–12 DAP while remaining attached to the plant to mature, while seed-grown wild type female plants were treated per the normal protocol described above. Plants were watered until 23–25 days after pollination, then watering was ceased, and plants and seed were dried down as described above.

Genotyping

Genomic DNA (gDNA) was extracted from maize leaf tissues using a previously published protocol (Edwards et al., 1991). About ∼2 cm^2 of fresh leaf tissue was ground in a 1.5 mL tube containing 500 μl of DNA extraction buffer (Edwards et al., 1991) with 100 μg/mL PureLink RNase A (Thermo Fisher Scientific, MA, USA), using a polypropylene homogenizing pestle attached to a cordless drill. After grinding for 10–15 s, an equal volume of chloroform (500 μL) was added to each tube and mixed thoroughly by gently inverting the tubes for 2 min. Sample tubes were centrifuged for 5 min at 21,130 × g and 300 μL of the aqueous phase was carefully transferred to a new 1.5 mL tube. To precipitate gDNA, 200 μL of isopropanol was added and thoroughly mixed by gentle inversions. gDNA was pelleted by centrifugation for 5 min and washed once with 500 μL of 80% ethanol and air dried for 10 min at room temperature. About 30–50 μL of ultrapure water was added to each tube and the gDNA concentration was quantified using the NanoDrop 1000 Spectrophotometer (Thermo Fisher Scientific, MA, USA) and adjusted to 50 ng/μL.

Genotyping analysis of *gl2* was performed by Sanger sequencing and trace data analyses using the Tracking of Indels by DEcomposition (TIDE, Brinkman et al., 2014) and Inference of CRISPR Edits (ICE, Hsiau et al., 2018). Briefly, an ∼1 kb region of *gl2* was PCR amplified using the Phusion high-fidelity DNA polymerase (NEB), primers Zm-gl2-F2 and Zm-gl2-R2 (Lee et al., 2019b), and about 50 ng of gDNA. Two pairs of primers were also used to screen for the presence of the T-DNA in the transgenic plants: zCas9-F1 and zCas9-R1 (Lee et al., 2019b) for the CRISPR-Cas9 and bar-RT-F5 and bar-RT-R5 (Testroet et al., 2017) for the *bar* gene. Detailed PCR reaction composition and the thermocycling conditions were as previously reported (Testroet et al., 2017; Lee et al., 2019b). Five microliters of the PCR product was used for agarose gel electrophoresis to verify single band amplification, and amplified PCR fragments were cleaned up by treating 5 μl of PCR product with 2 μl of ExoSAP-IT reagent (Thermo Fisher Scientific) according to the manufacturer's instruction. Sanger sequencing was carried out by the DNA Facility at the Iowa State University using the oligonucleotide ZmGl2-exon2-F1 as a primer (Lee et al., 2019b).

Sanger sequencing trace data were analyzed by TIDE (Brinkman et al., 2014) and ICE (Hsiau et al., 2018) using the default settings and the wild type FFMM-A *Gl2* sequencing trace file as a control.

Phenotyping and Mutant Inheritance Analysis

T0 plantlets were screened for loss-of-function *gl2* mutants by misting seedling leaves with water once the plants had acclimatized to the low-humidity conditions of the growth chamber, as well as by PCR as described above. T1 seeds were screened by germinating in vermiculite then screening roots for mCherry expression using a NIGHTSEA dual fluorescent protein flashlight and filter glasses designed to visualize RFP. Once seedling leaves emerged, leaves were misted with water to identify loss-of-function *gl2* mutants.

For T1 seed of marginal quality and likely incapable of germinating properly in vermiculite, an embryo rescuing method was used as described (Martinez and Wang, 2009). The surface sterilized mature embryos were placed embryo-axis-side up on MS medium containing 100 mg/L of benomyl to germinate. Rooted plants were moved to soil using the same method as described for a regenerated plantlet from transformation described above with the exception plants were moved to a 1 gallon (3.7-liter) pot and treated similarly to, and resembled, a seed grown plant once established.

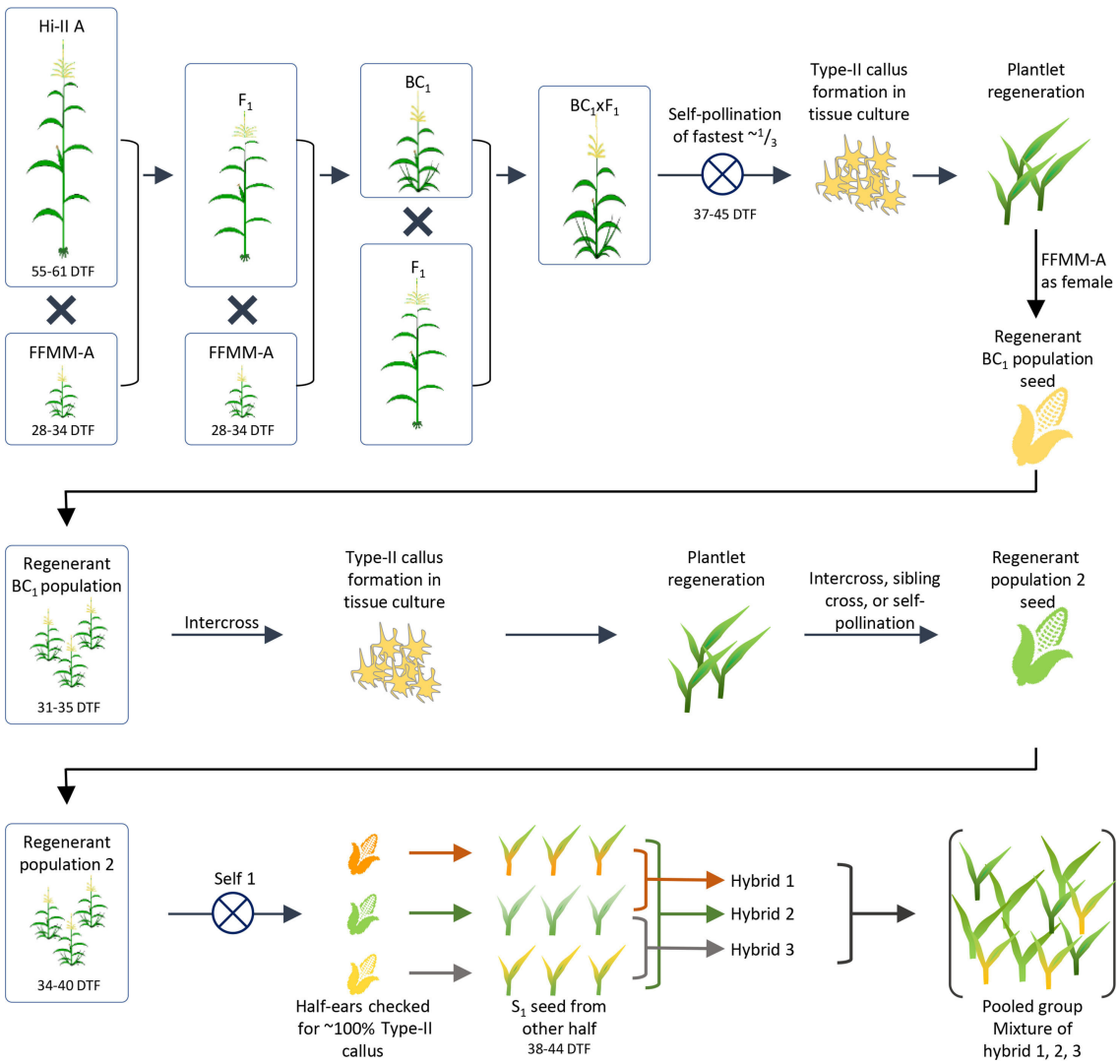

FIGURE 1 | Generation of initial FFMM-AT population. The breeding process used to create a population of plants with FFMM characteristics and the ability to form Type-II callus in tissue culture. From an initial F1 × BC1 crossing, callus was induced and regenerated plants were backcrossed as males to FFMM-A. The population was passed through tissue culture again to select for formation of Type-II callus, and regenerated plants formed a second population. Half-ears of selfed plants were checked for ~100% Type-II callus responses and presumed fixation of the trait. Plants derived from the seed of the other half of ears resembled FFMM-A but took too long to flower so they were intercrossed to form a final population from which fast-flowering lines could be selected. DTF, days to flowering.

RESULTS

Generation of Embryogenic Callus Producing FFMM Lines

Early efforts in attempting to transform FFMM–A and –B lines were unsuccessful in our hands because they are unable to produce embryogenic callus using standard conventional tissue culture and transformation protocols. To breed transformable FFMM lines, we performed a series of crosses and backcrosses by hybridizing the FFMM-A line with Hi-II Parent A (Hi-II A) (**Figure 1**). Hi-II is a transformable genotype; its immature embryos can readily produce friable, embryogenic callus culture (Armstrong et al., 1991). The goal was an introgression of competency to form embryogenic callus in tissue culture from Hi-II A into the FFMM-A genetic background to generate a transformable line FFMM-AT.

An initial F1 hybrid between Hi-II A and FFMM-A then a backcross 1 (BC1) to FFMM-A were produced. These materials were crossed to generate F1 × BC1 seed, which was grown to maturity. The fastest flowering plants were selfed (37–45 days after planting, representing about 1/3 of the total plants). Embryos were harvested 9 DAP and directly placed onto N6 callus induction medium (Wang and Frame, 2004) to evaluate their ability to produce Type-II callus. Type-II callus was produced by only 30 independent embryos and of those 15 callus events were able to form plantlets in regeneration media as described (Wang and Frame, 2004).

Plants resulting from nine separate callus events were backcrossed as a male to FFMM-A ear donors creating a ∼BC1.5. Grown from seed, these ∼BC1.5 plants strongly resembled FFMM-A in both plant architecture and flowering time (31–34 days). These backcrosses were intercrossed in as many unique combinations as possible, generating 18 ears from which embryos were extracted and taken through tissue culture as described above. The regenerated plants were grown in an isolated greenhouse and pollinated by pooling pollen then using it to fertilize open silks, creating a population of self-pollinated, sib-pollinated, and intercrossed seeds (**Figure 1**).

Seeds from the second round of tissue culture and regeneration were grown to maturity and self-pollinated

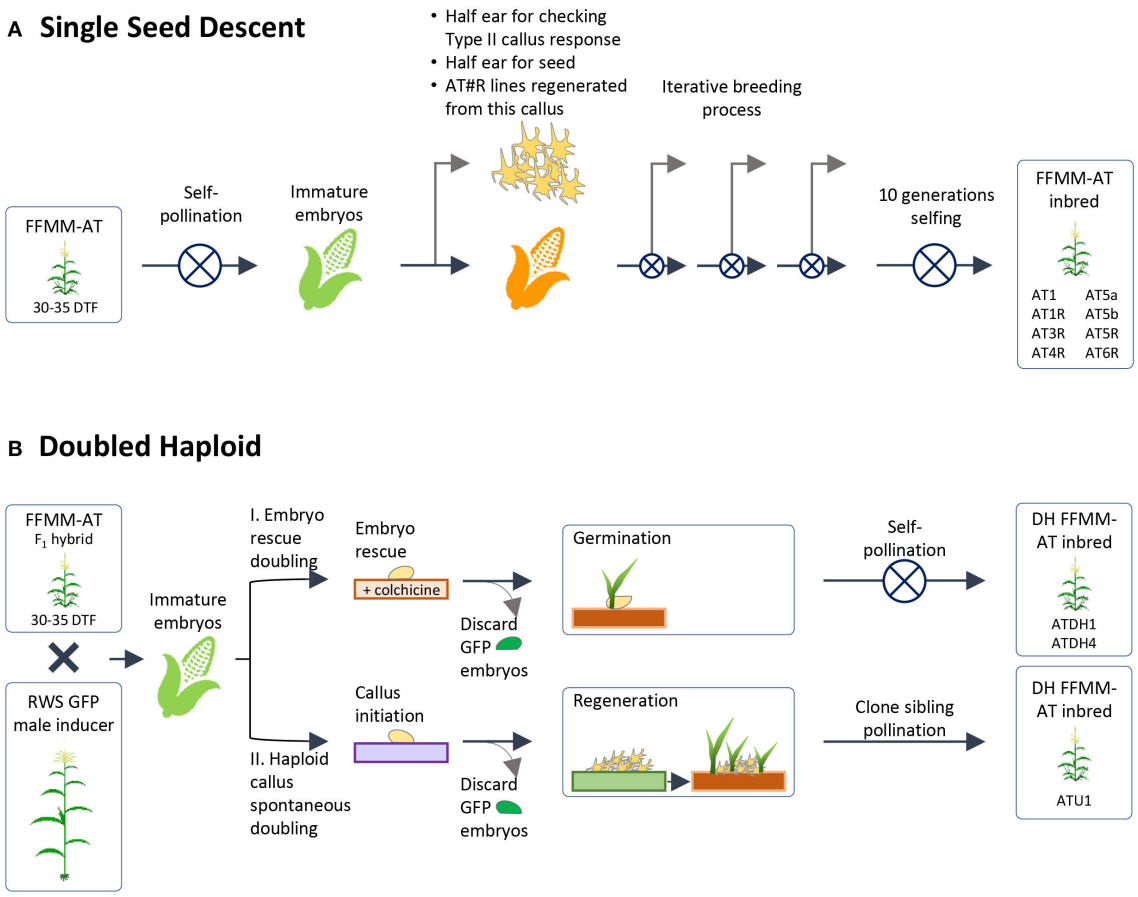

FIGURE 2 | Generation of homozygous lines. This figure depicts the two methods by which homozygous lines were produced from a heterozygous population selected for callus formation and regeneration, fast-flowering, and a Mini-Maize plant architecture. **(A)** Single Seed Descent method of inbreeding with further selection for callus formation and desired plant phenotype; **(B)** Doubled haploid methods. Starting FFMM-AT material was an F1 hybrid of lines from **(A)** that produced high rates of Type-II callus formation when half ears were checked and/or regenerated. DTF, days to flowering.

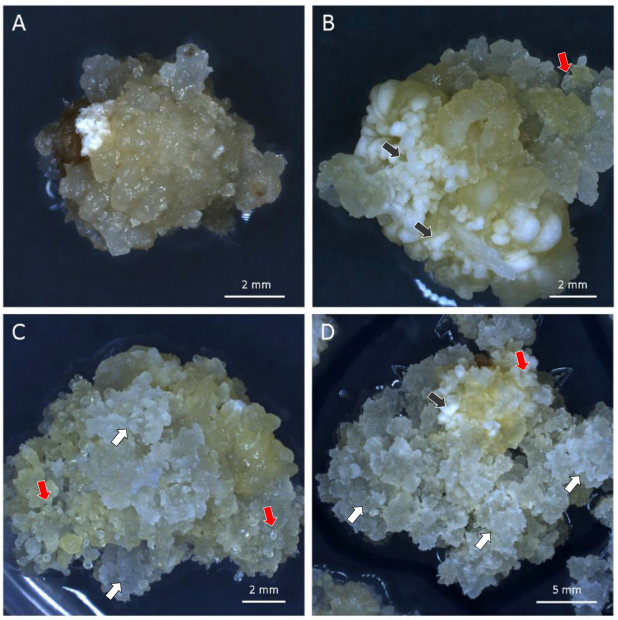

FIGURE 3 | Different types of embryogenic callus. **(A)** Non-embryogenic callus of FFMM-A; **(B)** Embryogenic callus of FFMM-ATU1; **(C,D)** Embryogenic callus of FFMM-AT6R. Black arrows, Type-I compact callus; White arrows, Type-II friable callus; Red arrows, Type-1.5 callus. All three regenerable types were produced from 9 DAP immature embryos and cultured on 605 J medium for 26 days.

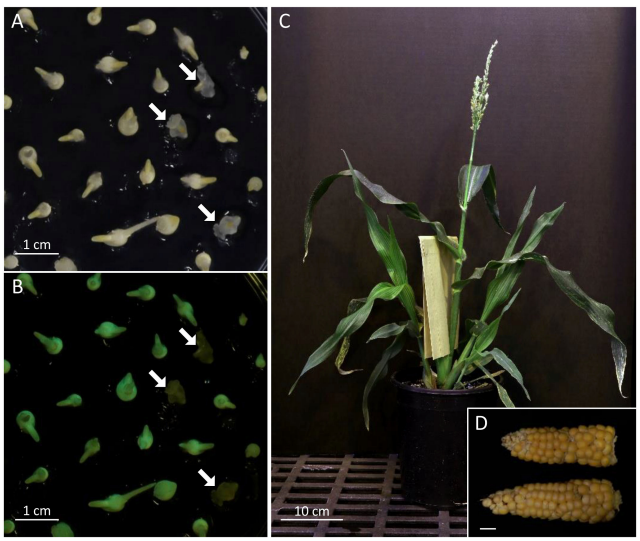

FIGURE 4 | FFMM-AT. Screening of haploid embryos under bright field **(A)** and NIGHTSEA flashlight with GFP filter glasses **(B)**. White arrows point to non-GFP-expressing haploid embryos. **(C)** A mature FFMM-AT plant; **(D)** Mature ears of AT6R; bar scale, 1 cm.

(**Figure 1**). The top half of ears were harvested 9–11 DAP when embryos were ∼1.5 mm long, and embryos were cultured on N6 medium to evaluate Type-II callus generation frequency. Three half-ears yielded ∼100% Type-II callus response and seeds in the remaining lower half of the ears were grown to maturity. Plants grown from these seeds resembled FFMM-A, but were slow to flower (38+ days vs. 28–34 days for FFMM-A), so these 3 lines were intercrossed once again. Seed from nine separate ears was then initiated into single seed descent inbreeding with selection for fast-flowering, good seed set, and ample pollen shed (**Figure 2A**). These lines were designated as FFMM-AT lines.

Embryogenic Type-II callus response was checked again at self-generation 2 (self-2) for one batch and self-3 for a second batch. Two independent lines, FFMM-AT1 and FFMM-AT5, which had close to 100% callus response, continued through single seed descent. These produced lines FFMM-AT1, FFMM-AT5a, and FFMM-AT5b. In addition, these three lines and three additional lines (FFMM-AT3, AT4, AT6) with reduced Type-II callus initiation frequencies were regenerated from callus once again before resuming selfing (**Figure 2A**). This produced lines FFMM-AT1R, AT3R, AT4R, AT5R, and AT6R. After self-hybridization for 10 generations, eight independent FFMM-AT inbred lines with the ability to produce embryogenic callus were established (**Figures 2A**, **3**). Compared to genotypes from the early breeding cycle, the embryogenic callus morphology produced from these finished lines is not as friable as the Type-II callus (**Figure 3D**), but rather somewhat resemble embryogenic Type-I callus type (**Figures 3B,C**), so we call it Type-1.5.

As an alternative to self-hybridization to reach homozygosity, we also attempted a faster breeding process using Doubled Haploid (DH) technology (**Figure 2B**). The F1 hybrid seeds from a cross between AT1 (self-4, 91% Type-II callus) and AT4R (self-3 regenerated from an ear with 66% Type-II callus) were grown and crossed as a female by RWS-GFP, a haploid inducer line carrying a green fluorescent marker gene (GFP) to facilitate identification of haploids (Röber et al., 2005; Yu and Birchler, 2016). Under the NIGHTSEA BlueStar flashlight, the immature diploid embryos were fluorescent due to the presence of the paternal *gfp* transgene, and thus were discarded (**Figure 2B**). Non-fluorescent embryos (**Figures 4A,B**) were treated either by embryo rescue doubling (ERD, Barton et al., 2014) or haploid callus spontaneous doubling (HCSD) method. Three doubled haploid FFMM-AT lines, ATDH1, ATDH4, and ATU1 were generated (**Figure 2B**).

Agrobacterium-Mediated Targeted Mutagenesis in FFMM-AT

Table 1 summarizes the transformation experiments carried out on 10 out of 11 advanced FFMM-AT genotypes that were generated from either > 7 generations of self-pollination or doubled haploid treatments. The CRISPR construct pKL2013 (**Figure 5**, **Supplementary Figure 1**) has an 11.5 kb T-DNA that carries a mCherry marker gene for visible selection, *bar* gene for plant selection, and SpCas9 and sgRNA for targeted mutagenesis of *Gl2*. The gene product of *Gl2* is responsible for the formation of a hydrophobic waxy cuticle layer in juvenile leaf tissues, and the knockout mutants can be easily identified by misting water on the young leaf surface (Bianchi et al., 1975). Water will roll off wild

TABLE 1 | Summary of FFMM-AT transformation experiments.

Exp ID	Genotype name	Self-generation	# of ear	# embs infected	# RFP+ callus	# event w/ shoot	# event rooted	# event to gh	# event to seed	% TF	Avg	Std
1	AT1	9	1	97	7	5	5	5	1	1.0%	**1.1%**	0.1%
2	AT1	10	2	81	4	2	2	2	1	1.2%		
3	AT1R	8	3	125	1	1	1	1	0	0.0%	**0.0%**	0.0%
4	AT1R	9	2	153	3	1	0	0	0	0.0%		
5	AT3R	7	2	145	1	5	5	3	2	1.4%	**N/A**	N/A
6	AT4R	8	2	156	14	9	9	5	4	2.6%	**1.5%**	1.5%
7	AT4R	10	4	241	2	1	1	1	1	0.4%		
8	AT5b	8	2	124	1	2	2	1	1	0.8%	**N/A**	N/A
9	AT5R	7	1	113	15	9	9	9	2	1.8%	**N/A**	N/A
10	AT6R	7	1	72	35	28	26	22	4	5.6%	**11.3%**	8.1%
11	AT6R	8	2	41	9	15	7	7	7	17.1%		
12	ATDH1	DH	2	79	5	2	2	2	2	2.5%	**3.4%**	1.3%
13	ATDH1	DH	2	23	2	1	1	1	1	4.3%		
14	ATDH4	DH	1	42	1	1	1	1	0	0.0%	**0.9%**	1.2%
15	ATDH4	DH	1	58	1	1	1	1	1	1.7%		
16	ATU1	DH	1	49	13	10	9	8	5	10.2%	**7.0%**	4.5%
17	ATU1	DH	2	103	12	6	6	6	4	3.9%		
Total			**31**	**1702**	**126**	**99**	**87**	**75**	**36**			

DH, germplasm generated using Doubled Haploid technology.
[#]RFP+ callus, putative transgenic callus with red fluorescence.
TF, transformation frequency (# event to seed/#embryos infected × 100).
Avg, average transformation frequency; Std, standard deviation; N/A, not applicable.

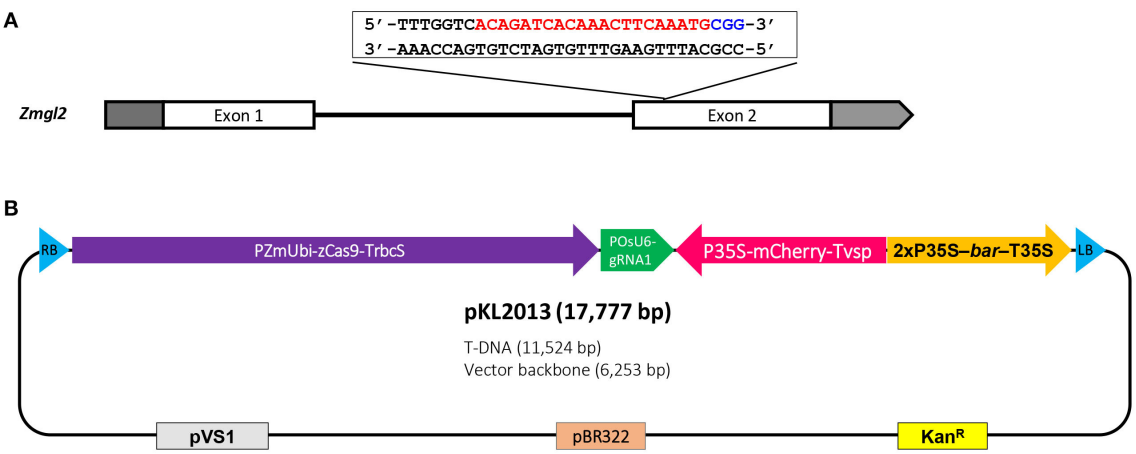

FIGURE 5 | Schematic illustration of maize *glossy2* (*gl2*) gene target sequence and CRISPR-Cas9 construct for *Agrobacterium*-mediated transformation. **(A)** Maize *Gl2* has two exons and the target sequence is located near the 5′ end of the second exon. The protospacer (red) and PAM (blue) are indicated; **(B)** The CRISPR-Cas9 construct, pKL2013, has an 11.5 kb T-DNA which includes maize-codon-optimized SpCas9 driven by maize ubiquitin promoter, sgRNA1 cassette driven by rice U6 promoter, mCherry cassette driven by CaMV 35S promoter, and *bar* selectable marker driven by CAMV 35S promoter. RB, T-DNA right border; PZmUbi-zCas9-TrbcS, maize ubiquitin promoter driving maize-codon-optimized SpCas9 (zCas9) with ribulose-1,5-bisphosphate carboxylase/oxygenase small subunit 2b terminator; POsU6-gRNA1, rice U6 promoter driving sgRNA1 with rice-U6-2 terminator; P35S-mCherry-Tvsp, CaMV 35S promoter driving mCherry with soybean vegetative storage protein terminator; 2xP35S-bar-T35S, CaMV 35S promoter driving phosphinothricin N-acetyltransferase (*bar*) with CaMV 35S terminator; LB, T-DNA left border; pVS1, origin of replication from the plasmid pVS1; pBR322, origin of replication from the plasmid pBR322; Kan^R, aminoglycoside phosphotransferase gene providing resistance to kanamycin.

TABLE 2 | Summary of T0 mutant genotypes†.

	# plants	% T0 mutant
Homozygous	20	23.3%
Biallelic	37	43.0%
Heterozygous	0	0.0%
Mosaic	11	12.8%
Wild type*	18	20.9%
Total analyzed	**86**	**100.0%**

†*Homozygous, one mutant sequence without wild type allele; Biallelic, two different mutant sequences; Heterozygous, wild type sequence and one mutant sequence; Mosaic, three or more mutant sequences in a single plant.*
**Among the 18 WT plants, 13 were Cas9 positive.*

type *Gl2* plants but droplets will adhere to the *gl2* homozygous or biallelic knockout individuals.

To enhance transformation, the construct is mobilized into an *Agrobacterium* thymidine auxotrophic strain LBA4404Thy- harboring a helper plasmid PHP71539 that carries an extra copy of virulence (*vir*) genes from the pTiBo542 plasmid (Anand et al., 2018). Extra copies of *vir* genes in an *Agrobacterium* strain have been shown to be effective in enhancing transformation frequency (Komari, 1990; Ishida et al., 1996; Anand et al., 2018). The Thy- strain was used to minimize *Agrobacterium* carryover during transformation process because this strain cannot survive on media without the addition of thymidine (Ranch et al., 2010). Over 1,700 immature embryos representing 31 ears were dissected and infected in a total of 17 individual experiments.

As shown in **Table 1**, immature embryos of all 10 FFMM-AT genotypes were capable of producing Type-1.5 embryogenic callus on media described in this work, with FFMM-ATU1 and FFMM-AT6R occurring at high frequencies (over 70%). FFMM-AT6R often produces a Type-II callus response in addition to Type-1.5 as can be seen in **Figure 3D**. After infection and co-cultivation, bialaphos-resistant callus pieces were monitored for the red fluorescent protein (RFP) mCherry expression throughout the selection stage. A total of 126 RFP-positive callus pieces (out of 1,702 infected embryos) were scored; 99 of the bialaphos-resistant callus pieces produced shoots and 87 of them made roots. Among 75 events transplanted to the soil, about half of them (36 events) produced seed. The transformation frequency (TF), defined as the number of transgenic events that produced T1 seeds per 100 embryos infected, ranged from 0.0% for genotype AT1R to 17.1% for AT6R. Among seven single seed descent, self-pollinated FFMM-AT genotypes tested, AT6R produced the highest TF with an average of 11.3 ± 8.1% (mean ± *SD*). Among the three doubled haploid lines, genotype ATU1 produced a high TF with an average of 7.0 ± 4.5% (**Table 1**).

T0 and T1 Analysis

Phenotyping and genotyping were performed for all T0 plants. The mCherry expression in root tissue was examined by a hand-held flashlight device. Leaf materials of T0 plantlets were analyzed by PCR for the presence of the *bar* and Cas9 genes. Then the target gene *gl2* was analyzed by Sanger sequencing and trace file analyses using the TIDE (Brinkman et al., 2014) and ICE (Hsiau et al., 2018) analyses.

Table 2 summarizes the T0 mutant genotypes. Out of 86 T0 plants sequenced, 68 plants carried mutations in the *gl2* gene, giving a mutagenesis frequency of 79%. Among the 18 plants with the wild-type genotype, 13 of them were Cas9-positive plants. It is possible that the Cas9 gene expression was silenced in these lines.

The *gl2* target sequences of selected T0 mutant lines are listed in **Figure 6**. As can be seen, most mutants have insertions or deletions (indels) near the PAM sequence. Some sibling plants derived from the same transgenic callus lines have the same mutation patterns, such as lines 1-2-1 and 1-2-3; 6-1-4, 6-1-5 and 6-1-6; 14-NR1-1, 14-NR1-3 and 14-NR1-4; as well as 15-4-1 and 15-4-2. In these events, targeted mutagenesis likely occurred at an early stage before the callus induction. Sometimes, plants produced from different callus lines can have the same mutation patterns, such as lines 11-2-8 and 11-4-2; 12-1-2 and 12-6-1; and 15-2-3 and 15-3-3. Two mutation patterns,−2/+1 (biallelic) and +1/+1 (homozygous), were prevalent and can be detected in a number of T0 mutants that were generated in different and separate infection experiments. Four plants (1-2-1, 1-2-3, 7-2-11, and 12-3-1) have the biallelic−2/+1 genotype and seven plants (11-2-8, 11-4-2, 9-1-7, 14-NR1-1,−3,−4 and 15-2-2) have the homozygous +1/+1 genotype (**Table 2**).

On the other hand, sibling plants derived from the same transgenic callus can often carry different mutation patterns (**Table 2**). For example, 11-2-1 and 11-2-8 were siblings from the same callus event. They have different mutant patterns; 11-2-1 is biallelic (-12/+2) and 11-2-8 is homozygous (+1/+1). Likewise, 9-1-5 and 9-1-7, 12-NR1-1 and 12-NR1-3, 15-1-2 and 15-1-3, 15-2-2 and 15-2-3 were all sibling plants with each other, but carried different mutant genotypes. This phenomenon has been reported in previous work (Char et al., 2017; Banakar et al., 2019; Lee et al., 2019b) and suggests that the *gl2* mutation might have occurred after initial cell divisions of the transformed cells. If the CRISPR reagents were not expressed fully at the early stage (single cell) of transformation, chimeric callus culture can generate multiple plants with different mutation patterns, even though they are all derived from a single transgenic event. There is also the possibility that multiple transgenic events were produced from a single embryo and were both represented during callus formation and selection.

Selected T0 mutant lines were either self-pollinated or out-crossed to FFMM-AT to produce T1 seeds. T1 seeds showed segregation of mCherry expressing transgene (**Figures 7A,B**) as well as *gl2* mutant phenotype (**Figures 7C,D**). T1 genotyping was carried out on progenies of either direct descendants or sibling plants from sequenced T0 mutant plants.

T1 seedlings from four self-pollinated lines (1-2-1, 11-4-1, 12-NR1-1, and 14-NR1-1) show parental genotypes, although lines 1-2-1 and 11-4-1 also produced some T1 seedlings with mutation patterns that were not detected in their T0 parental plants (**Figure 6**). Four out-crossed as female (OCF) lines and two out-crossed as male (OCM) lines gave various mutation patterns; some inherited the parent mutations but some did not. Out of the 10 T1 progenies analyzed, five of them (9-1-5, 14-NR1-1, 15-1-2, 15-2-2, and 15-4-1) were not direct descendants from their T0

Event IDs	Wild type	GTTTCTTTGGTCACAGATCACAAACTTCAAATGCGGTGGGCTGGCGCTGGGGTTCAGCTG	T0 genotype		Cross	# T1 analyzed	T1 genotype
AT1							
1-2-1,	Allele1:	GTTTCTTTGGTCACAGATCACAAACTTCAA--GCGGTGGGCTGGCGCTGGGGTTCAGCTG	-2 bp	(BI)	Self	14	-2/+1 (9x), +1/+1 (4x), -2/-2 (1x)
1-2-3	Allele2:	GTTTCTTTGGTCACAGATCACAAACTTCAAAATGCGGTGGGCTGGCGCTGGGGTTCAGCTG	+1 bp				
1-5-1	Allele1:	GTTTCTTTGGTCACAGATCACAAACTTCA----------GCTG	-27 bp	BI			
	Allele2:	GTTTCTTTGGTCACAGATCACAAACTTCAAAATGCGGTGGGCTGGCGCTGGGGTTCAGCTG	+1 bp				
AT4							
6-1-4,	Seq1:	GTTTCTTTGGTCACAGATCACAAACTTCAA-TGCGGTGGGCTGGCGCTGGGGTTCAGCTG	-1 bp	MO			
6-1-5,	Seq2:	GTTTCTTTGGTCACAGATCACAAACTTCAA------TGGGCTGGCGCTGGGGTTCAGCTG	-6 bp		OCF	2	-6/+1/0 (1x), -6/-3/+1 (1x)
6-1-6	Seq3:	GTTTCTTTGGTCACA----------TGCGGTGGGCTGGCGCTGGGGTTCAGCTG	-16 bp				
	Seq4:	GTTTCTTTGGTCACAGATCACAAACTTCAAAATGCGGTGGGCTGGCGCTGGGGTTCAGCTG	+1 bp				
AT6							
7-2-11	Allele1:	GTTTCTTTGGTCACAGATCACAAACTTCAA--GCGGTGGGCTGGCGCTGGGGTTCAGCTG	-2 bp	(BI)	OCF	12	-2/-2 (BI, 3x), -1/+1 (2x), +1/0 (2x), -2/0 (2x),
	Allele2:	GTTTCTTTGGTCACAGATCACAAACTTCAAAATGCGGTGGGCTGGCGCTGGGGTTCAGCTG	+1 bp				-1/-2 (1x), -2/+1 (1x), +1/+1 (1x)
7-3-1	Allele1:	GTTTCTTTGGTCACAGATCACAAACTTCA------------------------------	-51 bp	BI			
	Allele2:	GTTTCTTTGGTCACAGATCACAAACTTCAAAATGCGGTGGGCTGGCGCTGGGGTTCAGCTG	+1 bp				
11-2-1	Allele1:	GTTTCTTTGGTCACAGATCACAAACTTCAA----------GGCGCTGGGGTTCAGCTG	-12 bp	BI			
	Allele2:	GTTTCTTTGGTCACAGATCACAAACTTCAANNATGCGGTGGGCTGGCGCTGGGGTTCAGCTG	+2 bp				
11-2-8,	Allele1:	GTTTCTTTGGTCACAGATCACAAACTTCAAAATGCGGTGGGCTGGCGCTGGGGTTCAGCTG	+1 bp	(HM)			
11-4-2*	Allele2:	GTTTCTTTGGTCACAGATCACAAACTTCAAAATGCGGTGGGCTGGCGCTGGGGTTCAGCTG	+1 bp				
11-4-1	Allele1:	GTTTCTTTGGTCACAGATCACAAACTTCAA---CGGTGGGCTGGCGCTGGGGTTCAGCTG	-3 bp	HM	Self	13	-3/-3 (11x), -1/-2/-5 (1x), -42/-42 (1x)
	Allele2:	GTTTCTTTGGTCACAGATCACAAACTTCAA---CGGTGGGCTGGCGCTGGGGTTCAGCTG	-3 bp				
ATDH1							
9-1-5	Allele1:	GTTTCTTTGGTCACAGATCACAAAC----------TGGCGCTGGGGTTCAGCTG	-16 bp	HM	OCM	**12**	-16/-16 (5x), -15/+1 (3x), -4/-4 (1x),
	Allele2:	GTTTCTTTGGTCACAGATCACAAAC----------TGGCGCTGGGGTTCAGCTG	-16 bp				-1/-2 (1x), -16/-1 (1x), -1/0 (1x)
9-1-7	Allele1:	GTTTCTTTGGTCACAGATCACAAACTTCAAAATGCGGTGGGCTGGCGCTGGGGTTCAGCTG	+1 bp	(HM)			
	Allele2:	GTTTCTTTGGTCACAGATCACAAACTTCAAAATGCGGTGGGCTGGCGCTGGGGTTCAGCTG	+1 bp				
ATDH4							
10-1-1	Allele1:	GTTTCTTTGGTCACAGATCACAAACTTCA-ATGCGGTGGGCTGGCGCTGGGGTTCAGCTG	-1 bp	BI			
	Allele2:	GTTTCTTTGGTCACAGATCACAAACTT---ATGCGGTGGGCTGGCGCTGGGGTTCAGCTG	-3 bp				
ATU1							
12-1-2,	Allele1:	GTTTCTTTGGTCACAGATCACAAACTTCA--TGCGGTGGGCTGGCGCTGGGGTTCAGCTG	-2 bp	HM	OCM	15	-2/0 (4x), -2/-2 (BI, 3x), 0/0 (3x), -2/-2 (HM, 1x),
12-6-1*	Allele2:	GTTTCTTTGGTCACAGATCACAAACTTCA--TGCGGTGGGCTGGCGCTGGGGTTCAGCTG	-2 bp				-15/3 (1x), -1/+1 (1x), -2/+1 (1x), -1/-2 (1x)
12-3-1	Allele1:	GTTTCTTTGGTCACAGATCACAAACTTCAA--GCGGTGGGCTGGCGCTGGGGTTCAGCTG	-2 bp	(BI)			
	Allele2:	GTTTCTTTGGTCACAGATCACAAACTTCAAAATGCGGTGGGCTGGCGCTGGGGTTCAGCTG	+1 bp				
12-7-1	Allele1:	GTTTCTTTGGTCACAGATCACA---------TGCGGTGGGCTGGCGCTGGGGTTCAGCTG	-9 bp	BI			
	Allele2:	GTTTCTTTGGTCACAGATCACAAACTTCAAAATGCGGTGGGCTGGCGCTGGGGTTCAGCTG	+1 bp				
12-8-1	Allele1:	GTTTCTTTGGTCACAGATCACAAACTTCAA----------CTGGCGCTGGGGTTCAGCTG	-10 bp	BI			
	Allele2:	GTTTCTTTGGTCACAGATCACAAACTTCAAAATGCGGTGGGCTGGCGCTGGGGTTCAGCTG	+1 bp				
12-NR1-1	Allele1:	GTTTCTTTGGTCACAGATCACAAACTTCA-ATGCGGTGGGCTGGCGCTGGGGTTCAGCTG	-1 bp	HM	Self	15	-1/-1 (15x)
	Allele2:	GTTTCTTTGGTCACAGATCACAAACTTCA-ATGCGGTGGGCTGGCGCTGGGGTTCAGCTG	-1 bp				
12-NR1-3	Allele1:	GTTTCTTTGGTCACAGATCACAAACTTCA-ATGCGGTGGGCTGGCGCTGGGGTTCAGCTG	-1 bp	BI			
	Allele2:	GTTTCTTTGGTCACAGATCACAAACTTC--ATGCGGTGGGCTGGCGCTGGGGTTCAGCTG	-2 bp				
14-NR1-1,	Allele1:	GTTTCTTTGGTCACAGATCACAAACTTCAAAATGCGGTGGGCTGGCGCTGGGGTTCAGCTG	+1 bp	(HM)	Self	**14**	+1/+1 (14x)
-3. & -4	Allele2:	GTTTCTTTGGTCACAGATCACAAACTTCAAAATGCGGTGGGCTGGCGCTGGGGTTCAGCTG	+1 bp				
15-1-2	Allele1:	GTTTCTTTGGTCACAGATCACAAACTTCA----------CTGGCGCTGGGGTTCAGCTG	-11 bp	BI			
	Allele2:	GTTTCTTTGGTCACAGATCACAAACTTCAA----------TGGCGCTGGGGTTCAGCTG	-11 bp				
15-1-3	Allele1:	GTTTCTTTGGTCACAGATCACAAA--------GCGGTGGGCTGGCGCTGGGGTTCAGCTG	-8 bp	HM			
	Allele2:	GTTTCTTTGGTCACAGATCACAAA--------GCGGTGGGCTGGCGCTGGGGTTCAGCTG	-8 bp				
15-2-2	Allele1:	GTTTCTTTGGTCACAGATCACAAACTTCAAAATGCGGTGGGCTGGCGCTGGGGTTCAGCTG	+1 bp	(HM)	OCF	**9**	+1/0 (9x)
	Allele2:	GTTTCTTTGGTCACAGATCACAAACTTCAAAATGCGGTGGGCTGGCGCTGGGGTTCAGCTG	+1 bp				
15-2-3,	Allele1:	GTTTCTTTGGTCACAGATCACAAACTTC--ATGCGGTGGGCTGGCGCTGGGGTTCAGCTG	-2 bp	BI			
15-3-3*	Allele2:	GTTTCTTTGGTCACAGATCACAAACT----ATGCGGTGGGCTGGCGCTGGGGTTCAGCTG	-4 bp				
15-4-1,	Allele1:	GTTTCTTTGGTCACAGATCACAAACTTCA----CGGTGGGCTGGCGCTGGGGTTCAGCTG	-4 bp	BI	OCF	**20**	-6/0 (6x), -4/0 (5x), -4/-4 (BI1, 3x), -4/-4 (BI2, 3x),
15-4-2	Allele2:	GTTTCTTTGGTCACAGATCACAAACTTCA------GTGGGCTGGCGCTGGGGTTCAGCTG	-6 bp				-6/-6 (HM, 1x), -6/-6 (BI, 1x), -4/-2 (1x)

FIGURE 6 | Genotypes of selected T0 and T1 mutants. Red letters, target sequences in *Gl2* exon 2; Blue letters, PAM sequences; Black letter with underscore, insertion mutations; AT1, AT4R, AT6R, ATDH1, ATDH4, and ATU1, FFMM-AT genotypes; Event marked with star, separate event that had the same mutation pattern; BI, biallelic; HM, homozygous; MO, mosaic; (BI) and (HM), events with same mutation pattern in more than one sampled T0 plant; Self, self-pollination; OCF and OCM, an outcross with the T0 plant used as a female or male, respectively; Underlined numbers, T1 progenies of T0 plants of which their sibling T0 plants from the same transgenic event were sequenced; T1 genotypes, numbers in parentheses indicate the numbers of plants from the event that have the same mutation pattern.

sequenced parents, but rather progenies from their sibling plants derived from the same transgenic callus events. Some of them such as line 14-NR1-1 had exactly the same mutation pattern as its parent; other lines carried different patterns compared to their T0 sequenced counterparts.

DISCUSSION

Here we describe the successful development, transformation, and gene editing of new Fast-Flowering Mini-Maize lines, FFMM-AT. FFMM-AT lines reliably produce embryos ∼6 weeks after seed germination. The transformation process takes about 8–9 weeks, followed by about 3 weeks of regenerated plant growth in soil until crossing. Seed formation and maturation takes an additional 4 weeks. This gives a seed-to-T1 seed time of ∼5.5 months. Compared to transformation of over 9 months for Hi-II (Frame et al., 2015) and over 11 months for the B104 inbred (Raji et al., 2018), this is much shorter due largely to the faster generation time of FFMM on the pre-transformation material generation and post-regeneration stages. The callus selection step of FFMM-AT is also shorter than B104 and less labor intensive.

The challenges in using FFMM compared to standard maize lines are largely in adapting to care protocols that are specific to FFMM genotypes. It is important to grow FFMM in small containers such as 1-gallon (3.7-liter) pots [6.75 inches (17 cm) depth × 6.25 inches (16 cm) diameter] and avoid overwatering. Because of the rapid life cycle, stressed FFMM plants are unlikely to have enough time to recover and produce healthy pollen

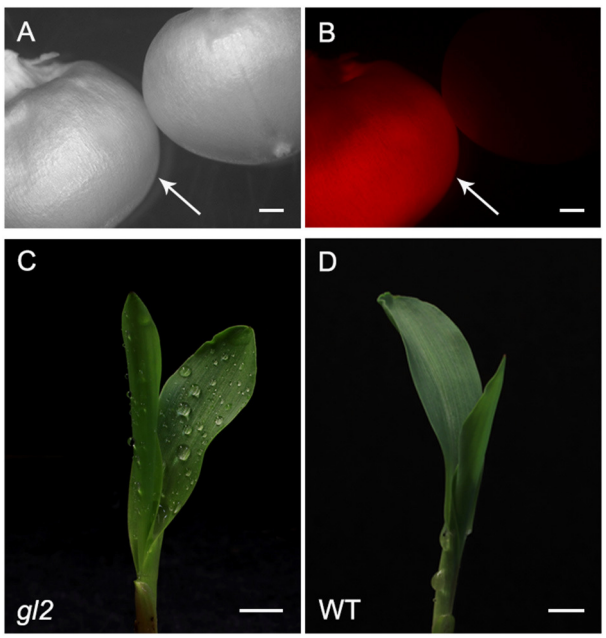

FIGURE 7 | Representative phenotypes of T1 transgenic lines. T1 progeny seed of RFP expressing (left, indicated by an arrow) and non-expressing segregant (right) under bright light **(A)** and RFP channel **(B)**. The phenotype of *gl2* loss-of-function mutant **(C)** and wild type **(D)**. Dull surface of juvenile leaf of *gl2* mutant retains sprayed water drops. Bar scale, 5 mm.

or ears. Seed production of 50 FFMM-AT transgenic plants generated in this study ranged from 5 to 199 with an average of 76 seeds per cob (**Figure 4D**), comparable to what has been observed in the original FFMM-A line (McCaw et al., 2016).

To date, successful maize transformation on a specific genotype often relies on the ability to produce embryogenic callus of the said genotype. The original FFMM lines lack this ability when using the conventional protocols and media regimes. Successful introgresssion of the ability to form Type-II callus into B73 has been reported, and the regions of the A188 genome that could be important to this ability have been identified (Armstrong et al., 1992; Lowe et al., 2006). Because of the possible existence of unknown repressors and other genetic factors, however, we decided to pursue the classic, albeit time consuming, breeding method and selected for a callus development phenotype rather than employing the marker-assisted breeding technology.

Once Type-II callus formation ability was introgressed into a background resembling FFMM, we produced homozygous lines by both inbreeding and doubled haploid approaches to achieve a uniform genetic background. Two doubled haploid methods were employed. In the ERD method invented by Barton et al. (2014), immature haploid embryos were cultured on colchicine-containing medium. In the HCSD method described in this work, immature haploid embryos were allowed to form haploid callus and undergo spontaneous chromosomal doubling without any doubling agent. Diploid plants generated from both methods showed good fertility restoration in the whole tassel, rather than sectors or branches as seen in traditional chromosome doubling methods that were used to treat haploid seedlings (Kato and Geiger, 2002; Vanous et al., 2017). The HCSD method may be particularly useful for generation of new lines capable of forming embryogenic callus because its success is determined by presence of callus formation ability in the haploid genome. Diploid homozygous lines are much more vigorous than their haploid counterpart; spontaneous genome doubling of haploid callus cells to produce diploid cells should increase the vigor of the callus and the increased growth rate can be selected for these events.

The FFMM-AT lines generated in this work demonstrated different tissue culture responses and transformation frequencies. Each line has unique characteristics to its phenotype. Line FFMM-AT6R appears to have robust performance in tissue culture and transformation capability in our study. When cultured on a 605J based medium this inbred line shows vigorous callus formation for both Type-1.5 and Type-II callus. It also has a high rate of infection by *Agrobacterium*, giving 44/113 embryos producing RFP-positive callus and 33/113 embryos producing shoots after selection.

FFMM-AT6R would be our preferred transformable line due to its robust response in callus, though it does have some differences compared to FFMM-A. FFMM-AT6R has a slightly more elongated stature that facilitates ear shoot bagging. The plant tends to produce a single-branched tassel or two tassel branches as compared to three or more in other FFMM lines; however, its pollen shed and nicking are still sufficient to pollinate the ear well. The ear tends to be shortened compared to FFMM-A, and often masculinized at the tip. It also tends to have larger kernels that are more disordered in kernel row ordering and kernel orientation. The larger kernels usually take longer to dry down before harvest. The plants have a slightly longer time to flowering, which makes FFMM-AT6R closer to seed-to-seed in 65–70 days, instead of 60 days for FFMM-A.

Several FFMM-AT lines were promising in early stages of breeding. For example, lines AT1 and AT4R produced plants that were subjectively superior to FFMM-A in plant architecture and ear size, while maintaining fast-flowering and fast seed maturity. At self-4, line AT1 showed strong ability in producing Type-II callus (over 90% from 1.2 to 1.8 mm ideal sized embryos) on the standard N6 medium used for Hi-II (Wang and Frame, 2004). At self-5 and self-6, line AT1 performed poorly on N6 medium, but performed well on 605J medium. Interestingly, at later selfed generations line AT1 performed poorly on both N6 and 605J media losing the ability to form embryogenic callus. This sudden change of tissue culture responses is puzzling. It is possible that one or a few alleles that were responsible for Type-II response were lost during the self-hybridization process.

The regeneration process of FFMM-AT is a key to success. The conventional maize transformation process for regular-sized genotypes such as Hi-II or B104 focused on producing a well-established plant with three to five leaves and a substantial root structure in tissue culture before moving to soil. Early attempts at regeneration of FFMM-AT lines by methods successful for Hi-II yielded plants with a small, fertile tassel, but they were unable to produce ears reliably. It was observed that when

producing transgenic FFMM-AT plants, it is important that the regenerated plantlets to be moved from culture media to soil much earlier. Regenerated FFMM-AT plants that closely resembled a freshly sprouted seedling, with just one or two leaves and established but short roots (just >7 cm total length of thick, not hair-fine), produced much more vigorous plants in soil in our hands. These plants were much more likely to produce ears that formed fertile tassels and produce viable seeds. Regenerated plants were often smaller than seed-grown FFMM-AT plants and produced excessive moisture within the ear. This moisture necessitates the dehusking of the ears around 11–12 DAP while remaining attached to the plant to prevent fungal growth but retain development by nourishment from the plant.

CRISPR-mediated targeted mutagenesis was efficient in FFMM-AT lines with a 79% mutation rate in T0 plants (**Table 2**). Observed mutation patterns were mostly short indels, similar to the maize B104 *gl2* mutant events transformed with construct A844B, which carried the same SpCas9-gRNA cassettes used in pKL2013 (Lee et al., 2019b). The combined frequencies of homozygous and biallelic mutants were comparable with 63% in B104 (**Table 1** in Lee et al., 2019b) and 66% in FFMM-AT. Interestingly, while no deletions larger than 7 bp were observed in B104 T0 plants, some FFMM-AT T0 lines showed large deletions over 10 bp (**Figure 5**). Another difference was the frequencies of heterozygous or mosaic mutants: while B104 showed a high frequency of heterozygous mutants with 37% (**Table 1** in Lee et al., 2019b), FFMM-AT T0 lines had no heterozygous mutants but had mosaic mutants in 11.8% of T0 plants. It is not clear if these differences reflect any genetic divergence in the FFMM-AT lines, but our data indicate that gene editing technologies can be used efficiently in FFMM-AT lines.

FFMM-AT has obvious and direct application to maize genomics studies, especially for large-scale indoor research. FFMM-AT provides unique benefits as a model organism by shortening the timeline and reducing the greenhouse space required for experiments. A full size FFMM plant can be grown in an inexpensive growth chamber that is too small for standard maize lines (Tran and Braun, 2017). Therefore, use of FFMM for research can potentially avoid the need for a greenhouse to grow maize. In 2018, a miniature rice germplasm, Xiaowei, was reported for large-scale indoor genomic research for rice (Hu et al., 2018). Compared to a typical rice variety Nipponbare (60 cm in height and 73 days-to-heading), Xiaowei measures 11.6 cm in height and 46 days-to heading. A regular maize genotype Hi-II is nearly 2 m in height and its seed-to-seed time is about 120 days. The FFMM-AT reported in this study, measures ∼90 cm in height (**Figure 4C**) and ∼65 days from seed to seed.

While FFMM will not be suitable for analyzing all gene functions, it can be useful for studying genes and pathways where a specific genetic background is not required. Coupled with CRISPR-Cas genome editing tools, it can accelerate maize genomic research. Moreover, pollen of FFMM can be potentially useful in small grain genomic research. Recently, Kelliher et al. (2019) has shown that transgenic maize pollen expressing CRISPR reagents could be used to generate haploid wheat with expected mutations in the targeted wheat gene. It is conceivable that FFMM-AT, the transformable, short stature and life cycle maize, can be an appealing tool for CRISPR-mediated mutagenesis in wheat and other small grain crops. In summary, with reduced space requirements and generation time, adding competency for genetic transformation completes FFMM-AT as an open source tool for maize genomic research.

DATA AVAILABILITY STATEMENT

The raw data supporting the conclusions of this article will be made available by the authors, without undue reservation. FFMM-AT seeds can be obtained from James A Birchler, birchlerj@missouri.edu.

AUTHOR CONTRIBUTIONS

MM and KW designed and oversaw the entire project. MM performed plant breeding, tissue culture evaluation, and data collection. KL designed/built the construct and performed molecular analysis. MM, MK, and JZ performed maize transformation. JZ contributed to regeneration protocol design. MM and MA took care greenhouse plants. MM, MK, and MA performed progeny phenotyping and figure preparation. JB contributed to breeding design and planning. MM, KW, and KL performed data analysis and prepared the manuscript. All authors contributed to discussion and revision of the manuscript.

FUNDING

This project was partially supported by National Science Foundation Plant Genome Research Program Grants 1725122 and 1917138, by the Agriculture and Food Research Initiative Competitive Grant # 2019-67013-29016 from the USDA National Institute of Food and Agriculture (NIFA) to KW, by NSF Plant Genome Research Program grant IOS-1339198 to JB, by Predictive Plant Phenomics Research Traineeship Program (National Science Foundation Grant DGE-1545453) to JZ, by the USDA NIFA Hatch project #IOW04714, by State of Iowa funds, and by the Crop Bioengineering Center of Iowa State University.

ACKNOWLEDGMENTS

The authors wish to thank Corteva Agriscience for providing *Agrobacterium* strain and accessory plasmid LBA4404Thy-(PHP71539); Ephraim Aliu for assisting in maize plant care; and Aaron Brand, Daniel Little, and Peter Lawlor for assistance and advice with greenhouse facilities.

SUPPLEMENTARY MATERIAL

The Supplementary Material for this article can be found online at: https://www.frontiersin.org/articles/10.3389/fgeed.2020.622227/full#supplementary-material

REFERENCES

Anami, S. E., Mgutu, A. J., Taracha, C., Coussens, G., Karimi, M., Hilson, P., et al. (2010). Somatic embryogenesis and plant regeneration of tropical maize genotypes. *Plant Cell Tissue Organ. Cult.* 102, 285–295. doi: 10.1007/s11240-010-9731-7

Anand, A., Bass, S. H., Wu, E., Wang, N., McBride, K. E., Annaluru, N., et al. (2018). An improved ternary vector system for *Agrobacterium*-mediated rapid maize transformation. *Plant Mol. Biol.* 97, 187–200. doi: 10.1007/s11103-018-0732-y

Armstrong, C. L., and Green, C. E. (1985). Establishment and maintenance of friable, embryogenic maize callus and the involvement of L-proline. *Planta* 164, 207–214. doi: 10.1007/BF00396083

Armstrong, C. L., Green, C. E., and Phillips, R. L. (1991). Development and availability of germplasm with high type II culture formation response. *Maize Genet. Coop. Newslett.* 65, 92–93.

Armstrong, C. L., Romero-Severson, J., and Hodges, T. K. (1992). Improved tissue culture response of an elite maize inbred through backcross breeding, and identification of chromosomal regions important for regeneration by RFLP analysis. *Theor. Appl. Genet.* 84, 755–762. doi: 10.1007/BF00224181

Banakar, R., Eggenberger, A. L., Lee, K., Wright, D., Murugan, K., Zarecor, S., et al. (2019). High-frequency random DNA insertions upon co-delivery of CRISPR-Cas9 ribonucleoprotein and selectable marker plasmid in rice. *Sci. Rep.* 9:19902. doi: 10.1038/s41598-019-55681-y

Barton, J. E., Maddock, S. E., Wu, X. E., Zhao, Z., Williams, M. E., Hussain, T., et al. (2014). *Doubling of chromosomes in haploid embryos. United States Patent US 8,859,846.*

Bianchi, G., Avato, P., and Salamini, F. (1975). Glossy mutants of maize. VI. chemical constituents of glossy-2 epicuticular waxes. *Maydica* 20, 165–173.

Bohorova, N., Zhang, W., Julstrum, P., McLean, S., Luna, B., Brito, R. M., et al. (1999). Production of transgenic tropical maize with cryIAb and cryIAc genes via microprojectile bombardment of immature embryos. *Theor. Appl. Genet.* 99, 437–444. doi: 10.1007/s001220051255

Brinkman, E. K., Chen, T., Amendola, M., and van Steensel, B. (2014). Easy quantitative assessment of genome editing by sequence trace decomposition. *Nucleic Acids Res.* 42:e168. doi: 10.1093/nar/gku936

Carvalho, C. H. S., Bohorova, N., Bordallo, P. N., Abreu, L. L., Valicente, F. H., Bressan, W., et al. (1997). Type II callus production and plant regeneration in tropical maize genotypes. *Plant Cell Rep.* 17, 73–76. doi: 10.1007/s002990050355

Char, S.-N., Neelakandan, A. K., Nahampun, H., Frame, B., Main, M., Spalding, M. H., et al. (2017). An *Agrobacterium*-delivered CRISPR/Cas9 system for high-frequency targeted mutagenesis in maize. *Plant Biotechnol. J.* 15, 257–268. doi: 10.1111/pbi.12611

Edwards, K., Johnstone, C., and Thompson, C. (1991). A simple and rapid method for the preparation of plant genomic DNA for PCR analysis. *Nucleic Acids Res.* 19:1349. doi: 10.1093/nar/19.6.1349

Frame, B. R., McMurray, J. M., Fonger, T. M., Main, M. L., Taylor, K. W., Torney, F. J., et al. (2006). Improved *Agrobacterium*-mediated transformation of three maize inbred lines using MS salts. *Plant Cell Rep.* 25, 1024–1034. doi: 10.1007/s00299-006-0145-2

Frame, B., Warnberg, K., Main, M., and Wang, K. (2015). "Maize (Zea mays L.)," in *Agrobacterium Protocols*, ed K. Wang (New York, NY: Springer Science+Business Media), 101–117. doi: 10.1007/978-1-4939-1695-5_8

Froger, A., and Hall, J. E. (2007). Transformation of plasmid DNA into *E. coli using the heat shock method. J. Vis. Exp.* 6:253. doi: 10.3791/253

Hsiau, T., Maures, T., Waite, K., Yang, J., Kelso, R., Holden, K., et al. (2018). Inference of CRISPR edits from sanger trace data. *bioRxiv* 251082. doi: 10.1101/251082

Hu, S., Hu, X., Hu, J., Shang, L., Dong, G., Zeng, D., et al. (2018). Xiaowei, a new rice germplasm for large-scale indoor research. *Mol. Plant.* 11, 1418–1420. doi: 10.1016/j.molp.2018.08.003

Ishida, Y., Saito, H., Hiei, Y., and Komari, T. (2003). Improved protocol for transformation of maize (*Zea mays* L.) mediated by *Agrobacterium tumefaciens*. *Plant Biotechnol.* 20, 57–66. doi: 10.5511/plantbiotechnology.20.57

Ishida, Y., Saito, H., Obta, S., Hiei, Y., Komari, T., and Kumashiro, T. (1996). High efficiency transformation of maize (*Zea mays* L.) mediated by *Agrobacterium tumefaciens*. *Nat. Biotechnol.* 14, 745–750. doi: 10.1038/nbt0696-745

Jinek, M., Chylinski, K., Fonfara, I., Hauer, M., Doudna, J. A., and Charpentier, E. (2012). A programmable dual-RNA-guided DNA endonuclease in adaptive bacterial immunity. *Science* 337, 816–821. doi: 10.1126/science.1225829

Jones, T., Lowe, K., Hoerster, G., Anand, A., Wu, E., Wang, N., et al. (2019). "Maize transformation using the morphogenic genes baby boom and wuschel2," in *Transgenic Plants, eds. S. Kumar, P. Barone and M. Smith (New York, NY: Humana Press),* 81–93. doi: 10.1007/978-1-4939-8778-8_6

Kato, A., and Geiger, H. H. (2002). Chromosome doubling of haploid maize seedlings using nitrous oxide gas at the flower primordial stage. *Plant Breed.* 121, 370–377. doi: 10.1046/j.1439-0523.2002.743321.x

Kelliher, T., Starr, D., Su, X., Tang, G., Chen, Z., Carter, J., et al. (2019). One-step genome editing of elite crop germplasm during haploid induction. *Nat. Biotechnol.* 37, 287–292. doi: 10.1038/s41587-019-0038-x

Komari, T. (1990). Transformation of cultured cells of *Chenopodium quinoa* by binary vectors that carry a fragment of DNA from the virulence region of pTiBo542. *Plant Cell Rep.* 9, 303–306. doi: 10.1007/BF00232856

Lee, K., Eggenberger, A. L., Banakar, R., McCaw, M. E., Zhu, H., Main, M., et al. (2019a). CRISPR/Cas9-mediated targeted T-DNA integration in rice. *Plant Mol. Biol.* 99, 317–328. doi: 10.1007/s11103-018-00819-1

Lee, K., Zhang, Y., Kleinstiver, B. P., Guo, J. A., Aryee, M. J., Miller, J., et al. (2019b). Activities and specificities of CRISPR-Cas9 and Cas12a nucleases for targeted mutagenesis in maize. *Plant Biotechnol. J.* 17, 362–372. doi: 10.1111/pbi.12982

Liu, K., Goodman, M., Muse, S., Smith, J. S., Buckler, E., and Doebley, J. (2003). Genetic structure and diversity among maize inbred lines as inferred from DNA microsatellites. *Genetics* 165, 2117–2128. Available online at: https://www.genetics.org/content/genetics/165/4/2117.full.pdf

Lowe, B. A., Way, M. M., Kumpf, J. M., Rout, J., Warner, D., Johnson, R., et al. (2006). Marker assisted breeding for transformability in maize. *Mol. Breed.* 18, 229–239. doi: 10.1007/s11032-006-9031-4

Lowe, K., La Rota, M., Hoerster, G., Hastings, C., Wang, N., Chamberlin, M., et al. (2018). Rapid genotype "independent" *Zea mays* L. *(maize) transformation via direct somatic embryogenesis. In vitro Cell. Dev. Biol. Plant* 54, 240–252. doi: 10.1007/s11627-018-9905-2

Lowe, K., Wu, E., Wang, N., Hoerster, G., Hastings, C., Cho, M.-J., et al. (2016). Morphogenic regulators baby boom and wuschel improve monocot transformation. *Plant Cell* 28, 1998–2015. doi: 10.1105/tpc.16.00124

Martinez, J. C., and Wang, K. (2009). A sterilization protocol for field-harvested maize mature seed used for *in vitro* culture and genetic transformation. *Maize. Genet. Coop. Newslett.* 83:2. Available online at: https://ftp.maizegdb.org/mnl/83/pdf%20files/01Martinez.pdf

Masters, A., Kang, M., McCaw, M., Zobrist, J., Gordon-Kamm, W., Jones, T., et al. (2020). *Agrobacterium*-mediated immature embryo transformation of recalcitrant maize inbred lines using morphogenic genes. *J. Vis. Exp.* 156:e60782. doi: 10.3791/60782

Mattanovich, D., Rüker, F., Machado, A. C., Laimer, M., Regner, F., Steinkellner, H., et al. (1989). Efficient transformation of *Agrobacterium* spp. *by electroporation. Nucleic Acids Res.* 17:6747. doi: 10.1093/nar/17.16.6747

McCaw, M. E., and Birchler, J. A. (2017). Handling fast-flowering mini-maize. *Curr. Protoc. Plant Biol.* 2, 124–134. doi: 10.1002/cppb.20051

McCaw, M. E., Wallace, J. G., Albert, P. S., Buckler, E. S., and Birchler, J. A. (2016). Fast-flowering mini-maize: seed to seed in 60 days. *Genetics* 204, 35–42. doi: 10.1534/genetics.116.191726

McCaw, M. E. (2017). *Pollinating Fast-Flowering Mini-Maize*. Available online at: https://www.youtube.com/watch?v=sK15NxMGFfg (accessed December 9, 2020).

Ombori, O., Muoma, J. V. O., and Machuka, J. (2013). *Agrobacterium*-mediated genetic transformation of selected tropical inbred and hybrid maize (*Zea mays* L.) lines. *Plant Cell Tissue Organ. Cult.* 113, 11–23. doi: 10.1007/s11240-012-0247-1

Raji, J. A., Frame, B., Little, D., Santoso, T., and Wang, K. (2018). "*Agrobacterium*- and biolistic- mediated transformation of maize B104 inbred," in *Maize: Methods and Protocols, ed. L. M. Lagrimini (New York, NY: Springer, USA)*, 15–40. doi: 10.1007/978-1-4939-7315-6_2

Ranch, J. P., Liebergesell, M., Garnaat, C. W., and Huffman, G. A. (2010). Auxotrophic *Agrobacterium* for plant transformation and methods thereof. *WO application WO 2010078445A1.*

Röber, F. K., Gordillo, G. A., and Geiger, H. H. (2005). *In vivo* haploid induction in maize – performance of new inducers and significance of doubled haploid lines in hybrid breeding. *Maydica* 50, 275–283.

Schnable, P. S., Pasternak, S., Liang, C., Zhang, J., Fulton, L., Graves, T. A., et al. (2009). The B73 maize genome: complexity, diversity, and dynamics. *Science* 326, 1112–1115. doi: 10.1126/science.1178534

Testroet, A., Lee, K., Luth, D., and Wang, K. (2017). Comparison of transformation frequency using *bar* gene driven by CaMV 35S or NOS promoter in *Agrobacterium*-mediated soybean (*Glycine max* L.) transformation. *In vitro Cell. Dev. Biol. Plant* 53, 188–199. doi: 10.1007/s11627-017-9810-0

Tomes, D. T., and Smith, O. S. (1985). The effect of parental genotype on initiation of embryogenic callus from elite maize (*Zea mays* L.) germplasm. *Theor. Appl. Genet.* 70, 505–509. doi: 10.1007/BF00305983

Tran, T. M., and Braun, D. M. (2017). An inexpensive, easy-to-use, and highly customizable growth chamber optimized for growing large plants. *Curr. Protoc. Plant Biol.* 2, 299–317. doi: 10.1002/cppb.20059

Valdez-Ortiz, A., Medina-Godoy, S., Valverde, M. E., and Paredes-López, O. (2007). A transgenic tropical maize line generated by the direct transformation of the embryo-scutellum by *A. tumefaciens. Plant Cell Tissue Organ. Cult.* 91, 201–214. doi: 10.1007/s11240-007-9286-4

Vanous, K., Vanous, A., Frei, U. K., and Lübberstedt, T. (2017). Generation of maize (*Zea mays*) doubled haploids *via* traditional methods. *Curr. Protoc. Plant Biol.* 2, 147–157. doi: 10.1002/cppb.20050

Wang, K., and Frame, B. (2004). "Maize transformation," in *Transgenic Crops of the World: Essential Protocols*. ed. I. Cutis (The Netherlands: Kluwer Academic Publisher), 45–62. doi: 10.1007/978-1-4020-2333-0_4

Yu, W., and Birchler, J. A. (2016). A green fluorescent protein-engineered haploid inducer line facilitates haploid mutant screens and doubled haploid breeding in maize. *Mol. Breed.* 36:5. doi: 10.1007/s11032-015-0428-9

Zetsche, B., Gootenberg, J. S., Abudayyeh, O. O., Slaymaker, I. M., Makarova, K. S., Essletzbichler, P., et al. (2015). Cpf1 is a single RNA-guided endonuclease of a class 2 CRISPR-cas system. *Cell* 163, 759–771. doi: 10.1016/j.cell.2015.09.038

Conflict of Interest: The authors declare that the research was conducted in the absence of any commercial or financial relationships that could be construed as a potential conflict of interest.

frontiers in Genome Editing

ORIGINAL RESEARCH
published: 20 January 2021
doi: 10.3389/fgeed.2020.621710

Fast-TrACC: A Rapid Method for Delivering and Testing Gene Editing Reagents in Somatic Plant Cells

Ryan A. Nasti[1,2,3], *Matthew H. Zinselmeier*[1,2,3], *Macy Vollbrecht*[1,2,3], *Michael F. Maher*[1,2,3,4] *and Daniel F. Voytas*[1,2,3]*

[1] Department of Genetics, Cell Biology and Development, University of Minnesota, St. Paul, MN, United States, [2] Center for Precision Plant Genomics, University of Minnesota, St. Paul, MN, United States, [3] Center for Genome Engineering, University of Minnesota, St. Paul, MN, United States, [4] Plant and Microbial Biology Graduate Program, University of Minnesota, St. Paul, MN, United States

The production of transgenic or gene edited plants requires considerable time and effort. It is of value to know at the onset of a project whether the transgenes or gene editing reagents are functioning as predicted. To test molecular reagents transiently, we implemented an improved, *Agrobacterium tumefaciens*-based co-culture method called Fast-TrACC (Fast Treated Agrobacterium Co-Culture). Fast-TrACC delivers reagents to seedlings, allowing high throughput, and uses a luciferase reporter to monitor and calibrate the efficiency of reagent delivery. We demonstrate the use of Fast-TrACC in multiple solanaceous species and apply the method to test promoter activity and the effectiveness of gene editing reagents.

Keywords: CRISPR, gene editing, plant, solanacaeae, *Agrobacterium tumefaciens*, reporter

OPEN ACCESS

Edited by:
Qi-Jun Chen,
China Agricultural University, China

Reviewed by:
Hui Zhang,
Shanghai Normal University, China
Keunsub Lee,
Iowa State University, United States

***Correspondence:**
Daniel F. Voytas
voytas@umn.edu

Specialty section:
This article was submitted to Genome Editing in Plants, a section of the journal Frontiers in Genome Editing

Received: *26 October 2020*
Accepted: *09 December 2020*
Published: *20 January 2021*

Citation:
Nasti RA, Zinselmeier MH, Vollbrecht M, Maher MF and Voytas DF (2021) Fast-TrACC: A Rapid Method for Delivering and Testing Gene Editing Reagents in Somatic Plant Cells. Front. Genome Ed. 2:621710. doi: 10.3389/fgeed.2020.621710

INTRODUCTION

Producing a gene edited plant requires considerable time, often from 6 to 9 months (Altpeter et al., 2016). Over this time period, significant effort must be put forth to identify edited cells in culture and induce them to form shoots and roots. Because of this investment in time and labor, it is important to know at the onset of an experiment whether the gene editing reagents can effectively create the desired genetic change. Typically, reagents are tested using transient assays to determine reagent efficacy within a shorter timescale. By comparing several different reagents in this manner the most efficient one can be selected and used to generate the gene edited plant. Currently, the most common transient delivery systems involve protoplasts (Lin et al., 2018) or leaf infiltrations (Janssen and Gardner, 1990; Ali et al., 2018). While both are effective, each has its own associated drawbacks. Protoplast isolation, where one removes the cell wall from plant cells, allows for transient transformation by chemical methods or electroporation. Isolating protoplasts is technically challenging and places the cells in an unnatural environment. On the other hand, leaf infiltration, performed by perfusion of *Agrobacterium tumefaciens* into a leaf with a needless syringe, is simple to perform but works with a limited number of plants, and time is required to grow plants to the proper stage for infiltration.

An alternative method, called AGROBEST, was developed for transient expression of transgenes in *Arabidopsis thaliana* (Wu et al., 2014). In this method Agrobacterium cultures are placed in media to promote expression of the *vir* genes, thereby improving the efficiency of T-DNA transfer to plant cells. With this increase in *vir* expression, one can deliver

a given T-DNA cargo by simply co-culturing Arabidopsis seedlings with the treated bacterial culture. We sought to use this approach to deliver T-DNA cargo to *Nicotiana benthamiana* seedlings, however, in order to achieve transformation, it was necessary to make changes to the concentration of bacteria used and the length of time the seedlings and bacteria were co-cultured (Maher et al., 2020). Specifically, increasing the Agrobacterium concentration and shortening co-culture times resulted in improvements in transgene delivery. This altered method, fast treated Agrobacterium co-culture (Fast-TrACC), was used to deliver developmental regulators to *N. benthamiana* seedlings to induce *de novo* meristems to create either transgenic or gene edited shoots (Maher et al., 2020).

The success of Fast-TrACC in *N. benthamiana* suggested that it might be generally useful as a transient DNA delivery method. Here we show success in using Fast-TrACC to efficiently deliver transgenes to other related species, including tomato (*Solanum lycopersicum*), potato (*Solanum tuberosum*), pepper (*Capsicum chinense*), and eggplant (*Solanum melongena*). We also used Fast-TrACC to compare the activity of various promoters in these species using a luciferase reporter, and we demonstrate that Fast-TrACC can quickly assess the activity of gene editing reagents at endogenous chromosomal targets. With relative ease, Fast-TrACC makes it possible to identify the reagents with highest activity prior to generating a gene edited plant line.

METHODS

DNA Constructs

All constructs generated for the Fast-TrACC experiments (**Supplementary Table 1**) were cloned into a T-DNA backbone to allow for Agrobacterium-mediated gene transfer. The majority of cloned T-DNA backbone includes sequence elements that produce Bean Yellow Dwarf Virus (BeYDV) or Tomato Leaf Curl Virus (ToLCV) geminiviral replicons, which circularize and replicate (Baltes et al., 2014). Replication increases copy number of the vector and consequently leads to high levels of gene expression. Whereas, replicons provide increased expression, they are not required, as non-replicon T-DNAs were used for the dual luciferase promoter comparison assay. Construct assembly was performed via a modular Golden Gate cloning platform (Čermák et al., 2017).

Two types of constructs were used in the Fast-TrACC experiments: luciferase reporter constructs and gene editing constructs. The reporter constructs were intended to express either firefly or Renilla luciferase (Thorne et al., 2010) using various promoters. Two types of promoters were tested: (1) strong promoters like cauliflower mosaic virus *35S* or Arabidopsis *Ubiquitin 10* (*AtUbi10*); (2) promoters with variable (Cestrum Yellow Leaf Curling Virus, *CmYLCV*) or undefined expression levels (Arabidopsis ribulose-1,5-bisphosphate carboxylase/oxygenase small subunit, *AtRbcs*) (Engler et al., 2014; Čermák et al., 2017). The gene editing T-DNA vectors were designed to express the RNA guided endonuclease, SpCas9, driven by the *35S* promoter along with either a single sgRNA expressed by the *AtU6* promoter or a sgRNA array expressed with the *35S* promoter (Čermák et al., 2017). Additionally, a luciferase reporter driven by either the *35S* or the *CmYLCV* promoter was used as a visual reporter for delivery of the gene editing construct.

Fast-TrACC

Fast-TrACC involves treating Agrobacterium cultures (GV3101) for 3 days prior to a 2 day co-culture with newly germinated seedlings. The first step is to grow the cultures overnight (8–12 h) in Luria broth (LB) with antibiotics [i.e., kanamycin (50 mg/mL) and gentamycin (50 mg/mL)] at 28°C. Next, cells are harvested by centrifugation and re-suspended to an OD_{600} of 0.3 in AB:MES200 salt solution (17.2 mM K_2HPO_4, 8.3 mM NaH_2PO_4, 18.7 mM NH_4Cl, 2 mM KCl, 1.25 mM $MgSO_4$, 100 μM $CaCl_2$, 10 μM $FeSO_4$, 50 mM MES, 2% glucose (w/v), 200 μM acetosyringone, pH 5.5) (Wu et al., 2014) and then grown overnight. The purpose of the AB:MES200 solution is to increase the expression of *vir* genes. The culture is again centrifuged and resuspended to OD_{600} within the range of 0.10–0.18 (typically 0.14) in a 50:50 (v/v) mix of AB:MES200 salt solution and ½ MS liquid plant growth medium (1/2 MS salt supplemented with 0.5% sucrose (w/v), pH 5.5).

Seeds are sterilized using 70% ethanol for 1 min and 50% bleach (v/v) (the hypochlorite concentration of the bleach was 7.4%) for 5 min. They are then rinsed 5 times with sterile water. Seeds are transferred to 6-well plates (∼5 seeds per well in 2 mL ½ MS) and maintained in growth chambers (24°C, 16/8 h light/dark cycle). Individual species vary on their germination times (defined as initial cotyledon emergence) in liquid ½ MS: canola seedlings germinate in 2–3 days, *N. benthamiana* seedlings germinate in 3–4 days, tomatoes and potatoes germinate in ∼7 days, peppers and eggplant germinate in ∼14 days. Two days post germination, ½ MS media is removed and the treated Agrobacterium culture is added. The co-cultured seedlings are incubated for 2 days before being washed free of Agrobacterium using sterile water. The washed seedlings are returned to liquid ½ MS containing the antibiotic timentin at a concentration of 100 μM to effectively counter-select against residual Agrobacterium.

GFP Imaging and Analysis

Seedlings were assessed for GFP fluorescence using a Nikon Model C-DSD115 stereoscope. Both bright field and GFP fluorescent images were captured from each individual seedling. Images were taken 3 days after removal from co-culture. The software ImageJ was used for GFP image analysis to count cells and determine effectiveness of delivery to each seedling. From the GFP images, the area corresponding to the cotyledons was selected, and background individual puncta were counted using the "Analyze Particles" function.

Firefly Luciferase Imaging

Seedlings are analyzed for delivery of the T-DNA constructs containing a firefly luciferase reporter through long exposure imaging. Luciferin substrate (5 μL of 50 mM in ddH_2O stock into 2 mL of ½ MS, final concentration of 125 μM luciferin in ½ MS) is added to the ½ MS liquid culture with the seedlings to produce light. The plate of seedlings is then lightly shaken for

5 min to ensure proper mixing of the luciferin solution. Long-exposure imaging (5.5 min exposure using a UVP BioImaging Systems EpiChemi^3 Darkroom) is then performed to capture the luminescence.

Dual Luciferase Assay

Dual luciferase assays were performed using the Promega Dual Luciferase® Reporter Assay System (Promega Cat. E1910) (Sherf et al., 1996). Treated seedlings were homogenized and resuspended in 1X passive lysis buffer, followed by passive lysis at 70 rpm for 15 min. Lysate was loaded into Grenier 96-well Lumitrac plates for analysis in the Berthold Technologies Centro XS^3 LB 960 Microplate Luminometer. One hundred microliter of prepared luciferase assay buffer II was injected into a single well, followed by measurement of firefly bioluminescence. Immediately following, 100 µL of prepared Stop & Glo® Buffer was injected into the same single well, and Renilla bioluminescence was measured. Relative Luciferase Units (RLUs) were calculated by taking the firefly:Renilla luminescence ratio, followed by normalization over the negative control. To perform fold change comparisons, the selected promoter's luminescence ratio was normalized over the luminescence ratio of the other promoters.

Testing for Editing

Gene editing frequencies in a given set of seedlings were measured by first extracting DNA extracted from selected tissues using CTAB. The isolated DNA was used as a template for PCR amplification of the target locus, and submitted either for next generation sequencing (NGS) (Campbell et al., 2015) or Sanger sequencing. Sanger traces were analyzed by TIDE (Brinkman et al., 2014), which uses software to de-convolute the Sanger peaks to determine editing efficiencies and outcomes. Sanger sequencing trace files from unedited plants were used as controls for the TIDE analysis. Primers for TIDE analysis were standard PCR primers, whereas the primers used for NGS contained 4bp barcodes in the forward and reverse directions, as well as Illumina adapters (**Supplementary Table 2**). Amplification products were submitted for NGS sequencing using GENEWIZ Amplicon-EZ services (www.genwiz.com). Each pool was de-multiplexed for unique forward and reverse adapters using ea-utils (Aronesty, 2013). Mutations were assessed for each de-multiplexed sample

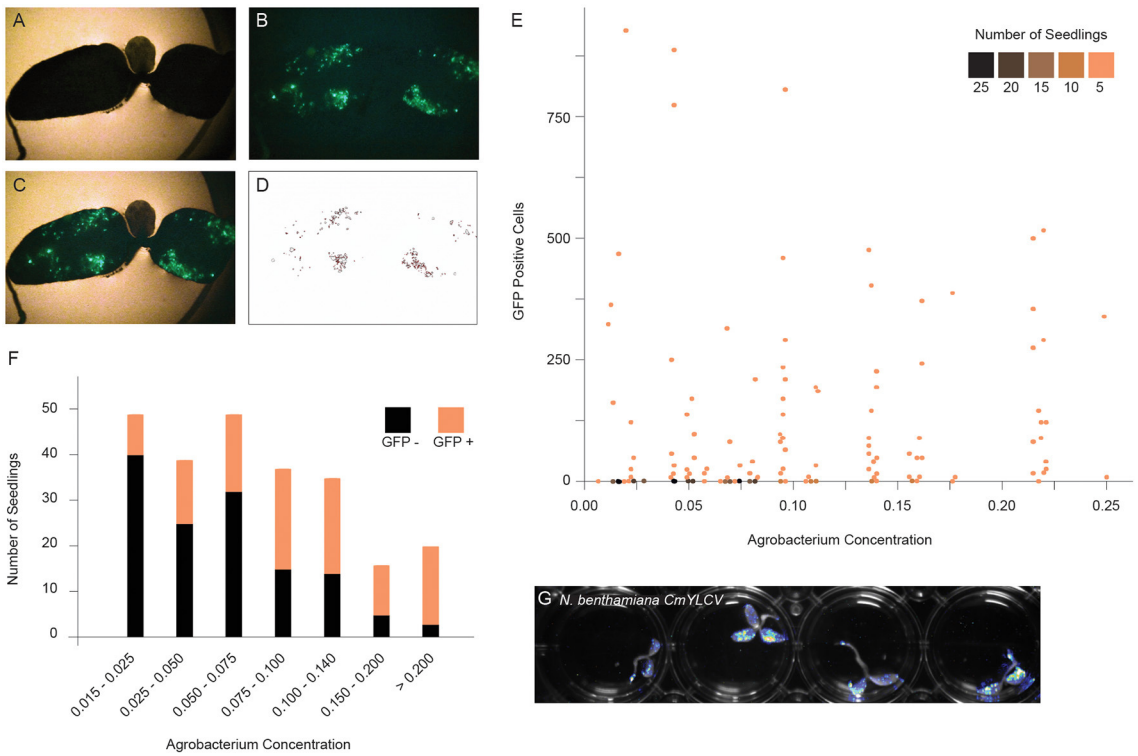

FIGURE 1 | Optimizing fast-TrACC conditions for *N. benthamiana*. To define the optimal co-culture conditions for gene transfer, constructs expressing GFP were delivered to *N. benthamiana* seedlings. After co-culture, seedlings were visualized for the presence of fluorescent signal. Bright field **(A)** and fluorescent images **(B)** were merged **(C)**, and the fluorescent signal was isolated over background **(D)**. Using these images, individual GFP positive sectors were counted. Seedlings were treated across a range of Agrobacterium concentrations, and the number of GFP positive sectors were tracked **(E)**. While seedlings with GFP positive sectors were observed at all bacterial concentrations, the number of negative seedlings was much higher at lower concentrations (**E,F**, black). The Agrobacterium concentration of $OD_{600} = 0.09$ represents the inflection point where an increasing percentage of seedlings showed fluorescence (**E,F**, orange). While the trend continued beyond $OD_{600} = 0.18$, there was a subsequent increase in tissue death beyond this concentration. In addition to fluorescent reporters, firefly luciferase can be delivered to *N. benthamiana* seedlings as illustrated here with the *CmYVLC* promoter **(G)**.

using Cas-Analyzer (Park et al., 2017). Minority read sequences (<10 reads) were considered background.

RESULTS

Optimizing Co-culture Conditions for Reliable Delivery of Transgenes to Multiple Species

The AGROBEST method was developed for Arabidopsis to deliver Agrobacterium T-DNAs to seedlings through co-culture (**Supplementary Figure 1A**) (Wu et al., 2014). When we tested the AGROBEST co-culture conditions (3 day co-culture, OD_{600} = 0.02) in *N. benthamiana,* we found that delivery of a GFP reporter, as measured by fluorescence, was barely detectable (Maher et al., 2020). Further, after a few days, considerable tissue necrosis was observed.

To implement a method for delivery of T-DNAs through co-culture to other plant species, we first developed a quantitative assay to measure expression of a GFP reporter in seedlings. The GFP reporter is on a geminiviral replicon to improve expression (**Supplementary Figure 1B**). Replicons undergo rolling circle replication and thereby significantly increase copy number of transgenes (Baltes et al., 2014). *N. benthamiana* seedlings were co-cultured with varying concentrations of bacteria, and after 2 days, seedlings were photographed under UV light, and GFP fluorescence was quantified by image analysis (**Figures 1A–D**, **Supplementary Figures 1C,D**). Although seedlings with GFP positive sectors were observed at all bacteria concentrations, the number of negative seedlings was much higher at lower concentrations (**Figure 1E**). The Agrobacterium concentration of OD_{600} = 0.09 was the inflection point, above which an increasing percentage of seedlings showed fluorescence (**Figure 1F**). While the trend of increased fluorescence continued beyond OD_{600} = 0.18, there was a subsequent increase in tissue death beyond this concentration. Ultimately, we selected a 2 day co-culture and an OD_{600} of ∼ 0.14. The GFP reporter could be swapped for firefly luciferase, allowing for rapid, whole plate imaging to monitor reagent delivery (**Figure 1G**).

The Fast-TrACC co-culture conditions used for *N. benthamiana* also worked well for tomato (**Figure 5**), potato (**Figure 6**), pepper, eggplant and canola (**Supplementary Figures 1F-H**). Constructs containing *AtUbi10:luciferase* were delivered to tomato seedlings and expression was observed across the seedlings (**Supplementary Figure 2**). To assess the transient nature of gene expression using Fast-TrACC, luciferase expression in tomato seedlings was monitored over a 72 h time period. T-DNAs containing either *35S: luciferase* or *AtUBQ10:luciferase* were imaged every 24 h after removal from co-culture. High levels of expression were observed at 24 h, which continually diminished over the next 48 h. Some expression is observed at all time points, which is presumably due to transgene integration. These observations define the timeframe of activity and allow for reagent assessment to be planned accordingly.

Using Fast-TrACC to Compare Promoter Activity in Different Species

We sought to determine if Fast-TrACC can be used to quickly assess promoter activity in different plant species. The *35S*, *AtUbi10* and *CmYLCV* promoters are all known to be effective at

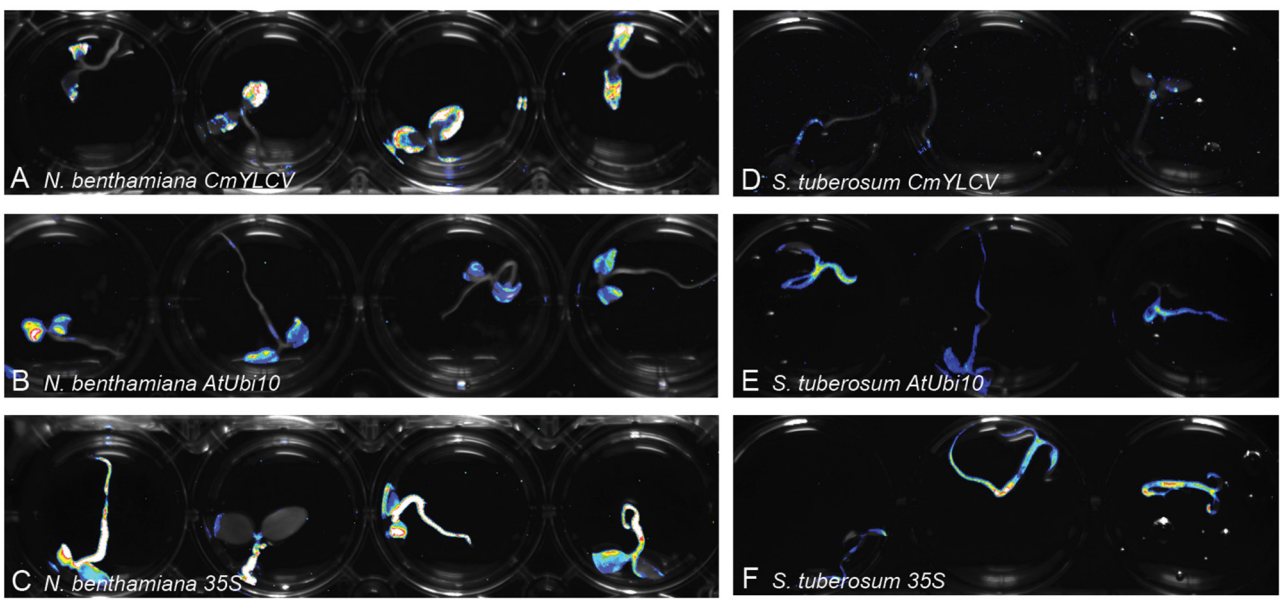

FIGURE 2 | Monitoring differences in promoter expression across species. Firefly luciferase expression was used to compare promoter activity in different species. Constructs encoding luciferase driven by the promoters *CmYLCV* **(A,D)**, *AtUbi10* **(B,E)**, and *35S* **(C,F)** were delivered to *N. benthamiana* **(A–C)** and potato **(D–F)** seedlings using Fast-TrACC. By taking long exposure images after delivery, promoter activity can be compared within a given species or across species. Expression patterns for each of the promoters was distinct. Out of the three tested promoters *CmYLCV* showed the greatest differences between species **(A,D)**. Testing new promoters to drive luciferase allows for their effectiveness to be determined in a species of interest.

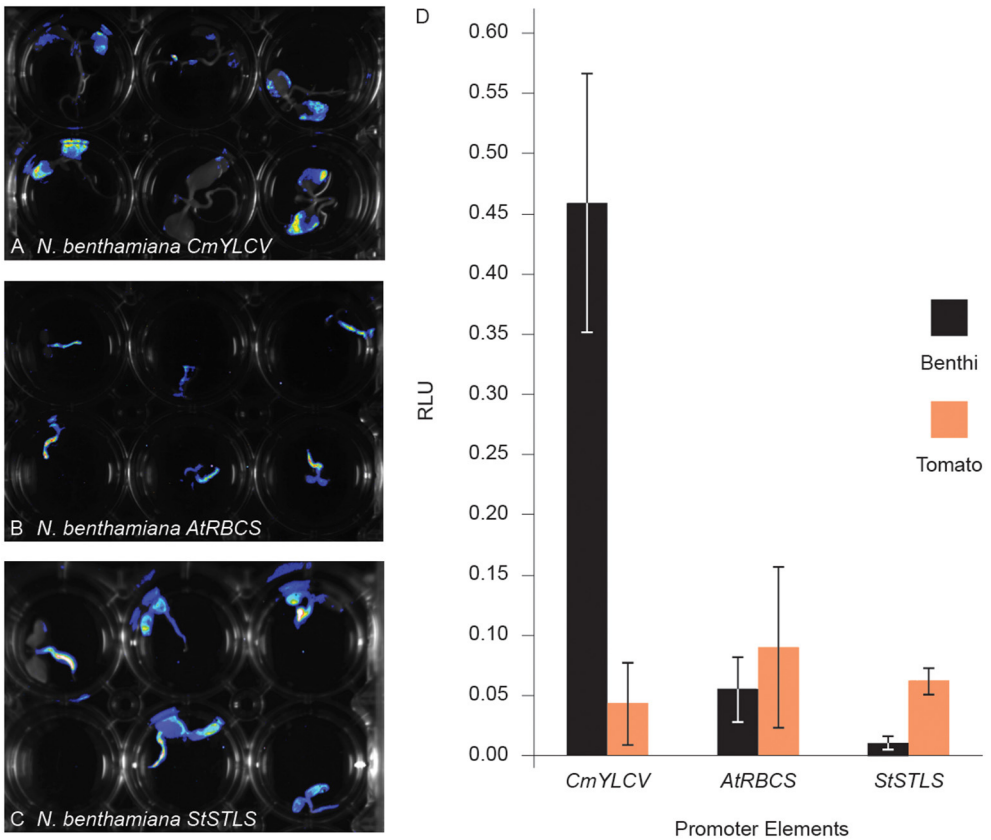

FIGURE 3 | Comparing promoter activity with fast-TrACC using a dual luciferase assay. Activity of three promoters, *CmYLCV* **(A)**, *AtRbcs3B* **(B)**, and *StSTLS* **(C)**, were compared in *N. benthamiana* and tomato. These promoters, driving firefly luciferase, were first delivered to *N. benthamiana* seedlings and qualitatively assessed for activity **(A–C)**. Once promoter activity was confirmed in *N. benthamiana*, T-DNAs with both *35S:Renilla* luciferase and the test promoters driving firefly luciferase were delivered to *N. benthamiana* and tomato seedlings. From seedling-derived lysates, luminescence was recorded for both luciferases. Between the two luminesce values, a relative luciferase unit (RLU) was calculated for the given promoter for direct comparison **(D)**. *CmYLCV* expression was 35-fold higher in *N. benthamiana* when compared to tomato, demonstrating the usefulness of Fast-TrACC for quantitative measurements of promoter activity. Error bars represent ± s.d.

driving gene expression in *N. benthamiana* (Engler et al., 2014; Čermák et al., 2017). We fused these promoters to luciferase, and delivered the constructs to potato (**Figure 2**), pepper, eggplant and canola via Fast-TrACC (**Supplementary Figure 3**). The *35S* and *AtUbi10* promoters performed well in all species; however, the *CmYLCV* was only functional in eggplant. Fast-TrACC, therefore, can be used to obtain a qualitative readout of promoter activity.

We next sought to determine if quantitative assessments of promoter activity can be achieved using Fast-TrACC. For this, we used a dual luciferase reporter assay (Sherf et al., 1996) to compare the 35S promoter to the *CmYLCV*, Arabidopsis ribulose-1,5-bisphosphate carboxylase/oxygenase small subunit 3B (*AtRbcs3B*), and the potato stem and leaf specific (*StSTLS*) promoters (**Figures 3A–C**). The three test promoters were fused to firefly luciferase and the *35S* promoter was fused to Renilla luciferase; all constructs were delivered to both *N. benthamiana* and tomato seedlings. While delivery varied, as determined by normalized Renilla luminescence (**Supplementary Figure 4**), relative expression trends for the test reporters could be discerned. *CmYLCV* yielded much higher expression in *N. benthamiana* than any other promoter in either species (**Figure 3D**), whereas the *AtRbcs3B* and *StSTLS* promoters were lower in expression and comparable in both species. Specifically, *CmYLCV* was 35-fold higher in expression in *N. benthamiana* relative to tomato, and within *N. benthamiana*, the *CmYLCV* promoter was 27- and 86-fold higher in expression than the *AtRbcs3B* and *StSTLS* promoters, respectively. These results demonstrate that quantitative comparisons can be made between promoter elements across species using Fast-TrACC.

Using Fast-TrACC to Test Activity of Gene Editing Reagents

We next tested whether Fast-TrACC could be used to deliver gene editing reagents to plants to assess their activity. In initial tests, we delivered 35S:Cas9 and a sgRNA targeting the *N. benthamiana phytoene desaturase* (*NbPDS*) locus (**Figure 4A**). DNA was isolated from each of six treated seedlings, the target site in *NbPDS* was PCR amplified, and the amplicon was subjected to NGS. Each of the six seedlings had gene editing efficiencies ranging from 30 to 95% (**Figure 4B**). No color change

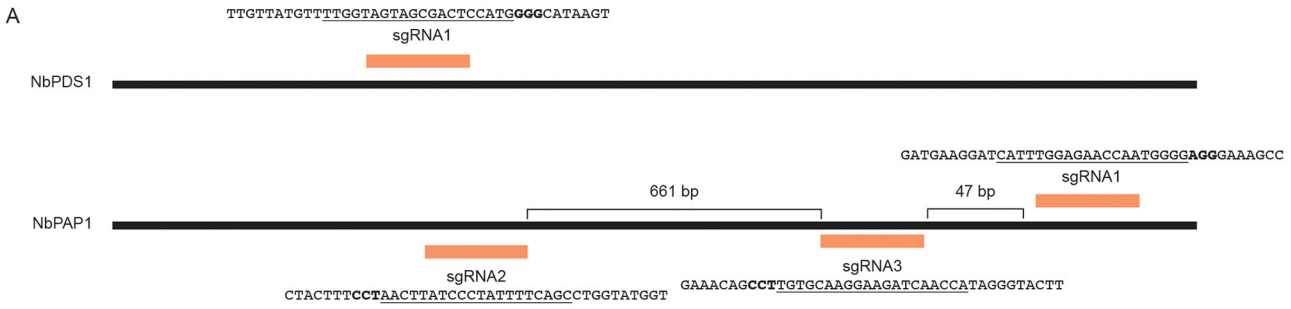

B

Sample	% Reads Edited	Most Common	2nd Common	3rd Common
1	88.1%	C Ins (48.9%)	8bp Del (14.8%)	A Ins (12.8%)
2	95.8%	C Ins (36.1%)	7bp Del (6.81%)	5bp Del (5.31%)
3	83.4%	C Ins (36%)	3bp Del (9.7%)	>10bp Del (9.1%)
4	92%	C Ins (37.3%)	8bp Del (9.6%)	>10bp Del (7.6%)
5	41%	>10bp Del (27.6%)	4bp Del (14.8%)	7bp Del (13.3%)
6	30.9%	C Ins (14%)	1bp Del (5.76%)	All other edits <5%

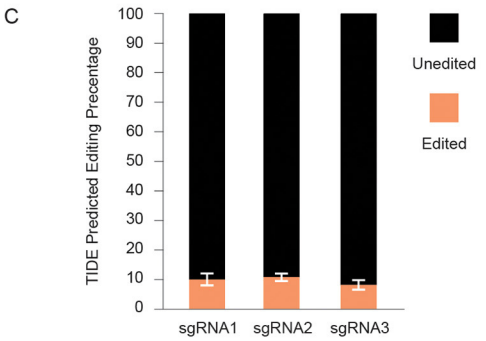

FIGURE 4 | Using fast-TrACC to determine gene editing efficiencies at distinct target sites in *N. benthamiana*. **(A)** Fast-TrACC was used to test a previously characterized sgRNA that targets *NbPDS1* in *N. benthamiana* as well as three untested sgRNAs targeting the *N. benthamiana* locus, *NbPAP1*. The sequences targeted by the sgRNAs are underlined and the PAM sequence is in bold. **(B)** DNA was prepared from six seedlings treated with reagents targeting *NbPDS1;* gene editing frequencies at *NbPDS1* were quantified by NGS. High frequency gene editing was observed in each sample, where editing efficiency is the percentage of total sequencing reads with a gene edit. **(C)** The frequency of editing for the three tested *NbPAP1* sgRNAs was substantially lower than the previously characterized *NbPDS1* sgRNA. sgRNA1 = 10.28% ± 2.18%; sgRNA2 = 11.12% ± 1.47; sgRNA3 = 8.38% ± 1.81.

was observed in the seedlings due to loss of *NbPDS*, likely because the cells were photosynthetically competent prior to editing. Additionally, three untested sgRNAs were designed to target the *PURPLE ACID PHOSPHATASE 1* (*NbPAP1)* locus (**Figure 4A**). Constructs expressing individual sgRNAs were delivered via Fast-TrACC, DNA was isolated from seedlings, and this time editing efficiency was estimated by Sanger-based TIDE analysis. Editing efficiencies were substantially lower for each sgRNA (9–13%, **Figure 4C**), demonstrating variability in editing across different targets within a species. Since these sgRNAs performed poorly, additional sgRNAs should be tested before attempting to make whole plants with edits in this gene.

We next determined if we could use Fast-TrACC to test the activity of gene editing reagents outside the *N. benthamiana* model. We delivered to tomato seedlings a constitutive *35S*::Cas9 and one of two sgRNAs (sgRNA1b & sgRNA7) (**Figure 5A**) that had previously been shown to work at the promoter of the tomato *Anthocyanin 1* (*SlANT1)* (Čermák et al., 2015). These reagents were assembled into T-DNA backbones that produce one of two different viral replicons derived from either Bean Yellow Dwarf Virus (BeYDV) or Tomato Leaf Curl Virus (ToLCV) (Baltes et al., 2014). Also included was a luciferase reporter. As evidenced by the pattern of luminescence (**Figures 5B–E**), delivery to tomato cotyledons was variable. Cotyledons with luciferase activity were collected, DNA was isolated, and the target site was PCR amplified and assessed for gene editing by NGS. The editing efficiency with sgRNA1b was modest, and editing was barely detectable with sgRNA7 (**Figure 5F**). When editing efficiencies were assessed at the individual seedling level, considerable variability was observed, likely due to differences in reagent delivery (**Figure 5G**). Despite the variable delivery, differences in the activity of sgRNAs could be discerned, with sgRNA1b editing at an appreciably higher efficiency on both replicons, whereas sgRNA7 showed little activity and only with the BeYDV replicon (**Figure 5F**). Thus, Fast-TrACC can be used to assess activity of gene editing reagents to inform decisions regarding sgRNA selection and vector design prior to engaging in lengthy protocols to create plants with heritable gene edits.

Fast-TrACC was also used to deliver Cas9, sgRNAs and a luciferase reporter to diploid potato seedlings. A previously published pair of sgRNAs targeting the *acetolactate synthase* (*StALS)* locus were used (**Figure 6A**) (Butler et al., 2015, 2016). The two sgRNAs were delivered together on a tRNA array to allow for individual sgRNAs to be processed from a single transcript. DNA was collected from the cotyledons of six seedlings with prominent luciferase expression (**Figures 6B–D**, numbered 1–6). The sgRNAs should at some frequency create a 235bp deletion

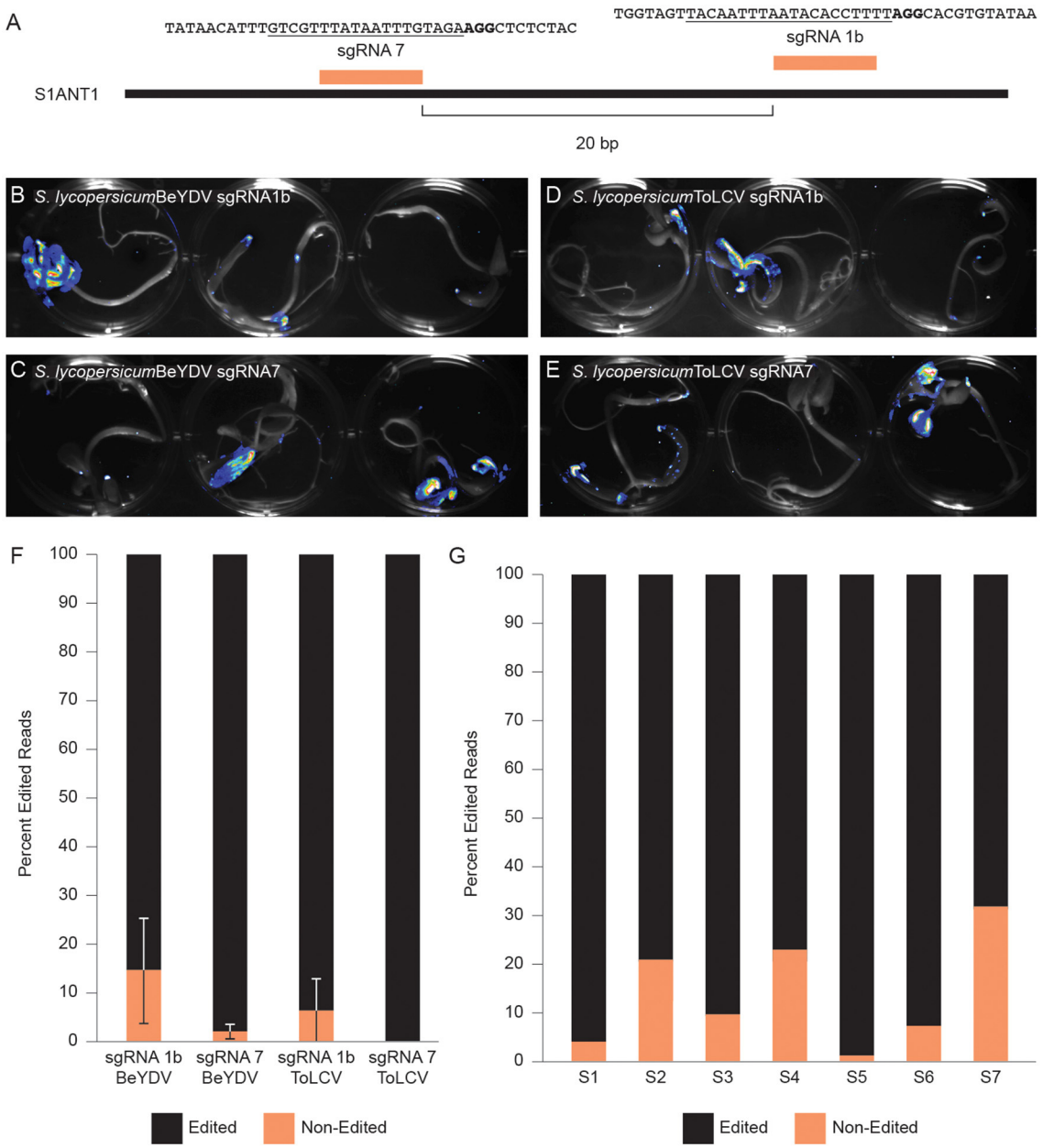

FIGURE 5 | Comparing gene editing efficiencies at a target locus in tomato. **(A)** Two distinct sgRNAs targeting the promoter of *SlANT1* were delivered via Fast-TrACC to tomato seedlings. The sequences targeted by the sgRNAs are underlined and the PAM sequence is in bold. The T-DNAs carried SpCas9, the sgRNAs and a luciferase reporter. These T-DNA sequences contain the required components to form either a BeYDV or ToLCV replicon. Delivery to tomato seedlings of BeYDV replicons with sgRNA1b **(B)** or sgRNA7 **(C)** or ToLCV replicons with sgRNA1b **(D)** or sgRNA7 **(E)** was monitored by luciferase expression and was variable across seedlings. From sectors showing strong luminescence, DNA was collected, and the target site was PCR- amplified and submitted for NGS. Based on the NGS sequencing results, sgRNA1b was more effective at generating edits **(F)** than sgRNA7. Additionally, the ToLCV replicon showed little or no activity **(F)**; Error bars represent ±s.d. When looking at individual seedlings treated with sgRNA1 on a BeYDV replicon, there was noticeable variability in the editing frequency **(G)** likely due to differential construct delivery.

between the sgRNA cut sites, which was observed in one of six tested seedlings (**Figure 6E**) and verified by DNA sequence analysis (**Figure 6F**). To this end, we were able to confirm a given set of reagents that generate edits in potato seedlings.

DISCUSSION

Creating transgenic or gene edited plants is a time-consuming task, often requiring months of effort. Prior to creating such plants, it is valuable to know whether the transgenes are

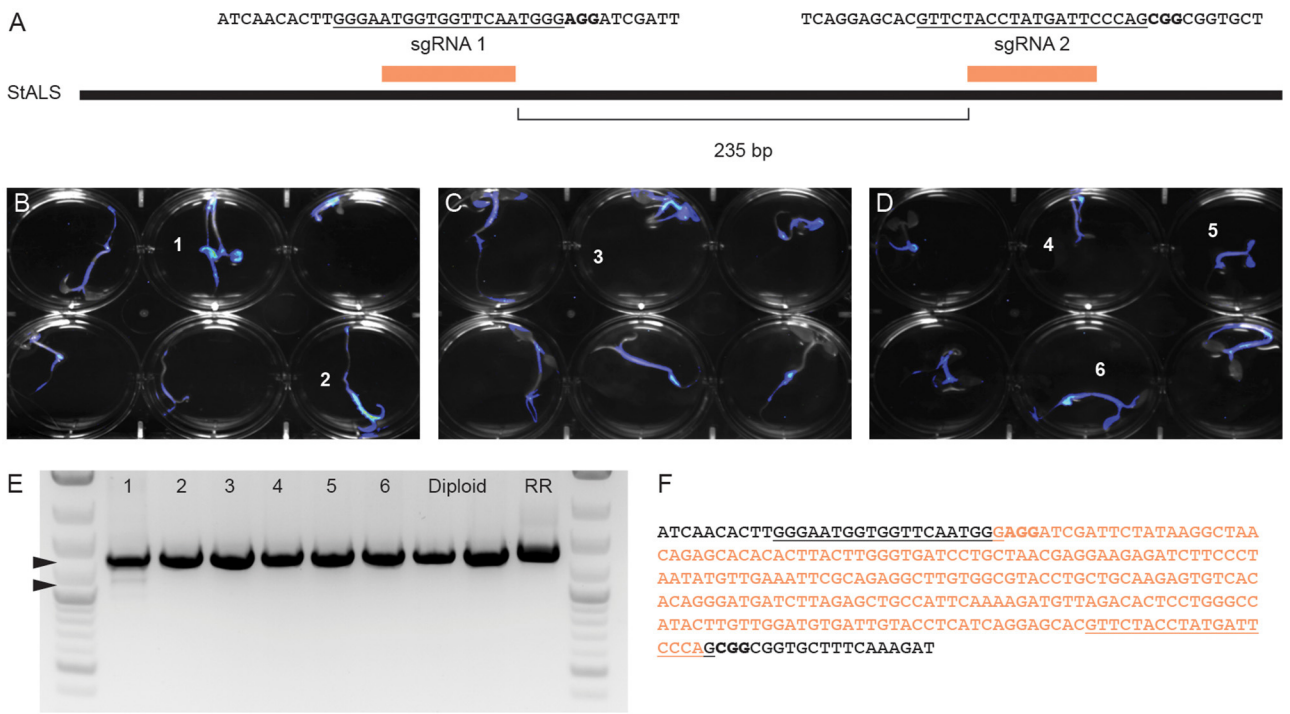

FIGURE 6 | Generating gene edits in potato seedlings. To test gene editing in diploid potato, two previously verified sgRNAs targeting *StALS* **(A)** were cloned into a single T-DNA vector and delivered via Fast-TrACC. The sequences targeted by the sgRNAs are underlined and the PAM sequence is in bold. DNA was isolated from the cotyledons of six seedlings (numbered) with the highest reporter expression **(B–D)**. The *StALS* locus was amplified **(E)** from these DNA samples and a deletion band (lower arrow) was observed in one of the six samples (sample 1, lower arrowhead). This deletion corresponds to the loss of the sequence between the cut sites of the two sgRNAs (**F**, removed sequence in orange, sgRNA sites underlined, PAM sites bolded).

functional or the gene editing reagents are effective in recognizing and cleaving their target sites. There are currently only a handful of ways to transiently test molecular reagents in plant cells, and each has drawbacks. The preparation of protoplasts from plant tissue is time-consuming, requires considerable expertise, and effective protocols are not available for many species. While leaf infiltrations with Agrobacterium are easy to perform, this method is only effective with a handful of plant species. Here we demonstrate that Fast-TrACC provides a quick, low-input, transient delivery method. Although the other methods may end up transforming a higher fraction of treated cells, Fast-TrACC's scalability and ease of implementation make it an attractive alternative for quickly testing the efficacy of molecular regents.

For expression control elements, such as promoters, we demonstrated that Fast-TrACC could be used for both qualitative and quantitative measurements using luciferase reporters. For example, it was very evident that the CmYLCV promoter had strong species specificity and functioned more effectively in *N. benthamiana* and eggplant than in tomato, potato or canola. Precise gene expression levels were quantified using a dual luciferase assay system. Because expression of test constructs is normalized to a Renilla luciferase cassette on the same T-DNA, the readout is analyzed only in the context of cells that received the construct. While promoters were the primary expression element tested, other expression control elements such as terminators and enhancers could also be tested in a similar fashion.

For gene editing reagents, comparisons could be made between individual sgRNAs targeting the same or different genomic loci. The editing efficiency discrepancies between sgRNAs at distinct genetic loci (as observed in *N. benthamiana*) or at a single locus (as observed in tomato) highlight how variable editing efficiencies can be at different genomic sites and with different sgRNAs and underscores the value in testing gene editing reagents prior to attempting to make gene edited plants. Further, broad species applicability was demonstrated by delivering editing reagents to three distinct species (*N. benthamiana*, tomato and potato). Fast-TrACC thus allows for rapid testing of editing reagents to inform reagent choice.

Fast-TrACC has applications beyond the testing of expression control elements or gene editing reagents. Other molecular reagents could be delivered, such as enzyme expression cassettes or T-DNA-encoded viruses. Previously, we used Fast-TrACC to deliver developmental regulators to whole seedlings, which promoted the formation of *de novo* shoots (Maher et al., 2020). When transgenes or gene editing reagents were co-delivered with the developmental regulators, transgenic or gene edited shoots were induced that transmitted genetic modifications to the next generation. Thus, Fast-TrACC enables a new approach for creating transgenic or gene edited plants.

One of the primary drawbacks to Fast-TrACC is variability in extent of transgene delivery. Agrobacterium is only able to transfer T-DNA to tissues in direct contact with the liquid

culture, which leads to certain portions of the seedling being missed, unless completely submerged. This mosaicism has an impact on the functional readout of either promoter activity or gene editing. As mentioned above, the dual luciferase assay addresses the problem of variable delivery, because the Renilla luciferase expression cassette is on the same T-DNA and therefore readouts of expression can be normalized to transformation frequency. For gene editing, efficiencies are underestimated because a fraction of cells never receive the T-DNA. This can be partially compensated for by co-delivering a reporter, and only harvesting and analyzing reporter-positive tissues. Finally, while we demonstrated delivery in a variety of different dicot species, with the exception of canola, all were members of the Solanaceae. Further experimentation will need to be done to determine how broadly Fast-TrACC can be applied across species, and whether, for example, it can be used to transiently transform monocots.

In summary, Fast-TrACC is a simple technique to quickly test molecular reagents for efficacy *in planta*. Although Fast-TrACC has limitations in that gene transfer is often not complete, this drawback is offset by the speed and high-throughput potential of the technique. We expect Fast-TrACC will quickly identify robust molecular reagents that can be applied to help answer lingering questions in the field of plant biology.

DATA AVAILABILITY STATEMENT

The raw data supporting the conclusions of this article will be made available by the authors, without undue reservation.

AUTHOR CONTRIBUTIONS

RN conceived of, implemented Fast-TrACC, directed all research, performed all experiments other than those noted below, and wrote the manuscript. MZ designed experiments to test promoter activity and carried out the dual luciferase assays. MM made some DNA constructs. MV carried out experiments in potato. DV edited the manuscript and supervised the research. All authors contributed to the article and approved the submitted version.

FUNDING

MZ and MM were funded from NIGMS T32-GM008347.

SUPPLEMENTARY MATERIAL

The Supplementary Material for this article can be found online at: https://www.frontiersin.org/articles/10.3389/fgeed.2020.621710/full#supplementary-material

REFERENCES

Ali, Z., Eid, A., Ali, S., and Mahfouz, M. M. (2018). Pea early-browning virus-mediated genome editing via the CRISPR/Cas9 system in *Nicotiana benthamiana* and *Arabidopsis*. *Virus Res.* 244, 333–337. doi: 10.1016/j.virusres.2017.10.009

Altpeter, F., Springer, N. M., Bartley, L. E., Blechl, A. E., Brutnell, T. P., Citovsky, V., et al. (2016). Advancing crop transformation in the era of genome editing. *Plant Cell* 28, 1510–1520. doi: 10.1105/tpc.16.00196

Aronesty, E. (2013). Comparison of sequencing utility programs. *Open Bioinformatics J.* 7, 1–8. doi: 10.2174/1875036201307010001

Baltes, N. J., Gil-Humanes, J., Cermak, T., Atkins, P. A., and Voytas, D. F. (2014). DNA replicons for plant genome engineering. *Plant Cell* 26, 151–163. doi: 10.1105/tpc.113.119792

Brinkman, E. K., Chen, T., Amendola, M., and van Steensel, B. (2014). Easy quantitative assessment of genome editing by sequence trace decomposition. *Nucleic Acids Res.* 42:e168. doi: 10.1093/nar/gku936

Butler, N. M., Atkins, P. A., Voytas, D. F., and Douches, D. S. (2015). Generation and inheritance of targeted mutations in potato (*Solanum tuberosum* L.) using the CRISPR/Cas system. *PLoS ONE* 10:e0144591. doi: 10.1371/journal.pone.0144591

Butler, N. M., Baltes, N. J., Voytas, D. F., and Douches, D. S. (2016). Geminivirus-mediated genome editing in potato (*Solanum tuberosum L.*) using sequence-specific nucleases. *Front Plant Sci.* 7:1045. doi: 10.3389/fpls.2016.01045

Campbell, N. R., Harmon, S. A., and Narum, S. R. (2015). Genotyping-in-Thousands by sequencing (GT-seq): a cost effective SNP genotyping method based on custom amplicon sequencing. *Mol. Ecol. Resour.* 15, 855–867. doi: 10.1111/1755-0998.12357

Čermák, T., Baltes, N. J., Čegan, R., Zhang, Y., and Voytas, D. F. (2015). High-frequency, precise modification of the tomato genome. *Genome Biol.* 16:232. doi: 10.1186/s13059-015-0796-9

Čermák, T., Curtin, S. J., Gil-Humanes, J., Čegan, R., Kono, T. J. Y., Konečná, E., et al. (2017). A multipurpose toolkit to enable advanced genome engineering in plants. *Plant Cell* 29, 1196–1217. doi: 10.1105/tpc.16.00922

Engler, C., Youles, M., Gruetzner, R., Ehnert, T. M., Werner, S., Jones, J. D., et al. (2014). A golden gate modular cloning toolbox for plants. *ACS Synth. Biol.* 3, 839–843. doi: 10.1021/sb4001504

Janssen, B. J., and Gardner, R. C. (1990). Localized transient expression of GUS in leaf discs following cocultivation with *Agrobacterium*. *Plant Mol. Biol.* 14, 61–72. doi: 10.1007/BF00015655

Lin, C. S., Hsu, C. T., Yang, L. H., Lee, L. Y., Fu, J. Y., Cheng, Q. W., et al. (2018). Application of protoplast technology to CRISPR/Cas9 mutagenesis: from single-cell mutation detection to mutant plant regeneration. *Plant Biotechnol. J.* 16, 1295–1310. doi: 10.1111/pbi.12870

Maher, M. F., Nasti, R. A., Vollbrecht, M., Starker, C. G., Clark, M. D., and Voytas, D. F. (2020). Plant gene editing through de novo induction of meristems. *Nat. Biotechnol.* 38, 84–89. doi: 10.1038/s41587-019-0337-2

Park, J., Lim, K., Kim, J. S., and Bae, S. (2017). Cas-analyzer: an online tool for assessing genome editing results using NGS data. *Bioinformatics* 33, 286–288. doi: 10.1093/bioinformatics/btw561

Sherf, B. A., Navarro, S. L., Hannah, R. R., and Wood, K. V. (1996). Dual-luciferaseTM reporter assay: an advanced co-reporter technology integrating firefly and Renilla luciferase assays. *Promega Notes* 57, 2–8.

Thorne, N., Inglese, J., and Auld, D. S. (2010). Illuminating insights into firefly luciferase and other bioluminescent reporters used in chemical biology. *Chem. Biol.* 17, 646–657. doi: 10.1016/j.chembiol.2010.05.012

Wu, H. Y., Liu, K. H., Wang, Y. C., Wu, J. F., Chiu, W. L., Chen, C. Y., et al. (2014). AGROBEST: an efficient Agrobacterium-mediated transient expression method for versatile gene function analyses in Arabidopsis seedlings. *Plant Methods* 10:19. doi: 10.1186/1746-4811-10-19

Conflict of Interest: The authors declare that the research was conducted in the absence of any commercial or financial relationships that could be construed as a potential conflict of interest.

frontiers in Genome Editing

BRIEF RESEARCH REPORT
published: 04 March 2021
doi: 10.3389/fgeed.2021.617553

Spelling Changes and Fluorescent Tagging With Prime Editing Vectors for Plants

*Li Wang[1], Hilal Betul Kaya[1,2], Ning Zhang[3], Rhitu Rai[1,4], Matthew R. Willmann[5], Sara C. D. Carpenter[1], Andrew C. Read[1], Federico Martin[6], Zhangjun Fei[3], Jan E. Leach[6], Gregory B. Martin[1,3] and Adam J. Bogdanove[1]**

[1] Plant Pathology and Plant-Microbe Biology Section, School of Integrative Plant Science, Cornell University, Ithaca, NY, United States, [2] Department of Bioengineering, Faculty of Engineering, Manisa Celal Bayar University, Manisa, Turkey, [3] Boyce Thompson Institute for Plant Research, Ithaca, NY, United States, [4] Plant Pathogen Interaction, National Institute for Plant Biotechnology (ICAR), New Delhi, India, [5] Plant Transformation Facility, School of Integrative Plant Science, Cornell University, Ithaca, NY, United States, [6] Department of Agricultural Biology, Colorado State University, Fort Collins, CO, United States

Prime editing is an adaptation of the CRISPR-Cas system that uses a Cas9(H840A)-reverse transcriptase fusion and a guide RNA amended with template and primer binding site sequences to achieve RNA-templated conversion of the target DNA, allowing specified substitutions, insertions, and deletions. In the first report of prime editing in plants, a variety of edits in rice and wheat were described, including insertions up to 15 bp. Several studies in rice quickly followed, but none reported a larger insertion. Here, we report easy-to-use vectors for prime editing in dicots as well as monocots, their validation in *Nicotiana benthamiana*, rice, and Arabidopsis, and an insertion of 66 bp that enabled split-GFP fluorescent tagging.

Keywords: prime editing, plant genome editing, fluorescent tagging, split GFP, *Oryza sativa*, Arabidopsis, *Nicotiana benthamiana*

OPEN ACCESS

Edited by:
Wendy Harwood,
John Innes Centre, United Kingdom

Reviewed by:
Anshu Alok,
University of Minnesota Twin Cities, United States
Tom Lawrenson,
John Innes Centre, United Kingdom

****Correspondence:***
Adam J. Bogdanove
ajb7@cornell.edu

Specialty section:
This article was submitted to Genome Editing in Plants, a section of the journal Frontiers in Genome Editing

Received: *15 October 2020*
Accepted: *10 February 2021*
Published: *04 March 2021*

Citation:
Wang L, Kaya HB, Zhang N, Rai R, Willmann MR, Carpenter SCD, Read AC, Martin F, Fei Z, Leach JE, Martin GB and Bogdanove AJ (2021) Spelling Changes and Fluorescent Tagging With Prime Editing Vectors for Plants. Front. Genome Ed. 3:617553. doi: 10.3389/fgeed.2021.617553

INTRODUCTION

Prime editing (PE) is an adaptation of the CRISPR-Cas system that uses a Cas9(H840A)-reverse transcriptase (RT) fusion and a guide RNA (pegRNA) amended with template and primer binding site (PBS) sequences to achieve RNA-templated conversion of the target DNA, allowing specified substitutions, insertions, and deletions (Anzalone et al., 2019). A second version of the system, PE2, incorporates an improved, engineered RT, and a third, PE3, adds to that a sgRNA directing a nick to the non-edited strand to drive its conversion (Anzalone et al., 2019).

Prime editing in plants was first reported by Lin et al. (2020), who achieved a variety of edits in rice and wheat. Several other studies in rice and one each in tomato, potato, and maize have been published since (Butt et al., 2020; Hua et al., 2020; Jiang et al., 2020; Li et al., 2020; Lu et al., 2020; Tang et al., 2020; Veillet et al., 2020; Xu et al., 2020a,b). While the editing efficiencies ranged from 1.55 to 31.3% in rice (Butt et al., 2020; Hua et al., 2020; Li et al., 2020; Lin et al., 2020; Tang et al., 2020; Xu et al., 2020a,b), the highest efficiency observed in tomato was 1.66% (Lu et al., 2020). Potato was similar to tomato (Veillet et al., 2020). The highest efficiency overall, 53.2%, was in maize, obtained by optimization of pegRNA expression (Jiang et al., 2020). In contrast to results in mammalian cells (Anzalone et al., 2019), PE3 did not increase editing efficiency in plants relative to PE2 (Butt et al., 2020; Lin et al., 2020; Veillet et al., 2020; Xu et al., 2020a). In some studies, in fact, PE2 yielded a much higher editing efficiency than PE3 (Jiang et al., 2020; Tang et al., 2020).

Unintended target site mutations including insertions, deletions, and substitutions were reported in almost all of the plant PE studies, though no unintended insertions or deletions were reported in maize (Jiang et al., 2020).

The largest targeted insertion by PE reported to date was in human cells, a 44-bp *loxP* tag (Anzalone et al., 2019). In plants, the largest insertion reported was 15 bp; attempts at larger insertions, up to 60 bp, were not successful (Lin et al., 2020). The apparent constraint on insertion length using prime editing potentially limits its application for introducing translational fusions, for example to a fluorescent protein for localization.

Here, we report easy-to-use vectors for PE in dicots and monocots, their validation in three plant species, and an insertion of 66 bp that enabled split-GFP fluorescent tagging. The vectors are suitable for PE2 or for PE3.

METHOD

Vector Construction

The binary vector for PE in dicots, pPPED, was constructed by replacing the 35S promoter and *Cas9* in binary vector p201N (Jacobs et al., 2015) with a double 35S promoter and *Cas9(H840A)* from pMOD_A0301 (Cermak et al., 2017) plus a commercially synthesized (Integrated DNA Technologies, Coralville, IA USA), tomato codon-optimized 34-aa flexible linker and engineered RT sequence (Anzalone et al., 2019), then adding a Gateway destination cassette (Thermo-Fisher, Waltham, MA USA). The smaller, non-binary vector for transfection or bombardment, pPPEDs, was created by moving these components into pBluescript KS(-). The binary vector for PE in monocots, pPPEM, was created by mutating pUbi-Cas9, which already contains a Gateway destination cassette (Zhou et al., 2014), to encode Cas9(H840A) using the Q5 Site-Directed Mutagenesis Kit (New England Biolabs, Ipswich, MA USA), then adding synthesized linker and RT sequence, optimized for rice. The entry vector for RNA modules, pPEG, was created by inserting into pCR8/GW/TOPO (Thermo-Fisher) a CmYLCV promoter-driven cassette containing two *Bsa*I sites across a short spacer for introducing module elements by Golden Gate cloning (Engler et al., 2008), with a gRNA scaffold downstream, together flanked one each side by an Arabidopsis pre-tRNA(Gly) gene sequence, and followed by the Arabidopsis *HSP18.2* gene terminator (sequences from Stavolone et al., 2003; Nagaya et al., 2010; Xie et al., 2015; Cermak et al., 2017) and, further downstream, a unique *Bae*I site downstream for inserting additional elements. Final PE constructs were prepared by introducing synthesized DNA sequence for the pegRNA with scaffold followed by tRNA(Gly) and an sgRNA spacer, and with a *Bsa*I site and compatible sequence at each end, into pPEG by Golden Gate reaction, then transferring the resulting module into pPPED, pPPEDs, or pPPEM by LR recombination.

Nicotiana benthamiana Agroinfiltration Assay

Transformants of *Agrobacterium tumefaciens* strain GV3101 carrying the helper plasmid pMP90 and pPPED or derivatives were grown in yeast extract peptone medium with the appropriate antibiotics overnight at 30°C. Bacteria were resuspended in infiltration buffer (10 mM $MgCl_2$, 10 mM MES [pH 5.6], and 200 mM acetosyringone) and were incubated with shaking for 2–4 h in the dark at room temperature. Bacterial cultures were then centrifuged, washed, resuspended in infiltration buffer, and adjusted to the final OD_{600} indicated in each experiment. Leaves of 5-week-old *Nicotiana benthamiana* plants were infiltrated using a needle-less syringe and were placed in a growth chamber (24°C day and 22°C night). Cell death was scored and photographed 6 or 12 days after infiltration. For amplicon sequencing, tissue was collected 6 days after infiltration, and DNA was extracted using the DNeasy Plant Mini Kit (Qiagen, Hilden, Germany), then PCR was performed using 50 ng of DNA and specific primers (**Supplementary Table 1**) with KAPA HiFi HotStart ReadyMix (Roche, Basel, Switzerland) in 25 μL reactions using the recommended protocol.

Rice Protoplast Assay

Seventy Oryza sativa ssp. japonica cv. Nipponbare seeds were sanitized in 70% ethanol for 2 min, followed by 40% commercial bleach for 30 min, then rinsed 5 times in autoclaved distilled water and dried on sterile filter paper. The sterile rice seeds were planted in 10 cm diameter glass jars on half MS media incubated in a growth chamber under a cycle of 12 h light at 28°C and 12 h dark at 25°C. After 12 days, the seedlings were used to isolate protoplasts as described (Shan et al., 2014) with the following modifications: filter-sterilized enzyme solution was added to the strips immediately (pre-incubation in 0.6 M mannitol was omitted), the strips were incubated in the dark for 7–8 h with gentle shaking at 100 rpm, and, after enzymatic digestion, W5 solution [2 mM MES (pH5.7), 154 mM NaCl, 125 mM $CaCl_2$, 5 mM KCl] was added and the digest shaken gently for 1 min to release the protoplasts; additionally, all centrifugation was carried out at 150 x g and supernatants were decanted by pouring. Protoplasts were quantified using a hemocytometer, and transfection was carried out using PEG as described (Shan et al., 2014) with the following modifications: the number of protoplasts used per transfection was 10^6, and in the final step, protoplasts were resuspended in 2 ml MMG solution [4 mM MES (pH5.7), 0.4 M mannitol, 15 mM $MgCl_2$] (instead of WI medium) before being incubated in a 6-well plate at 25°C in the dark for 2 days. Plasmid DNA for transfection was prepared using the HiSpeed Plasmid Maxi Kit (Qiagen) according to manufacturer instructions. For transfections with pPPEM or a derivative only, 15 μg was used. For transfections with an added pPEG construct, 15 μg of the pPPEM derivative and 4 μg of the pPEG construct were used. To estimate transformation efficiency, separately, protoplasts were transfected with 4 μg of pMOD_C3001 (Cermak et al., 2017) and 11 μg of pPEG (as carrier DNA) and imaged under an upright BX-50 fluorescence microscope (Olympus Corporation, Tokyo, Japan). For amplicon digests and sequencing, genomic DNA was isolated using the CTAB method (Allen et al., 2006), then PCR was performed using 40 ng of DNA and specific primers (**Supplementary Table 1**) with Q5 high-fidelity DNA polymerase (New England Biolabs) in 25-μL reactions using the recommended protocol. Selected PCR

products were digested using *Bst*Z17I (New England Biolabs) and analyzed by 1% agarose gel electrophoresis.

Arabidopsis Protoplast Assay

Arabidopsis protoplast transient expression experiments were done according to a published protocol (Yoo et al., 2007) except for a few modifications that follow. Plants were grown in Lambert Mix 1 (LM-1) in a Percival growth chamber at 22°C under a cycle of 16 h light and 8 h dark. Mesophyll protoplasts were isolated from fully-expanded leaves 5–8 of 4-week-old non-flowering plants. Digestion of 0.5–1.0 mm leaf strips was performed for 2 h in 1.5% cellulase R10 and 0.4% macerozyme R10 (Yakult Pharmaceutical Industry Company, Tokyo, Japan), 0.4 M mannitol, 20 mM KCl, 20 mM MES, pH 5.7, 10 mM $CaCl_2$, 0.1% BSA. The digest was then diluted 1:1 with W5 solution and filtered through Miracloth to remove undigested cellular debris. Following washing steps, the protoplasts were quantified using a hemocytometer and resuspended in MMG solution to 200,000 cells per ml. For each transfection, ∼50,000 protoplasts and 50 μg of plasmid DNA, prepared using the HiSpeed Plasmid Maxi Kit (Qiagen) according to manufacturer instructions, were used. Following transfection, the cells were transferred to WI solution as described (Yoo et al., 2007) except that following centrifugation, ∼100 ul of the buffer was left in the tube and used to resuspend and transfer the cells to one well of a 12-well culture dish having one 1 ml of WI solution. The cells were incubated at room temperature for 24 h prior to microscopy or centrifugation for DNA extraction. Transfection efficiency was estimated and DNA extraction was carried out as described for the rice protopasts, above, except that a 35S:eGFP construct was used (Chiu et al., 1996) and PCR was carried out with 10 ng of template DNA.

Amplicon Sequencing

Amplicons for sequencing (each <500 bp) were purified after 1% agarose gel electrophoresis by using the Monarch Gel Extraction Kit (New England Biolabs) and quantified with a NanoDrop 2000 spectrophotometer (Thermo Fisher). 500 ng of each was sent for commercial sequencing (Genewiz, South Plainfield, NJ USA) by indexed Illumina MiSeq paired-end (2 × 250 bp) reads. Reads were analyzed using CRISPResso2 v.2.0.37 (Clement et al., 2019). To determine the number of reads reflecting perfectly edited target DNA ("perfect-edit reads," with the edit and no other change) CRISPResso2 was run in HDR mode using a quantification window spanning 2 bp to the outside of the pegRNA and sgRNA nick sites and everything in between, and the number of perfect-edit reads was taken from the resulting alleles table (rather than being taken as the number of HDR reads, which does not exclude reads with a substitution or indel within the edit). Editing efficiency was calculated as (perfect-edit reads/total mapped reads)*100 divided by transfection efficiency and averaged across replicates (**Supplementary Table 2**). To calculate the proportion of "edit variants," reads containing the intended edit but also at least one other difference from the original sequence within the large quantification window, the total number of edit reads was first determined by a separate CRISPResso2 analysis using a smaller window that examined only the intended edit, then the number of perfect-edit reads was subtracted from that total and the result divided by the number of perfect-edit reads.

RESULTS AND DISCUSSION

Vectors and Strategy for PE in Plants

We created a binary vector for use in dicots, pPPED, and a binary vector for use in monocots, pPPEM; we also created a smaller, non-binary version of pPPED, pPPEDs, for transfection or bombardment (**Figure 1A**). The vectors encode, respectively, codon-optimized Cas9(H840A) fusions to the engineered RT and a Gateway destination cassette (Thermo-Fisher) for addition of an RNA module, either pegRNA for PE2 or pegRNA and sgRNA for PE3. We created an entry vector for the RNA modules, pPEG, that allows insertion of a synthetic dsDNA by Golden Gate cloning (Engler et al., 2008) (**Figure 1A**). pPEG also has a unique restriction enzyme site downstream of the RNA module cloning site and before the *attL2* site for introducing additional elements. To prepare a construct, pegRNA sequence without scaffold (PE2), or pegRNA with scaffold followed by tRNA(Gly) and an sgRNA spacer (PE3), with a *Bsa*I site and compatible sequence at each end, is synthesized and introduced by Golden Gate reaction into pPEG, then the resulting module is transferred by LR recombination into pPPED, pPPEDs, or pPPEM (**Figure 1B**). Our editing strategy for testing the vectors was PE3. Example peg- and sgRNAs are shown in **Figure 1C**. A schematic and sequence for preparing RNA modules is given in **Figure 1D**.

An Episomal 2-bp Substitution by Agroinfiltation of *N. benthamiana* Leaves

First, we tested pPPED by agroinfiltration of *N. benthamiana* leaves (**Figure 2A**). The target was a mutated allele of the *avrRpt2* gene of the bacterial plant pathogen *Pseudomonas syringae* (*avrRpt2[C122A]*; (Mazo-Molina et al., 2020), delivered on t-DNA by a co-infiltrated *Agrobacterium* strain. The AvrRpt2 protein elicits programmed cell death in *N. benthamiana*, and the C122A mutation abolishes this activity. The edit, GC to TG at codon 122, would correct the coding sequence to wild type and restore the gene's ability to elicit plant cell death, which can be assessed readily by eye. Together with *avrRpt2(C122A)*, pPPED carrying a pegRNA/sgRNA module for the edit (pPPED1), but not empty pPPED and not pPPED1 alone, resulted in cell death. To estimate efficiency, we determined the sensitivity of the assay by co-infiltrating different ratios of *avrRpt2* and *avrRpt2(C122A)* strains. The *avrRpt2* strain was sufficient for cell death at OD_{600} =0.0025 (1:19) but not at OD_{600} = 0.0005 (1:99). Thus, in the editing experiment, in which the *avrRpt2(C122A)* strain was at OD_{600} = 0.5, more than 0.1% (0.0005/0.5) and likely 0.5% (0.0025/0.5) or more of the delivered *avrRpt2(C122A)* was converted to wild type. Amplicon deep sequencing detected only 0.06 ± 0.03% (standard deviation, four infiltrations), likely because the template included *avrRpt2(C122A)* on the vector in *Agrobacterium*, not exposed to the PE reagent.

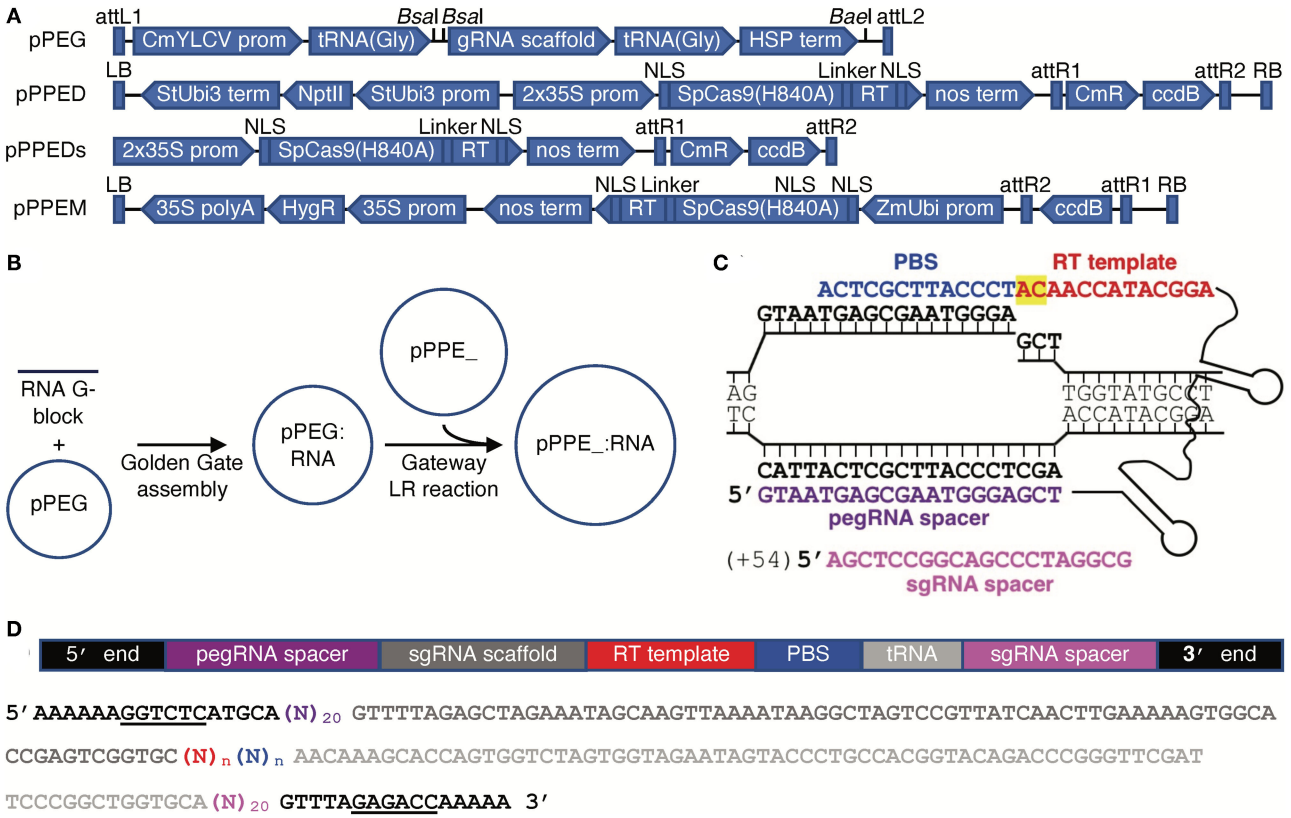

FIGURE 1 | Vectors and construct assembly for PE in plants. **(A)** Features of each vector (vectors and annotated sequences available at www.addgene.org). **(B)** Workflow for generating PE constructs. **(C)** A pegRNA on its target, showing the PBS (blue), RT template (red, with the edit highlighted in yellow), spacer (purple), and nick site, and, for PE3, the sgRNA (magenta) with the position of its nick site relative to the pegRNA-mediated nick in parentheses. **(D)** Schematic and color-matched sequence of an RNA module including compatible ends for Golden Gate cloning into pPEG (*Bsa*I sites underlined), pegRNA spacer, sgRNA scaffold, RT template and PBS (of unspecified lengths, *n*), and optionally a tRNA(Gly) and sgRNA spacer.

Chromosomal 2-bp Substitution and 25-bp Insertion Edits in Rice Protoplasts

Having established the functionality of the dicot binary vector by using agroinfiltration to edit a co-delivered t-DNA, we turned next to the monocot vector, pPPEM, and an endogenous chromosomal target. We tested pPPEM in rice (cv. Nipponbare) protoplasts, targeting two different edits to the bacterial leaf streak disease susceptibility gene *OsSULTR3;6* (LOC_Os01g52130; Cernadas et al., 2014) (**Figure 2B**). The first edit, GG to CC, eliminates the stop codon and introduces a *Bst*Z17I site. In three transfections with pPPEM carrying the pegRNA/sgRNA module for the edit (pPPEM2), but not in a control transfection with empty pPPEM, *Bst*Z17I digestion of PCR product spanning the target confirmed editing. Amplicon sequencing revealed efficiencies ranging from 0.7 to 2.2%, when adjusted for transfection efficiency (∼41%). An equimolar amount of entry vector carrying the RNA module, pPEG2, added to the pPPEM2 transfections did not increase average editing efficiency (unpaired, one tail *t*-test, $p < 0.05$).

The second edit we attempted, at the same location, was a 25-bp insertion for translational fusion of the FLAG epitope (**Figure 2C**). We carried out three transfections with the editing construct, pPPEM3, and three more with the corresponding pPEG plasmid, pPEG3, added. Amplicon sequencing confirmed insertion, but at relatively low adjusted efficiency, not significantly altered by pPEG3 (0.02 ± 0.01 and 0.01 ± 0.00%, respectively).

A 66-bp Insertion Allowing Split GFP Tagging in Arabidopsis Protoplasts

Finally, we tested pPPEDs in protoplasts of Arabidopsis lines expressing β strands 1–10 of optimized super-fold green fluorescent protein targeted to the cytoplasm, CYTO-sfGFP1-10^{OPT}, or nucleus, NUC-sfGFP1-10^{OPT} (Park et al., 2017). The edit was a 66-bp insertion encoding a linker and GFP11. We reasoned that a split-GFP approach could enable fluorescent tagging despite the apparent insertion size limitation of PE. Indeed, CYTO-sfGFP1-10^{OPT} transfections with a pPPEDs construct, pPPEDs4, targeting the insertion to the cytosolic prefoldin chaperone subunit family protein gene AT1G26660.1 yielded fluorescent protoplasts (**Figure 2D**), while control transfections of NUC-sfGFP1-10^{OPT} with the same construct,

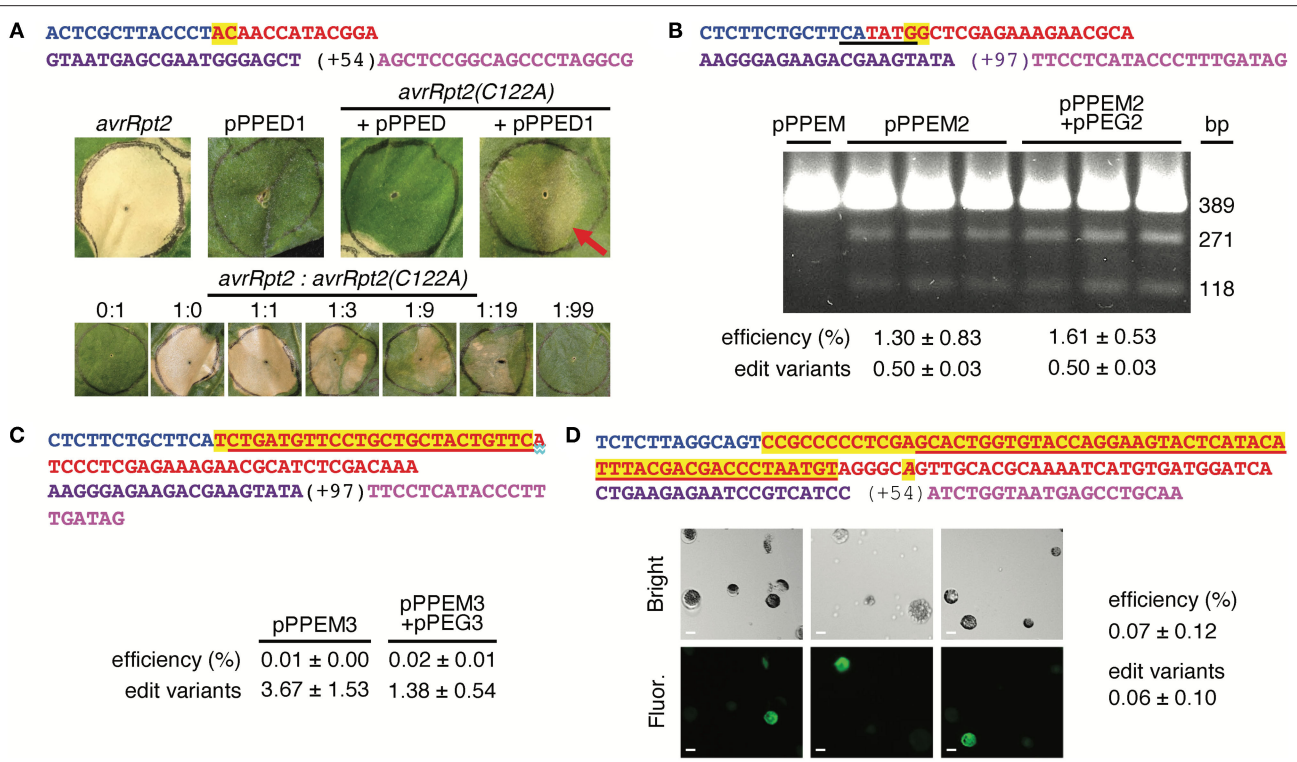

FIGURE 2 | Use of the vectors for spelling changes and tag insertions in three plant species. **(A)** A 2-bp edit of *avrRpt2*(*C122A*) using agroinfiltration of *Nicotiana benthamiana (N. benthamiana)* leaves. Top, features of the pegRNA and sgRNA, colored as in **Figure 1C**. Middle, leaves 12 days after introduction of *avrRpt2* (OD_{600} = 0.05), or pPPED1, *avrRpt2(C122A)* and empty pPPED, or *avrRpt2(C122A)* and pPPED1 (each at final OD_{600} = 0.5). Bottom, leaves 6 days after infiltration of different ratios of strains delivering *avrRpt2* or *avrRpt2(C122A)*, both at OD_{600} = 0.05 before mixing. These experiments were repeated twice and yielded results consistent with those shown. **(B)** A 2-bp substitution at *OsSULTR3;6* in rice protoplasts. Top, pegRNA and sgRNA features with *Bst*Z17I site underlined. Below, *Bst*Z17I digests of a 389-bp fragment spanning the target amplified from protoplasts transfected with empty pPPEM, pPPEM2, or pPPEM2 and equimolar pPEG2; 271-bp and 118-bp cleavage products indicate the presence of the *Bst*Z17I site introduced by the edit. **(C)** A 25-bp insertion for FLAG tagging at *OsSULTR3;6*. Top, pegRNA and sgRNA features, with FLAG coding sequence underlined. **(D)** A 60-bp insertion for fusion of GFP11 at AT1G26660.1 in Arabidopsis CYTO-sfGFP1-10^{OPT} protoplasts. Top, pegRNA and sgRNA features, with GFP11 coding sequence underlined and a substitution in the pegRNA PAM italicized. Below, bright field and fluorescence micrographs of protoplasts from replicate transfections; scale bar, 10 μm. Bottom of e-g, editing efficiencies determined by amplicon deep-sequencing adjusted for transfection efficiency, and, relative to the number of perfect-edit reads set as 1, the number of edit variant reads (see text). Only perfect-edit reads were counted in determining editing efficiency. Amplicon sequences were analyzed using CRISPResso2 (Clement et al., 2019).

or of CYTO-sfGFP1-10^{OPT} with a pPPEDs construct, pPPEDs5, targeting the insertion to the histone 2B gene (AT5G22880), did not. Transfection of NUC-sfGFP1-10^{OPT} protoplasts with pPPEDs5 targeting the histone 2B gene, though expected to yield fluorescence, did not detectably do so. The pPPEDs4 RT template includes a C to A substitution 6 bp after the GFP11 sequence that destroys the pegRNA PAM, a strategy proposed to limit indel formation between the PE3 nicks and to disfavor reversion of the edited strand (Anzalone et al., 2019). Amplicon sequencing of the CYTO- and NUC-sfGFP1-10^{OPT} transfections with pPPEDs4 (three each) confirmed successful insertion, averaging 0.07 ± 0.12% adjusted efficiency.

Editing Efficiencies

For all edits, the positive amplicon reads included some with other differences from the original sequence in the window encompassing the nick sites and edit plus 2 bp on either side, and some of the insertion edit reads had one or more substitutions or indels in the insertion. The frequencies of these "edit variants" (combined) are given in **Figure 2**. Edit variants were not counted in the reported efficiencies. They may represent non-templated changes during DNA repair, spontaneous mutations, or PCR or sequencing artifact. Notably, in the 66-bp insertion experiment in Arabidopsis protoplasts, sequencing of the AT1G26660.1 amplicon from negative control transfection of CYTO-sfGFP1-10^{OPT} with pPPEDs5, and from a transfection of NUC-GFP1-10^{OPT} with pPPEDs5, yielded an average of 6.4 ± 4.0% reads varying from the original sequence. This relatively high background suggests that editing efficiencies in this and the other experiments may have been higher than we calculated counting only perfect reads. Sequence variants without the edit but with an indel or substitution appearing to have arisen due to imperfect non-homologous end joining of a double strand break, presumably resulting from the pegRNA- and sgRNA-mediated nicks together, were detected in all of the sequenced test samples, at high frequencies relative to the edit (**Supplementary Figure 1**).

For the 2-bp substitution edits, it is possible that some of the perfect-edit reads resulted from substitutions that exactly duplicate the intended edit but that occurred by chance during repair of the cut DNA, or during PCR amplification or sequencing. To examine this possibility, we searched the variant reads from the 25-bp edit at *OsSULTR3;6* for any that by chance match the perfect-edit sequence for the 2-bp substitution at *OsSULTR3;6*, which was targeted to precisely the same nick site. Across the six total pPEM3 and pPEM3 plus pPEG3 sequence sets, an average of 0.04 ± 0.01% of the reads matched the perfect-read sequence for the 2-bp edit (**Supplementary Table 3**). This frequency is 17- to 55-fold lower than the frequencies of perfect-edit reads in the amplicon sequences from the actual 2-bp edit experiments (pPEM2 and pPEM2 plus pPEG2, above). Thus, contribution of non-templated substitutions, or PCR or sequencing artifact to the calculated efficiencies for the smaller edits can be considered negligible.

For the 25-bp and 66-bp insertion edits, the observation of fluorescent protoplasts for the latter notwithstanding, it is conceivable that the small numbers of positive reads are artifact resulting from template switching during PCR amplification. Template switching, first described in the 1990's (Paabo et al., 1990; Odelberg et al., 1995) has been found to be a rare source of erroneous, chimeric reads in high throughput sequence sets (Kebschull and Zador, 2015). In each of the two insertion-edit amplicon sequence sets, since the primers used anneal to the genomic DNA and not to the construct, two template switches would have had to occur for artifactual positive reads to have been generated, which can be expected to be exceedingly rare. Nonetheless, to control for the possibility in each case, we deep-sequenced amplicon generated from a mixed template of untransfected protoplast DNA and a 2-fold higher molar amount of the editing construct, 40 ng rice cv. Nipponbare DNA with pPPEM3 for the 25-bp edit and 10 ng Arabidopsis CYTO-sfGFP1-10^{OPT} DNA with pPPEDs4 for the 66-bp edit. None of the resulting aligned reads (averaging 16,672 and 46,631 reads, respectively, across two replicates each) contained the respective insertion sequences, perfect or variant.

SUMMARY

In summary, we developed vectors for straightforward plant PE construct assembly and demonstrated their efficacy in one monocot and two dicot species. Edits included two 2-bp codon changes, a 25-bp FLAG tag insertion, and a 66-bp GFP11 insertion. The 66-bp insertion is the largest reported for PE and provides important proof of concept for fluorescent tagging using PE. Editing efficiencies, especially for insertions, were low. However, efficiencies are likely to be higher in stably transformed plants or with meristem transformation (Maher et al., 2020), and possibly with optimization of RT template and PBS length (Lin et al., 2020; Tang et al., 2020; Xu et al., 2020a), and the vectors thus useful in extending PE to diverse plant species.

DATA AVAILABILITY STATEMENT

The datasets presented in this study can be found in online repositories. The names of the repository/repositories and accession number(s) can be found below: <https://www.ncbi.nlm.nih.gov/, PRJNA641949>.

AUTHOR CONTRIBUTIONS

LW, HK, NZ, RR, MW, AR, FM, JL, GM, and AB conceived and designed the study. LW, NZ, RR, and MW performed the experiments. LW, HK, NZ, RR, MW, SC, ZF, GM, and AB analyzed data. All authors contributed to preparation of the manuscript.

FUNDING

This work was supported by the National Science Foundation (IOS-1444511 to AB and JL, and IOS-1546625 to GM), the National Institute of Food and Agriculture of the U.S. Department of Agriculture (2018-67011-28025 to AR), the Indo-U.S. Science and Technology Forum, Government of India (fellowship to RR), and Manisa Celal Bayar University Scientific Research Projects funds (2017-113 to HK). Fluorescence microscopy was performed at the Imaging Facility of the Biotechnology Resource Center at Cornell University's Institute of Biotechnology, which was supported by the National Institutes of Health (S10RR025502).

ACKNOWLEDGMENTS

This manuscript has been released as a pre-print at bioRxiv (Wang et al., 2020).

SUPPLEMENTARY MATERIAL

The Supplementary Material for this article can be found online at: https://www.frontiersin.org/articles/10.3389/fgeed.2021.617553/full#supplementary-material

REFERENCES

Allen, G. C., Flores-Vergara, M. A., Krasynanski, S., Kumar, S., and Thompson, W. F. (2006). A modified protocol for rapid DNA isolation from plant tissues using cetyltrimethylammonium bromide. *Nat. Protoc.* 1, 2320–2325. doi: 10.1038/nprot.2006.384

Anzalone, A. V., Randolph, P. B., Davis, J. R., Sousa, A. A., Koblan, L. W., Levy, J. M., et al. (2019). Search-and-replace genome editing without double-strand breaks or donor DNA. *Nature* 576, 149–157. doi: 10.1038/s41586-019-1711-4

Butt, H., Rao, G. S., Sedeek, K., Aman, R., Kamel, R., and Mahfouz, M. (2020). Engineering herbicide resistance via prime editing in rice. *Plant Biotechnol. J.* 18:2370–2. doi: 10.1111/pbi.13399

Cermak, T., Curtin, S. J., Gil-Humanes, J., Cegan, R., Kono, T. J. Y., Konecna, E., et al. (2017). A multipurpose toolkit to enable advanced genome engineering in plants. *Plant Cell* 29, 1196–1217. doi: 10.1105/tpc.16.00922

Cernadas, R. A., Doyle, E. L., Nino-Liu, D. O., Wilkins, K. E., Bancroft, T., Wang, L., et al. (2014). Code-assisted discovery of TAL effector targets in bacterial leaf streak of rice reveals contrast with bacterial blight and a novel susceptibility gene. *PLoS Path.* 10:e1003972. doi: 10.1371/journal.ppat.1003972

Chiu, W., Niwa, Y., Zeng, W., Hirano, T., Kobayashi, H., and Sheen, J. (1996). Engineered GFP as a vital reporter in plants. *Curr. Biol.* 6, 325–330. doi: 10.1016/S0960-9822(02)00483-9

Clement, K., Rees, H., Canver, M. C., Gehrke, J. M., Farouni, R., Hsu, J. Y., et al. (2019). CRISPResso2 provides accurate and rapid genome editing sequence analysis. *Nat. Biotechnol.* 37, 224–226. doi: 10.1038/s41587-019-0032-3

Engler, C., Kandzia, R., and Marillonnet, S. (2008). A one pot, one step, precision cloning method with high throughput capability. *PLoS ONE* 3:e3647. doi: 10.1371/journal.pone.0003647

Hua, K., Jiang, Y., Tao, X., and Zhu, J. K. (2020). Precision genome engineering in rice using prime editing system. *Plant Biotechnol. J.* 18, 2167–2169. doi: 10.1111/pbi.13395

Jacobs T. B., LaFayette P. R., Schmitz R. J., Parrott W. A. (2015). Targeted genome modifications in soybean with CRISPR/Cas9. *BMC Biotechnol.* 15:16 doi: 10.1186/s12896-015-0131-2

Jiang, Y. Y., Chai, Y. P., Lu, M. H., Han, X. L., Lin, Q., Zhang, Y., et al. (2020). Prime editing efficiently generates W542L and S621I double mutations in two ALS genes in maize. *Genome Biol.* 21:257. doi: 10.1186/s13059-020-02170-5

Kebschull, J. M., and Zador, A. M. (2015). Sources of PCR-induced distortions in high-throughput sequencing data sets. *Nucleic Acids Res.* 43:e143. doi: 10.1093/nar/gkv717

Li, H., Li, J., Chen, J., Yan, L., and Xia, L. (2020). Precise modifications of both exogenous and endogenous genes in rice by prime editing. *Mol. Plant* 13, 671–674. doi: 10.1016/j.molp.2020.03.011

Lin, Q., Zong, Y., Xue, C., Wang, S., Jin, S., Zhu, Z., et al. (2020). Prime genome editing in rice and wheat. *Nat. Biotechnol.* 38, 582–585. doi: 10.1038/s41587-020-0455-x

Lu, Y., Tian, Y., Shen, R., Yao, Q., Zhong, D., Zhang, X., et al. (2020). Precise genome modification in tomato using an improved prime editing system. *Plant Biotechnol. J.* doi: 10.1111/pbi.13497. [Epub ahead of print].

Maher, M. F., Nasti, R. A., Vollbrecht, M., Starker, C. G., Clark, M. D., and Voytas, D. F. (2020). Plant gene editing through *de novo* induction of meristems. *Nat. Biotechnol.* 38, 84–89. doi: 10.1038/s41587-019-0337-2

Mazo-Molina, C., Mainiero, S., Haefner, B. J., Bednarek, R., Zhang, J., Feder, A., et al. (2020). *Ptr1* evolved convergently with *RPS2* and *Mr5* to mediate recognition of AvrRpt2 in diverse solanaceous species. *Plant J.* 103, 1433–1445. doi: 10.1111/tpj.14810

Nagaya, S., Kawamura, K., Shinmyo, A., and Kato, K. (2010). The HSP terminator of *Arabidopsis thaliana* increases gene expression in plant cells. *Plant Cell Physiol.* 51, 328–332. doi: 10.1093/pcp/pcp188

Odelberg, S. J., Weiss, R. B., Hata, A., and White, R. (1995). Template-switching during DNA synthesis by *Thermus aquaticus* DNA polymerase I. *Nucleic Acids Res.* 23, 2049–2057. doi: 10.1093/nar/23.11.2049

Paabo, S., Irwin, D. M., and Wilson, A. C. (1990). DNA damage promotes jumping between templates during enzymatic amplification. *J. Biol. Chem.* 265, 4718–4721. doi: 10.1016/S0021-9258(19)39621-8

Park, E., Lee, H. Y., Woo, J., Choi, D., and Dinesh-Kumar, S. P. (2017). Spatiotemporal monitoring of *Pseudomonas syringae* effectors via type III secretion using split fluorescent protein fragments. *Plant Cell* 29, 1571–1584. doi: 10.1105/tpc.17.00047

Shan, Q., Wang, Y., Li, J., and Gao, C. (2014). Genome editing in rice and wheat using the CRISPR/Cas system. *Nat. Protoc.* 9, 2395–2410. doi: 10.1038/nprot.2014.157

Stavolone, L., Kononova, M., Pauli, S., Ragozzino, A., De Haan, P., Milligan, S., et al. (2003). Cestrum yellow leaf curling virus (CmYLCV) promoter: a new strong constitutive promoter for heterologous gene expression in a wide variety of crops. *Plant Mol. Biol.* 53, 663–673. doi: 10.1023/B:PLAN.0000019110.95420.bb

Tang, X., Sretenovic, S., Ren, Q., Jia, X., Li, M., Fan, T., et al. (2020). Plant prime editors enable precise gene editing in rice cells. *Mol. Plant* 13, 667–670. doi: 10.1016/j.molp.2020.03.010

Veillet, F., Kermarrec, M.-P., Chauvin, L., Guyon-Debast, A., Chauvin, J.-E., Gallois, J.-L., et al. (2020). Prime editing is achievable in the tetraploid potato but needs improvement. *bioRxiv* 2020:159111. doi: 10.1101/2020.06.18.159111

Wang, L., Kaya, H. B., Zhang, N., Rai, R., Willmann, M. R., Carpenter, S. C. D., et al. (2020). Spelling changes and fluorescent tagging with prime editing vectors for plants. *bioRxiv* 2020:206276. doi: 10.1101/2020.07.16.206276

Xie, K., Minkenberg, B., and Yang, Y. (2015). Boosting CRISPR/Cas9 multiplex editing capability with the endogenous tRNA-processing system. *Proc. Natl. Acad. Sci. U.S.A.* 112, 3570–3575. doi: 10.1073/pnas.1420294112

Xu, R., Li, J., Liu, X., Shan, T., Qin, R., and Wei, P. (2020a). Development of plant prime-editing systems for precise genome editing. *Plant Commun.* 1:100043. doi: 10.1016/j.xplc.2020.100043

Xu, W., Zhang, C., Yang, Y., Zhao, S., Kang, G., He, X., et al. (2020b). Versatile nucleotides substitution in plant using an improved prime editing system. *Mol. Plant* 13, 675–678. doi: 10.1016/j.molp.2020.03.012

Yoo, S. D., Cho, Y. H., and Sheen, J. (2007). Arabidopsis mesophyll protoplasts: a versatile cell system for transient gene expression analysis. *Nat. Protoc.* 2, 1565–1572. doi: 10.1038/nprot.2007.199

Zhou, H., Liu, B., Weeks, D. P., Spalding, M. H., and Yang, B. (2014). Large chromosomal deletions and heritable small genetic changes induced by CRISPR/Cas9 in rice. *Nucleic Acids Res.* 42, 10903–10914. doi: 10.1093/nar/gku806

Conflict of Interest: The authors declare that the research was conducted in the absence of any commercial or financial relationships that could be construed as a potential conflict of interest.

frontiers in Genome Editing

ORIGINAL RESEARCH
published: 29 April 2021
doi: 10.3389/fgeed.2021.654996

Multiallelic, Targeted Mutagenesis of Magnesium Chelatase With CRISPR/Cas9 Provides a Rapidly Scorable Phenotype in Highly Polyploid Sugarcane

Ayman Eid[1,2], *Chakravarthi Mohan*[2], *Sara Sanchez*[1,2], *Duoduo Wang*[1,2] *and Fredy Altpeter*[1,2,3,4]*

[1] Agronomy Department, Institute of Food and Agricultural Sciences, University of Florida, Gainesville, FL, United States, [2] Department of Energy Center for Advanced Bioenergy and Bioproducts Innovation, Gainesville, FL, United States, [3] Genetics Institute, University of Florida, Gainesville, FL, United States, [4] Plant Molecular and Cellular Biology Program, Institute of Food and Agricultural Sciences, Gainesville, FL, United States

Genome editing with sequence-specific nucleases, such as clustered regularly interspaced short palindromic repeats (CRISPR)/CRISPR-associated protein 9 (Cas9), is revolutionizing crop improvement. Developing efficient genome-editing protocols for highly polyploid crops, including sugarcane (x = 10–13), remains challenging due to the high level of genetic redundancy in these plants. Here, we report the efficient multiallelic editing of magnesium chelatase subunit I (*MgCh*) in sugarcane. Magnesium chelatase is a key enzyme for chlorophyll biosynthesis. CRISPR/Cas9-mediated targeted co-mutagenesis of 49 copies/alleles of magnesium chelatase was confirmed via Sanger sequencing of cloned PCR amplicons. This resulted in severely reduced chlorophyll contents, which was scorable at the time of plant regeneration in the tissue culture. Heat treatment following the delivery of genome editing reagents elevated the editing frequency 2-fold and drastically promoted co-editing of multiple alleles, which proved necessary to create a phenotype that was visibly distinguishable from the wild type. Despite their yellow leaf color, the edited plants were established well in the soil and did not show noticeable growth retardation. This approach will facilitate the establishment of genome editing protocols for recalcitrant crops and support further optimization, including the evaluation of alternative RNA-guided nucleases to overcome the limitations of the protospacer adjacent motif (PAM) site or to develop novel delivery strategies for genome editing reagents.

Keywords: CRISPR/Cas9, genome editing, polyploid, magnesium chelatase, sugarcane, biolistic gene transfer, heat treatment

OPEN ACCESS

Edited by:
Wendy Harwood,
John Innes Centre, United Kingdom

Reviewed by:
Anshu Alok,
University of Minnesota Twin Cities, United States
Hongliang Zhu,
China Agricultural University, China

***Correspondence:**
Fredy Altpeter
altpeter@ufl.edu

Specialty section:
This article was submitted to Genome Editing in Plants, a section of the journal Frontiers in Genome Editing

Received: *18 January 2021*
Accepted: *15 March 2021*
Published: *29 April 2021*

Citation:
Eid A, Mohan C, Sanchez S, Wang D and Altpeter F (2021) Multiallelic, Targeted Mutagenesis of Magnesium Chelatase With CRISPR/Cas9 Provides a Rapidly Scorable Phenotype in Highly Polyploid Sugarcane. Front. Genome Ed. 3:654996. doi: 10.3389/fgeed.2021.654996

INTRODUCTION

The processing of sugarcane (*Saccharum* spp. hybrid) biomass provides 80% of the sugar and 26% of the ethanol produced globally. Sugarcane is one of the most productive crops under cultivation due to its superior light conversion and efficiencies of water and nitrogen use (Tew and Cobill, 2008; Byrt et al., 2011). It is also a prime candidate feedstock for the emerging bio-economy

(Altpeter and Ratna, 2018). The highly polyploid (x = 10 − 13; 2n = 100 − 130), heterozygous, interspecific, and aneuploid sugarcane genome decelerates attempts at crop improvement (Le Cunff et al., 2008; de Setta et al., 2014). Most parental sugarcane clones lack pollen fertility and any synchrony of flowering, posing challenges to conventional breeding (Moore and Nuss, 1987; Horsley and Zhou, 2013). Elite cultivars display a high level of heterozygosity and polyploidy, requiring vegetative propagation to prevent the loss of favorable alleles and the accumulation of detrimental ones during the disruptive process of meiosis. Therefore, adding superior alleles to improve an elite cultivar with the use of conventional breeding is a demanding and time-consuming undertaking. Genome editing using sequence-specific nucleases (SSNs) is a powerful approach for the genetic improvement of crops (Zhang et al., 2018). It has great potential for sugarcane and other vegetatively propagated, heterozygous, and polyploid crops (Weeks, 2017) by enabling precision genome modifications in elite varieties while bypassing meiosis. Among the SSNs, RNA-guided nucleases, including CRISPR/Cas9, are the most widely used gene editing tools due to their target specificity, efficiency, simplicity of design, multiplexing capacity, and versatility (Chandrasegaran and Carroll, 2016). They have been repurposed to targeted mutagenesis, gene stacking, targeted nucleotide substitutions, chromosomal translocations, transcriptional or translational regulation, and viral interference (Jinek et al., 2012; Shan et al., 2013; Ali et al., 2015; Baltes et al., 2015; Svitashev et al., 2015; Zhang et al., 2018; Huang and Puchta, 2019; Beying et al., 2020; Gao et al., 2020).

Most approaches to genome editing require a DNA double-strand break (DSB) in or near the target sequence to be edited. *Streptococcus pyogenes* Cas9 (spCas9) possesses innate nuclease activity, which is targeted by an engineered, single 20 nt guide RNA molecule to the DNA cleavage site adjacent to a protospacer-associated motif (PAM) (Jinek et al., 2012). Then DNA cleavage triggers cellular repair mechanisms, including non-homologous end joining (NHEJ), microhomology-mediated end joining (MMEJ), and homology-directed repair (HDR), to rectify the DSB. The error-prone NHEJ and MMEJ repair pathways enable the construction of knockout alleles through frameshift mutations caused by indels. By contrast, HDR supports precision edits, including targeted codon replacements and gene stacking. HDR relies on recombination, using a template that displays homology to the break site (Puchta, 1998; Shrivastav et al., 2008; Chapman et al., 2012; Butt et al., 2019; Huang and Puchta, 2019).

Targeted mutagenesis is more challenging in highly polyploid crops such as sugarcane than in diploid crops. The large number of homeologs and homologs in sugarcane causes functional redundancy. However, this also offers an opportunity to generate a range of phenotypes, depending on the number of co-mutated copies/alleles, similar to RNAi. The creation of knockdown or knockout phenotypes requires an efficient multiallelic editing platform. We recently reported the TALEN-mediated targeted co-mutagenesis of more than 100 copies/alleles of the lignin biosynthetic gene *caffeic acid O-methyltransferase* (*COMT*) in sugarcane. This action resulted in drastically improved saccharification efficiency and greater bioethanol yields from the lignocellulosic biomass without compromising agronomic performance (Jung and Altpeter, 2016; Kannan et al., 2018; Ko et al., 2018).

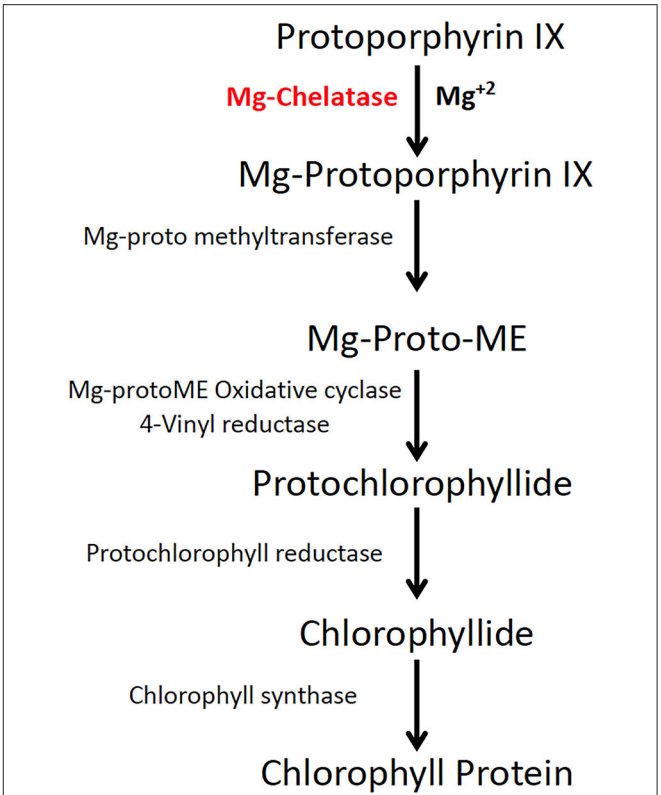

FIGURE 1 | Magnesium chelatase is a key enzyme in the chlorophyll biosynthesis pathway. Magnesium chelatase catalyzes the conversion of protoporphyrin IX (PPIX) to magnesium protoporphyrin IX, a precursor of chlorophyll b and a in the presence of Mg^{2+} and ATP. The enzyme is a hexameric motor complex made up of three proteins, ChlI, ChlD, and ChlH.

The establishment of CRISPR/Cas9-mediated genome editing for sugarcane is desirable for improving multiplexing capacity, versatility, and ease of design relative to TALEN (Eid and Mahfouz, 2016). This will involve the optimization of genome editing reagents and their delivery to enable efficient co-editing of a large number of copies/alleles.

These optimizations are accelerated with the help of a rapidly scorable screening system that allows the visual identification and quantification of targeted mutations as soon as plants regenerate from tissue cultures. To establish genome editing protocols in other crops, the phytoene desaturase (*PDS*) gene in the carotenoid biosynthetic pathway was targeted for mutagenesis (Shan et al., 2013; Fan et al., 2015). Unlike dwarf and albino phenotypes of PDS knockouts, Mg-chelatase mutants display a light green to yellow leaf phenotype with similar growth rates to the wild type (WT) (Walker et al., 2018). Mg-chelatase catalyzes Mg^{2+} attachment to protoporphyrin IX, which is the major regulatory point for the chlorophyll biosynthesis pathway (**Figure 1**) (Willows et al., 1996).

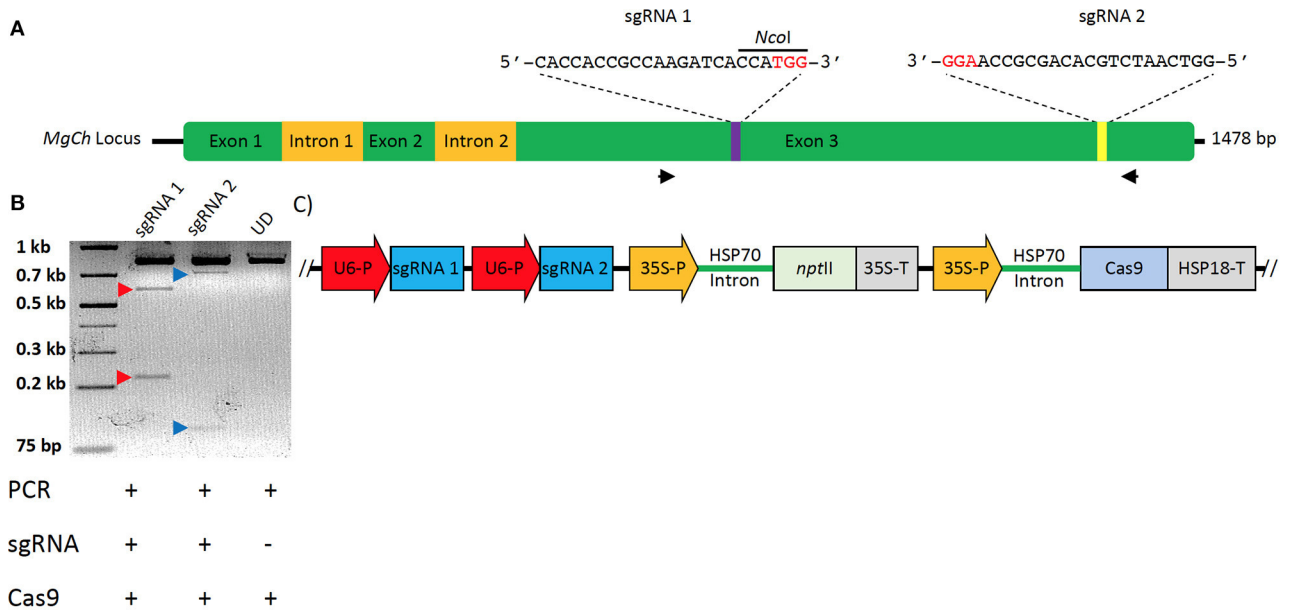

FIGURE 2 | Strategy for targeted mutagenesis of sugarcane *MgCh* and confirmation of *In-vitro* cleavage activity of sgRNAs. **(A)** Schematic representation of sugarcane *MgCh* locus and sgRNAs' target sites, sgRNA1 targeting nts 731–750 and sgRNA2 targeting nts 1223–1242. Mutations at sgRNA target site 1 would disrupt the *Nco*I restriction recognition site. Exons are indicated with green boxes, and introns with yellow boxes. **(B)** *In vitro* cleavage assay to validate sgRNA activity, the (810 nts) *MgCh* PCR amplicon is digested by ribonucleoprotein complex (RNP) of Cas9 and either sgRNA1 or sgRNA2 into ~581 and 229 nts or 701 and 109 nts, respectively. **(C)** Map of sugarcane gene editing plasmid (pMGE); Two sgRNAs are monoscistronically expressed under *Oryza sativa* U6 promoter, *npt*II is under transcriptional control of cauliflower mosaic virus (CaMV) 35S promoter and CaMV terminator, Cas9 is under transcriptional control of CaMV 35S promoter and *Sorghum bicolor* HSP18 terminator. Protospacer adjacent motifs (PAMs) are indicated in red font.

In this study, we explored whether targeted mutagenesis of magnesium chelatase subunit I with CRISPR/Cas9 provides a rapidly scorable phenotype for predicting the extent of multiallelic editing in highly polyploid sugarcane.

MATERIALS AND METHODS

Isolation of Allelic Variants of Mg Chelatase and Design of sgRNAs

The *MgCh* sequence in sugarcane was compared to sorghum and maize *MgCh* sequences via tBLASTn. This allowed the conserved domains to be identified, informing the primer design for the PCR amplification of multiple allelic *MgCh* variants from sugarcane target cultivar CP88-1762 (WT) (**Supplementary Table 1**). The amplicons were cloned into the p-GEMT® easy vector (A1360) (Promega, WI, USA), followed by the Sanger sequencing of multiple colonies. The sgRNAs were selected *in silico* using CRISPOR (http://crispor.tefor.net/). sgRNA1 was designed to cleave to a highly conserved region, while the sgRNA2 target was less conserved and included three allelic variants that differed in the number of mismatches (0, 1, or 2) in the genomic target sequence of the sgRNA (**Figure 2A**).

sgRNA Synthesis and *in vitro* Cleavage Assay

sgRNA templates were generated via PCR using Q5® High-Fidelity DNA Polymerase (NEB, MA, USA) using a DNA template encoding T7 promoter sequence corresponding to the target sequence. The optimized sgRNA scaffold (Chen et al., 2013) was assembled from oligonucleotides (Eurofins Genomics, KY, USA) through overlapping PCR, as previously described (Lin et al., 2014). Primer T7MgCh1F was combined with T7F, ScaffoldR1, and ScaffoldR2 to generate sgRNA1 DNA. The primer T7MgCh2F was combined with T7F, ScaffoldR1, and ScaffoldR2 to generate sgRNA2 DNA using the following PCR conditions: 30 cycles of 95°C for 10 s, 57°C for 10 s, and 72°C for 10 s (Lin et al., 2014). The reactions were purified with the GeneJET PCR Purification Kit (K0701) (Thermo Fisher Scientific, MA, USA) and were electrophoresed with 1% agarose gel. *In vitro* transcription was done using the HiScribe™ T7 Quick High Yield RNA Synthesis Kit (E2050S) (NEB) with 75 ng sgRNA DNA template. DNase I treatment and RNA cleanup were performed using Monarch® Total RNA Miniprep Kit (T2010) (NEB). The Mg-chelatase template PCR was amplified using Q5® High-Fidelity DNA Polymerase (M0491) (NEB) with primers C27 and C28 and the following cycle: initial denaturation at 98°C for 30 s, then 35 cycles of 98°C for 5 s, 68°C for 10 s, and 72°C for 20 s, with a final extension of 72°C for 2 min. sgRNAs validation was done by incubating 200 ng Mg-Chelatase template DNA, 250 ng sgRNA, 250 ng Cas9 protein (PNA Bio), and 2 μL NEB buffer 3 in a 20 μL reaction for 3 h at 37° C. The reaction was stopped with the addition of 1 μL PureLink™ RNase A (20 mg/mL) (12091021) (Thermo Fisher Scientific) and was incubated for 10 min at 65°C prior to electrophoresis with 2% agarose gel (**Figure 2B**).

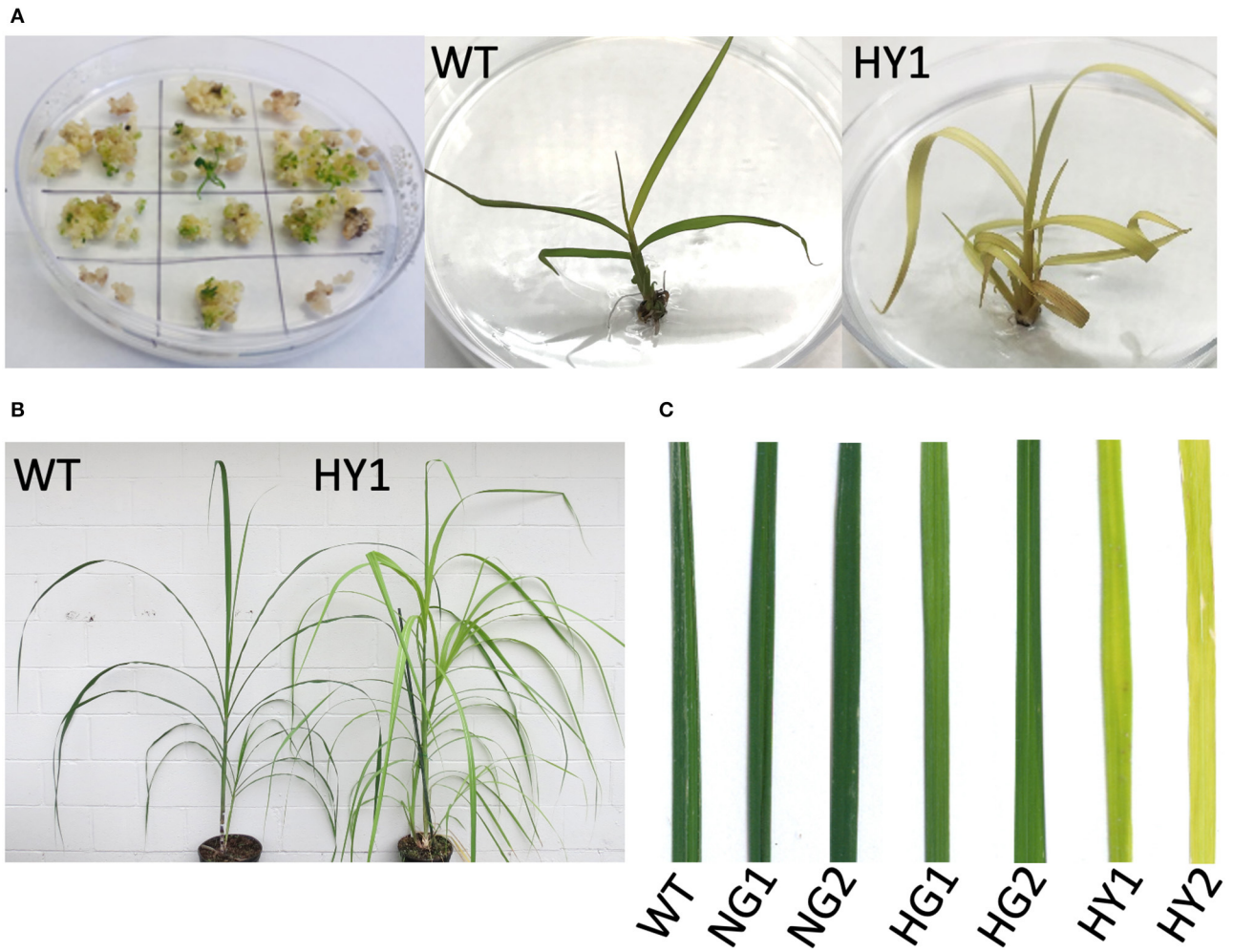

FIGURE 3 | Detection of chlorophyll depletion phenotype during *in vitro* propagation. **(A)** Development of chlorophyll depletion phenotype compared to the WT. Some of the genome-edited events (e.g., line HY1 [heat-treated, yellow 1]) displayed a distinguishable phenotype with yellow leaf color in plantlets that regenerated from tissue culture. **(B)** Comparison of line HY1 (right) to WT (left) after establishment in soil under greenhouse conditions. **(C)** Close-up of leaves from NG1, NG2, HG1, HG2, HY1, and HY2 compared to WT. HY = heat-treated yellow, NG = non-heat treated green, HG = heat treated green, WT = wild type.

Vector Construction

sgRNA vectors containing *Oryza sativa* U6 promoter were designed and custom synthesized in the pUC57 backbone (Genscript, NJ, USA) to generate pUCMg12. The Mg-chelatase target guide sequences were simultaneously cloned into the vector using annealed primer-dimers (**Supplementary Table 1**) holding 5′ overhangs to ligate into *Bbs*I and *Bsa*I restriction sites of pUC57. pUCMg12 vector was subcloned into the CRISPR backbone vector through digestion with *Srf*I and *Not*I enzymes, and the resultant colonies were confirmed via Sanger sequencing. The resulting vector MGE harbors a sugarcane codon-optimized *Streptococcus pyogenes* Cas9 driven by CaMV35S promoter with ZmHSP70 (heat shock protein) intron and AtHSP terminator. pMGE expresses the *npt*II (neomycin phosphotransferase II) gene as a plant selectable marker under transcriptional control of CaMV35S promoter with ZmHSP70 intron and CaMV35S terminator (**Figure 2C**).

Biolistic Transformation of Sugarcane

The MGE plasmid was linearized using the *Asc*I enzyme, and the minimal cassette was introduced into the embryogenic callus of sugarcane cultivar CP88-1762 through biolistic gene transfer, as described previously (Taparia et al., 2012). To evaluate the impact of heat treatment on mutation frequency, 50% of the calli were heat-treated at 37°C for 48 h, 4 days after bombardment, and they were compared to bombarded calli from the same experiment that were kept at the usual incubation temperature (28°C). The calli were subsequently incubated at 28°C and selected with geneticin (20 mg/L), as described by Taparia et al. (2012). Plantlets 5–10 cm in height were sampled for molecular analyses.

DNA Isolation, PCR, and Sanger and Next-Generation Sequencing

Genomic DNA was isolated from leaf tissues using the CTAB method (Murray and Thompson, 1980). The C5 and C9 primers

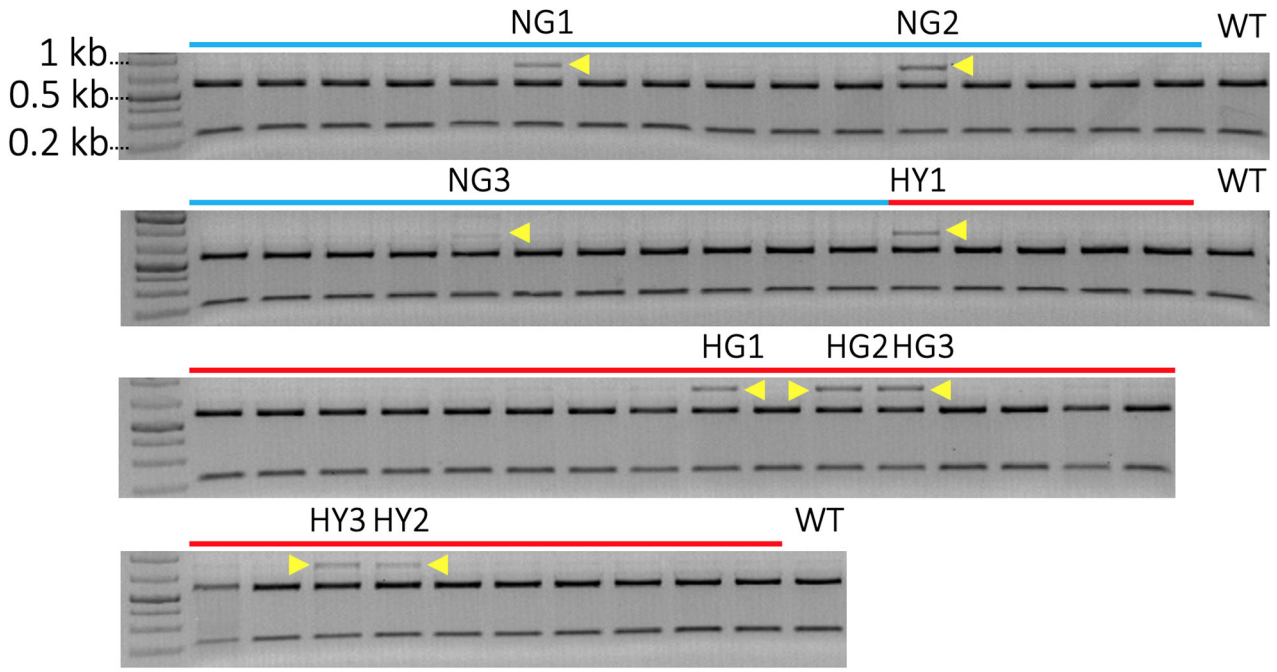

FIGURE 4 | Identification of mutants by detection of restriction site loss in sgRNA1 target site of *MgCh* PCR amplicons. Cleavage in sgRNA1 target site is likely to disrupt *Nco*I restriction site due to the creation of indels through an error-prone NHEJ-mediated repair process. A functional *Nco*I site would allow the cleavage of 810 bp PCR amplicon of *MgCh* into ∼578 bp and 232 bp products. Blue lines indicate transgenic lines generated without heat treatment, and red lines indicate transgenic lines that regenerate following heat treatment of bombarded callus at 37°C for 48 h. N = non-heat treated, G = green, H = heat-treated, Y = yellow. The *Nco*I digested *MgCh* PCR amplicon was electrophoresed on 2% agarose gel. Lines NG1, NG2, NG3, HY1, HG1 HG2, HG3, HY3, and HY2 all display partially undigested *MgCh* PCR amplicons following *Nco*I restriction digestions indicated by yellow arrows. HY = heat-treated, yellow; NG = non-heat treated, green; HG = heat treated, green; WT = wild type.

(**Supplementary Table 1**) used for PCR amplified a region of *MgCh*, spanning exon 3 (∼1,100 bp) from the genomic DNA template, including targets for sgRNAs 1 and 2 (**Figure 2A**). Q5® High-Fidelity DNA Polymerase (NEB, MA, USA) was used for PCR under the following conditions: 98°C for 30 s, 35 cycles of amplification at 98°C for 15 s, 55°C for 10 s, 72°C for 20 s, and final extension at 72°C for 2 min. The PCR amplicons used in the restriction enzyme assays to detect targeted mutations were amplified using C27 and C28 primers (**Supplementary Table 1**) and the Phire Plant Direct PCR Kit, under the following conditions: 98°C for 5 min, 35 cycles of amplification at 98°C for 5 s, 65.1°C for 5 s, 72°C for 20 s, and final extension at 72°C for 2 min, using PCR amplicons for Sanger sequencing ligated to pJET 1.2 blunt vector (Thermo Fisher Scientific, MA, USA). The plasmid DNA was prepared from cloned amplicons using the GeneJET miniprep kit (Thermo Fisher Scientific). Sanger sequencing of the cloned PCR amplicons was performed at Eurofins Genomics. The sequence chromatograms were visually checked for quality.

For next-generation sequencing, amplicons of 574 bp were generated using primers C31 and C32 (**Supplementary Table 1**) with Phire polymerase (Thermo Fisher Scientific) and the following amplification conditions: 98°C for 5 min, 35 cycles of amplification at 98°C for 5 s, 64.2°C for 5 s, 72°C for 20 s, and a final extension at 72°C for 2 min. The reactions were purified using a GeneJET PCR Purification Kit (K0701) (Thermo Fisher Scientific). Complete amplicon sequencing was performed using the CCIB DNA Core Facility at Massachusetts General Hospital (Cambridge, MA). Adapters with unique barcodes were ligated onto each sample during the library construction. The libraries were pooled into equimolar concentrations for multiplexed sequencing on the Illumina MiSeq platform (Illumina, San Diego, CA) with 2×150 run parameters.

To detect edited sgRNA target sites, all reads were examined in the corresponding fastq file to identify either the 5′ primer (C31) or the 3′ primer (C32) close to the beginning or the end of the read, respectively (exact match required). If primer C31 was found, a local alignment algorithm was run with the parameters match score = 1, mismatch penalty = −0.5, gap opening penalty = −0.5, and gap extension penalty = −0.2 to search for the sgRNA1 sequence in the 65 bp region downstream of C31. A minimum score of 15 was required to accept the alignment, in addition to a perfect match on the first two bases. If C32 was found, a search for the sgRNA2 sequence in the 50 bp region downstream of C32 was initiated, with the same parameters. If a match for the sgRNA sequence was found, the alignment was examined to determine the number of base substitutions, insertions, and deletions, and the number of reads that contained every possible combination of events (e.g., perfect match, substitutions only, substitutions and insertions,

substitutions and deletions, etc.) was reported. In addition, matrices showing the frequencies of all observed substitutions in each sample were generated.

For the sgRNA2 target, the results were computed separately for each of the three known sgRNA2 variants, based on single-nucleotide changes at positions 4 (C → T) and 15 (T → C). Only the three haplotypes CT, TT, and TC were observed at a significant frequency. To determine the indel sizes, the number of reads in which the sgRNA target sequence contained insertions (or deletions) totaling 1, 2, 3, 4, 5, or more than 5 base pairs (based on the local alignment) were also reported, as well as the average size of all insertions or deletions. The results for each of the three sgRNA2 variants were reported separately. To record the reads with severely modified sgRNA targets while preventing alignment with the sgRNA sequence, all reads that contained a valid primer (C31 or C32) but did not contain the sgRNA sequence were examined. This included searching for an 11 bp conserved sequence that could be located downstream of the sgRNA (at positions 56 and 61 downstream of C31 or C32, respectively). This search was performed using a local alignment algorithm with the following parameters: match score = 1, mismatch penalty = −1, gap opening penalty = −2, gap extension penalty = −2, and minimum score required for hit = 9. All analyses were performed with custom Python scripts using the Biopython package (specifically, the Bio.pairwise2 library).

Detecting Targeted Mutations Using Restriction Enzyme Digestion of PCR Amplicons

PCR products from C27–C28 were purified using GeneJET PCR Purification Kit (K0701) (Thermo Fisher Scientific). Following this, 200 ng of each purified product was incubated with 0.2 μL *Nco*I-HF (NEB) for 3 h at 37°C. The reactions were deactivated by incubation at 80°C for 20 min prior to loading on 2% agarose gel for visualization.

Phenotypic Evaluations

The plants were transferred from tissue culture media to Sunshine mix #8 (Sungrow Horticulture, Agawam, MA, USA) potting mix and grown in a walk-in growth chamber when the shoots were ∼10 cm long. During the first week after the transfer, a level of relative humidity near 100% was maintained, and then it was adjusted to 75% humidity. Plant growth occurred on a 16/8 h light/dark photoperiod and a light intensity of 400 μmol m^{-2} s^{-1}, at 28/22°C day/night temperature. The plants were fertilized every 2 weeks after their transfer to the soil by irrigation with Miracle Grow All Purpose Plant Food (ScottsMiracle-Gro, Maryville, OH, USA). Leaf greenness was measured on the fully expanded top leaf from three tillers per plant using a SPAD chlorophyll meter (Minolta SPAD-502, Konica-Minolta), and this was repeated twice at 3-week intervals.

Statistical Analyses

The means were compared using Fisher's least significant difference test. A minimum of three independent biological replicates were used for the statistical analyses.

RESULTS

Identification of Allelic Variants of *MgCh* in Sugarcane and Confirming sgRNA Activity *in vitro*

Sanger sequencing of cloned *MgCh* amplicons from WT DNA led to the identification of allelic variants in WT and informed the design of two sgRNAs that targeted exon 3. sgRNA1 targeted *MgCh* at nts 731–750, and sgRNA2 targeted *MgCh* at nts 1223–1242 (**Figure 2A**). Both sgRNAs were validated through *in vitro* cleavage assay. sgRNA1 guided the cleavage of the 810 nt long partial *MgCh* amplicons into 581 and 229 nt fragments. Targeting via sgRNA2 generates 701 and 109 nts fragments upon cleavage (**Figure 2B**).

Visual Detection of Mutant Phenotypes

Events that feature the depletion of chlorophyll are visually distinguishable as soon as the plantlets regenerate from tissue culture (**Figure 3A**). This included light green or yellow leaves, by contrast to the dark green shoots from the non-bombarded control plates.

Characterization of Mutant Lines With Restriction Enzyme Assay

A total of 52 transgenic lines were regenerated, including 22 lines from non-heat-treated tissue and 30 lines from heat-treated tissue from 10 bombardments with the pMGE construct for each treatment. The PCR amplicons of *MgCh* from these lines were analyzed for the loss of restriction sites in the target region of sgRNA1. Loss of the *Nco*I restriction site was expected if indels or nucleotide substitutions were generated in the target site of the sgRNA1 (**Figure 2A**). A total of nine lines were identified, including a partially undigested *MgCh* amplicon following *Nco*I treatment, by contrast to WT, which displayed a completely digested amplicon (**Figure 4**). Among the nine lines with altered *Nco*I restriction digest pattern, three lines originated from no-heat treatment (NG1, NG2, and NG3), and six lines were from heat-treated calli (HY1, HY2, and HY3 and HG1, HG2, and HG4; **Figure 4**).

Sanger Sequencing of Cloned PCR Amplicons of *MgCh*

Sanger sequencing of cloned PCR amplicons, including the 2 sgRNA target regions in exon 3 of *MgCh* (**Figure 2A**), confirmed the targeted mutations from the non-heat-treated set. Three mutant lines were confirmed by Sanger sequencing and restriction enzyme assay (14% of the regenerated lines; **Table 1** and **Supplementary Figure 1**). The heat-treated tissues regenerated six mutant lines (20% of the regenerated lines, **Table 1** and **Supplementary Figure 1**). All three of the lines with the most severe chlorophyll depletion HY1, HY2, and HY3 (heat-treated yellow 1, 2, and 3; **Table 1**) were derived from the heat treatment. In addition, three mutants with mild to moderate chlorophyll reduction were also regenerated from the heat treatment (HG1, HG2, and HG3; **Table 1**).

TABLE 1 | Summary of phenotyping and genotyping of regenerated plants following biolistic transfer of pMGE and treatment with 37°C or regular incubation temperature (28°C).

Temperature treatment	No. of shots	Cas9 (+ve) lines	Yellow Leaves	Mosaic Leaves	RSL (+ve)	Sanger (+ve)	Editing frequency/Shot	Editing frequency/Cas9 lines
28°C	10	22	0	0	3	3	3/10 (30%)	3/22 (14%)
37°C	10	30	3	1	6	6	6/10 (60%)	6/30 (20%)

Number of regenerated, transgenic, and edited lines following the biolistic transfer of pMGE minimal cassette and 48 h treatment with 37°C or regular incubation temperature (28°C). (+v) = PCR positive, RSL = restriction site loss.

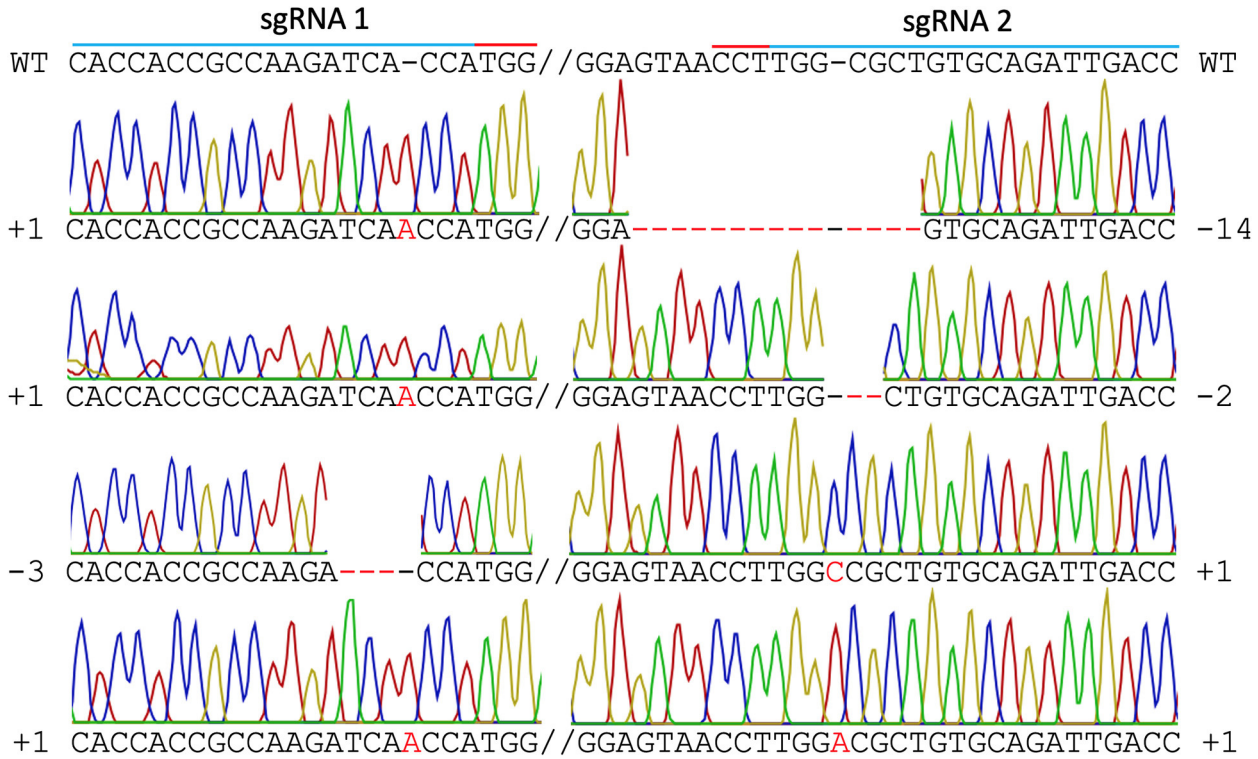

FIGURE 5 | Sanger sequencing of line HY1. Different types of edits are displayed. The blue line indicates both sgRNA target sites, the red line indicates PAM sites, the red font indicates insertions, and the red dashed line indicates deletions. WT = wild type.

Single-nucleotide polymorphism outside of the target regions for sgRNA1 and sgRNA2 allowed the identification of unique reads to represent individual *MgCh* copies/alleles. This allowed differentiation between single-edited and co-edited events within *MgCh* variants/alleles in the analyzed lines.

In mutant line HY1 (**Figure 3B**), 59 unique reads were identified from 175 cloned *MgCh* PCR amplicons, representing individual *MgCh* copies/alleles. In total, 49 of the 59 copies/alleles from HY1 were edited (83.1%), and 10 were not edited (16.9%). Among the 49 edited copies/alleles, 27 copies/alleles (45.8%) only displayed edits at the target site of sgRNA1 (PAM1), 3 (5.1%) only displayed edits at the target site of sgRNA2 (PAM2), and 19 (32.2%) displayed edits at both target sites (**Figure 5**, **Supplementary Tables 2**, **3**). Among the 49 edited copies/alleles, 40 (67.7% of all unique reads) carried frame-shift mutations, and 9 (15.3% of all unique reads) displayed a single amino acid deletion or in-frame isoform (**Supplementary Tables 2**, **4**). Indel analyses revealed that the most dominant deletions were 2–3 nt long, the longest deletion was 14 nt, and the detected insertions were all 1 nt long (**Figure 5**, **Supplementary Tables 2**–**4**).

SPAD Chlorophyll Meter Analyses to Quantify Leaf Greenness in Mutant *MgCh* Lines

Leaf greenness from mutant and WT plants was determined using the SPAD chlorophyll meter (Minolta SPAD-502, Konica-Minolta). Two lines were derived from incubation at 28°C following gene transfer (non-heat-treated green lines NG1 and NG3) that displayed SPAD values comparable to the WT leaves which was detected as 43.39 SPAD units (**Table 2**). Line NG2 displayed a 9% lower SPAD value than WT, but its greenness

was not visibly distinguishable from WT (**Figure 3C**). Therefore, mutant plants derived from incubation at 28°C were considered to be lacking a chlorophyll-depletion phenotype. The green lines originating from the heat-treated callus (37°C, HG1, HG2, and HG3) displayed SPAD values of 30.63, 34.7, and 31.07, respectively. This indicated a 20 to 29% reduction of chlorophyll compared to WT, although this was not visibly distinguishable from WT (**Table 2**; **Figure 3C**). The yellow lines (HY1, HY2, and HY3) originating from the heat-treated callus displayed SPAD values of 5.5, 6.63, and 12.53, respectively. This indicates a 71 to 87% reduction in chlorophyll compared to WT and was visibly distinguishable from the WT, NG, and HG lines (**Table 2**, **Figure 3C**).

TABLE 2 | Evaluation of leaf pigmentation of edited lines using a SPAD meter.

Line	Heat (37°C)	SPAD value
WT	-	43.93 ± 0.71
NG1	No	43.87 ± 1.85
NG2	No	40.03 ± 2.55
NG3	No	43.27 ± 0.95
HG1	Yes	30.63 ± 1.37
HG2	Yes	34.70 ± 2.27
HG3	Yes	31.07 ± 1.26
HY1	Yes	5.50 ± 1.08
HY2	Yes	6.63 ± 1.21
HY3	Yes	12.53 ± 1.3
LSD		3.8

Chlorophyll pigmentation values of edited lines (NG = non-treated green, HG = heat-treated green, HY = heat-treated yellow) as compared to non-modified sugarcane cultivar CP88-1762 (WT). Values were generated by SPAD chlorophyll meter from greenhouse-grown plants. The values following the means are standard deviation. Lines = 10; n = 3; LSD = least significant difference (3.8); $p < 0.01$.

Quantifying Multiallelic Co-editing Efficiency of *MgCh* With Next-Generation Sequencing

Next-generation sequencing data showed that the observed level of chlorophyll depletion largely corresponded to the proportion of edited reads. The exception to this was line HG3, which had only 4.4–4.8% of the reads edited at sgRNA target site 2 or 1, respectively, and displayed a 28% reduction of chlorophyll (**Tables 2**, **3**). *MgCh* reads aligning to the sgRNA1 target site displayed editing efficiencies ranging from 6.9 to 20.8% for NG lines, 4.8 to 28.8% for HG lines, and 42 to 82.3% for HY lines (**Table 3**). The editing efficiencies at the sgRNA2 target ranged from 5.7 to 8.7% for the NG lines, 4.4 to 29% for the HG lines, and 18.7 to 19.7% for the HY lines (**Table 3**). Taking the highest editing efficiency for each line at either the sgRNA1 or sgRNA2 target sites, NG lines displayed a range from 6.9 to 20.8%, HG lines from 4.8 to 29%, and HY lines from 42 to 82.3% of the *MgCh* reads as edited NGS reads (**Table 3**). The most common edit detected at the sgRNA1 target site was insertion, with an average of 24.3% of the total events across all of the lines. The most frequent editing event at sgRNA2 target site was a combination of substitution and insertion, with 8.6% of the total events across all of the lines (**Table 3**).

On average of all the edited lines, 33.1 or 15.3% of all NGS reads, that aligned to sgRNA1 or sgRNA2 displayed edits, respectively (**Table 3**). The sgRNA1 target site was located in a highly conserved region of *MgCh* with no sequence variants in WT. sgRNA2 was designed to target a site where three sequence variants were present in WT, with 0, 1, or 2 nt mismatches against the corresponding sgRNA. The editing efficiency was highest at the variant, with no mismatches to the sgRNA, reaching up to 28% of the *MgCh* reads in line HG1. Both variants, displayed low but detectable editing efficiencies with 1 or 2 mismatches (**Supplementary Table 5**). The NGS reads were also analyzed to

TABLE 3 | Summary of editing events detected by next-generation sequencing in the 20-nt sgRNA target sites.

Line	Type of edits in percent of NGS reads from target amplicon															
	sgRNA1 Target Site								sgRNA2 Target Site							
	Total edits	S	I	SI	D	SD	ID	SID	Total edits	S	I	SI	D	SD	ID	SID
NG1	6.9	4.2	1.8	0.9	0.0	0.0	0.0	0.0	5.7	3.7	0.2	1.5	0.2	0.0	0.1	0.0
NG2	12.4	3.9	3.7	0.8	3.9	0.1	0.0	0.0	7.6	3.7	0.3	3.1	0.5	0.0	0.0	0.0
NG3	20.8	3.5	16.3	1.0	0.0	0.0	0.0	0.0	8.7	3.7	0.5	4.2	0.3	0.0	0.0	0.0
HG1	28.8	2.9	15.7	1.1	0.4	0.1	8.4	0.2	29	2.5	0.2	25.9	0.4	0.0	0.0	0.0
HG2	22.5	3.5	11.9	0.9	0.3	0.0	5.8	0.1	24.3	3.0	0.2	20.8	0.3	0.0	0.0	0.0
HG3	4.8	4.3	0.4	0.1	0.0	0.0	0.0	0.0	4.4	3.7	0.2	0.3	0.1	0.0	0.1	0.0
HY1	78.1	1.3	64.3	12.5	0.0	0.0	0.0	0.0	19.7	3.4	0.2	4.4	11.7	0.0	0.0	0.0
HY2	82.3	1.0	67.9	13.4	0.0	0.0	0.0	0.0	18.7	3.2	0.2	2.7	12.5	0.0	0.1	0.0
HY3	42	3.3	36.9	1.8	0.0	0.0	0.0	0.0	19.4	3.4	1.3	14.6	0.1	0.0	0.0	0.0
Mean	33.1	3.1	24.3	3.6	0.5	0.0	1.6	0.0	15.3	3.4	0.4	8.6	2.9	0.0	0.0	0.0
WT	4.8	4.6	0.1	0.1	0.0	0.0	0.0	0.0	4.0	3.5	0.2	0.1	0.1	0.0	0.1	0.0

Values represent edited reads in percent of total reads that align to the target amplicon. Totals are the sums of all types of edits. The values at the sgRNA2 target site include the compilation of three allelic variants at this site. S = substitution, SI = substitution + insertion, D = deletion; SD = substitution + deletion, ID = insertion + deletion; SID = substitution + insertion + deletion; NG = not heat-treated, green; HG = heat-treated, green; HY = heat-treated, yellow; WT = unmodified sugarcane cultivar CP88-1762.

detect long insertions and long deletions at both sgRNA1 and sgRNA2 target sites. Long insertions were detected only at sgRNA site 1, in up to 6.5% of the *MgCh* reads as edited NGS reads for line HG1 (**Supplementary Table 6**). In lines with significant more long insertions than the wild type, the average length of long insertions ranged from 6.8 bp in NG1 to 9.4 bp in HG1 (**Supplementary Table 6**). Long deletions at sgRNA1 target site were detected in <0.1% of the NGS reads. At sgRNA2 target site long deletions were detected in 0.5% (HG3) to 19.4% (HY2) of the *MgCh* reads. In lines with significant more long deletions than the wild type, the average length of long deletions ranged from 5.9 bp in HY3 to 14.3 in HY2 (**Supplementary Table 6**).

DISCUSSION

Polyploidy is a common challenge in functional genomics and genetic improvement for many important crops. Sugarcane is an interspecific hybrid with a highly polyploid genome ($x = 10 - 13$; $2n = 100 - 130$) typically containing 10 or more homo(eo)logs at each locus (Le Cunff et al., 2008). This high level of genetic redundancy requires very efficient co-editing of multiple copies/alleles for the generation of knockout or knockdown mutant phenotypes. Here, we describe CRISPR/Cas9-mediated targeted mutagenesis of the magnesium chelatase gene (*MgCh*), which is a high-copy gene in sugarcane. Co-editing of up to 49 of the 59 detected copies/alleles was confirmed by Sanger sequencing. Of the 30 transgenic lines harboring the *MgCh* gene editing (MGE) construct, six were confirmed to have targeted mutations for an editing efficiency of 20%. Three events with the co-editing of the majority of the *MgCh* copies/alleles displayed severe chlorophyll depletion, which was visibly scorable as the plantlets regenerated from tissue culture.

In hexaploidy wheat, a tri-genome targeted sgRNA to the *PDS* gene was co-introduced with Cas9 in 38 independent transgenic lines, but no photobleaching phenotype was identified. Only 2 of the 38 transgenic wheat lines displayed targeted mutagenesis (editing efficiency of 5%), and none of them displayed co-editing of multiple copies/alleles (co-editing efficiency of 0%) (Howells et al., 2018). By contrast, the diploid barley displayed an editing efficiency that was three times higher than wheat, with the same construct. However, in barley, only chimeric events were identified, displaying the photo-bleaching phenotype in sections of the leaves that were associated with progressive somatic edits (Howells et al., 2018). Generally, short indels that include insertions, substitutions, and deletions are highly reported events in gene editing in the polyploid plant genomes (Naim et al., 2018; Shan et al., 2018; Wang et al., 2020; Wolabu et al., 2020).

To the best of our knowledge, this report is the first to describe the targeted mutagenesis of *MgCh* in plants. Naturally occurring mutations in the *MgCh* gene have previously been reported to cause impaired chlorophyll biosynthesis and thus to result in phenotypes with light green or yellow foliage (Campbell et al., 2014). RNA interference of *MgCh* in tobacco and peach results in light green phenotypes with significantly reduced chlorophyll contents (Papenbrock et al., 2000). By contrast to *MgCh* mutants, PDS mutants display impaired chlorophyll, carotenoid, and gibberellin biosynthesis resulting in dwarf or albino plantlets in both biallelic, homozygous, and biallelic heterozygous events (Qin et al., 2007). Albino plants may also be caused by somaclonal variation, and the dwarfing resulting from PDS suppression makes tissue collection to confirm molecular analyses more challenging. By contrast, Mg-chelatase-impaired natural mutants have been described with yields similar to (Slattery et al., 2017) or higher than WT plants (Pettigrew et al., 1989) despite 50% reduced chlorophyll content. The latter is associated with increased light penetration into the canopy, causing an increase in the CO_2 exchange rate there. The former results in a reduced nitrogen requirement. Therefore, manipulating chlorophyll content has been proposed as a strategy for improving canopy-level photosynthesis or nitrogen use efficiency under the dense canopies of tall biomass plants such as sugarcane (Kirst et al., 2017; Walker et al., 2018).

In this study, we demonstrated that the targeted mutagenesis of magnesium chelatase with CRISPR/Cas9 provides a rapidly scorable phenotype without leading to obvious growth retardation. Notably, the level of chlorophyll depletion was predictive of the extent of multiallelic co-editing of *MgCh*, which enables a rapid readout of the editing outcome.

The efficiencies of Cas9- and Cas12a-mediated mutagenesis can be elevated by the heat treatment of the callus following the delivery of editing reagents, as previously reported for *Arabidopsis*, rice, maize, and wheat (LeBlanc et al., 2018; Malzahn et al., 2019; Milner et al., 2020). Therefore, we deployed an MGE-based rapid readout system to compare co-editing efficiencies in response to heat treatment (37°C) or standard incubation temperature (28°C) for sugarcane callus. Three transgenic lines emerging from the heat treatment and none of the transgenic lines that regenerate under standard incubation temperatures displayed a phenotype with visible chlorophyll depletion. Genotyping with assaying restriction enzyme loss in the sgRNA target region, Sanger sequencing, and next-generation sequencing revealed a total of three mutant lines per 10 shots from callus regeneration under standard incubation temperatures and six mutant lines per 10 shots from heat-treated tissue. The events which were visibly distinguishable from WT due to severe chlorophyll depletion following heat treatment displayed editing of more than 40% of the *MgCh* NGS target amplicon reads. The events from standard temperature treatment displayed an editing rate of 6.9–20.8% of the *MgCh* NGS target amplicon reads without displaying a phenotype that could be visibly distinguished from WT. This suggested that heat treatment elevated the editing frequency 2-fold and drastically promoted the co-editing of multiple alleles to create a phenotype that was visibly distinguishable from WT. Efficient co-editing of multiple copies/alleles is of major importance for the generation of a distinct mutant phenotype in vegetatively propagated polyploid crops such as sugarcane and potato, where the combination of mutant alleles via sexual hybridization would disrupt the highly heterozygous, elite cultivar.

Multiallelic gene editing via CRISPR/Cas9 has been reported in several polyploid crops. In studies of both tetraploid potato and tetraploid switchgrass, only 2.0% of the T_0 transgenic plants displayed co-mutation of all four targeted alleles of the granule-bound starch synthase gene or phosphoglycerate mutase gene (Andersson et al., 2017; Liu et al., 2018). Using polycistronic delivery for four sgRNAs instead of a single one dramatically

elevated the editing efficiency in the tetraploid alfalfa. None of the 339 transgenic lines harboring a single sgRNA or Cas9 displayed tetra-allelic editing or the desired stay-green phenotype. By contrast, seven lines were confirmed with co-editing of all four alleles of the stay-green gene (MsSGR) in T_0 from 492 transgenic lines (Wolabu et al., 2020).

Co-delivery of two sgRNA instead of a single sgRNA also elevated the co-editing efficiency in this study. Analyses of unique reads following the Sanger sequencing of cloned PCR amplicons of line HY1 revealed that 45.8% of the reads were edited only at sgRNA site 1, 5.1% were edited only at sgRNA site 2, and 32.2% were edited at both sites. Both Sanger and next-generation sequencing analyses suggested that functional knockouts are mostly composed of short insertions and short deletions resulting in out of frame mutations. For example, in mutant line HY1, with severe depletion of chlorophyll, 67.8% of the alleles were out of frame.

To exploit the reduction in chlorophyll content for elevating the canopy level photosynthesis, it may be desirable to target a limited number of *MgCh* copies/alleles for mutagenesis. The choice of sgRNAs allows the targeting of specific alleles. Unlike sgRNA1, which was targeted to a highly conserved region with no allelic variants, sgRNA2 was targeted to a region that had three allelic variants with zero, one, or two mismatches to the sgRNA (**Supplementary Table 5**). Co-delivering both sgRNAs allowed a comparison of the impact of the individual sgRNA on the editing efficiency and the editing of the different allelic variants. Higher editing efficiency was found for all mutants for the target of sgRNA1 (33.1% edited NGS reads) than for sgRNA2 (15.3% edited NGS reads). The allelic variants with SNPs in sgRNA2 target region displayed very few edits and contributed to the overall lower editing efficiency at this site. This suggests that the choice of gRNA and the combination of sgRNAs offers opportunities to tailor the desired co-editing efficiency in sugarcane, similar to what is reported for other polyploid crops (Andersson et al., 2017; Liu et al., 2018; Wolabu et al., 2020).

The described approach will facilitate the establishment of genome-editing protocols for recalcitrant crops and will support important optimizations for the elevation of gene-editing efficiencies, including the evaluation of alternative tissue culture protocols, genome editing reagents, and their delivery.

DATA AVAILABILITY STATEMENT

The datasets presented in this study can be found in online repositories. The names of the repository/repositories and accession number(s) can be found below: https://www.ncbi.nlm.nih.gov/, Bioproject ID PRJNA704370.

AUTHOR CONTRIBUTIONS

FA conceived, designed, and managed the research project. DW and FA designed the sgRNAs. DW and AE validated sgRNAs with *in vitro* assays. CM generated the recombinant DNA constructs. CM and SS carried out the tissue cultures and generated the transgenic sugarcane plants. AE carried out the molecular and phenotypic analyses of the regenerated sugarcane lines. FA and AE wrote the manuscript. All authors read and approved the final manuscript.

FUNDING

This research was funded by the DOE Center for Advanced Bioenergy and Bioproducts Innovation (U.S. Department of Energy, Office of Science, Office of Biological and Environmental Research) under award number DE-SC0018420. Any opinions, findings and conclusions, or recommendations expressed in this publication are those of the authors and do not necessarily reflect the views of the U.S. Department of Energy. This work was also supported by the USDA National Institute of Food and Agriculture, Hatch project 1020425. We acknowledge the São Paulo Research Foundation for the visiting research fellowship (FAPESP Proc No. 2018/11544–5) to CM.

ACKNOWLEDGMENTS

The authors would like to thank Dr. Hardev Sandhu at The Everglades Research and Education Center, UF-IFAS, for providing sugarcane tops, and Sun Gro Horticulture, Apopka, FL, for the donation of potting mix. We would like to thank Alberto Riva from University of Florida Interdisciplinary Center for Biotechnology Research (ICBR) Bioinformatics Core for bioinformatics support with NGS data.

SUPPLEMENTARY MATERIAL

The Supplementary Material for this article can be found online at: https://www.frontiersin.org/articles/10.3389/fgeed.2021.654996/full#supplementary-material

Supplementary Figure 1 | Sanger sequencing reads exemplifying targeted mutations in different lines. The blue line indicates both sgRNA target sites, the orange line indicates PAM sites, the red font indicates insertions, and the red dashed line indicates deletions. Lines HY2, HY3, NG1, NG2, NG3, HG1, and HG3. HY = heat-treated, yellow; NG = non-heat treated, green; HG = heat treated, green; WT = wild type.

Supplementary Table 1 | Primers used in the experiment.

Supplementary Table 2 | Summary of edits of mutant line HY1 as detected by Sanger sequencing of cloned PCR amplicons of *MgCh*.

Supplementary Table 3A | Genotyping of 59 alleles/variants as detected by Sanger sequencing of cloned PCR amplicons of *MgCh* in mutant line HY1.

Supplementary Table 3B | Genotyping of 59 alleles/variants as detected by Sanger sequencing of cloned PCR amplicons of *MgCh* in mutant line HY1.

Supplementary Table 4 | Types of edits in *MgCh* gene in line HY1.

Supplementary Table 5 | Summary of Next Generation Sequencing revealing the editing frequency at target site for sgRNA2 for 3 different allelic variants of the *MgCh* gene.

Supplementary Table 6 | Analysis of NGS reads that did not align to sgRNA target sequence due to long insertions or long deletions.

REFERENCES

Ali, Z., Abul-faraj, A., Li, L., Ghosh, N., Piatek, M., Mahjoub, A., et al. (2015). Efficient Virus-Mediated Genome Editing in Plants Using the CRISPR/Cas9 System. *Mol. Plant* 8, 1288–1291. doi: 10.1016/j.molp.2015.02.011

Altpeter, F., and Ratna, K. (2018). "Genetic improvement of sugarcane by transgenic, intragenic and genome editing technologies," in *Achieving Sustainable Cultivation of Sugarcane, Vol. 2*, ed P. Rott (Cambridge: Burleigh Dodds Science Publishing), 133–154. doi: 10.19103/AS.2017.0035.07

Andersson, M., Turesson, H., Nicolia, A., Falt, A. S., Samuelsson, M., and Hofvander, P. (2017). Efficient targeted multiallelic mutagenesis in tetraploid potato (*Solanum tuberosum*) by transient CRISPR-Cas9 expression in protoplasts. *Plant Cell Rep.* 36, 117–128. doi: 10.1007/s00299-016-2062-3

Baltes, N. J., Hummel, A. W., Konecna, E., Cegan, R., Bruns, A. N., Bisaro, D. M., et al. (2015). Conferring resistance to geminiviruses with the CRISPR-Cas prokaryotic immune system. *Nat. Plants* 1:15145. doi: 10.1038/nplants.2015.145

Beying, N., Schmidt, C., Pacher, M., Houben, A., and Puchta, H. (2020). CRISPR-Cas9-mediated induction of heritable chromosomal translocations in Arabidopsis. *Nat. Plants* 6, 638–645. doi: 10.1038/s41477-020-0663-x

Butt, H., Eid, A., Momin, A. A., Bazin, J., Crespi, M., Arold, S. T., et al. (2019). CRISPR directed evolution of the spliceosome for resistance to splicing inhibitors. *Genome Biol.* 20, 73. doi: 10.1186/s13059-019-1680-9

Byrt, C. S., Grof, C. P., and Furbank, R. T. (2011). C4 plants as biofuel feedstocks: optimising biomass production and feedstock quality from a lignocellulosic perspective. *J. Integr. Plant Biol.* 53, 120–135. doi: 10.1111/j.1744-7909.2010.01023.x

Campbell, B. W., Mani, D., Curtin, S. J., Slattery, R. A., Michno, J. M., Ort, D. R., et al. (2014). Identical substitutions in magnesium chelatase paralogs result in chlorophyll-deficient soybean mutants. *G3* 5, 123–131. doi: 10.1534/g3.114.015255

Chandrasegaran, S., and Carroll, D. (2016). Origins of Programmable Nucleases for Genome Engineering. *J Mol Biol.* 428(5 Pt B), 963–989. doi: 10.1016/j.jmb.2015.10.014

Chapman, J. R., Taylor, M. R., and Boulton, S. J. (2012). Playing the end game: DNA double-strand break repair pathway choice. *Mol. Cell.* 47, 497–510. doi: 10.1016/j.molcel.2012.07.029

Chen, B., Gilbert, L. A., Cimini, B. A., Schnitzbauer, J., Zhang, W., Li, G. W., et al. (2013). Dynamic imaging of genomic loci in living human cells by an optimized CRISPR/Cas system. *Cell* 155, 1479–1491. doi: 10.1016/j.cell.2013.12.001

de Setta, N., Monteiro-Vitorello, C. B., Metcalfe, C. J., Cruz, G. M., Del Bem, L. E., Vicentini, R., et al. (2014). Building the sugarcane genome for biotechnology and identifying evolutionary trends. *BMC Genomics* 15:540. doi: 10.1186/1471-2164-15-540

Eid, A., and Mahfouz, M. M. (2016). Genome editing: the road of CRISPR/Cas9 from bench to clinic. *Exp. Mol. Med.* 48:e265. doi: 10.1038/emm.2016.111

Fan, D., Liu, T., Li, C., Jiao, B., Li, S., Hou, Y., et al. (2015). Efficient CRISPR/Cas9-mediated targeted mutagenesis in populus in the first generation. *Sci. Rep.* 5:12217. doi: 10.1038/srep12217

Gao, H., Mutti, J., Young, J. K., Yang, M., Schroder, M., Lenderts, B., et al. (2020). Complex Trait Loci in Maize Enabled by CRISPR-Cas9 Mediated Gene Insertion. *Front. Plant Sci.* 11:535. doi: 10.3389/fpls.2020.00535

Horsley, T., and Zhou, M. (2013). Effect of photoperiod treatments onpollen viability and flowering at the South African sugarcane research institute. *Proc. South Afr. Sugar Technol. Assoc.* 86, 286–290.

Howells, R. M., Craze, M., Bowden, S., and Wallington, E. J. (2018). Efficient generation of stable, heritable gene edits in wheat using CRISPR/Cas9. *BMC Plant Biol.* 18:215. doi: 10.1186/s12870-018-1433-z

Huang, T. K., and Puchta, H. (2019). CRISPR/Cas-mediated gene targeting in plants: finally a turn for the better for homologous recombination. *Plant Cell Rep.* 38, 443–453. doi: 10.1007/s00299-019-02379-0

Jinek, M., Chylinski, K., Fonfara, I., Hauer, M., Doudna, J. A., and Charpentier, E. (2012). A programmable dual-RNA-guided DNA endonuclease in adaptive bacterial immunity. *Science* 337, 816–821. doi: 10.1126/science.1225829

Jung, J. H., and Altpeter, F. (2016). TALEN mediated targeted mutagenesis of the caffeic acid O-methyltransferase in highly polyploid sugarcane improves cell wall composition for production of bioethanol. *Plant Mol. Biol.* 92, 131–142. doi: 10.1007/s11103-016-0499-y

Kannan, B., Jung, J. H., Moxley, G. W., Lee, S. M., and Altpeter, F. (2018). TALEN-mediated targeted mutagenesis of more than 100 COMT copies/alleles in highly polyploid sugarcane improves saccharification efficiency without compromising biomass yield. *Plant Biotechnol. J.* 16, 856–866. doi: 10.1111/pbi.12833

Kirst, H., Gabilly, S. T., Niyogi, K. K., Lemaux, P. G., and Melis, A. (2017). Photosynthetic antenna engineering to improve crop yields. *Planta* 245, 1009–1020. doi: 10.1007/s00425-017-2659-y

Ko, J. K., Jung, J. H., Altpeter, F., Kannan, B., Kim, H. E., Kim, K. H., et al. (2018). Largely enhanced bioethanol production through the combined use of lignin-modified sugarcane and xylose fermenting yeast strain. *Bioresour. Technol.* 256, 312–320. doi: 10.1016/j.biortech.2018.01.123

Le Cunff, L., Garsmeur, O., Raboin, L. M., Pauquet, J., Telismart, H., Selvi, A., et al. (2008). Diploid/polyploid syntenic shuttle mapping and haplotype-specific chromosome walking toward a rust resistance gene (Bru1) in highly polyploid sugarcane (2n approximately 12x approximately 115). *Genetics* 180, 649–660. doi: 10.1534/genetics.108.091355

LeBlanc, C., Zhang, F., Mendez, J., Lozano, Y., Chatpar, K., Irish, V. F., et al. (2018). Increased efficiency of targeted mutagenesis by CRISPR/Cas9 in plants using heat stress. *Plant J.* 93, 377–386. doi: 10.1111/tpj.13782

Lin, S., Staahl, B. T., Alla, R. K., and Doudna, J. A. (2014). Enhanced homology-directed human genome engineering by controlled timing of CRISPR/Cas9 delivery. *Elife* 3:e04766. doi: 10.7554/eLife.04766.010

Liu, Y., Merrick, P., Zhang, Z., Ji, C., Yang, B., and Fei, S. Z. (2018). Targeted mutagenesis in tetraploid switchgrass (*Panicum virgatum* L.) using CRISPR/Cas9. *Plant Biotechnol. J.* 16, 381–393. doi: 10.1111/pbi.12778

Malzahn, A. A., Tang, X., Lee, K., Ren, Q., Sretenovic, S., Zhang, Y., et al. (2019). Application of CRISPR-Cas12a temperature sensitivity for improved genome editing in rice, maize, and Arabidopsis. *BMC Biol.* 17:9. doi: 10.1186/s12915-019-0629-5

Milner, M. J., Craze, M., Hope, M. S., and Wallington, E. J. (2020). Turning up the temperature on CRISPR: increased temperature can improve the editing efficiency of wheat using CRISPR/Cas9. *Front. Plant Sci.* 11:583374. doi: 10.3389/fpls.2020.583374

Moore, P. H., and Nuss, K. J. (1987). "Flowering and flower synchronization," in *Sugarcane Improve-ment Through Breeding,* ed D. J. Heinz (Amsterdam: Elsevier), 273–311. doi: 10.1016/B978-0-444-42769-4.50012-6

Murray, M. G., and Thompson, W. F. (1980). Rapid isolation of high molecular weight plant DNA. *Nucleic Acids Res.* 8, 4321–4325. doi: 10.1093/nar/8.19.4321

Naim, F., Dugdale, B., Kleidon, J., Brinin, A., Shand, K., Waterhouse, P., et al. (2018). Gene editing the phytoene desaturase alleles of Cavendish banana using CRISPR/Cas9. *Transgenic Res.* 27, 451–460. doi: 10.1007/s11248-018-0083-0

Papenbrock, J., Pfundel, E., Mock, H. P., and Grimm, B. (2000). Decreased and increased expression of the subunit CHL I diminishes Mg chelatase activity and reduces chlorophyll synthesis in transgenic tobacco plants. *Plant J.* 22, 155–164. doi: 10.1046/j.1365-313x.2000.00724.x

Pettigrew, W. T., Hesketh, J. D., Peters, D. B., and Woolley, J. T. (1989). Characterization of canopy photosynthesis of chlorophyll-deficient soybean isolines. *Crop Sci.* 29, 1025–1029. doi: 10.2135/cropsci1989.0011183X002900040040x

Puchta, H. (1998). Repair of genomic double-strand breaks in somatic plant cells by one-sided invasion of homologous sequences. *Plant J.* 13, 331–339. doi: 10.1046/j.1365-313X.1998.00035.x

Qin, G., Gu, H., Ma, L., Peng, Y., Deng, X. W., Chen, Z., et al. (2007). Disruption of phytoene desaturase gene results in albino and dwarf phenotypes in Arabidopsis by impairing chlorophyll, carotenoid, and gibberellin biosynthesis. *Cell Res.* 17, 471–482. doi: 10.1038/cr.2007.40

Shan, Q., Wang, Y., Li, J., Zhang, Y., Chen, K., Liang, Z., et al. (2013). Targeted genome modification of crop plants using a CRISPR-Cas system. *Nat. Biotechnol.* 31, 686–688. doi: 10.1038/nbt.2650

Shan, S., Mavrodiev, E. V., Li, R., Zhang, Z., Hauser, B. A., Soltis, P. S., et al. (2018). Application of CRISPR/Cas9 to Tragopogon (*Asteraceae*), an evolutionary model for the study of polyploidy. *Mol. Ecol. Resour.* 18, 1427–1443. doi: 10.1111/1755-0998.12935

Shrivastav, M., De Haro, L. P., and Nickoloff, J. A. (2008). Regulation of DNA double-strand break repair pathway choice. *Cell Res.* 18, 134–147. doi: 10.1038/cr.2007.111

Slattery, R. A., VanLoocke, A., Bernacchi, C. J., Zhu, X. G., and Ort, D. R. (2017). Photosynthesis, Light Use Efficiency, and Yield of Reduced-Chlorophyll Soybean Mutants in Field Conditions. *Front. Plant Sci.* 8:549. doi: 10.3389/fpls.2017.00549

Svitashev, S., Young, J. K., Schwartz, C., Gao, H., Falco, S. C., and Cigan, A. M. (2015). Targeted mutagenesis, precise gene editing, and site-specific gene insertion in maize using Cas9 and guide RNA. *Plant Physiol.* 169, 931–945. doi: 10.1104/pp.15.00793

Taparia, Y., Gallo, M., and Altpeter, F. (2012). Comparison of direct and indirect embryogenesis protocols, biolistic gene transfer and selection parameters for efficient genetic transformation of sugarcane. *Plant Cell Tissue Organ. Cult.* 111, 131–141. doi: 10.1007/s11240-012-0177-y

Tew, T. L., and Cobill, R. M. (2008). "Genetic improvement of sugarcane (*Saccharum* spp.) as an energy crop," in *Genetic Improvement of Bioenergy Crops*, ed W. Vermerris (New York, NY: Springer New York), 273–294. doi: 10.1007/978-0-387-70805-8_9

Walker, B. J., Drewry, D. T., Slattery, R. A., VanLoocke, A., Cho, Y. B., and Ort, D. R. (2018). Chlorophyll can be reduced in crop canopies with little penalty to photosynthesis. *Plant Physiol.* 176, 1215–1232. doi: 10.1104/pp.17.01401

Wang, J., Wu, H., Chen, Y., and Yin, T. (2020). Efficient CRISPR/Cas9-mediated gene editing in an interspecific hybrid poplar with a highly heterozygous genome. *Front. Plant Sci.* 11:996. doi: 10.3389/fpls.2020.00996

Weeks, D. P. (2017). "Chapter Four - Gene editing in polyploid crops: wheat, camelina, canola, potato, cotton, peanut, sugar cane, and citrus," in *Progress in Molecular Biology and Translational Science, Vol. 149*, eds D. P. Weeks, and B. Yang (San Diego, CA: Academic Press), 65–80. doi: 10.1016/bs.pmbts.2017.05.002

Willows, R. D., Gibson, L. C., Kanangara, C. G., Hunter, C. N., and von Wettstein, D. (1996). Three separate proteins constitute the magnesium chelatase of Rhodobacter sphaeroides. *Eur. J. Biochem.* 235, 438–443. doi: 10.1111/j.1432-1033.1996.00438.x

Wolabu, T. W., Cong, L., Park, J. J., Bao, Q., Chen, M., Sun, J., et al. (2020). Development of a highly efficient multiplex genome editing system in outcrossing tetraploid alfalfa (*Medicago sativa*). *Front. Plant Sci.* 11:1063. doi: 10.3389/fpls.2020.01063

Zhang, Y., Massel, K., Godwin, I. D., and Gao, C. (2018). Applications and potential of genome editing in crop improvement. *Genome Biol.* 19:210. doi: 10.1186/s13059-018-1586-y

Conflict of Interest: The authors declare that the research was conducted in the absence of any commercial or financial relationships that could be construed as a potential conflict of interest.

frontiers in Genome Editing

ORIGINAL RESEARCH
published: 12 May 2021
doi: 10.3389/fgeed.2021.670529

Efficient Targeted Mutagenesis Mediated by CRISPR-Cas12a Ribonucleoprotein Complexes in Maize

Shujie Dong[1], Yinping Lucy Qin[1], Christopher A. Vakulskas[2], Michael A. Collingwood[2], Mariam Marand[1], Stephen Rigoulot[1], Ling Zhu[1], Yaping Jiang[1], Weining Gu[1], Chunyang Fan[1], Anna Mangum[1], Zhongying Chen[1], Michele Yarnall[1], Heng Zhong[1], Sivamani Elumalai[1], Liang Shi[1] and Qiudeng Que[1]**

[1] Syngenta Crop Protection, Research Triangle Park, Durham, NC, United States, [2] Integrated DNA Technologies, Coralville, IA, United States

Recent advances in the development of CRISPR-Cas genome editing technologies have made it possible to perform targeted mutagenesis and precise gene replacement in crop plants. CRISPR-Cas9 and CRISPR-Cas12a are two main types of widely used genome editing systems. However, when CRISPR-Cas12a editing machinery is expressed from a transgene, some chromosomal targets encountered low editing frequency in important crops like maize and soybean. Here, we report efficient methods to directly generate genome edited lines by delivering Cas12a-gRNA ribonucleoprotein complex (RNP) to immature maize embryos through particle bombardment in an elite maize variety. Genome edited lines were obtained at ~7% frequency without any selection during regeneration *via* biolistic delivery of Cas12a RNP into immature embryos. Strikingly, the gene editing rate was increased to 60% on average and up to 100% in some experiments when the Cas12a RNP was co-delivered with a PMI selectable marker gene cassette and the induced callus cultures were selected with mannose. We also show that use of higher activity Cas12a mutants resulted in improved editing efficiency in more recalcitrant target sequence. The advances described here provide useful tools for genetic improvement of maize.

Keywords: CRISPR-Cas12a, AsCas12a, LbCas12a, mutant Cas12a, ribonucleoprotein delivery, maize genome editing

OPEN ACCESS

Edited by:
Feng Zhang,
University of Minnesota Twin Cities, United States

Reviewed by:
Yanpeng Wang,
Chinese Academy of Sciences, China
Gunvant B. Patil,
Texas Tech University, United States

****Correspondence:***
Shujie Dong
shujie.dong@syngenta.com
Qiudeng Que
qiudeng.que@syngenta.com

Specialty section:
This article was submitted to Genome Editing in Plants, a section of the journal Frontiers in Genome Editing

Received: *21 February 2021*
Accepted: *14 April 2021*
Published: *12 May 2021*

Citation:
Dong S, Qin YL, Vakulskas CA, Collingwood MA, Marand M, Rigoulot S, Zhu L, Jiang Y, Gu W, Fan C, Mangum A, Chen Z, Yarnall M, Zhong H, Elumalai S, Shi L and Que Q (2021) Efficient Targeted Mutagenesis Mediated by CRISPR-Cas12a Ribonucleoprotein Complexes in Maize. Front. Genome Ed. 3:670529. doi: 10.3389/fgeed.2021.670529

INTRODUCTION

Clustered Regularly Interspaced Short Palindromic Repeats (CRISPR)/CRISPR-associated (Cas)-adaptive immune systems are widely distributed in nature to defend bacteria from invasion of phages and other mobile genetic elements, such as plasmids and transposons (Sapranauskas et al., 2011; Hille et al., 2018). CRISPR-Cas systems are classified into two main classes and six types (Bayat et al., 2018). The most widely used CRISPR-Cas systems for genome editing are the Types II and V members of the CRISPR/Cas Class 2 systems, Cas9 and Cas12a (aka Cpf1) effectors, respectively (Tang and Fu, 2018). CRISPR/Cas9 system has 2 functioning parts, the Cas9 endonuclease and a guide RNA (gRNA) comprised of two components, a target specific CRISPR RNA (crRNA) and a trans-activating RNA (tracrRNA) (Jinek et al., 2012; Memi et al., 2018). In

contrast to Cas9, Cas12a (Cpf1) has several distinct features such as T-rich protospacer-adjacent motif (PAM), a guide crRNA without the need for trans-activating RNA (tracrRNA), creation of sticky ends, and ability to self-process crRNA in addition to the DNA nuclease activity (Zetsche et al., 2015; Bayat et al., 2018). These RNA-guided Cas nucleases (RGNs) scan the genome to search for target DNA sequences complementary to the gRNA and generate a DNA double-strand break at the target sequence if there is a proper protospacer adjacent motif (PAM) present. The resulting chromosomal break is repaired by the host DNA repair machineries, either through non-homologous end joining (NHEJ) or homology-directed repair (HDR) (Chakrabarti et al., 2019).

CRISPR-Cas systems are flexible, precise, simple to use, and efficient. Both CRISPR-Cas9 and CRISPR-Cas12a nucleases have been used widely as highly sequence-specific tools for efficient genome modification (Murugan et al., 2017). CRISPR-Cas systems also have enormous potential for improving global crop production. Their uses in editing genomes have been expanding rapidly among different crops. CRISPR/Cas9 system has been used for genome editing in *Arabidopsis*, tobacco, rice, sorghum, maize, wheat, poplar, tomato, soybean, petunia, sweet orange as well as liverwort *Malcantia polymorpha* (El-Mounadi et al., 2020). Several engineered Cas9 enzymes with altered fidelity or target recognition specificity and Cas9 proteins fused with other types of DNA modification enzymes have also been developed (Sretenovic et al., 2020; Zhang Y. et al., 2020). For example, SpCas9-NGv1, an engineered CRISPR-Cas9 recognizing NG PAM edits has been shown to efficiently edit endogenous target sites with NG PAMs in both rice and *Arabidopsis*; furthermore, target-specific base editors have been generated by fusing NGv1 nickase to cytidine deaminase (Endo et al., 2019).

CRISPR-Cas12a is an alternative system to CRISPR-Cas9 for genome editing (Zetsche et al., 2015). The functionality of Cas12a systems for genome editing has been reported in many plant species including *Arabidopsis*, cotton, rice, tobacco, tomato and maize (Endo et al., 2016; Begemann et al., 2017; Tang et al., 2017; Xu et al., 2017; Zhong Z. et al., 2018; Lee et al., 2019; Li et al., 2020). LbCas12a variants, targeting alternative non-canonical PAMs, have also been used to edit plant genome sequences and broadened the range of targetable sequences by Cas12a (Li et al., 2018a). Recently, multiplex gene editing with CRISPR-Cas12a and CRISPR-Cas9 systems has also been achieved by expressing the nuclease and crRNA array from a single Pol II promoter for plant genome editing (Wang et al., 2018). Besides, synthesis-dependent repair of Cas12a-induced double strand DNA breaks enabled targeted gene replacement in rice (Li et al., 2018b). However, the editing efficiency is usually lower with Cas12a than with Cas9 and the efficiency varies considerably among different maize targets (Lee et al., 2019). It is possible that temperature is one of the main factors affecting Cas12a editing efficiency (Malzahn et al., 2019). Recently, a high activity variant of Cas12a with temperature tolerance was also reported to resulting in improved editing efficiency in plants (Schindele and Puchta, 2020).

Other than the activity of CRISPR-Cas system, efficient delivery of the editing machinery into the plant cells is key to genome editing applications in crops. In general, stable transformation of DNA expression vectors encoding the CRISPR-Cas components is achieved using *Agrobacterium tumefaciens*-mediated delivery or direct delivery method such as particle bombardment and protoplast transformation. However, stable transformation of plants is a long process and generates transgenic plants with CRISPR-Cas expression cassettes integrated into their genomes. The integration of DNA construct encoding for the editing machinery in plant genome and its continuous expression might lead to unwanted modifications at off-target genomic sequences (Murovec et al., 2018). Delivering ribonucleoproteins (RNPs) or RNA into cells without DNA is an alternative method to generate transgene-free targeted genome edits (Woo et al., 2015; Svitashev et al., 2016; Zhang et al., 2016; Andersson et al., 2018; Liang et al., 2018). DNA-free delivery is also preferred in crops that are vegetatively propagated since it is not an option to use crossing to breed out the transgene inserts (Murovec et al., 2018; Que et al., 2019). Genome editing through DNA-free delivery with RNP may also ease up regulatory concerns related to transgenes. Editing through transfection of protoplasts with pre-assembled Cas9 RNP complexes has been demonstrated in many plant species (Woo et al., 2015; Malnoy et al., 2016; Svitashev et al., 2016; Andersson et al., 2018; Liang et al., 2018; Murovec et al., 2018; Sant'Ana et al., 2020). However, due to the technical difficulties and long timeline in regenerating plants from protoplasts, the routine use of protoplasts with RNP delivery for generating of stably edited lines has not been reported in economically important crops including cotton, maize, soybean and wheat. On the other hand, some of these crops have well-established high efficiency biolistic transformation systems and successful generation of heritable edits has been achieved using CRISPR-Cas9 *in vitro* transcripts or RNPs delivered with biolistic method (Svitashev et al., 2016; Liang et al., 2018).

During our research in applying Cas12a editing system to maize we have also observed low editing efficiency in some editing targets when the Cas12a editing machinery was expressed from integrated transgenes. In order to understand why we observed variable editing efficiencies, we have tested several parameters such as different Cas12a enzymes and delivery methods. Here we report efficient gene editing in maize with Cas12a RNP delivered into leaf protoplasts and immature embryos. When RNP was delivered via particle bombardment, the average editing efficiency in immature embryos is above 60% using co-selection with the phosphomannose isomerase (PMI) marker gene. A large proportion of mutants generated using this protocol carried biallelic mutations, suggesting efficient cleavage of target sites by Cas12a RNP. The results also indicate that Cas12a RNP-mediated editing has much reduced target dependency. We also show that edited plants can be generated with DNA-free RNP delivery method without any selection in a shorter timeline, albeit at much lower efficiency. We also compared different versions of AsCas12a and LbCas12a genes and showed that higher activity Cas12a mutants resulted in improved editing efficiency at recalcitrant target sequences.

MATERIALS AND METHODS

Plant Materials

Syngenta's proprietary elite maize inbred variety NP2222 was used in all experiments. Stock plant care, maize ear production, immature embryo extraction and transformation with PMI as selectable marker gene was carried out as described before (Zhong H. et al., 2018).

Cas12a and crRNA Reagents Used for Plant Transformation

Cas12a (aka. Cpf1) enzymes including AsCas12a-WT, AsCas12a-V3, AsCas12a-Ultra and LbCas12a-V3 (**Supplementary Table 1**) (Behlke et al., 2018; Vakulskas et al., 2020; Zhang L. et al., 2020) and crRNA were purchased from or provided by IDT (Integrated DNA Technologies, Inc. USA). Guide or spacer sequence of the crRNAs and their corresponding maize gene target are shown in **Supplementary Table 2**. The crRNA scaffold used for LbCas12a is based on CRISPR-LbCpf1 system, while the crRNA scaffold used for AsCas12a is based on CRISPR-AsCpf1 system (Zetsche et al., 2015).

CRISPR-Cas12a Expression Vectors and Generation of Transgenic Maize Plants

Binary transformation vector 12672 contains 2 gene expression cassettes, one for the PMI selectable marker gene driven by the maize Ubiquitin-1 promoter and another for the AmCyan fluorescent protein gene driven by the maize Ubiquitin-1 promoter (Zhong H. et al., 2018). For expression of LbCas12a, the rice codon-optimized coding sequence (Tang et al., 2017) was used with 3 bp changes to remove 2 Bsp119I and one RsrII recognition sites. The Cas12a transformation vectors (**Supplementary Table 3**, **Supplementary Figure 1**) contain 3 expression cassettes: Cas12a expression cassette driven by sugarcane ubiquitin-4 promoter (prSoUbi4) followed by the NOS terminator, crRNA-ribozymes expression cassette and PMI selectable marker cassette. The *Bx9* gene target sequences for the crRNAs of these Cas12a vectors are listed in **Supplementary Table 3**. Transgenic plants were generated through particle bombardment using isolated immature embryos as targets and PMI as a selectable marker (Wright et al., 2001; Chen et al., 2018; Zhong H. et al., 2018). Briefly, immature embryos were isolated from harvested ears at about 9–11 days after pollination and pre-cultured for 1–3 days on osmoticum media. Pre-cultured embryos were then bombarded with the DNA described above using the BioRad PDS-1000 He™ Biolistic particle delivery system. Bombarded embryos were then incubated in callus induction media. For 33°C treatment, bombarded embryos were incubated at 33°C for 2 days before moving back to regular culture temperature at 28°C. Induced calli were then moved onto mannose selection media. Mannose resistant calli were transferred to regeneration media to induce shoot formation. Shoots were then sub-cultured onto rooting media. Leaf samples were harvested from rooted plants for Taqman® assays to detect mutations in the target site using a previously described real time quantitative polymerase chain reaction (qPCR) Taqman® method (Ingham et al., 2001; Chen et al., 2018).

RNP (Ribonucleoprotein) Complex Preparation, Particle Bombardment, and Plant Regeneration

To generate Cas12a-crRNA RNP complexes, 0.3 nmol of Cas12 protein and 0.3 nmol of crRNA were mixed together in a total volume of 11 μl and incubated at room temperature for 10 min. For RNP delivery alone, the RNPs were coated onto 0.6 μm gold particles (Bio-Rad, USA) as follows: 100 μl of gold particles (water suspension of 10 mg/ml) and 20 μl of glycogen (20 mg/ml) were added to the premixed RNPs, mixed gently, and then incubated on ice for 10 min. For co-delivery of RNP with DNA, the RNPs and DNA vector plasmid 12672 were coated onto gold particles as follows: 100 μl of gold particles (water suspension of 10 mg/ml) and 20 μl of glycogen (20 mg/ml) were added to the premixed RNPs and DNA vector, mixed gently, and incubated on ice for 10 min. The RNP/DNA coated gold particles were then centrifuged at 8,000 g for 40 s and the supernatant was removed. The pellet was resuspended with 30 μl of sterile water by brief sonication, and then spread onto a macrocarrier disc (10 μl each) followed by air dry in the laminar flow hood (2–4 h). Immature embryos were isolated, pre-cultured and bombarded with RNP complex alone or RNP complex with 12672 plasmid DNA as described above for DNA delivery. For experiments with RNP delivery alone and those that did not go through mannose selection, the embryos were cultured on callus induction medium for 2 weeks before transferring to regeneration medium for shoot regeneration. Shoots were then sub-cultured onto rooting media. For RNP-DNA delivery, induced calli were selected on mannose containing media and the resistant calli were placed on regeneration media for transgenic plant production as described above for generation of transgenic plants containing Cas12a expression vectors.

Etiolated Maize Leaf Protoplast Isolation and Transfection

Protoplasts were isolated from etiolated maize leaves grown under dark conditions as described (Sheen, 1991). Cas12a RNP was assembled as above. Protoplast transfection was carried out as described, with modification (Sant'Ana et al., 2020). Transfection reactions consisted of 5 x 10^5 protoplasts per reaction and were incubated with PEG solution (40% PEG-4000, 0.6 M Mannitol, 100 mM $CaCl_2$) for 15 min. Following termination by W5 solution (154 mM NaCl, 125 mM CaCl2, 5 mM KCl and 2 mM MES, pH 5.7), transfected protoplasts were resuspended in 300 μl W1 solution (0.6 M Mannitol, 4 mM MES, pH 5.7, 4 mM KCl), transferred to 96-well clear bottom microplate and incubated for 2 days in the dark at 28°C without shaking. DNA was isolated from transfected protoplasts after 2 days and analyzed for mutant identification (Chen et al., 2018).

Molecular Analysis and Mutant Identification

For detection of mutation in immature embryos bombarded with Cas12a-crRNA RNP complex, genomic DNA was extracted from embryos cultured for 2 days after bombardment. Genomic sequences flanking the crRNA target sites were PCR-amplified by specific primers: Bx9-Forward (5′- AAACA CTAAA CACTC CCCTC TG−3′), Bx9-Reverse (5′- GTTTA CCCAT CTCTT TTAAC ACTAT−3′), MIR604-Forward (5′- GGATA TGACT CCACT GACCA−3′) and MIR604-Reverse (5′- CATTT CTCCA TAGCC CGTTT−3′). Amplicons were purified through Ampure XP beads (Beckman Coulter Inc., Brea, CA) following the manufacturer's instructions. Samples containing 40 μl of > 1 ng/μl of purified amplicon DNA were sequenced by SeqWell Inc. (Beverly, MA). NGS raw FASTQ files were aligned to corresponding reference sequences. Reads with Indels were extracted. The reads were further filtered by two criteria: first, the variant region must overlap with gRNA target sequence and second, the variant size must be equal to or larger than 2 bp. The percentage of reads with edits was calculated using the number of filtered Indels divided by total read count covering the gRNA target region. For analysis of editing in regenerated plants, leaf samples were harvested, and total genomic DNA was extracted from rooted plants for Taqman assays were used to detect putative mutations in target sites (Ingham et al., 2001, Chen et al., 2018). Identified putative mutants were further characterized by Sanger or NGS sequencing analysis.

RESULTS AND DISCUSSION

Editing of Chromosomal Target Sequences by Cas12a RNP Delivered Into Maize Immature Embryos and Leaf Protoplasts

DNA-free delivery of editing reagents in the form of protein, mRNA or RNP has great potential to address potential regulatory requirements and public concerns associated with the incorporation of recombinant DNA molecule into edited plants. Successful genome editing using CRISPR-Cas9 RNPs delivered using the biolistic method has been previously demonstrated in wheat and maize using immature embryos as explants (Svitashev et al., 2016, Liang et al., 2018). However, biolistic delivery for Cas12a RNP has yet to be established in maize. We were therefore interested in investigating whether Cas12a RNP could be delivered similarly using particle bombardment to achieve efficient editing in maize. We chose two genomic regions as targets: one is the genic region of *Bx9* gene which encodes for the UDP-glucosyltransferase involved in benzoxazinoid DIMBOA biosynthesis (von Rad et al., 2001) (GRMZM2G161335 in B73 RefGen_v3) **(Sequence File 1 in Supplementary Material)** and another is the non-genic region corresponding to the transgene insertion locus of a commercial event MIR604 for root worm control (Chen et al., 2018), (MIR604FS, **Sequence File 2 in Supplementary Material**).

Table 1 shows the transient editing results of target sequences by AsCas12a-Ultra RNP complexes delivered via particle bombardment. The results show that some genomic targets such as Bx9TS2 can be edited efficiently using AsCas12a RNP. Since only a small percentage of the embryo cells (i.e., those at the scutellum surface and adjacent 1–2 cell layers) can be targeted by microparticles during bombardment, it is expected that a maximum of 5–10% of the total cells in an immature embryo explant can receive Cas12a RNP. Assuming a 10-day immature maize embryo has around 1,000 cells, it has a maximum of 50–100 cells that can be targeted by the delivered RNP complex. Assuming an editing efficiency of ∼50%, it is estimated that only 25–50 cells will get edited and this translates into 2.5–5.0% of sequence reads having mutant variants. It is remarkable that one of the tested crRNAs (crBx9GS2) resulted in 3.42% reads with edits, suggesting that AsCas12a RNP has been delivered to many of the surface cells and it is very active in editing the *Bx9* gene sequence. Other tested crRNAs resulted in lower editing efficiency, with crMIR604GS2 and crMIR604GS4 having 0.35 and 0.19% edited reads, and crMIR604GS1 and crMIR604GS3 having the lowest percentage of edited reads (∼0.10%) (**Table 1**). The reason for lower editing efficiency is not clear, but it is possible both gRNA and target accessibility may play a role. The results suggest that RNP delivery directly into immature embryos, the transformation target explants, can be a quick way to screen gRNAs for Cas12a-mediated editing.

We also validated the top performing crRNAs (crBx9GS2 and crMIR604GS2) from the immature embryo bombardment assay for editing efficiency using protoplast-mediated transfection (**Table 2**). AsCas12a-Ultra RNP transfection in maize protoplasts

TABLE 1 | Transient editing of maize chromosomal target sequence by AsCas12a-Ultra RNP complexes delivered *via* particle bombardment of immature embryos.

Experiment ID	Target site	crRNA	Total sequence read number	Variant (InDel) read number	% Reads with edits (Mean ± SD) (rep number)
Blank control 1	MIR604TS2	None	12,841	1	0.01% ($n = 1$)
Blank control 2	MIR604TS4	None	14,410	2	0.01% ($n = 1$)
MIR604T1A	MIR604TS1	crMIR604GS1	39,267	38	0.10% ± 0.10% ($n = 3$)
MIR604T2A	MIR604TS2	crMIR604GS2	37,750	133	0.35% ± 0.24% ($n = 3$)
MIR604T3A	MIR604TS3	crMIR604GS3	15,922	15	0.09% ± 0.04% ($n = 3$)
MIR604T4A	MIR604TS4	crMIR604GS4	36,445	69	0.19% ± 0.18% ($n = 3$)
Bx9T2A	Bx9TS2	crBx9GS2	35,040	1,198	3.42% ± 0.18% ($n = 3$)

TABLE 2 | Transient editing of maize chromosomal target sequence by AsCas12a-Ultra RNP complexes delivered *via* PEG-mediated protoplast transfection.

Experiment ID	Target site	crRNA	Total read number	Variant (InDel) read number	% Reads with edits (Mean ± SD) (rep number)
Blank control 1	MIR604TS2	None	29,788	87	0.29% ± 0.10% ($n = 3$)
MIR604T2A	MIR604TS2	crMIR604GS2	43,716	15,729	35.98% ± 5.57% ($n = 6$)
Blank control 2	Bx9TS2	None	71,716	153	0.21% ± 0.04% ($n = 3$)
Bx9T2A	Bx9TS2	crBx9GS2	149,313	30,528	20.45% ± 15.06% ($n = 6$)

resulted in high efficiency editing at both targets, with 20.45 and 35.98% of the reads having edits, respectively. It is surprising that crMIR604GS2-RNP resulted in a high percentage of edited reads in leaf protoplasts, at even higher percentage than was observed for crBx9GS2-RNP (**Table 2**). It is not clear why the crMIR604GS2-RNP has a higher editing rate in leaf protoplasts as compared to immature embryos. One possible explanation is that the presence of a more open chromatin structure for the MIR604TS2 target locus in leaf *vs.* immature embryos. It should be noted that protoplast transfection has been widely applied to assess Cas9 RNP activity against different targets in various plant species including maize (Woo et al., 2015; Malnoy et al., 2016; Svitashev et al., 2016; Andersson et al., 2018; Liang et al., 2018; Lin et al., 2018; Murovec et al., 2018; Sant'Ana et al., 2020). Since a much higher percentage of cells can receive RNP in comparison with direct embryo bombardment, protoplast transfection is expected to result (on average) in much higher editing efficiencies. With our maize leaf protoplast transfection experiments with vector expressing green fluorescent protein as reporter, a typical transfection efficiency of 60–70% is obtained (results not shown). However, protoplast isolation is time-consuming and tedious, and direct bombardment of immature embryos coupled with targeted deep sequencing can offer a straightforward alternative to evaluate gRNA performance directly in the transformation target tissues.

High Efficiency Recovery of Edited Lines by Co-delivery of Cas12a RNP With a Selectable Marker Gene Vector

Since reasonable editing efficiencies were achieved using AsCas12a RNP in direct immature embryo bombardment, we also tested whether stably edited lines can be recovered from immature embryos bombarded with RNPs targeting *Bx9* gene. We co-delivered RNP with a plasmid named pBSC12672 which contains the PMI selectable marker gene (Zhong H. et al., 2018). We tested three different versions of AsCas12a nuclease: AsCas12a-WT, AsCas12a-V3 and AsCas12a-Ultra; the AsCas12a-WT and AsCas12a-V3 proteins contain the wild-type AsCas12a sequence with AsCas12a-V3 also containing an optimized NLS sequence, whereas the AsCas12a-Ultra is an engineered-version of AsCas12a-V3 with mutations that were isolated using directed evolution in bacteria to achieve higher editing efficiencies in living cells (Zhang L. et al., 2020) (**Supplementary Table 1**).

To optimize mutation rate, we tested multiple parameters including different versions of AsCas12a, helium pressure for bombardment and culture temperature (**Supplementary Table 4**). Incubation at 37°C produced more mutants but transformation efficiency was negatively affected. Overall, the results showed that 1,100 psi, 0.3 nmol RNP and culture of bombed embryos at 33°C for 2 days immediately after bombardment is a good combination for high efficiency editing of Bx9TS1 target (**Supplementary Table 4**). We also directly compared performance of AsCas12a-WT with AsCas12a-Ultra (**Table 3**). With AsCas12a-WT protein, only about 1.2–7.1% of transgenic plants derived from immature embryos co-bombarded with RNP and 12672 plasmid DNA showed successful editing at the Bx9TS1 target according to Sanger sequencing results (**Table 3**). The sequencing profile of 5 mutants was examined and these results indicated five distinct deletions had occurred at the expected loci (**Supplementary Figure 2**). Remarkably, the use of the improved AsCas12a nuclease (AsCas12a-Ultra) resulted in about a 10-fold improvement in editing rate to 68.8% (**Table 3**). In addition, a high percentage of the edits are biallelic, suggesting high activity of AsCas12a-Ultra in recognizing and cutting the genomic target sequences in maize cells.

Lines With Heritable Edits Can Be Generated Directly From Maize Immature Embryos Bombarded With Cas12a RNP Without Selection

Considering the high editing rate of AsCas12a RNP in direct immature embryo bombardment (**Table 3**, **Supplementary Table 4**), we wondered whether stably edited lines could be recovered from immature embryos that have been bombarded with RNP targeting *Bx9* gene in the absence of selection. After AsCas12a RNP was delivered into maize immature embryos, regenerated plant lines (E0) were obtained within 1 month. Putative mutants were identified using high-throughput Taqman assays (Chen et al., 2018) to identify mutations in the Bx9TS2 target sequence (**Supplementary Tables 2**, **5**, **Sequence File 1 in Supplementary Material**). Mutant plants were further characterized by sequencing to confirm the identity of genomic edits. **Table 4** shows that 24 mutants at Bx9TS2 target were identified from a total of 419 immature embryos bombed

TABLE 3 | Targeted mutagenesis of *Bx9* target Bx9TS1 with ribonucleoprotein (RNP) complex of two versions of AsCas12a in maize co-delivered with PMI selectable marker gene vector 12672.

Treatment	AsCas12a enzyme	Embryo explants used	Events[#]	Transformation frequency	Putative mutant (Taqman assay)	Biallelic mutants	Seq. confirmed mutants	Editing rate*
A	AsCas12a-WT	2,093	84	4.0%	1	0	1	1.2%
B	AsCas12a-WT	490	99	20.2%	2	1	2	2.0%
C	AsCas12a-WT	2,165	28	1.3%	2	0	2	7.1%
D	AsCas12a-Ultra	2,670	77	2.9%	53	49	53	68.8%

[#]*Selectable marker plasmid (pBSC12672) was co-precipitated and co-delivered into precultured immature embryos at 1,100 psi; Bombarded embryos were incubated at 33°C for 2 days before moving back to regular culture temperature at 28°C. Calli selected with mannose.*
**Editing rate: number of edited lines/100 regenerated plants.*

TABLE 4 | Mutation frequency of Bx9TS2 target in E0 plants directly generated from bombarded immature embryos with RNP without selection.

Treatment	AsCas12a	Embryo explants used	Plants sampled[&]	Biallelic mutant	Monoallelic mutant	Total number of plants with InDel	Editing rate*	Editing efficiency[#]
A	V3	288	585	11	5	16	2.7%	5.6%
B	Ultra	131	204	7	1	8	3.9%	6.1%
Total		419	789	18	6	24	3.0%	5.7%

[&]*For this experiment only, all regenerated shoots from an explant were sampled for mutation analysis. Therefore, some explants had more than 1 shoot.*
**Editing rate: number of edited lines/100 regenerated plants.*
[#]*Editing efficiency: number of edited plants/100 starting immature embryo explants.*

with AsCas12a RNP and crBx9GS2 gRNA. NGS sequencing confirmed that 16 of the 24 mutants have biallelic mutations.

E0 plants were self-pollinated to produce E1 seeds. **Supplementary Table 5** shows that all E1 progeny of the biallelic E0 mutants have biallelic mutations. Of the 3 monoallelic mutant E0 lines, two of them had poor germination, resulting in small number of E1 lines and thus not meaningful for statistical analysis. However, for unknown reasons line MZKE192601A571A's segregation does not fit the expected 1:2:1 (HOM/HET/WT) ratio. Overall, the results indicated that edits in E0 mutant lines generated using RNP delivery and without selection can be stably inherited to the progeny plants.

Cas12a RNP Results in Comparable or Higher Editing Efficiency in Comparison With Editing Machinery Expressed From Transgenes

Maize transformation is usually done using particle bombardment or *Agrobacterium*-mediated delivery. Therefore, genome editing machinery is commonly delivered in the form of DNA expression cassettes. For example, Cas9 nuclease and gRNA are controlled under PolII and PolIII promoters, respectively (Svitashev et al., 2016). We were interested in comparing the relative efficiency of Cas12a editing delivered by either RNP or DNA delivery methods. For biolistic-mediated delivery of Cas12a editing machinery targeting Bx9TS1 and Bx9TS2 sites, binary vectors containing various AsCas12a and LbCas12a variants were constructed that express crRNA targeting Bx9TS1 or Bx9TS2 sequence, respectively (**Supplementary Tables 2, 3, Supplementary Figure 1**); Each of the vectors contains three expression cassettes: PMI selectable marker, Cas12a and crRNA flanked by self-processing ribozymes (**Supplementary Figure 1**). Both Cas12a and crRNA were controlled by sugarcane ubiquitin-4 promoter (prSoUbi). Embryos bombarded with different DNA vectors were then selected on mannose to recover transgenic plants. Plants were assayed for editing at Bx9TS1 and Bx9TS2 target sequences.

The results in **Table 5** shows that in general the editing rate and efficiency are higher for Bx9TS2 than Bx9TS1 target sites. It is interesting that the editing efficiency of Bx9TS1 is significantly improved when higher activity mutant AsCas12a-Ultra were used in comparison with the wild-type AsCas12a protein (V3). However, the editing efficiency at Bx9TS2 was already very high with the wild-type AsCas12a protein, and the use of improved variant had a negligible effect on editing efficiency (**Table 5**). We also compared the editing efficiency of two different temperatures on two different editing targets Bx9TS1 and Bx9TS2. Both AsCas12a and LbCas12a vectors worked well for editing of both targets at both 28 and 33°C (**Table 5**). However, higher editing rates at both Bx9TS1 and Bx9TS2 target were achieved when bombed cultures were incubated at 33°C (**Table 5**). For LbCas12a, editing rate at both target sites is somewhat higher with LbCas12a-V3 in comparison with the LbCas12a version with rice optimized codon (Lb, Qi in **Table 5**).

It is also interesting that the editing rate of Bx9TS1 target sequence with AsCas12a-Ultra RNP was higher than when the editing machinery was expressed from a transgene (**Tables 3**, **5**). The lower editing efficiency with AsCas12a expressed from a transgene is probably due to several reasons.

TABLE 5 | Editing efficiency of *Bx9* target sequences in transgenic plants expressing different versions of Cas12a enzymes.

Vector ID	Target site	Cas12a gene	Culture temp	Embryo explants used	PMI positive events+	Transformation frequency	Biallelic	Monoallelic	Total Mutants	Editing rate[#]	Editing efficiency*
pBIDT1	Bx9TS1	As, V3	33°C	714	85	11.9%	2	9	11	12.9%	1.5%
pBIDT2	Bx9TS1	As, Ultra	33°C	400	34	8.5%	9	5	14	41.0%	3.5%
pBIDT2	Bx9TS1	As, Ultra	28°C	180	12	6.7%	1	4	5	41.0%	2.8%
pBIDT3	Bx9TS1	Lb, V3	33°C	756	106	14.0%	15	7	22	23.6%	2.9%
24096	Bx9TS1	Lb, Qi	33°C	793	73	17.8%	8	7	13	17.8%	1.6%
pBIDT4	Bx9TS2	As, V3	33°C	702	132	18.8%	64	35	99	78.0%	14.1%
pBIDT5	Bx9TS2	As, Ultra	33°C	380	31	8.2%	18	10	28	83.9%	7.4%
pBIDT5	Bx9TS2	As, Ultra	28°C	205	15	7.3%	3	3	6	33.3%	2.9%
pBIDT6	Bx9TS2	Lb, V3	33°C	720	74	10.3%	30	30	60	83.8%	8.3%
24100	Bx9TS2	Lb, Qi	33°C	787	86	10.9%	30	26	58	67.4%	7.4%

[#]*Editing rate: number of edited lines/100 transgenic events.*

**Editing efficiency: number of edited plants/100 starting immature embryo explants. For 33°C treatment, bombed embryos were incubated at 33°C for 2 days before moving back to regular culture temperature at 28°C.*

While DNA delivery is efficient, efficient transcription and translation of delivered transgenes can be highly variable depending on the activity of promoters and post-transcriptional regulatory features, and poor codon optimization can also negatively influence overall transgene expression. DNA transgene expression also depends on proper gRNA processing and transport of Cas12a protein back to the correct nuclear compartment for proper RNP assembly; whereas *in vitro* assembly of Cas12a RNP is very efficient and the pre-assembled RNP can start doing editing once delivered into the nucleus.

CONCLUSION

CRISPR-Cas12a is an attractive alternative system to CRISPR-Cas9 for crop genome editing (Zetsche et al., 2015; Tang et al., 2017). However, it has several limitations in comparison with Cas9 including less flexibility due to its longer PAM sequence requirements (TTTV-3′), low activity at room temperature, higher percentage of non-functional gRNA (Lee et al., 2019, Malzahn et al., 2019). Therefore, it is highly desirable to have a fast and efficient prescreen system for gRNAs or Cas12a expression vectors to test their functionality before investing resources to carry out stable transformation which is resource-intensive and also usually takes 2–3 months before regenerated materials are available for molecular analysis. In this report we have demonstrated that the commonly used maize transformation target explants, i.e., immature embryos can be directly bombed with RNPs for assessing their genome editing capability. Alternatively, leaf protoplasts can be an efficient RNP screening system. We have also shown that RNP led to high efficiency editing when delivered into maize immature embryo targets; In addition, stable lines with heritable edits can be efficiently generated *via* RNP delivery with or without co-selection. Finally, we have demonstrated that both AsCas12a, LbCas12a and their mutants with enhanced activities can be used to generate targeted genome modifications at high rate. The techniques described in this paper provide us useful tools for precision genome engineering of maize, an important field crop.

DATA AVAILABILITY STATEMENT

The datasets used and/or analyzed during the current study are available from the corresponding author on reasonable request.

AUTHOR CONTRIBUTIONS

SD, WG, MY, SR, and QQ conceived and designed experiments. YQ, CV, and MC constructed the vectors. AM, SE, MM, and SD did transformation experiments. SR did protoplast experiments. CF, YJ, LZ, MY, and WG did assay design and molecular analysis. CV and MC provided Cas12a enzymes. QQ, HZ, ZC, and LS provided suggestions, research, and laboratory support. SD and QQ wrote the manuscript. All authors contributed to the article and approved the submitted version.

ACKNOWLEDGMENTS

The authors would like to thank Anna Prairie, Sam Nalapalli, and Xiujuan Su for generating transgenic plants. James Roberts, Rafaela Miranda Lunny Castro, and Tim Strebe for providing maize ears on a timely manner and taking care of the edited plants in greenhouse. David Bradley and Ping Wu for making the media required for tissue culture and transformation. We also like to thank Jianping Xu, Wan Shi, and Ian Jepson for helpful discussions and suggestions.

SUPPLEMENTARY MATERIAL

The Supplementary Material for this article can be found online at: https://www.frontiersin.org/articles/10.3389/fgeed.2021.670529/full#supplementary-material

REFERENCES

Andersson, M., Turesson, H., Olsson, N., Fält, A. S., Ohlsson, P., Gonzalez, M. N., et al. (2018). Genome editing in potato via CRISPR-Cas9 ribonucleoprotein delivery. *Physiol. Plant* 164, 378–384. doi: 10.1111/ppl.12731

Bayat, H., Modarressi, M. H., and Rahimpour, A. (2018). The conspicuity of CRISPR-Cpf1 system as a significant breakthrough in genome editing. *Curr. Microbiol.* 75, 107–115. doi: 10.1007/s00284-017-1406-8

Begemann, M. B., Gray, B. N., January, E., Gordon, G. C., He, Y., Liu, H., et al. (2017). Precise insertion and guided editing of higher plant genomes using Cpf1 CRISPR nucleases. *Sci. Rep.* 7:11606. doi: 10.1038/s41598-017-11760-6

Behlke, M. A., Collingwood, M. A., Turk, R., and Vakulskas, C. A. (2018). *CRISPR/Cpf1 Systems and Methods*. United States Patent Application Publication, US20180187176A1. Available online at: https://patents.google.com/patent/US20180187176A1/en (accessed July 5, 2018).

Chakrabarti, A. M., Henser-Brownhill, T., Monserrat, J., Poetsch, A. R., Luscombe, N. M., and Scaffidi, P. (2019). Target-specific precision of CRISPR-mediated genome editing. *Mol. Cell.* 73, 699–713. doi: 10.1016/j.molcel.2018.11.031

Chen, Z., Kim, M., Chilton, M. D., Zhong, H., Gu, W., Jiang, Y., et al. (2018). *Methods and Compositions for Identifying and Enriching for Cells Comprising Site Specific Genomic Modifications*. United States Patent 9,963,710.

El-Mounadi, K., Morales-Floriano, M. L., and Garcia-Ruiz, H. (2020). Principles, applications, and biosafety of plant genome editing using CRISPR-Cas9. *Front. Plant Sci.* 11:56. doi: 10.3389/fpls.2020.00056

Endo, A., Masafumi, M., Kaya, H., and Toki, S. (2016) Efficient targeted mutagenesis of rice and tobacco genomes using Cpf1 from *Francisella novicida*. *Sci. Rep.* 6:38169. doi: 10.1038/srep38169

Endo, M., Mikami, M., Endo, A., Kaya, H., Itoh, T., Nishimasu, H., et al. (2019). Genome editing in plants by engineered CRISPR–Cas9 recognizing NG PAM. *Nat. Plants* 5, 14–17. doi: 10.1038/s41477-018-0321-8

Hille, F., H., Richter,Wong, S. P., Bratovič, M., Ressel, S., and Charpentier, E. (2018). The biology of CRISPR-Cas: backward and forward. *Cell* 172, 1239–1259. doi: 10.1016/j.cell.2017.11.032

Ingham, D. J., Beer, S., Money, S., and Hansen, G. (2001). Quantitative real-time PCR assay for determining transgene copy number in transformed plants. *Biotechniques* 31, 132–134. doi: 10.2144/01311rr04

Jinek, M., Chylinski, K., Fonfara, I., Hauer, M., Doudna, J. A., and Charpentier, E. (2012). A programmable dual-RNA-guided DNA endonuclease in adaptive bacterial immunity. *Science* 337, 816–821. doi: 10.1126/science.1225829

Lee, K., Zhang, Y., Kleinstiver, B. P., Guo, J. A., Aryee, M. J., Miller, J., et al. (2019). Activities and specificities of CRISPR/Cas9 and Cas12a nucleases for targeted mutagenesis in maize. *Plant Biotech. J.* 17, 362–372. doi: 10.1111/pbi.12982

Li, S., Li, J., Zhang, J., Du, W., Fu, J., Sutar, S., et al. (2018b). Synthesis-dependent repair of Cpf1-induced double strand DNA breaks enables targeted gene replacement in rice. *J. Exp. Bot.* 69, 4715–4721. doi: 10.1093/jxb/ery245

Li, S., Zhang, X., Wang, W., Guo, X., Wu, Z., Du, W., et al. (2018a). Expanding the scope of CRISPR/Cpf1-mediated genome editing in rice. *Mol. Plant* 11, 995–998. doi: 10.1016/j.molp.2018.03.009

Li, S., Zhang, Y., Xia, L., and Qi, Y. (2020). CRISPR-Cas12a enables efficient biallelic gene targeting in rice. *Plant Biotech. J.* 18, 1351–1353. doi: 10.1111/pbi.13295

Liang, Z., Chen, K., Zhang, Y., Liu, J., Yin, K., Qiu, J. L., et al. (2018). Genome editing of bread wheat using biolistic delivery of CRISPR/Cas9 *in vitro* transcripts or ribonucleoproteins. *Nat. Protocol.* 13, 413–430. doi: 10.1038/nprot.2017.145

Lin, C. S., Hsu, C. T., Yang, L. H., Lee, L. Y., Fu, J. Y., Cheng, Q. W., et al. (2018). Application of protoplast technology to CRISPR/Cas9 mutagenesis: from single-cell mutation detection to mutant plant regeneration. *Plant Biotech. J.* 16, 1295–1310. doi: 10.1111/pbi.12870

Malnoy, M., Viola, R., Jung, M. H., Koo, O. J., Kim, S., Kim, J. S., et al. (2016). DNA-free genetically edited grapevine and apple protoplast using CRISPR/Cas9 ribonucleoproteins. *Front. Plant Sci.* 7:1904. doi: 10.3389/fpls.2016.01904

Malzahn, A. A., Tang, X., Lee, K., Ren, Q., Sretenovic, S., Zhang, Y., et al. (2019). Application of CRISPR-Cas12a temperature sensitivity for improved genome editing in rice, maize, and Arabidopsis. *BMC Biol.* 17:9. doi: 10.1186/s12915-019-0629-5

Memi, F., Ntokou, A., and Papangeli, I. (2018). CRISPR/Cas9 gene-editing: research technologies, clinical applications and ethical considerations. *Semin. Perinatol.* 42, 487–500. doi: 10.1053/j.semperi.2018.09.003

Murovec, J., Guček, K., Bohanec, B., Avbelj, M., and Jerala, R. (2018). DNA-free genome editing of *Brassica oleracea* and *B. rapa* protoplasts using CRISPR-Cas9 ribonucleoprotein complexes. *Front. Plant Sci.* 9:1594. doi: 10.3389/fpls.2018.01594

Murugan, K., Babu, K., Sundaresan, R., Rajan, R., and Sashital, D. G. (2017). The revolution continues: Newly discovered systems expand the CRISPR-Cas toolkit. *Mol Cell.* 68, 15–25. doi: 10.1016/j.molcel.2017.09.007

Que, Q., Chen, Z., Kelliher, T., Skibbe, D., Dong, S., and Chilton, M. D. (2019). Plant DNA repair pathways and their applications in genome engineering. *Methods Mol Biol.* 1917, 3–24. doi: 10.1007/978-1-4939-8991-1_1

Sant'Ana, R. R. A., Caprestano, C. A., Nodari, R. O., and Agapito-Tenfen, S. Z. (2020). PEG-delivered CRISPR-Cas9 ribonucleoproteins system for gene-editing screening of maize protoplasts. *Genes* 11:1029. doi: 10.3390/genes11091029

Sapranauskas, R., Gasiunas, G., Fremaux, C., Barrangou, R., Horvath, P., and Siksnys, V. (2011). The Streptococcus thermophilus CRISPR/Cas system provides immunity in Escherichia coli. *Nucleic Acids Res.* 39, 9275–9282. doi: 10.1093/nar/gkr606

Schindele, P., and Puchta, H. (2020). Engineering CRISPR/LbCas12a for highly efficient, temperature-tolerant plant gene editing. *Plant Biotech. J.* 18, 1118–1120. doi: 10.1111/pbi.13275

Sheen, J. (1991). Molecular mechanisms underlying the differential expression of maize pyruvate, orthophosphate dikinase genes. *Plant Cell* 3, 225–245. doi: 10.1105/tpc.3.3.225

Sretenovic, S., Yin, D., Levav, A., Selengut, J. D., Mount, S. M., and Qi, Y. (2020). Expanding plant genome-editing scope by an engineered iSpyMacCas9 system that targets A-rich PAM sequences. *Plant Commun.* 2:100101. doi: 10.1016/j.xplc.2020.100101

Svitashev, S., Schwartz, C., Lenderts, B., Young, J., and Cigan, A. M. (2016). Genome editing in maize directed by CRISPR–Cas9 ribonucleoprotein complexes. *Nat. Commun.* 7:13274. doi: 10.1038/ncomms13274

Tang, X., Lowder, L., Zhang, T., Malzahn, A. A., Zheng, X., and Voytas, D. F. (2017). A CRISPR–Cpf1 system for efficient genome editing and transcriptional repression in plants. *Nat. Plants* 3:17018. doi: 10.1038/nplants.2017.103

Tang, Y., and Fu, F. (2018). Class 2 CRISPR/Cas: an expanding biotechnology toolbox for and beyond genome editing. *Cell Biosci.* 8:59. doi: 10.1186/s13578-018-0255-x

Vakulskas, C. A., Bode, N. M., Collingwood, M. A., and Beaudoin, S. (2020). *Cas12a Mutant Genes and Polypeptides Encoded by Same*. United States Patent Application Publication, US20200216825A1. Available online at: https://patents.google.com/patent/US20200216825A1/en (accessed July 9, 2020).

von Rad, U., Hüttl, R., Lottspeich, F., Gierl, A., and Frey, M. (2001). Two glucosyltransferases are involved in detoxification of benzoxazinoids in maize. *Plant J.* 28, 633–642. doi: 10.1046/j.1365-313x.2001.01161.x

Wang, M., Mao, Y., Lu, Y., Wang, Z., Tao, X., and Zhu, J. K. (2018). Multiplex gene editing in rice with simplified CRISPR-Cpf1 and CRISPR-Cas9 systems. *J. Integr. Plant Biol.* 60, 626–631. doi: 10.1111/jipb.12667

Woo, J. W., Kim, J., Kwon, S. I., Corvalan, C., Cho, S. W., et al. (2015). DNA-free genome editing in plants with preassembled CRISPR-Cas9 ribonucleoproteins. *Nat. Biotechnol.* 33, 1162–1164. doi: 10.1038/nbt.3389

Wright, M., Dawson, J., Dunder, E., Suttie, J., Reed, J., Kramer, C., et al. (2001). Efficient biolistic transformation of maize (*Zea mays* L.) and wheat (*Triticum aestivum* L.) using the phosphomannose isomerase gene, pmi, as the selectable marker. *Plant Cell Rep.* 20, 429–436. doi: 10.1007/s002990100318

Xu, R., Qin, R., Li, H., Li, D., Li, L., Wei, P., et al. (2017) Generation of targeted mutant rice using a CRISPR-Cpf1 system. *Plant Biotech. J.* 15, 713–717. doi: 10.1111/pbi.12669

Zetsche, B., Gootenberg, J. S., Abudayyeh, O. O., Slaymaker, I. M., Makarova, K. S., Essletzbichler, P., et al. (2015). Cpf1 is a single RNA-guided endonuclease of a class 2 CRISPR-Cas system. *Cell* 163, 759–771. doi: 10.1016/j.cell.2015.09.038

Zhang, L., Vakulskas, C. A., Bode, N. M., Collingwood, M. A., Beltz, K. R., and Behlke, M. A. (2020). *Novel Mutations That Enhance the DNA Cleavage Activity of Acidaminococcus sp. cpf1*. United States Patent Application Publication, US20200109382A1. Available online at: https://patents.google.com/patent/US20200109382A1/en (accessed April 9, 2020).

Zhang, Y., Liang, Z., Zong, Y., Wang, Y., Liu, J., and Chen, K. (2016). Efficient and transgene-free genome editing in wheat through transient expression of CRISPR/Cas9 DNA or RNA. *Nat. Commun.* 7:12617. doi: 10.1038/ncomms12617

Zhang, Y., Pribil, M., Palmgren, M., and Gao, C. (2020). A CRISPR way for accelerating improvement of food crops. *Nat. Food* 1, 200–205. doi: 10.1038/s43016-020-0051-8

Zhong, H., Elumalai, S., Nalapalli, S., Richbourg, L., Prairie, A., Bradley, D., et al. (2018). Advances in Agrobacterium-mediated maize transformation. *Methods Mol. Biol.* 1676, 41–59. doi: 10.1007/978-1-4939-7315-6_3

Zhong, Z., Zhang, Y., You, Q., Tang, X., Ren, Q., Liu, S., et al. (2018). Plant genome editing using FnCpf1 and LbCpf1 nucleases at redefined and altered PAM sites. *Mol. Plant* 11, 999–1002. doi: 10.1016/j.molp.2018.03.008

Conflict of Interest: SD, YQ, MM, SR, LZ, YJ, WG, CF, AM, ZC, MY, HZ, SE, LS, and QQ were employed by Syngenta Crop Protection, LLC. CV and MC are employed by Integrated DNA Technologies which manufactures genome editing reagents.

frontiers in Genome Editing

ORIGINAL RESEARCH
published: 15 June 2021
doi: 10.3389/fgeed.2021.663380

In-planta Gene Targeting in Barley Using Cas9 With and Without Geminiviral Replicons

*Tom Lawrenson, Alison Hinchliffe, Martha Clarke, Yvie Morgan and Wendy Harwood**

John Innes Centre, Norwich Research Park, Norwich, United Kingdom

Advances in the use of RNA-guided Cas9-based genome editing in plants have been rapid over the last few years. A desirable application of genome editing is gene targeting (GT), as it allows a wide range of precise modifications; however, this remains inefficient especially in key crop species. Here, we describe successful, heritable gene targeting in barley at the target site of Cas9 using an *in-planta* strategy but fail to achieve the same using a wheat dwarf virus replicon to increase the copy number of the repair template. Without the replicon, we were able to delete 150 bp of the coding sequence of our target gene whilst simultaneously fusing in-frame mCherry in its place. Starting from 14 original transgenic plants, two plants appeared to have the required gene targeting event. From one of these T0 plants, three independent gene targeting events were identified, two of which were heritable. When the replicon was included, 39 T0 plants were produced and shown to have high copy numbers of the repair template. However, none of the 17 lines screened in T1 gave rise to significant or heritable gene targeting events despite screening twice the number of plants in T1 compared with the non-replicon strategy. Investigation indicated that high copy numbers of repair template created by the replicon approach cause false-positive PCR results which are indistinguishable at the sequence level to true GT events in junction PCR screens widely used in GT studies. In the successful non-replicon approach, heritable gene targeting events were obtained in T1, and subsequently, the T-DNA was found to be linked to the targeted locus. Thus, physical proximity of target and donor sites may be a factor in successful gene targeting.

Keywords: wheat dwarf virus, homology-dependent recombination, knock-in, precise insertion, repair template

OPEN ACCESS

Edited by:
Yiping Qi,
University of Maryland, College Park, United States

Reviewed by:
Goetz Hensel,
Heinrich Heine University Düsseldorf, Germany
Filiz Gürel,
University of Maryland, College Park, United States

****Correspondence:***
Wendy Harwood
wendy.harwood@jic.ac.uk

Specialty section:
This article was submitted to Genome Editing in Plants, a section of the journal Frontiers in Genome Editing

Received: *02 February 2021*
Accepted: *29 April 2021*
Published: *15 June 2021*

Citation:
Lawrenson T, Hinchliffe A, Clarke M, Morgan Y and Harwood W (2021) In-planta Gene Targeting in Barley Using Cas9 With and Without Geminiviral Replicons. Front. Genome Ed. 3:663380. doi: 10.3389/fgeed.2021.663380

INTRODUCTION

Genome editing has exploded in recent years due to advances in programmable nucleases which allow a double-stranded DNA break to be created at a predefined locus. First on the scene were Zinc-finger nucleases (Kim et al., 1996) followed by transcription activator-like effector nucleases (TALENS) (Christian et al., 2010) and, more recently, clustered regularly interspaced short palindromic repeats (CRISPR) systems, especially the *Sp*Cas9 (Jinek et al., 2012) which was the first CRISPR nuclease reported to function in plants (Feng et al., 2013; Li et al., 2013; Nekrasov et al., 2013; Shan et al., 2013; Xie and Yang, 2013). Although insertion of exogenously supplied DNA into plant genomes has been possible for many years *via Agrobacterium*-mediated transformation or physical delivery, location was impossible to control precisely. Some success is reported inserting DNA in a precise manner by homologous recombination in rice without creating

a double-strand break (DSB) at the target site, although it was necessary to use a positive/negative selection system (Terada et al., 2002) which was later shown to produce no successful modifications in barley (Horvath et al., 2017). The value of creating a DSB at the target site to initiate DNA repair and facilitate insertion by homologous recombination was shown early on in plants with the non-programmable *I-SceI* meganuclease (Fauser et al., 2012), so it was a natural progression to repurpose Cas9 for precise insertional modifications. Many DSBs are repaired by non-homologous end-joining (NHEJ) mechanisms which are error prone but shown to be capable of inserting an exogenously supplied DNA template at the break point in plants (Salomon and Puchta, 1998; Chilton and Que, 2003; Tzfira et al., 2003; Lee et al., 2019) although precision is likely to be compromised by indels created at the spliced junctions as well as issues controlling orientation, truncation and concatenation.

Targeted DSBs can be introduced very efficiently and with great precision into plant genomes using RNA-guided Cas9, and this has made it facile over recent years to produce gene knockouts by the introduction of indels and larger deletions due to the error-prone nature of NHEJ. Many reports now exist describing single and multiple gene knockouts at efficiencies often approaching 100% although the precise nature of the edit is often not possible to predict. Lesions typically lead to a shift in reading frame and a premature stop codon. Base and prime editing technologies (Komor et al., 2016; Gaudelli et al., 2017; Anzalone et al., 2019) have partially addressed the precision issue allowing defined single base changes as well as short insertions and deletions, although larger precise changes such as adding an in-frame reporter fusion are unlikely to be possible in this way.

Gene targeting (GT) can be defined as the introduction of a precise predefined modification into a plant genome, either an insertion, deletion or replacement *via* the introduction of a supplied repair template using homology-dependent recombination (HDR) and usually a DSB at the target site. By making available a repair template containing the required modification flanked by sequence homologous to each side of the DSB, a precise change can be introduced into the genome. This change can be either small, for example, a single amino acid conversion (Budhagatapalli et al., 2015; Sun et al., 2016; Svitashev et al., 2016; Wolter et al., 2018; Danilo et al., 2019; Wolter and Puchta, 2019), or large such as the in-frame insertion of a reporter gene (Zhao et al., 2016; Wang et al., 2017; Miki et al., 2018).

Whilst GT is able to address both large and small precise modifications, it is usually much harder to achieve than knockout, and so researchers have sought ways in which rare events can be screened for easily and means to boost the frequency at which they occur. Early GT efforts in crops have focussed on creating a precise change resulting in resistance to an herbicide or antibiotic which can then be used to select for resistant plants containing the desired GT event. *ALS* (acetolactate synthase) is a plant gene essential in the production of branched chain amino acids that is a target for inhibitors used as herbicides which has been extensively used in plants for GT experiments (Svitashev et al., 2015, 2016; Sun et al., 2016; Wolter et al., 2018; Danilo et al., 2019). Sometimes, a visual marker has been used in the screen such as insertion of a 35s promoter upstream of *ANT1* leading to a purple phenotype (Cermak et al., 2015), or restoration of *gl1* leading to trichome production in *Arabidopsis* (Hahn et al., 2018). This approach, however, means that modification is restricted to genes which allow such a selectable or visible phenotype, which many editing projects will not.

Many crop plants may only be transformed at efficiencies of a few percent or less, which, when combined with the low efficiency of GT, makes regeneration of T0 gene targeted plants hugely labour intensive or just inconceivable. One way around this is to adopt an *in-planta* strategy whereby just a few primary transgenics containing the editing reagents are created, but the numbers required to retrieve the rare GT events are generated by the plants themselves through the normal process of flowering and seed production (Fauser et al., 2012; Schiml et al., 2014, 2017). Each progeny plant may give rise to successful GT events, perhaps just as somatic sectors, but these can enter the germline and prove to be heritable in subsequent generations. In this approach, all the editing reagents can be included on a single T-DNA with a selection cassette to allow transgenic production, a nuclease programmed to create a DSB at the target site and a repair template containing the desired modification with flanking sequence homologous to each side of the target site DSB. Recognition sequences for the nuclease can also be added to the ends of the repair template to allow cutting and its transfer to the target site (Schiml et al., 2014; Zhao et al., 2016). Here, the screen can be based on the genotype rather than the phenotype, with plants containing the required edits being detected by PCR for example. A widely adopted approach is to PCR screen using one primer within the modified region of the repair template and the second primer outside of the repair template in the sequence flanking the target site. In this way, the PCR must cross the junction where the repair template stops, and the flanking genomic sequence begins.

It has been suggested that one major constraint on successful GT is the availability of repair template sequence at the correct time and in sufficient quantity for it to be incorporated as intended. In order to address this, Geminivirus replicons have been utilised (Baltes et al., 2014; Butler et al., 2016; Gil-Humanes et al., 2017; Wang et al., 2017; Dahan-Meir et al., 2018; Hahn et al., 2018; Vu et al., 2020), simultaneously pushing plant cells into more of an S phase-like state where HDR repair occurs more frequently and by replicating to high copy numbers providing many copies of the repair template to the target site. Here, the coat and movement protein section of the viral genome can be replaced by the repair template and then supplied in linear form to the plant on a T-DNA for *Agrobacterium*-mediated delivery. Once within the plant cell, the viral REP proteins are expressed leading to rolling circle replication and many copies of the repair template. Cas9 can also be delivered on the same T-DNA allowing simultaneous DSB at the target site and production of large quantities of the repair template. This approach has been most successful in tomato (Cermak et al., 2015; Dahan-Meir et al., 2018; Vu et al., 2020) but has also been described in wheat (Gil-Humanes et al., 2017), rice (Wang et al., 2017) and potato (Butler et al., 2016) although

Arabidopsis appeared to be recalcitrant to any GT benefits (Hahn et al., 2018).

To date, there have been two reports of GT in barley: one a transient single amino acid conversion of a GFP transgene to YFP (Budhagatapalli et al., 2015) and the second a stable modification of a non-functional *hptII* transgene to a functional form (Watanabe et al., 2016). The former was identified in epidermal cells and the latter was one-sided GT events—one side of the repair was by HDR and the other by NHEJ. Our aim was to achieve heritable Cas9 GT in barley which would modify a locus of interest that was not a transgene and could be selected genotypically; thus, we chose to create a partial deletion of a native barley gene of interest, simultaneously fusing an in-frame reporter to the remaining part. To keep the number of transgenics required to a minimum and to potentially make the approach suitable for genotypes more recalcitrant to transformation, we used an *in-planta* strategy and attempted to increase efficiency by incorporating the repair template within a Geminivirus replicon. We present efficiencies using strategies with and without inclusion of the replicon.

MATERIALS AND METHODS

PCR and Sanger Sequencing of HORVU4Hr1G061310 Target Locus for Indel Detection

PCR was done using 30 ng of genomic DNA as template, 400 nM of primers F4 and R5 (**Supplementary Table 6**), Qiagen 2× PCR Master Mix and a total reaction volume of 25 μl being completed by water. After initial denaturation at 94°C for 3 min, 40 cycles of 94°C for 30 s/58°C for 1 min/72°C for 45 s were performed. A final extension of 72°C for 5 min was given. One microliter of the cleaned product (see Sanger sequencing PCR products) was then used in separate Sanger reactions with both F4 and R5 primers. ABI chromatograms were compared with known WT chromatograms using the web-based ICE CRISPR analysis tool (www.synthego.com/products/bioinformatics/crispr-analysis) to identify lines carrying indels at target sites A and B.

Sanger Sequencing of PCR Products

PCR reactions were prepared for Sanger sequencing by adding 10 units of exonuclease 1 and 1 unit of shrimp alkaline phosphatase to 10 μl of PCR reaction before incubation at 37°C for 30 min followed by 80°C for 10 min to inactivate the enzymes. One microliter of the cleaned product was used as sequencing template where the amplicon was 1 kb or less in size and 2 μl when over 1 kb. Sequencing reactions were in 10 μl volumes with 100 nM primer, 1.5 μl BigDye buffer and 1 μl BigDye 3.1, made up to 10 μl with water. After a denaturation step of 96°C for 2 min, 35 cycles of 96°C for 10 s/52°C for 15 s/60°C for 3 min were performed. Finally, reactions were held at 72°C for 1 min, sent for commercial data extraction and returned in the form of ABI files.

qPCR Assay for T-DNA (*HptII*) and Repair Template (mCherry) Copy Number Determination

Hydrolysis probe-based quantitative real-time PCR (qPCR) was used to determine copy number of the T-DNA (*HptII*) and repair template (mCherry) in transgenic barley lines. The reaction compared the Cq values of an *HptII* amplicon to a single-copy barley gene *CO2* (*Constans-like*, AF490469) amplicon and the Cq values of an mCherry amplicon to a single-copy barley gene *CO2* (*Constans-like*, AF490469) amplicon within FAM/VIC duplexed assays (see **Supplementary Table 6**). The reactions used Thermo ABGene Absolute qPCR Rox Mix (Cat. number AB1139) with the probes and primers at final concentrations of 200 nM (*HptII* and mCherry) and 100 nM (*CO2*). The assay contained 5 μl DNA solution and was optimised for DNA concentrations of 1–10 ng/μl (5–50 ng DNA in the assay). PCRs were carried out as 25 μl reactions in a Bio-Rad CFX96 machine (C1000 Touch, Bio-Rad, Hercules, CA, USA). The detectors used were FAM-TAMRA and VIC-TAMRA. The PCR cycling conditions were 95°C for 15 min (enzyme activation), 40 cycles of 95°C for 15 s, and 60°C for 60 s. Cq values were determined using CFX96 software (version 3.1), with Cq determination set to regression mode. Values obtained were used to calculate copy number according to published methods (Weng et al., 2004).

PCR Screening for GT

F1/R1 (left junction) and F2/R2 (right junction) primer sequences are given in **Supplementary Table 6**. Each left and right junction PCR reaction contained 30 ng genomic DNA template, 2.5 μl 10× buffer 1, 200 μM dNTPs, 200 nM primers, 0.625 units AmpliTaq Gold (Thermo Fisher, Waltham, MA, USA) and water to 25 μl. Reactions were cycled as follows: 95°C 10 min (enzyme activation), then 40 cycles of 95°C for 30 s/58°C for 30 s/72°C for 1 min. The final extension was at 72°C for 5 min. Amplicons were sequenced with the following primers (**Supplementary Table 6**): F1/R1 amplicon: Seq1, Seq2, Seq3 and Seq10; F2/R2 amplicon: Seq6, Seq7, Seq8, Seq9 and Seq1. Primers for the less sensitive but fully diagnostic F1/R3 PCR are given in **Supplementary Table 6**. Each reaction contained 30 ng genomic DNA template, 10 μl 5× GoTaq buffer, 1.5 mm $MgCl_2$, 200 nM primers, 200 μM dNTPs, 5 units GoTaq DNA polymerase (Promega, Madison, WI, USA) and water to 50 μl. Reactions were cycled at 94°C for 3 min then 40 cycles of 94°C for 30 s/58°C for 30 s/72°C for 2 min and 30 s, before final extension at 72°C for 5 min. F1/R3 amplicons were sequenced with the following primers (**Supplementary Table 6**): Seq1, Seq2, Seq3, Seq4, Seq5, Seq6, Seq7, Seq8, and Seq10.

gDNA Prep and Quantification by Qubit

Genomic DNA was prepared from the leaves according to a published protocol (Edwards et al., 1991). Preps were quantified using the Qubit dsDNA HS Assay Kit (Thermo Fisher) according to the manufacturer's instructions and diluted to a concentration of 30 ng/μl.

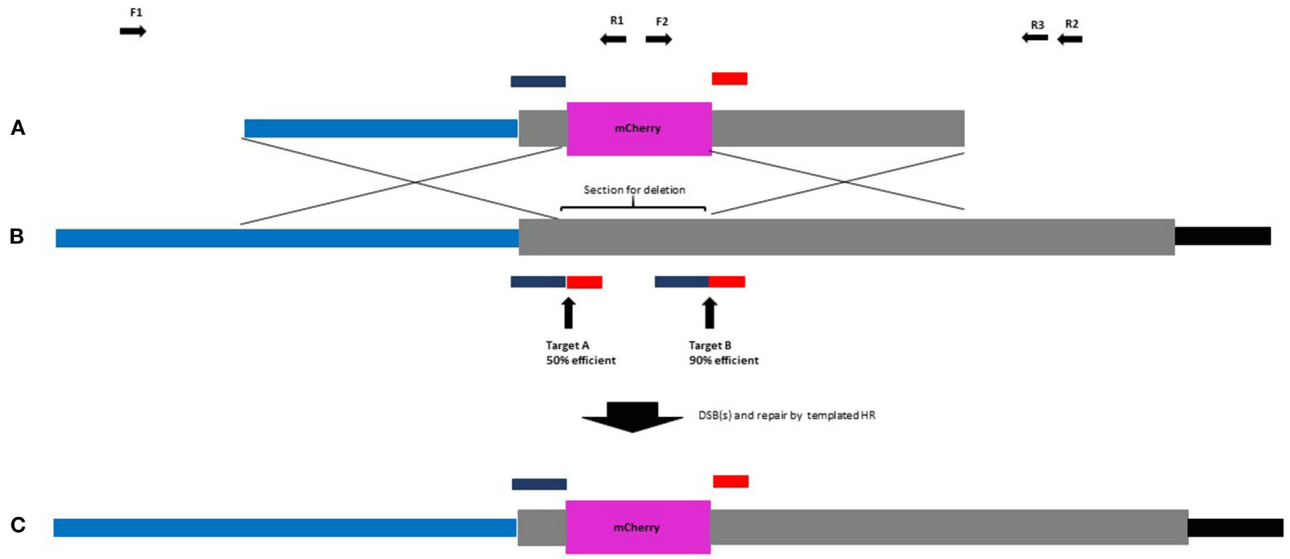

FIGURE 1 | (A) Repair template, **(B)** target locus and **(C)** successful GT into the target locus. Promoter region of HORVU4Hr1G061310 in light blue, mCherry CDS in purple, HORVU4Hr1G061310 CDS in grey, and 3′ UTR in black. Protospacer sequences **(A,B)** in dark blue. Associated PAMs in red. Guide efficiency is shown as % of lines in which indels are detected. Complete protospacer/PAM sequences are absent from **(A,C)** to prevent cleavage by Cas9. A successful event leads to a partial deletion of the HORVU4Hr1G06131 CDS with the remainder being fused in-frame to mCherry. Forward (F) and reverse (R) screening primers are indicated as black horizontal arrows.

Barley Transformation

Barley (cv. "Golden Promise") was transformed by *Agrobacterium tumefaciens*-mediated transformation of immature embryos as described by Hinchliffe and Harwood (2019).

Construct Assembly

Constructs were assembled using previously described parts and methods (Lawrenson et al., 2015), except for the protospacers, repair template, and wheat dwarf virus (WDV) components. Protospacers, repair template, extended repair template, and replicon sequences are given in **Supplementary Table 6**. Protospacer, repair template, extended repair template, and replicon sequences were commercially synthesised as modules compatible with the parts and cloning methods previously described (Lawrenson et al., 2015). Sequence-confirmed constructs A, B, C, and D were transformed into *Agrobacterium* strain AGL1 (Lazo et al., 1991).

Crossing

Barley was crossed according to a published protocol (Thomas et al., 2019).

Chromosome Walking

A published PCR-based protocol (Wang et al., 2007) was used to determine sequences flanking the T-DNA borders. Primer sequences used are shown in **Supplementary Table 6**. SP2 products were cloned into pGEMT-Easy (Promega) and sequenced with M13 and M13R universal primers (Eurofins, Louisville, KY, USA). pGEMT-Easy, left and right T-DNA border sequences were identified in the reads showing that the remaining barley sequence represented the sequence flanking the T-DNA in the barley genome.

RESULTS

GT Construct Design

In our design strategy, high-efficiency introduction of DSBs was considered important as the benefits of DSBs to GT have been reported (Fauser et al., 2012). As part of a gene knockout project, HORVU4Hr1G061310 was identified as being efficiently targeted by protospacers A and B when provided to barley plants simultaneously in the same DNA construct. Here, 18 T0 barley lines were created containing a construct with architecture according to a published work (Lawrenson et al., 2015) and screened by Sanger sequencing amplicons which spanned target sites A and B. Chromatograms from the 18 lines were compared with wild-type controls using the web-based ICE CRISPR analysis tool. Protospacer A was able to create indels in 9/18 (50%) of independent transgenic lines and protospacer B 16/18 (89%) of the same lines (**Supplementary Table 7**). Therefore, for our selected native barley target (HORVU4Hr1G061310), these two protospacers were used and allowed for a strategy to delete around 150 bp of the coding sequence of this single exon gene whilst simultaneously fusing in-frame mCherry in its place (**Figures 1A–C**). To maximise the chance of success, we decided to incorporate both guides into our design as two DSBs at the target site might be better than one. In the repair template, homology to the target site was maximised by continuing the right and left homology arm sequences fully up to the Cas9 cuts sites, i.e., 3 bp from the native PAM. This allowed omission of

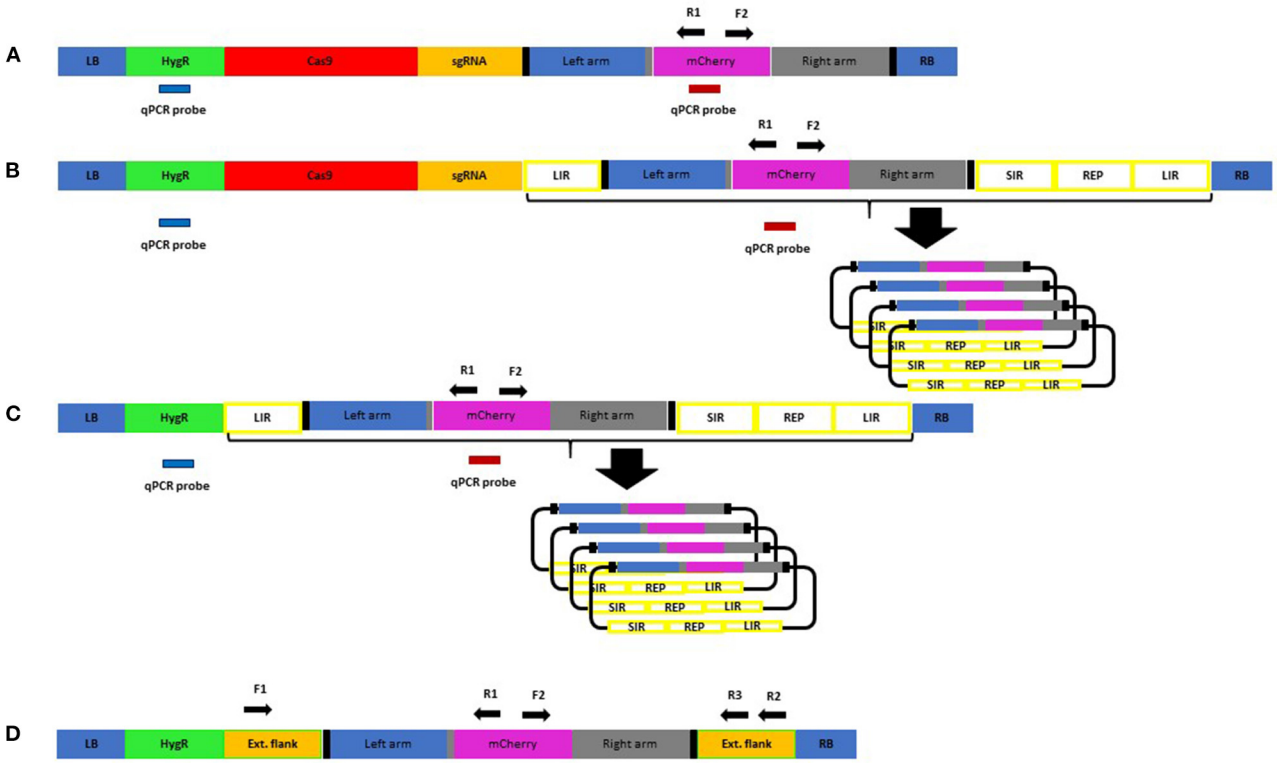

FIGURE 2 | Constructs for plant transformation used in this study: RB, right border; LB, left border; HygR, hygromycin resistance cassette; Cas9 *Hs*, codon-optimised *Sp*Cas9 driven by Zm Ubiquitin promoter; sgRNA, guide RNA expression cassette for two guides **(A,B)**; Left arm, left homology arm; mCherry, mCherry reporter CDS; Right arm, right homology arm; LIR, long intergenic region; SIR, short intergenic region; REP, replicase proteins; qPCR probe used for copy number determination. Thick black vertical bars indicate target sites for the Cas9/guides. Construct **(A)** is the basic GT version, and construct **(B)** is the same except the repair template is contained between replicon sequences. Construct **(C)** is the same as **(B)** but lacks the Cas9/gRNA and ability to introduce DSBs. Construct **(D)** has no Cas9/gRNA or replicon but has the repair template with extended homology arms. It was transformed into barley and used to establish a sensitive PCR assay. F1, R1, F2, R2, and R3 are PCR primers used for screening.

the PAM on the left arm and the protospacer on the right arm of the repair template, preventing the Cas9 from cutting within it, both before and after GT (**Figures 1A,C**). Target sequences (full protospacer and PAM) were included in the flanks of the repair template (**Figure 2**) to allow cutting and facilitate its incorporation into the target site. The repair template was added to the construct containing Cas9 and the guide A and B cassettes to arrive at construct A (**Figure 2A**) which was similar in architecture to a previous example shown to enable GT in *Arabidopsis* (Schiml et al., 2014). The predicted GT event is shown in **Figure 1C**.

WDV is part of the Geminivirus family, whose members have been used in both dicotyledonous and monocotyledonous plants previously as replicons to deliver genome editing reagents and, in particular, the repair template for GT (Baltes et al., 2014; Butler et al., 2016; Gil-Humanes et al., 2017; Wang et al., 2017; Dahan-Meir et al., 2018; Hahn et al., 2018; Vu et al., 2020). The coat and movement protein coding sequence can be completely removed and replaced by a fragment of no maximally determined size whilst still retaining the ability to replicate within its host to high copy numbers after introduction by *Agrobacterium* or physical means. We used the basic template (LIR-SIR-REP-LIR) previously used with success (Gil-Humanes et al., 2017; Wang et al., 2017) but supplemented for our purposes by using the genome sequence from a strain of WDV isolated from barley (WDV-Bar [Hu]) (Ramsell et al., 2009). The WDV-Bar[Hu] version of LIR-SIR-REP-LIR was included in construct B (**Figure 2B**) such that it would allow rolling circle replication of the repair template already present in construct A. We chose not to include the Cas9 within the replicon such that it would replicate to a high copy number as no benefit was previously seen in GT experiments when this was done with other sequence-specific nucleases (Baltes et al., 2014). Only when the repair template was inserted into the replicon was GT boosted, suggesting that it was largely an increase in copy number of the donor and not a replicon-induced increase in DSB formation that was beneficial to GT. Previously, such replicons have often been shown functional in terms of replicative ability by using PCR to detect the circular replicating form of the linearly supplied unit. We chose to develop a qPCR copy number assay using amplicon/probe combinations in the repair template, hygromycin selection cassette (**Figure 2**) and a single-copy barley gene to enable quantification of replication in stable transgenic lines.

Construct C (**Figure 2C**) was identical to B other than lacking the Cas9 and sgRNA cassettes, so it was able to amplify the repair template but unable to induce the site-specific DSBs. This was to test the importance of targeted DSBs in GT which have been shown to be beneficial (Fauser et al., 2012) although not always essential (Terada et al., 2002).

Design of Assay for Detection of GT Events

Construct D (**Figure 2D**) was produced as a means of optimising the PCR screening strategy for GT detection, as high sensitivity and specificity would be vital due to the rarity of GT events and the expectation that we could be searching for somatic sectors which might represent a small proportion of the cells within leaf samples taken for analysis (Schiml et al., 2017). Somatic sectors can be inherited through the germline and also indicate active lines where further events are likely to occur. Construct D contains the repair template as found in constructs A, B, and C; however, the homology arms have been extended for a few 100 nucleotides with the native HORVU4Hr1G061310 genomic sequence to include the binding sites for the F1, R2, and R3 primers (**Figure 2D**; **Supplementary Table 6**). By creating a single-copy transgenic line with construct D, as determined by qPCR assay, a more realistic scenario to derive template for optimisation was possible than by using plasmid alone. In order to allow distinction from true GT events, polymorphisms at the junctions of the extended flanks and the homology arms were introduced which would not be present in the predicted true GT events (**Supplementary Table 6**). Various PCR conditions were tried and the best (see *Methods*) were found to work well with primer combinations F1/R1, F2/R2, and F1/R3. The most sensitive were found to be junction PCRs F1/R1 and F2/R2 which would identify GT events at either the left or right junction, respectively. By serially diluting 30 ng of construct D genomic DNA, considering the 5.3-Gbp haploid barley genome and the average weight of 650 Da per base pair, it was possible to calculate the number of template copies in each PCR reaction and thus determine the threshold sensitivity. This was found to be in the region of 40 copies for the F1/R1 primer pair (**Supplementary Figure 1**), so theoretically capable of identifying a somatic sector containing the same number of cells with a GT event. PCR with primers F1/R3, although covering the entire GT event over both left and right junctions, was less sensitive, presumably due to the greater amplicon size and the competitive tendency of the smaller WT allele to amplify and dominate the products (see **Figure 3**). The limit of detection for the F1/R3 amplicon was in the region of 1,000 template copies (data not shown). For this reason, it was decided to use the more sensitive F1/R1 and F2/R2 junction combinations for screening primary transgenics where small somatic GT sectors were likely.

Production and Analysis of the T0 Generation

Barley cv. "Golden Promise" was transformed with constructs A, B, C, and D using *Agrobacterium* delivery, and selection of transgenic plants was done on hygromycin-containing media (Hinchliffe and Harwood, 2019). Two hundred immature embryos were inoculated each for constructs A, B, and C. One hundred embryos were inoculated for construct D. Construct A yielded 14 T0 lines (1826 prefix), construct B (2158 prefix) 39 T0 lines, construct C (2291 prefix) 17 lines, and construct D 8 lines. Transformation efficiencies for constructs A–D, respectively, were 7, 19.5, 8.8, and 8%. As the purpose of construct D lines was to optimise PCR conditions for screening, they were destructively harvested for genomic DNA once rooted in tissue culture. After qPCR copy number determinations for construct D lines, suitable genomic DNA template containing a single-copy T-DNA insertion was identified for PCR screen optimisation as described in the previous section. The 1826, 2158, and 2291 T0 lines were screened and scored using the F1/R1 and F2/R2 primer pairs as well as being assayed by qPCR for their HptII (T-DNA) and mCherry (repair template) copy numbers. These data are given in **Supplementary Table 1** which show that in the case of construct A (1826) lines, the copy numbers of HptII and mCherry correspond as expected for two single-copy elements on a T-DNA. The 39 construct B (2158) lines, however, show an average of 7,575 copies of mCherry, whilst the HptII copy number remains largely one or two. This indicates that in many of the 2158 lines, rolling circle replication is occurring giving rise to huge numbers of repair template copies. **Supplementary Table 1** also shows the presence or absence of F1/R1 and F2/R2 PCR products of the correct size, and for 1826 lines, 2/14 (14%) scored positive for both left and right junction PCRs, whilst for 2158 lines, 22/39 (56%) scored positive for the same two PCRs.

To check the identity and fidelity of these PCR products, F1/R1 and F2/R2 products were purified and Sanger sequenced for the lines 2158-9-1, 2158-14-1, 1826-5-2, and 1826-8-1 and found to be identical and, as expected, perfect for GT events (**Supplementary Table 2**). As expected, construct C lines (2291 prefix) also generated many copies of repair template, but unexpectedly, also produced correctly sized PCR products with primers F1/R1 and F2/R2 which are shown in **Supplementary Table 1**. In fact, 8/16 (50%) of the 2291 lines gave both left and right junction PCR products of the size indicative of a GT event and, furthermore, when purified and sequenced, gave exactly the same sequence as seen with the 1826 and 2158 lines. Looking at the relation between mCherry copy number and the presence/absence of F1/R1 and F2/R2 PCR products (**Supplementary Table 1**), it was apparent that high numbers of repair template and PCR success were linked. Whilst this could mean that increasing the number of repair template copies was causing GT, it could also indicate that false PCR positives were being triggered by the high number of repair templates produced by the replicon.

To test this latter idea, plasmid DNA containing the repair template was mixed with wild-type Golden Promise DNA (where GT could not have occurred) and F2/R2 PCR was performed. Initially, 30 ng of barley DNA (as used in all other screening PCRs described) was mixed with around 7.72×10^9 copies of repair template, and this resulted in the production of the 1,047-bp F2/R2 band. This plasmid was then titrated against the 30-ng wild-type barley DNA (representing 5,240 target site copies) to determine the minimum number of repair template copies per target site necessary to trigger the false positive when 30 ng of barley DNA was used as template. This is shown in

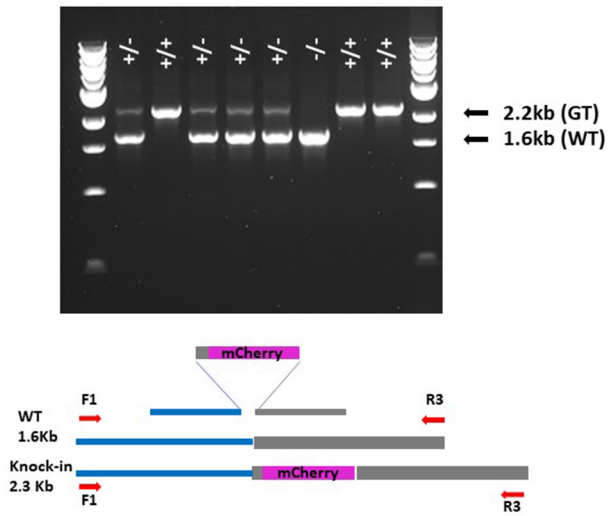

FIGURE 3 | Gel showing segregation of GT event in 1826-8-1_A T2. Bands are the products of F1/R3 primers. + indicates GT allele; – indicates WT allele.

Supplementary Figure 2 and was found to be in the region of 700 copies per target site, based on the 5.3-Gbp genome size and the average weight of a single base pair to be 650 Da. This result can be related to the qPCR copy number determinations for mCherry (repair template) in the replicon lines where the numbers in **Supplementary Table 1** relate to copies per haploid genome or in other words per target site (there is one copy of HORVU4Hr1G061310 per haploid genome). Looking at **Supplementary Table 1**, it is evident that F1/R1 and F2/R2 products begin to appear in 2158 and 2291 lines at around 600 or 700 copies of mCherry per genome/target site, meaning it is likely that many of the PCR bands produced in replicon lines are false positives. This was further confirmed by sequencing a band from the plasmid titration test (**Supplementary Figure 2**) in the lane labelled 736641 which proved identical in sequence to the F2/R2 bands obtained for the 2158, 2291, and 1826 lines. Presumably, by increasing the number of repair template copies with the replicon, we had inadvertently also increased the likelihood of partial primer extension from within the repair template. For example, R1 could in one cycle of PCR be partially extended from within mCherry to somewhere in the left homology arm. After denaturation, the partially extended product would be free to anneal at its 5′ end with the homologous site in the target region (template switching) where it could then be extended beyond the position of the F1 primer binding site. F1 could then prime against this site and extend to produce double-stranded DNA of sequence identical to the predicted GT event and allow exponential amplification and production of the false positive.

The 1826 lines all had relatively low copy numbers of repair template (highest was 2), way below 600 per target site, and so our testing indicated that the lines 1826-8-1 and 1826-5-2 would be true positives. These were the only two 1826 lines with both F1/R1 and F2/R2 bands, indicating HR events at the left and right junctions, suggestive of a perfect GT event. Other lines such as 1826-3-1 showed an F2/R2 band but not F1/R1, which could be indicative of imperfect, one-sided GT events, for example, homologous recombination at the right junction but NHEJ at the left junction. Of course, false positives in the replicon lines could be masking true positives in the background, so the 39 individual 2158 lines were subject to F1/R3 PCR which was expected to be more specific due to the requirement for two template switches for false amplification to occur. The 14 individual 1826 lines also underwent the F1/R3 PCR; however, no T0 lines produced a band although this was unsurprising due to the low sensitivity of this large amplicon PCR. Accordingly, lines 1826-8-1 and 1826-5-2 were sown out for T1 screening due to being likely true positive GT lines, whilst 17 F1/R1 and F2/R2 positive 2158 lines were selected for T1 screening based on the assumption that some true positive GT events may be masked by false positives created ***via*** replicon amplification.

Analysis of the T1 Generation and Beyond

Because of the false-positive PCR issue, and to detect GT events and somatic sectors of significant size likely to become heritable, it was decided to screen T1 plants with the less sensitive F1/R3 primer pair. For each of the 17 selected T0 2158 lines, ∼70 siblings were sown out, giving a total of around 1,200 from which no F1/R3 positives were identified. T0 line 1826-5-2 produced 228 seeds and all were sown and screened producing no F1/R3 positive band. T0 line 1826-8-1 was, however, more productive and yielded 467 seeds, and from these, 3 T1 plants produced a band of 2.2 kb indicative of the sought-after GT event as well as a second band of 1.6 kb corresponding to the wild-type allele. These 3 T1 siblings were designated 1826-8-1_A, 1826-8-1_B and 1826-8-1_C. The 2.2-kb band was purified for all three siblings and sequenced from end to end, showing that all were identical to the predicted GT event (**Supplementary Table 2**). The three sibling T1 plants were grown to maturity and harvested before sowing out seeds for T2 screening. Ninety-four individual 1826-8-1_A T2 siblings were screened and 75 gave the GT PCR product and 19 gave no band, corresponding to a 3:1 ratio (**Supplementary Table 3**), which is expected if the event was heterozygous in the T1 parent. Eight of these T2 siblings are shown in **Figure 3** after F1/R3 PCR, where homozygous, heterozygous and wild-type plants can all be clearly seen. This strongly indicates that the GT event occurred either in the T0 generation or very early in T1, i.e., just after fertilisation. All 94 of the 1826-8-1_A T2 siblings contained two copies of the T-DNA (homozygous) as determined by qPCR, so homozygous GT plants (**Figure 3**) were selected for crossing to wild-type Golden Promise in order to segregate away the T-DNA from the GT event in F2.

T1 line 1826-8-1_B was also sown out for T2 screening, but out of 94 siblings, none screened positive for GT. This indicates that the event which was detected in T1 with F1/R3 primers and sequencing would, according to the sensitivity of the assay, represent a somatic sector of at least 1,000 cells, which was unable to pass through the germline into T2 plants and was therefore lost. All 94 of the 1826-8-1_B T2 siblings contained two copies of the T-DNA (homozygous).

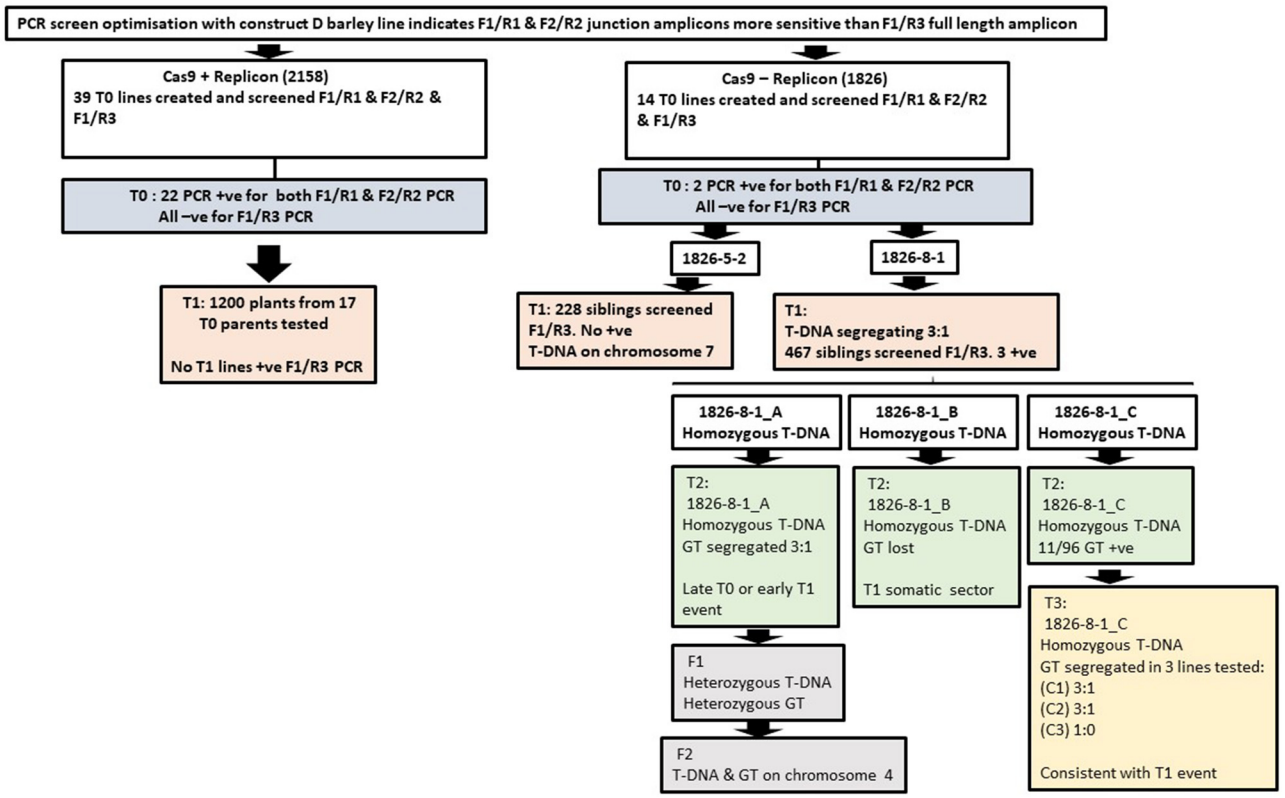

FIGURE 4 | Key findings comparing *in-planta* GT with and without geminiviral replicon; 2158 are replicon lines (construct B) and 1826 lines are non-replicon lines (construct A).

T1 line 1826-8-1_C was sown out for T2 screening, and this time, 11/94 screened positive for GT. All 94 of the 1826-8-1_C T2 siblings contained two copies of the T-DNA (homozygous). Three of the GT-positive T2 siblings were designated 1826-8-1_C1, 1826-8-1_C2, and 1826-8-1_C3 and sown out again for T3 screening; 17/24 1826-8-1_C1 siblings (3:1), 16/24 1826-8-1_C2 siblings (3:1) and 24/24 1826-8-1_C3 siblings were positive for GT indicating that T2 parents were likely GT heterozygotes (C1, C2) or GT homozygotes (C3) (see **Supplementary Table 3**). This is consistent with a T1 parent which was a cellular mosaic of the GT event(s) which passed through the germline into T2 progeny at a subsequently lower fraction than the 75% expected from a heterozygous parent. Alternatively, GT could have occurred independently in the T2 lines 1826-8-1_C1, 1826-8-1_C2, and 1826-8-1_C3 to give the same T3 GT zygosity.

As with line 1826-8-1_A, all T2 siblings of 1826-8-1_C were homozygous for the T-DNA insertion, so it was not possible to lose the transgene without backcrossing to Golden Promise. As all 1826-8-1 lines share the same T-DNA insertion and the crossing was already underway for 1826-8-1_A, this was not done for 1826-8-1_C.

Linkage of the T-DNA and GT Event

All 19 F1 lines produced for the 1826-8-1_A × Golden Promise cross were heterozygous for the T-DNA and GT as determined by qPCR and F1/R3 PCR. In F2, 74/96 (3:1) siblings screened positive for GT as expected. All 96 were also tested for the presence of the transgene by qPCR which showed that all siblings containing the GT also contained the T-DNA and all GT free plants were also free of the T-DNA (**Supplementary Table 3**); in other words, the T-DNA and GT locus are linked. To see how close the GT and T-DNA were to each other, a chromosome walking technique was used to determine the flanking sequences of the T-DNA. BLAST search using the sequence obtained as query against the barley genome revealed the T-DNA to be located 4.23 Mb from the GT locus on chromosome 4 in line 1826-8-1 (**Supplementary Table 4**). The same chromosome walking was also done for line 1826-5-2 which was found to harbour the T-DNA on chromosome 7 (**Supplementary Table 4**).

DISCUSSION

Figure 4 summarises the key findings described above for all plants analysed. Heritable GT was confined to line 1826-8-1 with the event in 1826-8-1_A occurring either in T0 or very early T1 and the 1826-8-1_C events occurring in T1 or T2. Additionally, a significant event leading to detection with the low sensitivity primer pair F1/R3 was recovered in 1826-8-1_B but lost by T2 so must have occurred in T1. This shows that the 1826-8-1 family tree had diverged before the origin of these independent GT

events, and so for some reason, the line 1826-8-1 was relatively prolific in terms of GT. A comparable line 1826-5-2 showed somatic GT in T0 but did not go on to result in subsequent heritable GT. This may be related to the T-DNA containing the repair template being linked to the target site in 1826-8-1 but not in 1826-5-2. It was previously reported that if the repair template and target site were present on the same chromosome, then GT was around twice as frequent as when they were on different chromosomes (Fauser et al., 2012). Successful GT in line 1826-8-1 also makes sense in light of evidence that DNA repair by HDR using a sister chromatid template is common in barley (Vu et al., 2014). Being on the same chromosome is likely to impact on the physical proximity of target and donor site. It was recently reported in rice that using a Cas9-VirD2 fusion to direct the repair template to the target site had a beneficial effect on GT (Ali et al., 2020). It is also reported that the zygosity of the repair template has a similar impact (Puchta et al., 1995), where a homozygous transgene was 50% more likely to lead to intrachromosomal HR-based gene repair than if hemizygous. In line with this, all three 1826-8-1 T1 siblings of interest were homozygous for the T-DNA, whilst the overall T1 T-DNA inheritance in this line showed 3:1 segregation.

A limitation of our study is the establishment of a causal role for Cas9 in the GT observed. Although we have no results from a control containing the repair template in the absence of Cas9 and guides, it has previously been reported (Horvath et al., 2017) that GT in barley did not occur from an estimated 6,838 independent transformation events where DSBs were not induced. In this GT report, successful targeting would have led to herbicide resistance allowing whole plant regeneration in tissue culture. Comparison of these 6,838 events to the 14 transformed T0 plants we created with construct A (1826 lines) does not necessarily indicate the benefit of induced DSBs as the number of chances for GT to occur in a multicellular regenerated plant containing the editing reagents is much greater than in a single transformation event that does not proceed beyond the single-cell stage in tissue culture. However, the benefits to GT of creating such targeted DSBs in plants are now extensively shown (Puchta et al., 1996; de Pater et al., 2009, 2013; Shukla et al., 2009; Townsend et al., 2009; Zhang et al., 2013; Endo et al., 2016).

We did not carry out any microscopy study to see if the in-frame mCherry HORVU4Hr1G061310 fusion created was functional as screening all 19 1826-8-1_A F1 plants produced showed that they still contained the T-DNA-based repair template (data not shown). Similarly, six GT-positive T3 plants from each of 1826-8-1_C1, 1826-8-1_C2, and 1826-8-1_C3 all contained the T-DNA-based repair template (data not shown). This repair template contains the promoter region, mCherry and much of the HORVU4Hr1G061310 CDS so may well have given a fluorescent signal despite not being integrated at the target locus by GT. This would not allow distinction of a signal arising from GT at the target locus and a signal from the repair template still located in the T-DNA.

We did not find F1/R3 detectable GT events in 2158 lines despite screening twice the number of plants in T1 compared with the 1826 lines; 2158 lines had very high copy numbers of repair template in T0 and in T1 where its amplification co-segregated with the T-DNA (**Supplementary Table 5**). Although the replicationally functional linear replicon form is thus able to pass through the germline successfully, we do not have any data to support whether donor amplification was occurring in cells giving rise to sex cells, and so a failure to achieve heritable replicon GT events could be a result of cell-specific type variation in replicon activity. With this in mind, it is still possible that the replicon had a positive effect on GT in leaf cells where rolling circle replication was detectable. However, titration of repair template plasmid against wild-type Golden Promise DNA *in vitro* indicated that the GT activity detected in T0 2158 lines was potentially a PCR artefact as junction PCR bands begin to appear at around 700 copies of repair template per target site, which is very close to the ratio seen *in-planta* with the replicon where the junction PCR began yielding product.

Future GT experiments utilising high copy numbers of repair template should be aware that such a junction PCR approach is liable to produce false-positive results and would benefit from strategies to prevent them. One way to do this may be to reduce the length of homology arms to a minimum, thus reducing the size of the region in which partial primer extension may occur before template switching during PCR. Whilst reducing the length of homology arms may result in a decrease in overall GT efficiency, relatively short homology arms of 196 and 74 bp have been shown to function in rice (Li et al., 2020). Another way to reduce false-positive junction PCR may be to simply increase the size of the amplicon by moving the primer in the flanking non-repair template region further out, which may in turn reduce the chances of a partially extended product being fully extended after template switching. However, larger amplicons are likely to reduce sensitivity, which could affect the detection of small somatic sectors, that may go on to be usefully heritable. A third way to reduce or remove false junction PCRs could be to do one round of full-length PCR with primers outside the repair template—F1/R3 in this case, and then to use the product as template for nested junction PCR—F1/R1 or F2/R2 in this case. The requirement for two template switching events to occur with F1/R3 in the production of a false positive may be sufficient to produce only true full-length GT products even with small somatic sectors which could then be amplified to detection point in a second round of nested junction PCR after template dilution. On the other hand, it is also possible that the increased sensitivity of nested junction PCR would also lead to false positives due to counteracting the reduced but not completely removed potential of the full-length F1/R3 PCR to switch template. Future GT experiments may benefit from trialling PCR screening methods thoroughly before implementation. It could be that junction PCR is a suitable method of screening where repair template copy number is low such as in our non-replicon approach. In our setup, plasmid/genomic DNA titration suggested that false positives were only triggered when the molar ratio of repair template:target site exceeded 600. This is currently mainly an issue with replicon and particle bombardment approaches.

Although we screened a greater number of T1 progeny (1,200 $>$ 695) from a greater number of T0 parents (17 $>$ 2) for

the replicon (2158) compared with the non-replicon (1826) lines, we cannot be sure that this is a valid replicon/non-replicon comparison as indel formation at target sites may have been unequal for some reason. Using Cas9 has the potential disadvantage that indel formation is likely to mutate the "seed region" of the target site such that further DSBs are not possible as the relevant guide no longer matches the site. We know that both guides A and B were able to induce indels in 50 and 90% of T0 lines tested, respectively, often representing half of the alleles detected which may well indicate that many target sites would no longer be available for GT. The target sites in T0, T1, T2, etc. lines created could be sequenced to gain more insight into the remaining availability of WT target sites. As we only had one non-replicon (1826) T0 transgenic that yielded heritable GT events, a larger number of true GT events would need to be investigated in order to make a replicon/non-replicon comparison.

Recently, it has been shown in *Arabidopsis* that timing the occurrence of DSBs to the egg cell greatly increases GT efficiency (Miki et al., 2018; Wolter et al., 2018). Similarly, by using Cas12a instead of Cas9, GT efficiency was increased (Wolter and Puchta, 2019). Two features here address the potential lack in availability of WT target sites that may be shutting down DSB formation in our experiment. Firstly, restricting DSBs to egg cells would mean each female gamete has the potential for DSBs to occur and in turn undergo GT, rather than a reduced or non-existent fraction resulting from indels formed earlier during development under ubiquitous Cas9 expression. Secondly, Cas12a cuts outside of its seed region and would be expected to resist a certain amount of indel formation and may therefore keep creating DSBs for an increased length of time compared with Cas9, giving more potential for GT to occur. It will be interesting to see if the benefits to GT of egg cell-specific Cas12a can be translated to crops. It has been shown in tomato that the frequency of GT using Cas9 increased in line with temperature when it was carried out between 18 and 31°C, from around 1% at the lower temperature to around 5% at the higher temperature (Vu et al., 2020). Such a temperature regime may have been beneficial in our experiments although care would be needed to avoid a detrimental effect on fertility as high temperatures are known to have a negative impact in the latter stages of the barley life cycle (Jacott and Boden, 2020).

A previous report of *in-planta* GT in *Arabidopsis* (Hahn et al., 2018) found no beneficial effect from including the repair template within a replicon, whilst a single-copy repair template (similar to our construct A) gave rise to inheritable GT. However, this study investigated the progeny of just three primary transformant lines per DNA construct and may also suffer from indels shutting down target sites. In tomato, bean yellow dwarf virus-based replicons have been shown to result in heritable GT events (Cermak et al., 2015; Dahan-Meir et al., 2018; Vu et al., 2020). In one tomato study utilising an *in-planta* approach, it increased the percentage of inheritable T0 events from 8% without a replicon to 25% with a replicon (Dahan-Meir et al., 2018). Rice (Wang et al., 2017), wheat (Gil-Humanes et al., 2017) and potato (Butler et al., 2016) replicon/GT reports describe junction PCR/sequencing assays similar to our false-positive-prone F1/R1 and F2/R2 and no GT heritability. It could be that the benefits of replicons to heritable GT are restricted to certain plant species, which according to existing literature would include only tomato.

Our work in barley has extended what has previously been shown in this species as we created the first heritable true GT events at a native locus. However, we were unable to segregate away the editing reagents on the T-DNA, possibly due to an inadvertent selection for linkage. Whilst it may be possible to separate the two loci by searching for meiotic recombinants, this probably represents an unreasonable amount of work. Increasing the number of heritable GT events detected will probably allow the isolation of unlinked versions which would in turn be easier if GT efficiency was boosted in other ways, such as egg cell Cas12a expression. Additionally, a pooling strategy may enable more plants to be screened which should increase the numbers of GT events recovered.

DATA AVAILABILITY STATEMENT

The raw data supporting the conclusions of this article will be made available by the authors, without undue reservation.

AUTHOR CONTRIBUTIONS

TL designed the experiments, conducted the molecular work and analysis, and prepared the manuscript. AH carried out barley transformations. MC carried out the crossing programme. YM assisted with molecular analysis and crossing. WH contributed to the study design and manuscript preparation. All authors read and approved the final manuscript.

FUNDING

We acknowledge the support from the project Engineering Nitrogen Symbiosis for Africa (ENSA) currently supported through a grant to the University of Cambridge by the Bill and Melinda Gates Foundation and the Foreign, Commonwealth and Development Office (FCDO). The work was also supported by the UK Biotechnology and Biological Sciences Research Council (BBSRC) through grant BB/P013511/1.

ACKNOWLEDGMENTS

We thank JIC Horticultural Services for plant care.

SUPPLEMENTARY MATERIAL

The Supplementary Material for this article can be found online at: https://www.frontiersin.org/articles/10.3389/fgeed.2021.663380/full#supplementary-material

Supplementary Figure 1 | Gel showing sensitivity obtained in F1/R1 PCR screen setup. Construct D was transformed into barley and DNA extracted from a regenerated plant (transgene copy number 1) and quantified by Qubit fluorescence. Serial dilutions were made of this DNA for subsequent PCR. The copy number of transgene D are shown for each lane. The limit of detection is around 40 copies of the target.

Supplementary Figure 2 | Copies of repair template plasmid per target site. Thirty ng of wild type barley DNA was mixed with serial dilutions of plasmid DNA containing the repair template. The lane numbers represent the copies of repair template: target site ratio. Positive control was a construct D line. The 1047 bp band in lane 736641 was excised, purified and sequenced.

Supplementary Table 1 | qPCR determined copy numbers of HptII (TDNA), mCherry (repair template), and presence/absence of junction PCR products (left: F1/R1; right: F2/R2) for T0 lines.

Supplementary Table 2 | Sequences of GT events for lines 2158-9-1, 2158-14-1, 1826-5-2, and 1826-8-1 showing F1/R1 (T0), F2/R2 (T0), and F1/R3 (T1) products.

Supplementary Table 3 | Table showing zygosity of T-DNA and GT events in interesting descendants of 1826-8-1 throughout the generations analysed in this study.

Supplementary Table 4 | Flanking sequences of the T-DNA in lines 1826-8-1 and 1826-5-2.

Supplementary Table 5 | T1 inheritance of the T-DNA and associated replicon activity.

Supplementary Table 6 | Primer and probe sequences used in the study and sequences of construct components.

Supplementary Table 7 | Analysis of T0 lines for indels at target sites A and B in HORVU4Hr1G061310.

REFERENCES

Ali, Z., Shami, A., Sedeek, K., Kamel, R., Alhabsi, A., Tehseen, M., et al. (2020). Fusion of the Cas9 endonuclease and the VirD2 relaxase facilitates homology-directed repair for precise genome engineering in rice. *Commun. Biol.* 3:44. doi: 10.1038/s42003-020-0768-9

Anzalone, A. V., Randolph, P. B., Davis, J. R., Sousa, A. A., Koblan, L. W., Levy, J. M., et al. (2019). Search-and-replace genome editing without double-strand breaks or donor DNA. *Nature* 576, 149–157. doi: 10.1038/s41586-019-1711-4

Baltes, N. J., Gil-Humanes, J., Cermak, T., Atkins, P. A., and Voytas, D. F. (2014). DNA replicons for plant genome engineering. *Plant Cell* 26, 151–163. doi: 10.1105/tpc.113.119792

Budhagatapalli, N., Rutten, T., Gurushidze, M., Kumlehn, J., and Hensel, G. (2015). Targeted modification of gene function exploiting homology-directed repair of TALEN-mediated double-strand breaks in barley. *Genes Genomes Genet.* 5, 1857–1863. doi: 10.1534/g3.115.018762

Butler, N. M., Baltes, N. J., Voytas, D. F., and Douches, D. S. (2016). Geminivirus-mediated genome editing in potato (*Solanum tuberosum* L.) using sequence-specific nucleases. *Front. Plant Sci.* 7:1045. doi: 10.3389/fpls.2016.01045

Cermak, T., Baltes, N. J., Cegan, R., Zhang, Y., and Voytas, D. F. (2015). High-frequency, precise modification of the tomato genome. *Genome Biol.* 16:232. doi: 10.1186/s13059-015-0796-9

Chilton, M. D. M., and Que, Q. D. (2003). Targeted integration of T-DNA into the tobacco genome at double-stranded breaks: new insights on the mechanism of T-DNA integration. *Plant Physiol.* 133, 956–965. doi: 10.1104/pp.103.026104

Christian, M., Cermak, T., Doyle, E. L., Schmidt, C., Zhang, F., Hummel, A., et al. (2010). Targeting DNA double-strand breaks with TAL effector nucleases. *Genetics* 186, 757–761. doi: 10.1534/genetics.110.120717

Dahan-Meir, T., Filler-Hayut, S., Melamed-Bessudo, C., Bocobza, S., Czosnek, H., Aharoni, A., et al. (2018). Efficient in planta gene targeting in tomato using geminiviral replicons and the CRISPR/Cas9 system. *Plant J.* 95, 5–16. doi: 10.1111/tpj.13932

Danilo, B., Perrot, L., Mara, K., Botton, E., Nogue, F., and Mazier, M. (2019). Efficient and transgene-free gene targeting using Agrobacterium-mediated delivery of the CRISPR/Cas9 system in tomato. *Plant Cell Rep.* 38, 459–462. doi: 10.1007/s00299-019-02373-6

de Pater, S., Neuteboom, L. W., Pinas, J. E., Hooykaas, P. J. J., and van der Zaal, B. J. (2009). UN-induced mutagenesis and gene-targeting in Arabidopsis through Agrobacterium-mediated floral dip transformation. *Plant Biotechnol. J.* 7, 821–835. doi: 10.1111/j.1467-7652.2009.00446.x

de Pater, S., Pinas, J. E., Hooykaas, P. J. J., and van der Zaal, B. J. (2013). ZFN-mediated gene targeting of the Arabidopsis protoporphyrinogen oxidase gene through Agrobacterium-mediated floral dip transformation. *Plant Biotechnol. J.* 11, 510–515. doi: 10.1111/pbi.12040

Edwards, K., Johnstone, C., and Thompson, C. (1991). A simple and rapid method for the preparation of plant genomic dna for pcr analysis. *Nucleic Acids Res.* 19, 1349–1349. doi: 10.1093/nar/19.6.1349

Endo, M., Mikami, M., and Toki, S. (2016). Biallelic gene targeting in rice. *Plant Physiol.* 170, 667–677. doi: 10.1104/pp.15.01663

Fauser, F., Roth, N., Pacher, M., Ilg, G., Sanchez-Fernandez, R., Biesgen, C., et al. (2012). In planta gene targeting. *Proc. Natl. Acad. Sci. U.S.A.* 109, 7535–7540. doi: 10.1073/pnas.1202191109

Feng, Z., Zhang, B., Ding, W., Liu, X., Yang, D.-L., Wei, P., et al. (2013). Efficient genome editing in plants using a CRISPR/Cas system. *Cell Res.* 23, 1229–1232. doi: 10.1038/cr.2013.114

Gaudelli, N. M., Komor, A. C., Rees, H. A., Packer, M. S., Badran, A. H., Bryson, D. I., et al. (2017). Programmable base editing of A.T to G.C in genomic DNA without DNA cleavage. *Nature* 551, 464–471. doi: 10.1038/nature24644

Gil-Humanes, J., Wang, Y., Liang, Z., Shan, Q., Ozuna, C. V., Sanchez-Leon, S., et al. (2017). High-efficiency gene targeting in hexaploid wheat using DNA replicons and CRISPR/Cas9. *Plant J.* 89, 1251–1262. doi: 10.1111/tpj.13446

Hahn, F., Eisenhut, M., Mantegazza, O., and Weber, A. P. M. (2018). Homology-directed repair of a defective glabrous gene in arabidopsis with Cas9-based gene targeting. *Front. Plant Sci.* 9:424. doi: 10.3389/fpls.2018.00424

Hinchliffe, A., and Harwood, W. A. (2019). Agrobacterium-mediated transformation of barley immature embryos. *Methods Mol. Biol.* 1900, 115–126. doi: 10.1007/978-1-4939-8944-7_8

Horvath, M., Steinbiss, H. H., and Reiss, B. (2017). Gene targeting without DSB induction is inefficient in barley. *Front. Plant Sci.* 7:1973. doi: 10.3389/fpls.2016.01973

Jacott, C. N., and Boden, S. A. (2020). Feeling the heat: developmental and molecular responses of wheat and barley to high ambient temperatures. *J. Exp. Bot.* 71, 5740–5751. doi: 10.1093/jxb/eraa326

Jinek, M., Chylinski, K., Fonfara, I., Hauer, M., Doudna, J. A., and Charpentier, E. (2012). A programmable dual-RNA-guided DNA endonuclease in adaptive bacterial immunity. *Science* 337, 816–821. doi: 10.1126/science.1225829

Kim, Y. G., Cha, J., and Chandrasegaran, S. (1996). Hybrid restriction enzymes: zinc finger fusions to Fok I cleavage domain. *Proc. Natl. Acad. Sci. U.S.A.* 93, 1156–1160. doi: 10.1073/pnas.93.3.1156

Komor, A. C., Kim, Y. B., Packer, M. S., Zuris, J. A., and Liu, D. R. (2016). Programmable editing of a target base in genomic DNA without double-stranded DNA cleavage. *Nature* 533, 420–424. doi: 10.1038/nature17946

Lawrenson, T., Shorinola, O., Stacey, N., Li, C., Ostergaard, L., Patron, N., et al. (2015). Induction of targeted, heritable mutations in barley and Brassica oleracea using RNA-guided Cas9 nuclease. *Genome Biol.* 16:258. doi: 10.1186/s13059-015-0826-7

Lazo, G. R., Stein, P. A., and Ludwig, R. A. (1991). A DNA transformation-competent arabidopsis genomic library in agrobacterium. *Bio-Technology* 9, 963–967. doi: 10.1038/nbt1091-963

Lee, K., Eggenberger, A. L., Banakar, R., McCaw, M. E., Zhu, H., Main, M., et al. (2019). CRISPR/Cas9-mediated targeted T-DNA integration in rice. *Plant Mol. Biol.* 99, 317–328. doi: 10.1007/s11103-018-00819-1

Li, J.-F., Norville, J. E., Aach, J., McCormack, M., Zhang, D., Bush, J., et al. (2013). Multiplex and homologous recombination-mediated genome editing in Arabidopsis and Nicotiana benthamiana using guide RNA and Cas9. *Nat. Biotechnol.* 31, 688–691. doi: 10.1038/nbt.2654

Li, S. Y., Zhang, Y. X., Xia, L. Q., and Qi, Y. P. (2020). CRISPR-Cas12a enables efficient biallelic gene targeting in rice. *Plant Biotechnol. J.* 18, 1351–1353. doi: 10.1111/pbi.13295

Miki, D., Zhang, W., Zeng, W., Feng, Z., and Zhu, J.-K. (2018). CRISPR/Cas9-mediated gene targeting in Arabidopsis using sequential transformation. *Nat. Commun.* 9:1967. doi: 10.1038/s41467-018-04416-0

Nekrasov, V., Staskawicz, B., Weigel, D., Jones, J. D. G., and Kamoun, S. (2013). Targeted mutagenesis in the model plant Nicotiana benthamiana using Cas9

RNA-guided endonuclease. *Nat. Biotechnol.* 31, 691–693. doi: 10.1038/nbt.2655

Puchta, H., Dujon, B., and Hohn, B. (1996). Two different but related mechanisms are used in plants for the repair of genomic double-strand breaks by homologous recombination. *Proc. Natl. Acad. Sci. U.S.A.* 93, 5055–5060. doi: 10.1073/pnas.93.10.5055

Puchta, H., Swoboda, P., Gal, S., Blot, M., and Hohn, B. (1995). Somatic intrachromosomal homologous recombination events in populations of plant siblings. *Plant Mol. Biol.* 28, 281–292. doi: 10.1007/BF00020247

Ramsell, J. N. E., Boulton, M. I., Martin, D. P., Valkonen, J. P. T., and Kvarnheden, A. (2009). Studies on the host range of the barley strain of Wheat dwarf virus using an agroinfectious viral clone. *Plant Pathol.* 58, 1161–1169. doi: 10.1111/j.1365-3059.2009.02146.x

Salomon, S., and Puchta, H. (1998). Capture of genomic and T-DNA sequences during double-strand break repair in somatic plant cells. *EMBO J.* 17, 6086–6095. doi: 10.1093/emboj/17.20.6086

Schiml, S., Fauser, F., and Puchta, H. (2014). The CRISPR/Cas system can be used as nuclease for in planta gene targeting and as paired nickases for directed mutagenesis in Arabidopsis resulting in heritable progeny. *Plant J.* 80, 1139–1150. doi: 10.1111/tpj.12704

Schiml, S., Fauser, F., and Puchta, H. (2017). CRISPR/Cas-mediated in planta gene targeting. *Methods Mol. Biol.* 1610, 3–11. doi: 10.1007/978-1-4939-7003-2_1

Shan, Q., Wang, Y., Li, J., Zhang, Y., Chen, K., Liang, Z., et al. (2013). Targeted genome modification of crop plants using a CRISPR-Cas system. *Nat. Biotechnol.* 31, 686–688. doi: 10.1038/nbt.2650

Shukla, V. K., Doyon, Y., Miller, J. C., DeKelver, R. C., Moehle, E. A., Worden, S. E., et al. (2009). Precise genome modification in the crop species Zea mays using zinc-finger nucleases. *Nature* 459, 437–441. doi: 10.1038/nature07992

Sun, Y., Zhang, X., Wu, C., He, Y., Ma, Y., Hou, H., et al. (2016). Engineering herbicide-resistant rice plants through CRISPR/Cas9-mediated homologous recombination of acetolactate synthase. *Mol. Plant* 9, 628–631. doi: 10.1016/j.molp.2016.01.001

Svitashev, S., Schwartz, C., Lenderts, B., Young, J. K., and Cigan, A. M. (2016). Genome editing in maize directed by CRISPR-Cas9 ribonucleoprotein complexes. *Nat. Commun.* 7:13274. doi: 10.1038/ncomms13274

Svitashev, S., Young, J. K., Schwartz, C., Gao, H. R., Falco, S. C., and Cigan, A. M. (2015). Targeted mutagenesis, precise gene editing, and site-specific gene insertion in maize using Cas9 and guide RNA. *Plant Physiol.* 169, 931–945. doi: 10.1104/pp.15.00793

Terada, R., Urawa, H., Inagaki, Y., Tsugane, K., and Iida, S. (2002). Efficient gene targeting by homologous recombination in rice. *Nat. Biotechnol.* 20, 1030–1034. doi: 10.1038/nbt737

Thomas, W. T. B., Bull, H., Booth, A., Hamilton, R., Forster, B. P., and Franckowiak, J. D. (2019). A practical guide to barley crossing. *Methods Mol. Biol.* 1900, 21–36. doi: 10.1007/978-1-4939-8944-7_3

Townsend, J. A., Wright, D. A., Winfrey, R. J., Fu, F., Maeder, M. L., Joung, J. K., et al. (2009). High-frequency modification of plant genes using engineered zinc-finger nucleases. *Nature* 459, 442–445. doi: 10.1038/nature07845

Tzfira, T., Frankman, L. R., Vaidya, M., and Citovsky, V. (2003). Site-specific integration of Agrobacterium tumefaciens T-DNA via double-stranded intermediates. *Plant Physiol.* 133, 1011–1023. doi: 10.1104/pp.103.032128

Vu, G. T. H., Cao, H. X., Watanabe, K., Hensel, G., Blattner, F. R., Kumlehn, J., et al. (2014). Repair of site-specific DNA double-strand breaks in barley occurs via diverse pathways primarily involving the sister chromatid. *Plant Cell* 26, 2156–2167. doi: 10.1105/tpc.114.126607

Vu, T. V., Sivankalyani, V., Kim, E.-J., Doan, D. T. H., Tran, M. T., Kim, J., et al. (2020). Highly efficient homology-directed repair using CRISPR/Cpf1-geminiviral replicon in tomato. *Plant Biotechnol. J.* 18, 2133–2143. doi: 10.1111/pbi.13373

Wang, M. G., Lu, Y. M., Botella, J. R., Mao, Y. F., Hua, K., and Zhu, J. K. (2017). Gene targeting by homology-directed repair in rice using a geminivirus-based CRISPR/Cas9 system. *Mol. Plant* 10, 1007–1010. doi: 10.1016/j.molp.2017.03.002

Wang, S., He, J., Cui, Z., and Li, S. (2007). Self-formed adaptor PCR: a simple and efficient method for chromosome walking. *Appl. Environ. Microbiol.* 73, 5048–5051. doi: 10.1128/AEM.02973-06

Watanabe, K., Breier, U., Hensel, G., Kumlehn, J., Schubert, I., and Reiss, B. (2016). Stable gene replacement in barley by targeted double-strand break induction. *J. Exp. Bot.* 67, 1433–1445. doi: 10.1093/jxb/erv537

Weng, H., Pan, A. H., Yang, L. T., Zhang, C. M., Liu, Z. L., and Zhang, D. B. (2004). Estimating number of transgene copies in transgenic rapeseed by real-time PCR assay with HMG I/Y as an endogenous reference gene. *Plant Mol. Biol. Rep.* 22, 289–300. doi: 10.1007/BF02773139

Wolter, F., Klemm, J., and Puchta, H. (2018). Efficient in planta gene targeting in Arabidopsis using egg cell-specific expression of the Cas9 nuclease of Staphylococcus aureus. *Plant J.* 94, 735–746. doi: 10.1111/tpj.13893

Wolter, F., and Puchta, H. (2019). In planta gene targeting can be enhanced by the use of CRISPR/Cas12a. *Plant J.* 100, 1083–1094. doi: 10.1111/tpj.14488

Xie, K., and Yang, Y. (2013). RNA-guided genome editing in plants using a CRISPRCas system. *Mol. Plant* 6, 1975–1983. doi: 10.1093/mp/sst119

Zhang, Y., Zhang, F., Li, X., Baller, J. A., Qi, Y., Starker, C. G., et al. (2013). Transcription activator-like effector nucleases enable efficient plant genome engineering. *Plant Physiol.* 161, 20–27. doi: 10.1104/pp.112.205179

Zhao, Y., Zhang, C., Liu, W., Gao, W., Liu, C., Song, G., et al. (2016). An alternative strategy for targeted gene replacement in plants using a dual-sgRNA/Cas9 design. *Sci. Rep.* 6:23890. doi: 10.1038/srep23890

Conflict of Interest: The authors declare that the research was conducted in the absence of any commercial or financial relationships that could be construed as a potential conflict of interest.

Advantages of publishing in Frontiers

OPEN ACCESS
Articles are free to read for greatest visibility and readership

FAST PUBLICATION
Around 90 days from submission to decision

HIGH QUALITY PEER-REVIEW
Rigorous, collaborative, and constructive peer-review

TRANSPARENT PEER-REVIEW
Editors and reviewers acknowledged by name on published articles

Frontiers
Avenue du Tribunal-Fédéral 34
1005 Lausanne | Switzerland

Visit us: www.frontiersin.org
Contact us: frontiersin.org/about/contact

REPRODUCIBILITY OF RESEARCH
Support open data and methods to enhance research reproducibility

DIGITAL PUBLISHING
Articles designed for optimal readership across devices

FOLLOW US
@frontiersin

IMPACT METRICS
Advanced article metrics track visibility across digital media

EXTENSIVE PROMOTION
Marketing and promotion of impactful research

LOOP RESEARCH NETWORK
Our network increases your article's readership